Universidade de Lisboa

Faculdade de Medicina de Lisboa

ROLE OF *PLASMODIUM* TRANSLATIONALLY REPRESSED GENE PRODUCTS IN MALARIA TRANSMISSION

Jorge Manuel Santos

Doutoramento em Ciências Biomédicas

Especialidade de Microbiologia e Parasitologia

2014

Universidade de Lisboa

Faculdade de Medicina de Lisboa

ROLE OF *PLASMODIUM* TRANSLATIONALLY REPRESSED GENE PRODUCTS IN MALARIA TRANSMISSION

Jorge Manuel Santos

Tese orientada pelo Doutor Gunnar R. Mair e co-orientada pela Professora Doutora Maria M. Mota

Doutoramento em Ciências Biomédicas

Especialidade de Microbiologia e Parasitologia

A impressão desta dissertação foi aprovada pelo Conselho Científico da Faculdade de Medicina de Lisboa em reunião de 28 de Outubro de 2014.

TABLE OF CONTENTS

ACKNOWLEDGMENTS

I would like to start by thanking Gunnar Mair, my supervisor, for receiving me in his lab, for accepting me as his student and for giving me freedom to try things my way. Also for teaching me all the basic and advanced tricks of working on *Plasmodium* molecular biology, and for setting the pace for my PhD while insisting on perfection and always expecting the best from me. I thank Maria Mota, my co-supervisor, for her determined and pragmatic character that many times helped me to see with clarity through the fog. Thank you also for your encouragement words and honest opinions throughout these years.

Thank you Céline Carret, for the close supervision when I most needed, Miguel Prudêncio, for the attentive eye to my work and my person, and Rita Zilhão, for being a true tutor since college days. After all, it is thanks to you that I have embraced the decision of doing a PhD.

I have to thank many people at Instituto de Medicina Molecular, colleagues that became friends, for their help on the daily life in the lab but not less important for the lovely crazy environment we all lived together, especially in the end of the working days: Afonso Almeida, Alice Melão, Ana Guerreiro, Ana Parreira, Ana Rita Gomes, António Mendes, Bethania Cassani, Fabien Guegan, Fernanda Baptista, Filipa Ferreira, Filipa Teixeira, Francisco Branco, Hélder Ribeiro, Inês Albuquerque, Iset Vera, Joana Pissarra, Leonor Pinho, Mafalda Pimentel, Margarida Vaz, Marija Markovic, Marta Machado, Miguel Duarte, Patrícia Inácio, Patrícia Meireles, Patrícia Silva, Rita Domingues, Sandra Trindade, Sílvia Madeira, Telma Lança. My apologies to those who I might have missed here, namely my partners in the IMM/CAML PhD Students Commission. We all have lived unforgettable moments together. My thoughtful gratitude goes to Vanessa Luís, for the special guidance in the last phase of my work, and for the sincere friendship, and to Andreia Pinto, for some of the most exciting moments of my journey at IMM; I simply loved working with both of you.

I am thankful to Chris Janse and Blandine Franke-Fayard for kindly receiving me in their lab in Leiden, The Netherlands, where I have generated with their help most of the parasite mutants used in the present work. Our collaboration was certainly fruitful and I am sure essential for the accomplishment of my PhD goals. Thank you Hans, Jai and Onny, it would not be possible without your support as well. A special word for Blandine, one of the kindest and wisest persons I ever met in Science. I wish all the very best for your career as I know you also aspire for mine.

I thank Fundação para a Ciência e a Tecnologia (FCT) for awarding me a PhD fellowship during the four years of this work, as well as for financially supporting my stay in Chris Janse's lab in late 2011.

My final words go to my closest friends and family. Amado, Antas, Gaspar, Guilherme, Inês, Joel, Lima, Maria, Marialva, Nelson, Palha, Pena (also an IMM fellow) and Sara: when we are together, problems just do not seem so overwhelming and everything feels like the old days;

thank you for that. I am sincerely grateful for my mother's support, not just during this last four years but also throughout my life. She was and is unconditionally proud of me and that pride has always kept me going. She deserves my absolute admiration and is undoubtedly my hero in life. Thank you for staying by my side in the good but mostly in the difficult moments.

Finally, I deeply thank my dear Diogo, who has been by my side since the beginning of this journey and before, who has constantly kept me on track, brought my feet back to ground when I felt lost and above all, who never let me forget what should be the priorities in life. May I be able to absorb your strength for many more years to come.

ABBREVIATIONS

2-BMP	2-bromopalmitate
ABE	Acyl-Biotin Exchange
Alba	acetylation lowers binding affinity
ALD	aldolase
AMA1	apical membrane antigen 1
AP2	Apetala2
AP2-O	Apetala2 in ookinetes
AP2-Sp	Apetala2 in sporozoites
ApiAP2	Apicomplexan Apetala2
ATP	adenosine triphosphate
BRE	Bruno response element
BSA	Bovine Serum Albumin
CAP	cyclase-associated protein
CB	crystalloid body
cDNA	complementary DNA
CDPK	calcium-dependent protein kinase
CelTOS	cell-traversal protein for ookinetes and sporozoites
CHT1	chitinase
CITH	*C. elegans* CAR-1 and fly Trailer hitch Homologue
CM	cerebral malaria
CPEB	cytoplasmic polyadenylation element binding protein
CRD	cysteine-rich domain
CSP	circumsporozoite protein
CTRP	circumsporozoite- and TRAP-related protein
DARF	DOZI-associated repressor factors
DEAD	Asp-Glu-Ala-Asp = Aspartate-Glutamate-Alanine-Aspartate
dhfr/*ts*	dihydrofolate reductase/thymidylate synthase
DHHC	Asp-His-His-Cys = Aspartate-Histidine-Histidine-Cysteine
DIC	differential interference contrast

DMSO	dimethyl sulfoxide
DNA	deoxyribonucleic acid
DOZI	Development Of Zygote Inhibited
DTT	dithiothreitol
EEF	exoerythrocytic from
eef1a	eukaryotic translation elongation factor 1α
eIF2α	eukaryotic translation initiation factor 2α
eIF4E	eukaryotic translation initiation factor 4E
eIF4G	eukaryotic translation initiation factor 4G
EM	electron microscopy
EMP1	Erythrocyte Membrane Protein 1
EPSF	Essential Protein for Sporozoite Formation
EST	Expressed Sequence Tag
EuPathDB	Eukaryotic Pathogen Database Resources
FACS	fluorescence-activated cell sorting
F-actin	filamentous actin
FBS	Fetal Bovine Serum
FIGE	Field-Inversion Gel Electrophoresis
FLP-FRT	flippase-flippase recognition target
FPKM	Fragments Per Kilobase of transcript per Million mapped reads
GAK	cyclin G-associated kinase
GAP	glideosome-associated protein
GAPM	glideosome associated protein with multiple membrane spans
gDNA	genomic DNA
GEST	gamete egress and sporozoite traversal
GFP	green fluorescent protein
GMP	cyclic guanosine monophosphate
HA	haemagglutinin
Hda2	histone deacetylase 2
HoBo	Homologue of *Drosophila* Bruno

HoMu	Homologue of Musashi1
HP1	heterochromatin protein 1
HPRT	hypoxanthine-guanine phosphoribosyltransferase
HRP	horseradish peroxidase
HSP20	heat shock protein 20
HSP70	heat shock protein 70
HSPG	heparan sulphate proteoglycan
i.p.	intraperitoneally
i.v.	intravenously
ICP	inhibitor of cysteine proteases
IFA	immunofluorescence assay
IgG	immunoglobulin G
IK2	eukaryotic translation initiation factor 2α kinase
IMC	inner membrane complex
IP	immunoprecipitation
iRBC	infected red blood cell
ISP	IMC sub-compartment protein
KH	K-homology
KO	knock-out
lncRNA	long non-coding RNA
Lsm	like-Sm
MAEBL	merozoite adhesive erythrocytic binding-like protein
MAOP	membrane-attack ookinete protein
MAP-2	mitogen-activated protein kinase 2
MBOAT	membrane-bound *O*-acyl-transferase
mRNA	messenger ribonucleic acid
mRNP	messenger ribonucleoprotein
MSP1	merozoite surface protein 1
MTBV	malaria transmission blocking vaccine
MTIP	MyoA tail domain interacting protein

MTOC	microtubule organizing centre
MyoA	Myosin A
ncRNA	non-coding RNA
NIMA	Never in Mitosis Gene A
NRE	Nanos response element
ORF	open reading frame
p.i.	post-infection
PABP	poly(A)-binding protein
PAM	pregnancy-associated malaria
PAT	palmitoyl-S-acyl-transferase
Pb	*Plasmodium berghei*
PBE	Pumilio binding element
P-body	processing-body
PBS	Phosphate Buffered Saline
PCR	polymerase chain reaction
PCRMP	*Plasmodium* cysteine repeat modular protein
Pf	*Plasmodium falciparum*
PFA	paraformaldehyde
Pg	*Plasmodium gallinaceum*
PGAM	phosphoglycerate mutase family member
PK7	protein kinase 7
PlasmoDB	*Plasmodium* Genomics Resource
*Plasmo*GEM	*Plasmodium* Genetic Modification Project
PM	plasma membrane
PP	protein phosphatase
PPKL	kelch-like motifs protein phosphatase
PPLP	*Plasmodium* perforin-like protein
PPM	metallo-dependent protein phosphatase
PRE	Prx Regulatory Element
PREBP	PRE Binding Protein

PSII	photosystem II
PSOP	putative secreted ookinete protein
PTM	post-translational modification
PTPLA	protein tyrosine phosphatase-like A homolog
Puf	Pumilio
PUM-HD	Pumilio homology domain
PV	parasitophorous vacuole
PVM	parasitophorous vacuole membrane
Pvs	*Plasmodium vivax*
Py	*Plasmodium yoelii*
qPCR	quantitative real-time PCR
RBC	red blood cell
RBS	ribosome binding site
RFP	red fluorescent protein
RMgmDB	Rodent Malaria genetically modified Parasites Database
RNA	ribonucleic acid
RNAi	RNA interference
RNA-IP	RNA-immunoprecipitation
RNAseq	RNA sequencing
RON4	rhoptry neck protein 4
RPMI	Roswell Park Memorial Institute medium
RT	reverse transcriptase or room temperature
RT-PCR	reverse transcriptase-polymerase chain reaction
S6/TREP	sporozoite-specific gene 6/TRAP-related protein
SA	severe anaemia
SDS-PAGE	sodium dodecyl sulfate-polyacrylamide gel electrophoresis
SEM	standard error of the mean
SHLP1	Shewanella-like protein phosphatase 1
SIP2	SPE2-interacting protein
SNP	single nucleotide polymorphism

SOAP	secreted ookinete adhesive protein
SP	signal peptide
SPECT	sporozoite microneme protein essential for cell traversal
SPM	subpellicular microtubule protein
SR	serine/arginine
SRPK	serine/arginine-rich protein kinase
Sub2	subtilisin-like serine protease (subtilase)
TB	transmission blocking
TEM	transmission electron microscopy
TF	transcription factor
Tg	*Toxoplasma gondii*
TJ	tight junction
TLP	TRAP-like protein
TM	transmembrane
ToxoDB	*Toxoplasma* Genomics Resource
TR	translational repression
TRAP	thrombospondin-related anonymous protein
TRSP	thrombospondin-related sporozoite protein
UIS	upregulated in infectious sporozoites
UTR	untranslated region
VSP	variant-specific surface protein
WARP	von Willebrand factor A domain-related protein
WT	wild-type
ZOT	zygote-to-ookinete transformation

FIGURE AND TABLE INDEX

INTRODUCTION

EPSF:* A NOVEL CRYSTALLOID BODY PROTEIN WITH A CRITICAL ROLE FOR PLASMODIUM *SPOROZOITE DEVELOPMENT

PALMITOYLATION DEFINES KEY EVENTS DURING MALARIA LIFE CYCLE PROGRESSION IN THE MOSQUITO VECTOR

LIMP:* *A SURFACE PROTEIN ESSENTIAL FOR MALARIA PARASITE MOTILITY AND INVASION THROUGH REGULATION OF ADHESION SITE TURNOVER

RESUMO

A Malária é uma doença causada por espécies parasitas do género *Plasmodium* pertencentes ao filo Apicomplexa. Estes parasitas causam doença no seu hospedeiro quando invadem e se desenvolvem dentro de eritrócitos e apresentam um ciclo de vida deveras complexo, incluindo uma fase de transmissão por um mosquito fêmea do género *Anopheles*. A infecção deste vector depende de células precursoras sexuais designadas gametócitos que se desenvolvem na corrente sanguínea do hospedeiro vertebrado. Nesta fase, os parasitas apresentam dimorfismo sexual, evidente quer a nível morfológico, quer molecular. Por forma a colonizar com sucesso o intestino médio do mosquito, os gametócitos femininos armazenam de forma quiescente ácidos ribonucleicos mensageiros (mRNAs) específicos em ribonucleoproteínas mensageiras (mRNPs) através de um mecanismo molecular designado repressão da tradução. Após uma refeição sanguínea, estes transcriptos são traduzidos no zigoto em desenvolvimento, iniciando desta forma as alterações morfológicas e funcionais que permitem aos parasitas formar o oocineto dotado de motilidade e estabelecer um oocisto replicativo por debaixo do epitélio do intestino médio.

Previamente à transição entre zigoto e oocineto, a repressão da tradução de determinados mRNAs depende dum complexo multiproteico onde as proteínas DOZI e CITH são componentes centrais. Quando estes estão ausentes, os mRNAs outrora silenciados são sobexpressos, prevenindo assim a expressão não oportuna de proteínas na corrente sanguínea do hospedeiro que poderia gerar anticorpos de bloqueio da transmissão da Malária. Parasitas depletados em DOZI ou CITH realizam fertilização, mas ficam impossibilitados de prosseguir mais além no seu desenvolvimento. Os primeiros genes traducionalmente reprimidos a serem identificados foram *p25* e *p28*; estes codificam para as duas mais abundantes proteínas de superfície do oocineto envolvidas na sobrevivência do oocineto, na penetração do epitélio do intestino médio e no desenvolvimento dos oocistos. A repressão da tradução destes mRNAs depende de uma região rica em uridinas nas suas regiões não traduzidas (UTRs), nomeadamente na UTR 5' de *p25* e na UTR 3' de *p28*. Para além disto, estes genes são também dos alvos líder no desenvolvimento de vacinas de bloqueio da transmissão da Malária. Tais vacinas baseiam-se na presença de anticorpos contra antigénios de *Plasmodium* que, quando ingeridos por um mosquito durante uma refeição sanguínea, se ligam ao parasita em desenvolvimento, prevenindo assim a infecção do vector. É portanto evidente que a repressão da tradução é crucial para a produção cronometrada de moléculas do parasita que de outra forma poderiam gerar anticorpos de bloqueio da transmissão com consequências deletérias para a transmissão de *Plasmodium*.

Existem evidências de que a repressão da tradução também ocorre em esporozoítos nas glândulas salivares do mosquito. Os esporozoítos são a forma infecciosa do parasita responsável pela transmissão da doença do mosquito para um hospedeiro não infectado. A deleção do gene *puf2* em *P. berghei*, a espécie causadora de Malária em roedores, resulta em alterações transcripcionais e traducionais que normalmente têm lugar em estádios hepáticos do

parasita. Estas modificações moleculares precedem alterações morfológicas reminiscentes da transição esporozoíto-forma exoeritrocítica quando o parasita ainda se encontra no interior das glândulas salivares do mosquito, sugerindo que a quiescência do esporozoíto depende do controlo pós-transcripcional de certos mRNAs e da função da proteína Pumilio 2 ou Puf2.

O presente trabalho centra-se nos factores que controlam a progressão do ciclo de vida do parasita no mosquito, desde o despontar do desenvolvimento sexual ainda no interior do eritrócito, à formação do esporozoíto e à invasão do fígado. O mesmo caracteriza a função de novos produtos génicos traducionalmente reprimidos de *P. berghei* e determina a sua contribuição para o desenvolvimento do parasita no interior do mosquito e, consequentemente, para a sua transmissão. Este estudo debruça-se essencialmente em três genes principais – *epsf*, *dhhc10* e *limp* – e suas correspondentes proteínas. Todos estes genes são sobexpressos em gametócitos de parasitas Δ*dozi*. É aqui demonstrado que os mesmos são traducionalmente reprimidos em gametócitos femininos, que os seus transcritos interagem com DOZI e CITH e, uma vez traduzidos, as respectivas proteínas se localizam nos corpos cristalóides do oocineto, organelos efémeros e enigmáticos cuja função não é ainda totalmente conhecida.

EPSF (*Essential Protein for Sporozoite Formation*) é uma proteína conservada entre os membros do filo Apicomplexa mas a sua função era até à data desconhecida. Esta proteína apresenta, embora com baixa probabilidade bioinformática, um domínio semelhante a TPM, que em plantas é conhecido por participar no ciclo de síntese/degradação de proteínas do fotossistema II no cloroplasto. DHHC10 é um membro de uma família evolutivamente conservada de palmitoil-S-acil-transferases (PATs) caracterizada pela presença de um domínio rico em cisteínas compreendendo o motivo Asp-His-His-Cys (DHHC), ou por vezes DHYC. Estas proteínas são responsáveis pela adição de palmitato (ácido gordo de cadeia C-16) a resíduos de cisteína de outras proteínas, uma modificação pós-traducional reversível que modifica a afinidade dos seus alvos para membranas lipídicas. Por sua vez, LIMP é uma pequena proteína (110 aminoácidos de comprimento) exclusiva do género *Plasmodium* e não exibe qualquer domínio funcional identificável.

Os mutantes Δe*psf* estabelecem números normais de oocistos que permanecem vacuolizados e não desenvolvem esporozoítos. Os mesmos atingem dimensões superiores aos oocistos *wild-type* (WT) sem concomitante replicação de ácido desoxirribonucleico (DNA) ou expressão de *circumsporozoite protein*. Consequentemente, os parasitas Δe*psf* não apresentam qualquer capacidade de transmissão.

Os mutantes Δ*dhhc10* apresentam um fenótipo muito semelhante ao nível dos oocistos, não obstante neste caso a replicação do seu DNA não ser afectada. Apesar da palmitoilação de proteínas e a relevância de DHHC-PATs para a biologia das fases sanguíneas de *Plasmodium* terem sido foco de muita atenção recentemente, nada é sabido actualmente acerca da importância desta modificação pós-traducional no desenvolvimento do parasita no seu vector. Através do uso de inibidores e de modificação genética este estudo demonstra pela primeira vez que a palmitoilação é crucial para processos biológicos que têm lugar em diversas

fases da infecção do mosquito: é indispensável para a transformação do zigoto em oocineto e define a eficiência de invasão de hepatócitos por esporozoítos, sendo no entanto redundante para a motilidade do tipo *gliding* e para o atravessamento de células hospedeiras. Ao remover *dhhc10* é demonstrado neste trabalho que esta DHHC-PAT é basilar para a correcta localização de outros componentes dos corpos cristalóides e para a própria formação destes organelos.

Tal como para outras proteínas localizadas nos corpos cristalóides (membros da família proteica de adesinas LCCL), EPSF e DHHC10 têm um papel essencial na esporogonia de *P. berghei* (formação de esporozoítos dentro dos oocistos) e portanto na progressão do ciclo de vida do parasita no mosquito. Os dados aqui apresentados reforçam a noção de que proteínas residentes dos corpos cristalóides são vitais para a esporulação dos oocistos. LIMP também se localiza nos corpos cristalóides do oocineto mas, contrariamente a EPSF e DHHC10, a sua função nada tem que ver com a formação de esporozoítos. De facto, os oocistos Δ*limp* são igualmente eficientes na produção de esporozoítos quanto parasitas WT.

Este ensaio estabelece LIMP como um novo factor de motilidade do tipo *gliding* específico de parasitas da Malária. O mesmo é importante para uma eficiente infectividade do oocineto e essencial para a motilidade do esporozoíto, assim com para a sua capacidade de aderir, atravessar e invadir células do fígado. A ausência desta proteína reduz a transmissão para o mosquito em metade, a invasão das glândulas salivares em dez vezes e torna os parasitas incapazes de infectar ratinhos *naïve*, quer por picada de mosquito, quer por injecção intravenosa de esporozoítos. Por um lado, os parasitas depletados em LIMP não dispõem de qualquer motilidade. Por outro, a fusão deste factor com a proteína fluorescente GFP resulta num movimento imperfeito caracterizado por velocidade reduzida e frequente alongamento do esporozoíto, particularidades relacionadas com uma redução da reciclagem de locais de adesão entre o parasita e o substrato. Conjuntamente com a localização de LIMP na membrana plasmática do esporozoíto, os actuais resultados sugerem que LIMP desempenha um papel crítico no estabelecimento/dissolução de locais de adesão durante o movimento do parasita e invasão de células hospedeiras.

De forma geral, a presente dissertação sublinha a relevância da repressão da tradução e dos seus mRNAs alvo para a biologia de *Plasmodium* e demonstra que os genes traducionalmente reprimidos são cruciais para a transmissão do parasita e sua sobrevivência em múltiplas fases do seu desenvolvimento no interior do mosquito. Este trabalho indicia novas abordagens conceptuais no combate à Malária, nomeadamente a inibição da formação de corpos cristalóides e a interferência com a maquinaria de motilidade do parasita.

SUMMARY

Malaria is caused by parasite species of the genus *Plasmodium* belonging to the phylum Apicomplexa. *Plasmodium* parasites cause disease when they infect red blood cells of the mammalian host and present a very complex life cycle that includes transmission by a female anopheline mosquito vector. The infection of this vector depends on sexual precursor cells called gametocytes that develop in the blood stream of the vertebrate host. At this stage, parasites display sexual dimorphism that is evident at both morphological and molecular levels. In order to successfully colonise the mosquito midgut, female gametocytes quiescently store specific messenger ribonucleic acids (mRNAs) in messenger ribonucleoproteins (mRNPs) by a molecular mechanism designated translational repression (TR). Following a blood meal, these transcripts are translated in the developing zygote, thereby initiating the morphological and functional changes that allow the parasites to form the motile ookinete and establish a replicating oocyst underneath the midgut epithelium cell layer.

Prior to the zygote-to-ookinete transformation (ZOT), TR of selected mRNAs depends on a multiprotein complex where DOZI and CITH are core components. When absent, the otherwise silenced mRNAs are downregulated, preventing mistimed protein expression in the mammalian host's blood stream that could allow for the generation of malaria transmission blocking antibodies. Parasites lacking DOZI or CITH take part in fertilisation but cannot develop further. The first *Plasmodium* translationally repressed genes to be identified were *p25* and *p28*; they encode for the two major ookinete surface proteins involved in ookinete survival, penetration of midgut epithelium and development into oocysts. TR of these mRNAs depends on uridine-rich regions in their untranslated regions (UTRs), namely in the 5' UTR of *p25* and in the 3' UTR of *p28*. Additionally, these have also been the gold standard and leading target candidates for malaria transmission blocking vaccines (MTBVs). These vaccines rely on the presence of antibodies against *Plasmodium* antigens that, when taken up by a mosquito during a blood meal, bind to the developing parasite preventing infection of the vector. It is then evident that TR is paramount for the timely production of parasite molecules that otherwise could raise transmission blocking antibodies with deleterious consequences for *Plasmodium* transmission.

TR is also believed to take place in salivary gland sporozoites, the mammalian-infective parasite form that is responsible for disease transmission from the mosquito to the human or rodent host. Deletion of *puf2* in the rodent malaria parasite species *P. berghei* results in transcriptional and translational alterations that normally take place in hepatic stages. These molecular modifications precede morphological changes reminiscent of sporozoite-to-liver stage transformation while still in the mosquito salivary glands, suggesting that sporozoite quiescence relies on post-transcriptional control of certain mRNAs and on the function of the protein Pumilio 2 or Puf2.

We are interested in the factors that drive parasite life cycle progression in the mosquito vector, from the onset of sexual development in the erythrocyte to sporozoite formation and liver

cell invasion. In the present study we characterised the function of novel putative translationally repressed gene products of *P. berghei* and determine their contribution to parasite development within the mosquito and consequently to malaria transmission. Three main genes (and corresponding proteins) are addressed herein – *epsf*, *dhhc10* and *limp* – all of which were found downregulated in the *Δdozi* parasite line. We show here that they are translationally repressed in female gametocytes, are bound by DOZI and CITH and are targeted to the ookinete crystalloid bodies (CBs) upon translation, a short-lived and enigmatic organelle with unclear function.

EPSF (Essential Protein for Sporozoite Formation) is conserved among apicomplexans but its function was so far unknown. This protein contains, although with low probability, a bioinformatically annotated TPM-similar domain that in plants has been implicated in the synthesis/degradation cycle of photosystem II proteins in the chloroplast. DHHC10 is a member of an evolutionarily conserved family of palmitoyl-S-acyl-transferases (PATs) characterised by the presence of an Asp-His-His-Cys (DHHC) motif (sometimes DHYC) within a cysteine-rich domain. These proteins are responsible for the addition of palmitate (C-16-long chain fatty acids) to cysteine residues of other proteins, a reversible post-translational modification (PTM) that tethers its targets to lipid membranes. On the other hand, LIMP is a small (110 amino acids-long) protein unique to *Plasmodium* spp. and exhibits no identifiable functional domains.

Δe*psf* mutants establish normal oocyst numbers but fail to develop sporozoites, remain vacuolated and continue to increase in size without concomitant deoxyribonucleic acid (DNA) replication or circumsporozoite protein expression. Consequently, Δe*psf* parasites are completely blocked in transmission.

Δ*dhhc10* mutants show a very similar oocyst phenotype despite the fact that DNA replication does not seem to be affected in this case. Although protein palmitoylation and the relevance of DHHC-PATs in *Plasmodium* biology have recently been the focus of much interest in blood stage parasites, nothing is know about the importance of such PTM in parasite development within its mosquito vector. Using drug inhibitor and gene deletion studies we show for the first time that palmitoylation is crucial for the execution of developmental and cell biological processes during several phases of mosquito stage infection: it is indispensable for ZOT and defines the efficiency of sporozoite invasion of the host hepatocyte while being redundant for rapid protein turn-over during gliding motility and cell traversal. By deleting *dhhc10* we demonstrate that this DHHC-PAT is key to the correct targeting of other CB components and to the formation of the ookinete CB itself.

Similar to other CB-associated proteins (the members of the LCCL protein family of adhesins), both EPSF and DHHC10 have an essential role for *P. berghei* sporogony (formation of sporozoites within oocysts) and therefore for progression of the parasite life cycle in the mosquito. Our data thus further establishes the vital function of CB-resident proteins in oocyst sporulation. LIMP is also localised to the ookinete CBs but, on the contrary to EPSF and

DHHC10, is not involved in the formation of sporozoites. In fact, Δ*limp* oocysts are equally efficient as wild-type (WT) parasites in producing midgut sporozoites.

We establish LIMP as a novel malaria-specific gliding motility factor that is important for efficient ookinete infectivity and essential for sporozoite motility and capability to adhere, traverse and invade host liver cells. The absence of this protein reduces transmission to the mosquito vector by half, salivary gland invasion 10-fold and renders parasites unable to infect naïve mice by mosquito bite or when injected intravenously. While LIMP-depleted parasites display no gliding motility, *in situ* green fluorescent protein (GFP) tagging of this protein resulted in a limping movement characterised by reduced speed and frequent stretching, which has been correlated with reduced turnover of parasite-substrate adhesion sites. Together with the plasma membrane localisation of LIMP in sporozoites, our results suggest that LIMP plays a critical role in regulating the attachment/detachment of adhesion sites during gliding motility and invasion of host target cells.

Overall, this dissertation highlights the relevance of TR and its target mRNAs for *Plasmodium* biology and demonstrates that translationally repressed gene products are crucial for parasite transmission and survival at multiple steps of its development within the mosquito. This work raises new conceptual approaches to combat malaria, namely by inhibiting the formation of CBs and interfering with the parasite gliding motility machinery.

INTRODUCTION

I – APICOMPLEXA

The phylum Apicomplexa is composed of a large group of unicellular, eukaryotic protozoa and contains obligate intracellular parasites causing disease to humans, livestock, wild animals and invertebrates, such as those belonging to the genera *Plasmodium*, *Toxoplasma*, *Cryptosporidium*, *Babesia* and *Theileria* [1]. The hallmark of the phylum from which the name Apicomplexa derives is the presence of an apical complex involved in motility and host cell adhesion and penetration and composed of secretory organelles such as rhoptries and micronemes and one or more polar rings [2]. Polar rings are circular structures from which subpellicular microtubules emanate and were thus postulated to be a microtubule organizing centre (MTOC) [3]. Some members such as *Toxoplasma* possess a set of spirally arranged tubulin fibers forming a truncated cone structure called conoid [4]. This organelle is thought to play a mechanical role in invasion of host cells [2]. Another characteristic feature of most apicomplexans is the apicoplast, a non-photosynthetic plastid thought to be derived from the engulfment of a red alga in a secondary endosymbiotic event [5, 6]. As a result, the apicoplast presents not two, but four membranes, with the outermost and second outermost membranes deriving from the parasite and algal plasma membranes, respectively [5, 6]. The overall function of this organelle is still elusive but evidence exists that it is involved in type II fatty acid, isoprenoid, iron-sulphur cluster and haem synthesis [6].

II – *PLASMODIUM* AND MALARIA

Although the global malaria burden has decreased in last few years, it still exerts a severe negative impact on the social and economic development of most African and South-East Asian countries. According to World Health Organization estimates, there were 219 million malaria cases worldwide in 2010, including 660 thousand deaths. Most of the cases (80%) and deaths (91%) occur in sub-Saharan Africa. Strikingly, 86% of the malaria deaths took place in children under 5 years of age. *Plasmodium falciparum*, the deadliest human parasite species, was responsible for 90% of the total malaria cases in that year [7].

Malaria is caused by parasites species of the genus *Plasmodium* belonging to the phylum Apicomplexa and is a complex disease including several different symptoms and clinical manifestations. The invasion of the liver and development of the parasite within hepatocytes are disease-free phases of the parasitic infection. The pathogenic process starts when parasites infect the red blood cells (RBCs) of its host. The first and most common signs of malaria infection are periodic fever peaks and chills. These symptoms occur at the time of erythrocyte rupture, a necessary step for the subsequent infection of new RBC and continuation of parasite asexual multiplication, and are believed to be caused by the release of malarial toxins. Consecutive RBC burst typically leads to anaemia [8]. Severe forms of disease exist and include cerebral malaria (CM), acute lung injury, acute respiratory distress syndrome, pregnancy-associated malaria (PAM) and severe anaemia (SA) [9]. In addition to SA, which affects mostly children under the age of 3, CM, accompanied by characteristic seizures and sometimes coma, is one of the leading causes of death in non-immune patients and African children [8]. The onset of this severe condition depends on high blood parasitaemias [8] but also on the concomitant sequestration of CD8-expressing T cells and infected RBCs (iRBCs) in the brain, as determined in animal models [10]. In *P. falciparum*, the endothelial cytoadherence feature of iRBCs depends on the expression of PfEMP1 (Erythrocyte Membrane Protein 1) at the surface of the iRBC, a protein encoded by the *var* family of genes [11, 12]. Non-immune women are particularly susceptible to PAM, which may lead to abortions and stillbirths. Other frequent consequences of PAM for the newborns are low birth weight, caused by intrauterine growth retardation and/or premature delivery, neonatal infection and mortality. These pregnancy outcomes are likely to be associated with the accumulation of iRBCs in the placental vasculature [8]. In agreement with this idea, VAR2CSA, a PfEMP1 variant, is implicated in iRBC sequestration in the placenta [13].

Malaria parasites are transmitted from and to mammalian hosts (human, simian and rodent) during the blood meal of female anopheline mosquitoes (*Anopheles* spp.), which feed on blood in order to produce and lay eggs. On the other hand, culicine mosquitoes such as *Aedes* spp. and *Culex* spp. are, similarly to *Anopheles* spp., capable of transmitting *P. gallinaceum* and *P. relictum* to avian vertebrate hosts but have never been reported transmitting mammalian parasites [14]. Out of the numerous *Plasmodium* species known to date, only four routinely cause disease in humans: *P. falciparum, P. vivax, P. malariae* and *P. ovale* [15].

Traditionally viewed as a zoonotic infectious agent, *P. knowlesi* has recently been reported in humans [16, 17]. Five major anopheline species act as human malaria vectors in Africa: *A. gambiae*, *A. arabiensis*, *A. funestus*, *A. nili* and *A. moucheti*. They all belong to species complexes that are very difficult to distinguish based on morphological characters. The predominance and overlap of these species largely depends on the geographic region and ecosystems but in certain areas as much as all five species co-habit and transmit parasites to humans [18].

The malaria parasite was first discovered in Algiers by Alphonse Laveran, a French army surgeon who observed flagellated cells moving in a blood sample from a malaria patient. He was observing what today is known as the exflagellation of male gametocytes [19]. The erythrocytic cycle and the name *Plasmodium* were established a few years later by Ettiore Marchiafava and Angelo Celli [20]. The vectorial capacity of *Anophelles* mosquitoes for *Plasmodium* parasites was only discovered in 1902 by Ronal Ross, a British medical doctor working at the Presidency General Hospital in Calcutta at the time. By carefully examining histological sections of stomachs from mosquitoes fed on malaria patients four days before he found perfectly round parasite forms: the oocyst [21]. One year later he describes the complete parasite 'metamorphosis' in the mosquito, including the ookinete to oocyst development, the release of sporozoites into the haemocoel and their journey to the salivary glands, using *P. relictum* (then called *Proteosoma*) infecting sparrows and larks [22]. This major scientific breakthrough earned Sir Ross the second Nobel Prize for Physiology or Medicine in 1902. However, it was only in the second half of the 20th century that the whole malaria life cycle became complete, when the English protozoologist Cyril Garnham (in collaboration with is colleague Hugh Shortt) unravelled the exoerythrocytic stage of species infecting non-human primate hosts [23-25] and later on of the human malaria parasites *P. vivax* [26, 27], *P. falciparum* [28], *P. ovale* [29] and *P. malariae* [30].

The *Plasmodium* life cycle is complex. Within the RBCs, the majority of parasites follow an asexual multiplication cycle termed schizogony [31], while some develop into non-dividing sexual precursor cells called gametocytes [32, 33]. Following a mosquito blood meal, the ingested male (micro) and female (macro) gametocytes form male and female gametes, respectively; these mate inside the mosquito midgut and the resulting zygote develops into an ookinete. This motile parasite form escapes from the midgut peritrophic matrix, a chitin-containing sheath secreted by midgut cells to contain the blood meal [34], traverses the midgut epithelium and establishes a sessile oocyst that produces thousands of sporozoites. Oocyst rupture results in the release of motile sporozoites that migrate through the haemocoel to the mosquito salivary glands where they await another blood meal [35, 36]. After being injected into the skin of the vertebrate host (e.g., human or mouse model), the parasites migrate to the blood stream and reach the liver where they traverse a few cells before definitely establishing themselves within a hepatocyte [37]. There, a single sporozoite develops into an exoerythrocytic from (EEF), which releases thousands of newly formed, RBC-infective merozoites into the

bloodstream [38]. Some species such as the non-human primate parasite *P. cynomolgi* and the human parasites *P. vivax* and *P. ovale* are capable of producing liver dormant cells called hypnozoites, responsible for malaria relapses (with concomitant blood parasitaemias) months or even years after the infectious bite took place. The discovery of this deviation to the standard life cycle is also due to the work of Garnham as well as other British and American scientists [39, 40]. Please see **Figure 1** for a diagram of the complete life cycle of *P. falciparum*.

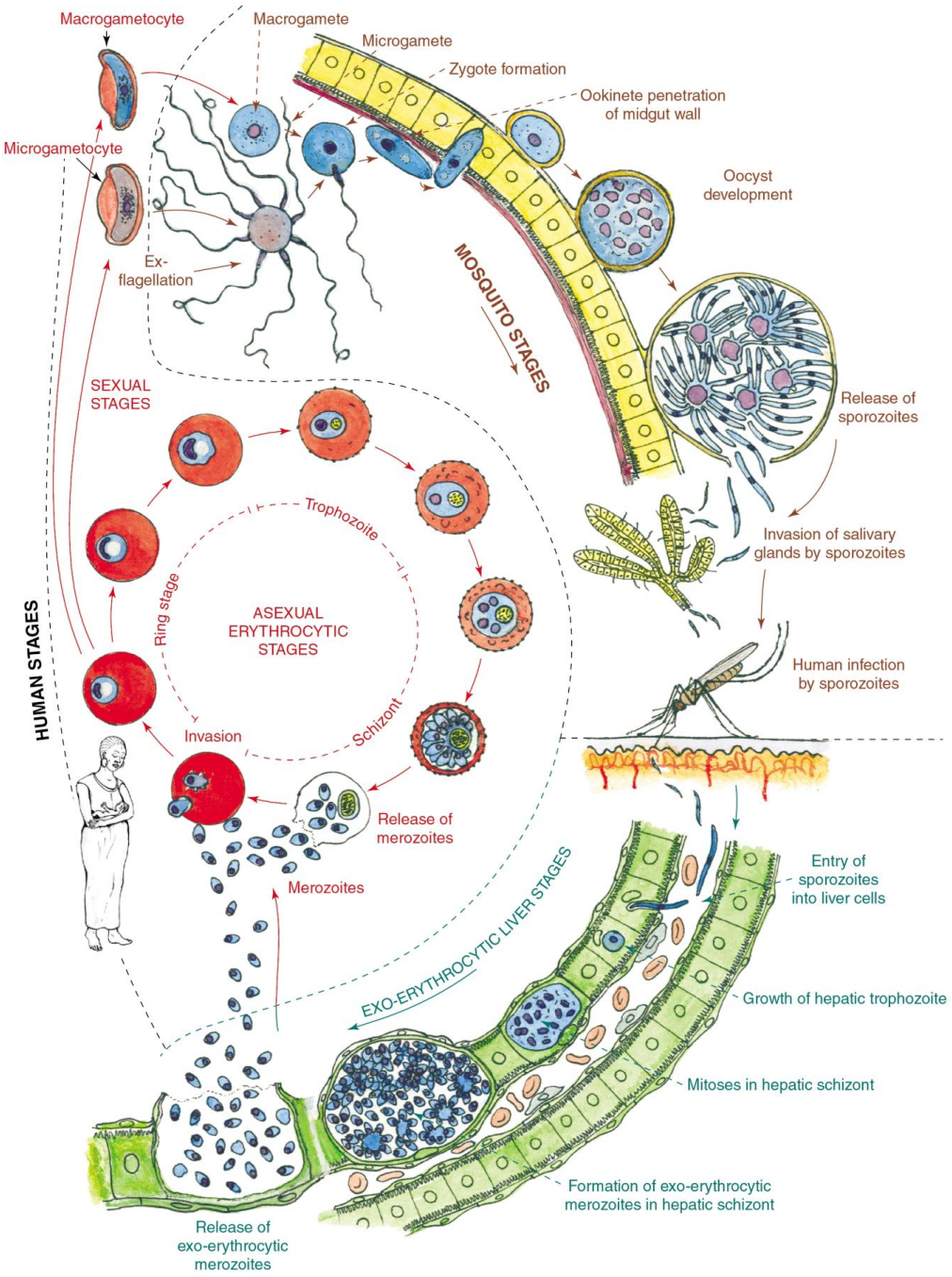

Figure 1 – Life cycle of *Plasmodium falciparum*.
The complete life cycle including the liver and blood stages of infection in the human host, as well as the gut and salivary gland phases in the mosquito vector are depicted. [Adapted from Bannister and Mitchell, *Trends Parasitol* 2003, 19(5): 209-13]

The developmental time frame of each one of *Plasmodium* life cycle steps is highly variable and species-dependent. For example, in *P. berghei*, a rodent malaria species, the exoerythrocytic phase takes about 48 hours, but can last up to 16 days depending on the parasite species [38]. The completion of the asexual blood cycle is achieved in 24 hours in *P. berghei* [41], *P. chabaudi* (another species infecting rodents) [42] and *P. knowlesi* [43]. In *P. falciparum* this cycle takes approximately 48 hours [44-46] but is isolate-dependent. Gametocyte maturation takes 7-8 days in the case of *P. falciparum*, passing through five morphological stages [32, 36], and 26-30 hours in *P. berghei*, only slightly longer than the duration of the asexual cycle [32]. Fertilisation occurs within approximately one hour after mosquito blood feeding and zygote-to-ookinete transformation (ZOT) in different *Plasmodium* species varies from 10 to 30 hours. The entire duration of parasite development within the mosquito, from the ingestion of infected blood to the presence of infective sporozoites in the salivary glands, is complete in approximately 14 days at 26 °C in the case of *P. falciparum* [36] and takes at least 18 days at 20 °C in the case of *P. berghei*.

Two major bottlenecks exist in the malaria life cycle, each one of them followed by extensive population expansion: they occur during transmission to and from the mosquito vector. While it is estimated that less than 5% of the 10–10,000 female gametocytes ingested during a blood meal successfully develops into oocysts [35, 36] (**Figure 2**), not more than a few hundred sporozoites are injected in the skin of the host during mosquito probing prior to a subsequent blood feeding [35, 38, 47]. In between, a less pronounced population constraint takes place during development within the mosquito: only a quarter of the sporozoites that are released from the oocysts to the mosquito hemolymph successfully reach the salivary glands, which can harbour up to 100,000 parasites [35]. Therefore, intervention strategies targeting such density limiting stages are likely to be successful, as substantially less parasitic cells need to be eliminated at those specific moments. Recently, a studied performed in laboratory-

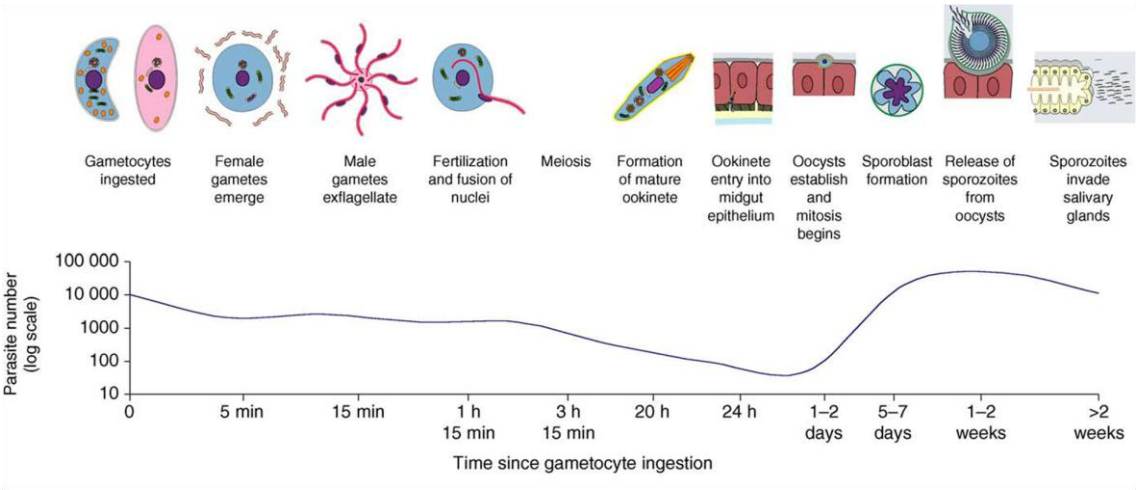

Figure 2 – Dynamics of *Plasmodium* development in the mosquito vector.
The sequence of developmental events (top) is accompanied by drastic fluctuations in parasite density (bottom). The plot should is merely an indication of changes in density over time and should not be regarded as an indication of absolute parasite numbers. [Adapted from Baton and Ranford-Cartwright, *Trends Parasitol* 2005, 21(12): 573-80]

controlled vector populations has shown that the administration of the transmission blocking (TB) drug atovaquone to infected mice reduces parasite burden and prevalence of infection in mosquitoes by 57 and 32%, respectively. Even so, this mild effect was capable of eliminating malaria from both the mosquito and mouse populations in only three cycles of transmission at low mosquito biting rates, i.e., one or two potentially infectious mosquito bites per mouse in each generation. At higher transmission rates, parasites were however not eliminated from either population, indicating that more efficacious TB strategies would be needed to achieve malaria elimination in this scenario [48].

III – *PLASMODIUM* GENE REGULATION

The *Plasmodium* proteome is tightly regulated throughout its intricate life cycle, with high percentages of stage-specific proteins [49-51]. How exactly malaria parasites control gene expression to achieve such specificity is still being unravelled but involves molecular mechanisms at the transcriptional, post-transcriptional and translational level. One very relevant observation with great impact on how these organisms regulate gene expression is that they do not possess the core RNA interference (RNAi) machinery components, such as Argonaute and Dicer [52].

The mutually exclusive expression of *var* genes has been extensively studied and depends to a great extent on epigenetic regulators such as chromatin-remodelling proteins, histone modification marks, histone variants and long non-coding RNAs (lncRNAs) [53]. Conserved eukaryotic epigenetic factors have been correlated with gene expression on a *P. falciparum* genome-wide scale. The dynamic occupancy pattern of eight euchromatic and heterochromatic histone marks in either histone H3 (H3K4me3, H3K9ac, H3K14ac and H3K56ac) or H4 (H4K8ac, H4K16ac, H4K20me1 and H4K4,8,12,16ac) displayed a strong positive correlation with transcript levels across the parasite genome and intraerythrocytic development cycle. Interestingly, and similarly to what is observed in plants, these histone modifications were mainly associated with the 5' end of coding sequences and not with intergenic regions [54]. Non-coding RNAs (ncRNAs) may also contribute to epigenetic regulation of transcription by possibly binding to general histone-modifying enzymes and providing them with target specificity [55]. Recently, an unprecedented type of post-transcriptional gene regulation mechanism involving RNase II-mediated degradation of nascent RNAs was shown to contribute to the silencing of upsA-type *var* genes in *P. falciparum*, known to be associated with obstruction of brain blood vessels in cerebral malaria human patients [56].

Evidence suggests that nuclear positioning of specific *loci* participates in the activation/silencing of genes. For instance, silent *var* genes are observed in perinuclear clusters while they move towards the nucleus centre upon activation. Nonetheless, general active transcription sites are also observed at the nuclear periphery [57]. Overall *P. falciparum* genome architecture has also been recently implicated in gene regulation, with a strong correlation between the transcription of specific genes and their spatial localisation within the three-dimensional genome structure [58].

Unlike most eukaryotes, not many transcription factors (TFs) are known in the genomes of *Plasmodium* parasites. Only one family of TFs is known in malaria parasites, the Apicomplexan Apetala2 (ApiAP2) family [59], with 27 predicted members in *P. falciparum* and 26 in *P. berghei* (PlasmoDB version 11.1). *Toxoplasma gondii* strains on the other hand encode up to 68 of such proteins in their genomes ([60, 61] and ToxoDB version 11.0). This is a family of plant TFs characterised by the presence of at least one AP2 domain, a DNA binding domain of approximately 60 amino acids [62].

Given the scarcity of TFs, *locus*-specific, promoter-based transcriptional control of gene expression was long thought not to be the dominant mode of gene regulation in *Plasmodium*. A significant delay between the transcript and protein maximum abundances for a vast percentage of the malarial genes pointed towards this view [63]. Instead, post-transcriptional mechanisms would play a major role in achieving a tight regulation of gene expression [64]. But recent and current work done on the ApiAP2 gene family is challenging this theory.

Remarkably, the AP2 domains of different ApiAP2 proteins show specific affinities for distinct DNA motifs enriched in the upstream region of functionally-related genes, underscoring the importance of both *cis*- and *trans*-acting factors in parasite gene regulation [65]. In recent years, specific ApiAp2 TFs have been ascribed to defined biological processes and life cycle stage transitions. The ApiAP2 member PfSIP2 (SPE2-interacting protein) was shown to co-localise with PfHP1 (heterochromatin protein 1) and to bind almost exclusively to heterochromatic domains upstream of subtelomeric *var* genes containing the SPE2 DNA motif. Interestingly, this work described for the first time the participation of an ApiAP2 TF in the formation of heterochromatin (tightly condensed form of DNA) and thus in gene silencing in *P. falciparum* blood stages [66]. Also in *P. falciparum*, it was recently demonstrated that sexual commitment is dependent on the DNA-binding protein PfAP2-G [67], which in turn is negatively controlled by PfHP1 [68] and PfHda2 (histone deacetylase 2) [69]. Both these epigenetic regulators contribute to the maintenance of heterochromatin at the *pfap2-g locus*. Similarly, the *P. berghei* ortholog PbAP2-G was also shown to be a master regulator of sexual differentiation in this rodent malaria parasite species, while a second transcription factor, PbAP2-G2, modulates the numbers of gametocytes, as its absence does not result in the complete abolishment of gametocytogenesis [70]. AP2-O (Apetala2 in ookinetes) on the other hand was shown to regulate the expression of *P. berghei* ookinete-specific genes, particularly invasion-related factors, by binding to a DNA motif in their 5' upstream regions [71]. The AP2 domain of another ApiAP2 TF in *P. berghei*, AP2-Sp (Apetala2 in sporozoites), was found to bind to a conserved *cis* element in the promoter region of known sporozoite-specific genes. In agreement with this finding, ablation of AP2-Sp led to the development of abortive oocysts in mosquito midguts, demonstrating its essentiality for sporozoite formation, most likely through the transcriptional activation of genes necessary for sporozoite morphogenesis [72]. On the other hand, AP2-L is essential for the development of malaria liver stages and responsible for the expression of *uis3*, *uis4*, *exp1* and *lisp1*, genes encoding for proteins of the parasitophorous vacuole membrane (PVM) surrounding intrahepatic parasites. Although AP2-L-depleted parasites invade hepatocytes normally, they arrest development during liver schizogony [73]. Lastly, a non-ApiAP2 intraerythrocytic stage TF of *P. falciparum* but well conserved within the *Plasmodium* genus was shown to activate the expression of *pf1-cys-prx* [74], a trophozoite/schizont-specific peroxiredoxin family member [75, 76]. This TF was named PREBP (PRE Binding Protein) based on its ability to bind to DNA stretches including the 102 base pair-long Prx Regulatory Element (PRE) and contains four K-homology (KH) domains [74] characteristic of single-stranded DNA and RNA binding proteins [77, 78].

Regardless of the continuously growing evidence that TFs are master regulators of parasite virulence and development, co-transcriptional and post-transcriptional mechanisms of gene regulation are critical players in controlling gene expression in *Plasmodium*. One example of co-transcriptional mechanisms is pre-mRNA alternative splicing. Approximately 53% of *P. falciparum* genes are predicted to contain introns ([79] and PlasmoDB version 11.1) and many of these give rise to alternative mRNA splice variants, which arise through use of alternative 5' and/or 3' splice sites, intron retention/creation or exon skipping. Splicing can also be observed in the 5' and 3' untranslated regions (UTRs) of certain genes [80, 81]. In some cases, these alternative splicing events generate mature mRNAs containing premature stop codons [81], which might encode for non-functional proteins or instead, protein variants with distinct functions and subcellular localisations [82]. One important post-transcriptional mechanism of malaria gene expression control is translational repression (TR), by which specific mRNAs are kept translationally quiescent in the parasite cytoplasm in association with protein repressor complexes until the right environmental cues trigger their release from such complexes and initiate protein synthesis. TR in *Plasmodium* and as a general evolutionarily conserved mechanism will be described in greater detail in the next section of this Introduction.

Finally, a polysome profiling study along the parasite erythrocytic cell cycle identified a delay between the peak of mRNA abundance in steady-state versus that associated with polysomes for over 30% of *P. falciparum* genes, implying a strong translational control of gene expression. Abundant and widespread transcription of ncRNAs which could influence translation efficiency was also highlighted in the same work [83]. Over 300 antisense, ncRNAs were also detected in another study on *P. falciparum* blood stages and believed to act as silencers of the cognate genes in the transition from asexual to sexual development [84].

IV – TRANSLATIONAL REPRESSION

IV.1 – TRANSLATIONAL REPRESSION IS AN ANCIENT AND CONSERVED MECHANISM

TR is a broad molecular concept that consists in inhibiting the translation of certain genes/transcripts. It is an evolutionarily conserved post-transcriptional gene regulatory process exerted by both prokaryotic and eukaryotic organisms which general principle is to interfere with the formation of translational initiation complexes.

In bacteria this can be achieved by three mechanisms: a temperature-induced mRNA conformational change that generates a *cis*-acting mRNA sequence responsible for preventing ribosomal 30S subunit access to the ribosome binding site (RBS), binding of a protein to its own mRNA in a negative loop feedback effect and binding of a *trans*-acting allosteric repressor to the mRNA. The first two mechanisms are called competitive mechanisms as they compete with the ribosome for binding to the RBS. The latter one is an entrapment mechanism, as the repressor does not impair interaction of ribosomal subunits with the RBS, but instead induces entrapped ternary complexes that inhibit the formation of stable translational initiation complexes [85, 86].

In eukaryotes, TR is accomplished through the binding of microRNAs or RNA binding proteins to target mRNAs [87-89]. Although not fully dissected, a model for the involvement of microRNAs in TR suggests they interact with GW182 and Argonaute proteins leading to: (i) competition with the translation initiation factor eIF4G for association with poly(A)-binding protein (PABP), (ii) prevention of 60S-40S ribosomal subunit interaction to form 80S ribosomes, (iii) ribosome stalling along the mRNA, (iv) premature translation termination and/or (v) co-translational degradation of synthesised proteins [89]. One of the best studied families of translational repressors is the Puf family of RNA binding proteins. This is an evolutionarily conserved family present in highly divergent eukaryotic organisms, from yeast to zebrafish, *Xenopus*, mouse, humans and plants, but also in the invertebrates *Drosophila*, *Anopheles* and *Caenorhabditis elegans*. Puf proteins are related to the Pumilio protein of *Drosophila* and the fem-3 mRNA binding factor of *C. elegans* (founder members of the family) and typically contain eight tandem Pumilio homology domains (PUM-HDs). They control mRNA translation by promoting its repression or degradation and generally interact with transcripts by binding to conserved motifs [UGUA/G$(N)_{1-2}$AUA] on their UTRs, often the 3' UTR, the so called Pumilio binding elements (PBEs) [90-93].

TR allows a bi-dimensional regulation of gene expression (i.e., both in time and in space). For example, in the case of *Drosophila*, *hunchback* mRNA (encoding for a transcription factor critical for embryonic patterning) is specifically repressed in posterior regions of the fly embryo. This is mediated by the binding of a protein complex containing Pumilio and Nanos proteins to the Nanos response elements (NREs) on *hunchback* 3' UTR and ensures that Hunchback protein is exclusively expressed at the anterior pole of the embryo [94, 95]. The

maternally-derived mRNA *oskar* is also target of TR, in this case through the interaction with the repressor Bruno, which binds to Bruno response elements (BREs) present on the 3' UTR of *oskar* [96, 97]. On the other hand, the maternally inherited xCR1 mRNA is both temporally and spatially regulated. The transcript is present in the egg but only translationally activated at the 16- to 32-cell stage embryo, and although the mRNA is equally distributed throughout all *Xenopus* embryonic cells, it is not translated in the vegetal half of the embryo and consequently protein accumulates in the animal half. The repression of xCR1 translation in vegetal cells is conferred by a region in its 3' UTR that contains both PBEs and binding sites for the CUG-BP1 protein, a homologue of the *Drosophila* Bruno [98]. The binding of Pumilio proteins to PBEs in the RINGO mRNA of *Xenopus* oocytes has also been shown to lead to its TR [99], and the interaction of CUG-BP1 (also known as EDEN-BP) with the 3' UTR of certain mRNAs is known to negatively regulate mRNA translation in *Xenopus* embryos [100].

IV.2 – TRANSLATIONAL REPRESSION IN *PLASMODIUM*

In *Plasmodium*, TR was first described more than 20 years ago [101], and several subsequent studies highlighted its importance [49, 102-104]. As in multicellular eukaryotes [105, 106], TR in *Plasmodium* is particularly important in sexual differentiation and is exerted in female inherited mRNAs [107, 108]. In 1993, Paton and colleagues reported the transcript of *p28* to be abundant in *P. berghei* gametocytes, while the corresponding protein was only observed after gametocyte in zygotes and ookinetes [101]. However, it was only in 2006 that the exact mechanism responsible for the lag between transcription and translation of certain genes became clear. Known and predicted translationally repressed mRNAs were shown to physically interact in cytoplasmic messenger ribonucleoproteins (mRNPs) with the RNA binding protein DOZI (Development Of Zygote Inhibited) [107], a member of the DEAD(Asp-Glu-Ala-Asp)-box family of RNA helicases [109] particularly enriched in female gametocytes [50]. DOZI homologues in other organisms include Dhh1p in *Saccharomyces cerevisiae*, CGH-1 in *C. elegans*, Me31B in *Drosophila melanogaster* and DDX6/Rck54 in humans. DDX6 RNA helicase homologues are implicated in both mRNA silencing in mRNP complexes [110, 111] and diversion of mRNAs to processing (P)-bodies, cellular centres of mRNA degradation [112]. P-bodies are not necessarily the end point of mRNAs, as P-body-associated transcripts can still return to translation [113]. In parasite mutants lacking DOZI, ookinete development is completely abolished. Although fertilization takes place and zygotes are formed, they all abort development before meiosis, which can be explained by the degradation of more than 370 transcripts including several essential for ookinete biology [107]. Among those are *p25*, *p28* (genes encoding for the two major ookinete surface molecules) and others previously shown to be translationally repressed [49].

In a subsequent study, the protein CITH (*C. elegans* CAR-1 and fly Trailer hitch Homologue) was shown to play a role in the silencing of *Plasmodium* maternal mRNAs [108]. CITH/CAR-1/Trailer hitch are Scd6 family members and contain an Lsm (like-Sm) domain and

an FDF amino acid motif. Lsm domains interact with each other [113] and both Lsm and FDF domains are required for the binding of these proteins to RNA [114]. The FDF motif of *S. cerevisiae* Edc3p is also known to bind to Dhh1p [115]. Scd6 proteins have also been shown to associate with mRNAs in mRNPs, which suggests that they function in the control of mRNA translation and/or degradation. Moreover, in *D. melanogaster* oocytes Trailer hitch co-localises with mRNP particles containing Me31B, while in *C. elegans* developing oocytes and embryos CAR-1 localizes to P-body-related granules containing CGH-1, indicating that Scd6 proteins may bind specific mRNAs and control their translation [113]. Indeed, mass-spectrometry analysis of *Plasmodium* female gametocyte P granules determined that these contain 16 core factors and that DOZI and CITH co-localise in these complexes (**Figure 3**). Among those 16 mRNP components other RNA binding proteins were found, such as HoBo (Homologue of *Drosophila* Bruno) and HoMu (Homologue of Musashi1) [108]. Musashi1 is known to contribute to the immature state and self-renewal activity of neuronal stem cells through TR by competing with eIF4G for binding to PABP [116]. Remarkably, PABP is also present in the *Plasmodium* female P granules, while eIF4G is absent [108]. Moreover, three (out of four) *P. berghei* Alba-domain proteins (acetylation lowers binding affinity) also take part in this mRNP; these are homologues of the archaeal protein Alba, a DNA/RNA-binding protein thought to maintain the stability of RNA and ribosomes, as well as to play a role in establishment or maintenance of chromatin architecture and thereby in transcription repression [117-120]. While some of the identified factors are known RNA binding proteins, others have an obscure function in TR. Enolase and PGAM (phosphoglycerate mutase family member) are glycolytic enzymes but were also found in the repressor complex. However, it is well established that enolase can participate in other biological processes such as transcription and heat-shock, and also plays a part in the bacterial degradasome [121]. On the other hand, PGAM family members are known to participate in complexes responsible for repressing gene transcription [122].

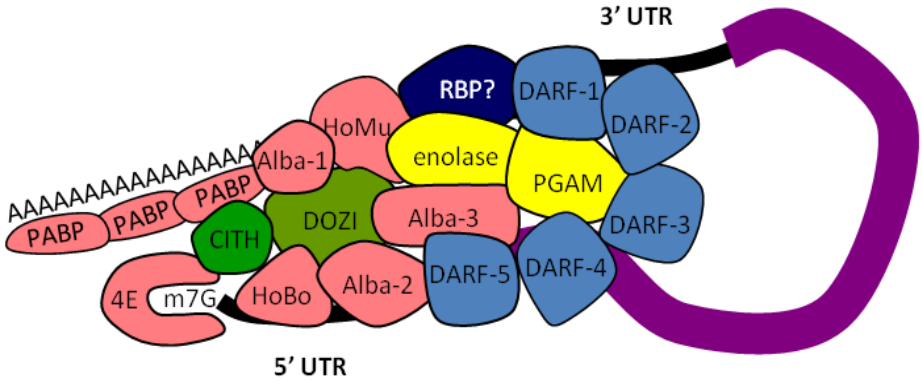

Figure 3 – Putative mRNP responsible for translational repression in *Plasmodium berghei* female gametocytes.
A pool of mRNAs (depicted by the purple string) interacts with the different components of the repressor complex via their 5' and/or 3' UTRs. Main constituents of the complex are depicted. DOZI: development of zygote inhibited; CITH: CAR-1/Trailer hitch homologue; HoBo: homologue of Bruno; HoMu: homologue of Musashi1; PABP: poly(A)-binding protein (possibly interacts with the poly(A) tail of mRNAs); 4E: eukaryotic translation initiation factor 4E (eIF4E); PGAM: phosphoglycerate mutase family member; DARF: unidentified DOZI-associated repressor factors; RBP: other unidentified RNA binding proteins. [Image credits: Gunnar R. Mair, unpublished]

The depletion of CITH resulted in the downregulation of 183 transcripts in female gametocytes. This is substantially less (49%) than the number of downregulated mRNAs in Δ*dozi* parasites (370). However, of these, 117 are common between the two lines. This is a remarkable overlap and clearly indicates that DOZI and CITH assist each other in the stabilisation of large numbers of mRNAs but do not have redundant functions as one cannot compensate for the other. Nonetheless, there is a considerable pool of mRNAs that are only affected by the absence of either DOZI (253/370, 68%) or CITH (66/183, 36%). This observation suggests that there may be different mRNP complexes within the parasite cytoplasm, possibly with distinct functions, and containing different subsets of mRNAs that depend on DOZI, CITH or both proteins for their stabilisation. Independent results indicate that there may be multiple compositional and functional classes of CGH-1- and CAR-1-containing P-body-like granules in *C. elegans* [113].

The phenotype of Δ*cith* parasites is very similar with that of those lacking DOZI. Both result in complete abortion of ZOT. However, the absence of DOZI is more severe for parasite development as zygotes do not perform meiosis and remain diploid, while Δ*cith* parasites complete meiotic DNA replication and establish tetraploidy [108]. Interestingly, similar gene deletion phenotypes for DOZI and CITH homologues have also been reported in *C. elegans*, where depletion of CGH-1 or CAR-1 causes defects in cytokinesis and apoptosis [123]. These studies pinpointed TR as a central feature of sexual development and malaria transmission to the mosquito vector, probably acting upon several hundreds of mRNAs.

TR is believed to take place as well in *Plasmodium* sporozoites. In *P. berghei*, the absence of PbPuf2 results in transcriptional changes in the salivary gland sporozoite, which precedes visible morphological changes reminiscent of sporozoite to liver stage transformation, when the parasite is still present in the mosquito salivary glands. Upregulated genes in Δ*puf2* sporozoites are a signature of increased metabolic activity, while genes encoding for inner membrane complex (IMC) components and motility and invasion-related proteins (e.g., CelTOS, SPECT, SPECT2, TRSP, S6/TREP, P36p) are downregulated. Consequently, Δ*puf2* sporozoites are impaired in gliding motility and host cell traversal and invasion [124, 125]. Overall, the lack of Puf2 renders parasites incapable of remaining in the quiescent state characteristic of wild-type (WT) salivary gland sporozoites, which suggests that Puf2 is responsible for the TR of key factors in the transition from the sporozoite to early hepatic stages [124]. On the other hand, PbPuf1, originally referred to as UIS9 (upregulated in infectious sporozoites 9) [126], was shown to have a redundant function throughout the parasite's life cycle [124, 125]. Very similar observations were made in the rodent malaria parasite *P. yoelii*. One interesting result from this study is that *dozi* was upregulated in Δ*pypuf2* sporozoites, pinpointing for the first time a potential role for DOZI in the sporozoite, possibly related with the function of Puf2 [127].

The function assigned for *P. falciparum* Puf2 is however quite different. PfPuf2 is expressed in both male and female gametocytes and regulates sexual development and sex

differentiation; its deletion promoted gametocytogenesis and differentiation of microgametocytes [128]. In agreement with these results, *pfpuf2* mRNA but also the corresponding protein had previously been shown to be upregulated in *P. falciparum* gametocytes [129]. Despite of acting in a very distinct phase of the life cycle when compared to PbPuf2 and PyPuf2, the data obtained for PfPuf2 confirm that *Plasmodium* Pumilio 2 proteins exert the conserved function of suppressing differentiation. PfPuf1 and 2 were first characterised in 2002 [130] and both of them interact with the NREs in the *hunchback* mRNA of *D. melanogaster* [129, 130], confirming their evolutionarily conserved function as RNA binding proteins and likely translational repressors. Regardless of the many studies done on the characterization of *Plasmodium* Puf2, no direct evidence to date implicates Puf2 as a *bona fide* translational repressor.

Another protein known to be a determinant for sporozoite latency is the eukaryotic translation initiation factor 2α (eIF2α) kinase (IK2), initially termed UIS1 [126]. This kinase phosphorylates eIF2α and leads to general inhibition of protein synthesis and accumulation of stalled mRNAs into granules. eIF2α is dephosphorylated upon hepatocyte invasion and TR is alleviated. As in Δ*puf2* parasites, Δ*ik2* sporozoites suffer premature metamorphosis into EEFs in the mosquito and loose infectivity although not as significantly as in the absence of Puf2 [131]. How Puf2 and IK2 coordinate translation inhibition and developmental arrest is not known, neither is it clear whether the role of Puf2 is mediated through eIF2α. It is although worth noting that Δ*puf2* sporozoites do downregulate *ik2* [124, 125].

Interestingly, the consequence of interfering with TR in *Plasmodium* gametocytes and sporozoites is quite different. While in the case of gametocytes, absence of DOZI and CITH leads to the loss of otherwise quiescent mRNAs and complete abolishment of ZOT [107, 108], the lack of Puf2 in sporozoites leads to premature developmental progression [124], likely by alleviating Puf2-dependent TR of factors necessary for sporozoite transformation into EEFs. It was hypothesised that mistimed translation of otherwise repressed transcripts encoding these factors takes place, instead of the mRNA loss happening in gametocytes.

TR was shown to depend on uridine-rich regions present on either 5' or 3' UTRs of certain genes [49, 132]. These are for instance present in the 5' UTR of *p25* and in the 3' UTR of *p28* and are sufficient to target transgenes for TR specifically in female gametocytes [132]. More recently, TR of at least part of the *uis4* mRNA pool in salivary gland sporozoites was demonstrated to depend on its open reading frame (ORF), whereas the 5′ and 3′ UTRs are dispensable for its silencing [133]. Whether *uis4* is maintained in a quiescent state until after invasion of hepatocytes through the interaction with Puf2 remains to be elucidated but it is interesting to note that several *uis* genes were downregulated in Δ*pypuf2* sporozoites [127]. *uis4* was however not differentially regulated in Δ*pbpuf2* parasites [125] but UIS4 protein was upregulated in Δ*pbik2* salivary gland sporozoites [131].

How silenced *Plasmodium* mRNAs are activated for translation is not fully understood, but it has recently been shown to depend on the parasite calcium-dependent protein kinase 1 (CDPK1) during parasite sexual development [134]. For instance, translational activation of

certain transcripts in *Xenopus* oocytes involves phosphorylation of the RNA binding protein CPEB (cytoplasmic polyadenylation element binding protein) [135]. It is possible that CDPK1 regulates translational activation by phosphorylating a component of the repressor complex.

IV.3 – TRANSLATIONAL REPRESSION AND MALARIA TRANSMISSION BLOCKING VACCINES

In *Plasmodium*, the hallmarks of translationally repressed genes are *p25* and *p28*. These genes are involved in ookinete survival in the mosquito midgut, penetration of midgut epithelium and development into oocysts [136, 137]. Some insight has been made in the putative interaction of P25 and P28 with the mosquito midgut. Pvs25 (P25 orthologue in *Plasmodium vivax*) has been shown to interact *in vitro* with *Anopheles albimanus* calreticulin, a molecule expressed in midgut microvilli [138], while Pb25 binds to laminin γ1 in the midgut basal lamina of *A. gambiae* [139] but also to collagen IV [140]. On the other hand, anti-annexin antibodies inhibit *P. berghei* oocyst development in mosquitoes and confocal microscopy analysis of infected midguts showed a co-localisation of Pb28 with annexin, suggesting that P28 binds to *Anopheles* annexin [141].

Because of their function and even and abundant distribution over the entire ookinete surface [142], P25 and P28 have been the leading target candidates for malaria transmission blocking vaccines (MTBVs). MTBVs rely on the presence of antibodies against *Plasmodium* antigens that, when taken up by a female mosquito during a blood meal, bind to the developing parasite preventing infection of the vector and subsequent transmission of the parasite to naïve human hosts [143]. The target molecules of a MTBV, unlike other malaria vaccines, are proteins expressed in sexual and ookinete stages of the parasite. Some of these are transcribed but not translated during mammalian host-associated life cycle stages [144]. Consequently, these proteins are not under immune selection and may represent good TB antigens [144, 145]. Therefore, MTBVs are promising agents of malaria control, especially when used in conjunction with other intervention strategies [143]. Indeed, the presence of anti-P25 and anti-P28 antibodies during a blood meal clearly reduces mosquito infection [144, 146-151]. So far, only Pfs25- and Pvs25-based TB strategies have gone through phase 1 clinical trials. Different immunisation schedules, doses and adjuvants have been tested but local and systemic mild to adverse effects and suboptimal TB effects have been reported [143, 152, 153]. Nonetheless, mathematical modelling suggests that current formulations of Pfs25 are likely to achieve useful malaria transmission reduction in the field [154]. Other theoretical studies have predicted that TB interventions could significantly impact the number of malarial cases in the field under a variety of transmission rates and even if at low intervention efficacy and coverage [155, 156]. Notably, malaria elimination could be successfully achieved in laboratory populations of mice and *Anopheles stephensi* over three transmission cycles conditions using a mildly effective TB drug under low bite rates [48].

The MTBV concept started almost 40 years ago when Robert Gwadz and Richard Carter showed that immunising chickens with *P. gallinaceum* gametocytes generated antibodies that killed the parasite not when still circulating in the blood, but after it had egressed from the RBC in the mosquito blood meal [157, 158]. MTBVs are an unusual vaccine type and are often called 'altruistic' vaccines, as they cannot affect the course of infection in a vaccinated individual. Instead, they would benefit others by means of reducing parasite transmission rates. In the perspective of national health programmes this should however not induce ethical rejection as protection of communities as wholes is intended [159]. Nevertheless, a number of challenges are posed to the development and application of such vaccines. For example, natural boosting for antigens that are never expressed in human hosts will not occur and so a MTBV would have to generate long lasting antibody titres. A considerable population-wide vaccination effort would also have to be undertaken to guarantee that an effective fraction of gametocyte carrier individuals generate TB immunity [160]. This means that the impact of MTBVs is exclusively based on herd immunity. But reducing malaria transmission in particular endemicity scenarios could also be dangerous. By interfering with the acquisition of natural immunity, the number of life threatening disease cases may increase [161].

MTBV target antigen research has focused on few surface and soluble molecules belonging to two groups: pre-fertilisation antigens, expressed in gametocytes and gametes, or post-fertilisation antigens, expressed in zygotes and ookinetes [142, 145]. Pre-fertilisation antigens include P48/45 [162-166] and P230 [167-170], while P25 and P28 (see above), CHT1 (chitinase) [171-173], CTRP [172] and WARP [172, 174] are post-fertilisation antigens. However, several more proteins (e.g., SOAP, MAOP, PbSub2, LAPs, CelTOS, PPLPs and PSOPs) have been shown to contribute for mosquito infection using gene knock-out (KO) parasites [142, 160, 175, 176]. Different production methods, adjuvants and immunisation routes have been tested for the several MTBV candidates mentioned above. Antigens have been produced using insect and mammalian viruses [165, 177-181], bacteria [162, 164, 174, 182, 183], yeast (either *Saccharomyces* or *Pichia* [146, 148, 151, 153, 166, 184-186], algae [187-189], as well as plant virus-based [190, 191] and wheat germ cell-free expression systems [169]. More recently, DNA-based vaccination strategies have also been developed [147, 192-195]. Most of these studies used intramuscular immunisation route, while others have tested intranasal [178, 196-198], intradermal [193], subcutaneous [198] and oral [189] administrations, but also skin/muscle electroporation [192, 193, 195]. Besides the common aluminium-based [184, 199, 200] and water-in-oil Montanide emulsion [149, 150, 152, 199] adjuvants, several studies have assayed Alhydrogel [150, 153, 201] and bacterial proteins/toxins [189, 197, 198, 200-203].

Some of the above mentioned malaria TB targets are ookinete micronemal proteins: circumsporozoite- and TRAP-related protein (CTRP), chitinase (CHT1) and von Willebrand factor A domain-related protein (WARP) [172]. Micronemes are secretory organelles of the malaria invasive stages (merozoites, ookinetes and sporozoites) that are necessary for parasite

motility (in the case of ookinetes and sporozoites) and host cell invasion [204]. Interestingly, *warp* is downregulated in the absence of DOZI or CITH, suggesting it is also translationally repressed [107, 108], and the protein is only detectable several hours after gametocyte activation [205]. Transcription of these genes but also of *soap* (secreted ookinete adhesive protein) was shown to be regulated by AP2-O, while storage of *ap2-o* mRNA in female gametocytes is itself dependent on DOZI [107]. Independently on whether DOZI and CITH act directly to repress micronemal genes or control their expression by regulating AP2-O, it is evident that TR is paramount for the timely production of parasite molecules that otherwise could raise TB antibodies with deleterious consequences for *Plasmodium* infection of the mosquito.

V – MALARIA CRYSTALLOID BODIES

mRNAs that rely on the translational repressors DOZI and CITH for stability in *P. berghei* female gametocytes (and are thus putative or known translationally repressed gene products) include (among others) those encoding for surface coat antigens (P25, P28), transcription factors (AP2-O), micronemal proteins (WARP) and proteins linked to ookinete motility and invasion such as IMC proteins (IMC1b), alveolins and proteins of the gliding motility molecular motor (MyoA, GAP45, MTIP). The list is extensive and comprises as well three transcripts that encode for members of the LCCL protein family (also known as LAP family in *P. berghei* [206] and CCp family in *P. falciparum* [207]) [107, 108]. These are *pblap4*, *pblap5*, and *pblap6* and indeed these genes have been shown to be translationally repressed as corresponding proteins were detected in mature ookinetes but not in gametocytes [208]. LCCL proteins are modular proteins with multiple adhesive-type domains implicated in the binding of proteins, lipids and carbohydrates [209, 210]. This family comprises six proteins and all with no exception have been found to localise to the ookinete crystalloid bodies (CBs) [208, 211, 212].

The CB is an enigmatic organelle. It is a short-lived, cytoplasmic, subunit-based inclusion easily visualised under live differential interference contrast (DIC) microscopy that assembles during ookinete development and dissociates in the growing oocyst [210]. The malaria CB is formed by electron-dense, 25 to 42 nm-wide particles arranged in a tight honeycomb pattern [210, 213] and whether it possess or not a surrounding membrane is still a matter of debate [210]. CBs vary in size between 0.5 µm and 2.0 µm [214] and represent a conserved feature of *Plasmodium* species [210]. In *P. berghei*, haemozoin-containing vacuoles, remnants of the blood stage food vacuole where haemoglobin is digested, accumulate around the edges of the crystalloid inclusion bodies [215, 216]. CBs are sometimes found in association with smooth endoplasmic reticulum and Golgi-like vesicles [215-218]. This can indicate that crystalloids have their origin on these subcellular compartments. The CB persists until the early stages of oocyst maturation [210]. While in the ookinete crystalloids are highly organized, in the oocyst CB particles are more randomly assembled and can be found dispersed in the parasite cytoplasm. As the oocyst matures, CBs disassemble and subunit-like particles are observed at the edges of *P. berghei*, *P. gallinaceum* and *P. cynomolgi* older oocysts [219, 220].

The geometrical arrangement of CB particles in electron microscopy samples (hence the name ‘crystalloid’) led some researchers to postulate that the CB was the result of a viral infection taking place within the mosquito midgut, thus explaining its transient nature [221, 222]. However, the fact that CBs can also be observed when ookinetes are cultured *in vitro* posed a problem to this theory [213], and the definitive proof that CBs are not of viral origin came with the report of the first parasite protein, LAP1 or PbSR (another member of the LCCL family), with essential role in CB biogenesis [211].

The exact function of the CB is still elusive. CBs are believed to function as temporal storage compartments, acting as an atypical trafficking route for (lipo)proteins from the female gametocyte to the oocyst that will be necessary for oocyst maturation and sporozoite

development [210, 215, 223]. However, the CB proteome is poorly determined, and includes only the six members of the LAP protein family [208, 211, 212]. Nonetheless, all *P. berghei* LAP proteins studied to date by reverse genetics (LAP1 or PbSR, LAP2 and LAP4-6) revealed a crucial role during sporogony in mosquitoes [176, 211, 224-226], although under certain *in vitro* culture conditions PbSR KO oocyst sporulation rates are comparable to that of WT parasites [211]. On the contrary, deletion of *P. falciparum* CCp2 (ortholog of PbLAP4) and CCp3 (ortholog of PbSR) did not affect oocyst sporulation. Rather, KO sporozoites were not able to invade the mosquito salivary glands [207]. Despite these discrepancies, it seems clear that LCCL proteins have key roles in the development of infective sporozoites, having the oocyst as their likely site of action [210].

As mentioned above, the formation of the ookinete relies on numerous translationally repressed mRNAs provided by the female gametocyte; they are translated following fertilisation and are crucial for morphogenesis [107, 108, 134]. Among the set of repressed mRNAs are also such that are translated but redundant for ookinete formation, invasion of the midgut epithelium or establishment of the oocyst. This is the case, for example, of *pblap4-6* [208]. The remaining members of the LAP family (PbSR [211] and PbLAP2-3 [212]) are not targets of TR and protein can be found throughout the macrogametocyte cytoplasm that is later on redirected to the CB upon ookinete development.

VI – PROTEIN PALMITOYLATION IN *PLASMODIUM* AND RELATED APICOMPLEXA

In the list of downregulated genes in Δ*dozi* parasites one can find three encoding for palmitoyl-S-acyl-transferases belonging to the DHHC family (DHHC2, DHHC3 and DHHC10), suggesting an involvement of protein palmitoylation in the development of the parasite within the mosquito vector. While the essential nature of this post-translational modification (PTM) has recently been determined for *P. falciparum* blood stages [227], its role in malaria life cycle progression in the mosquito remains completely unexplored.

The morphological changes during ZOT and the formation of thousands of individual sporozoites from a single oocyst requires extensive protein translation and trafficking as well as membrane biogenesis to support the generation of organelles and plasma membrane (PM) surrounding each new parasite. A large proportion (36%) of proteins found in the oocyst and oocyst-derived sporozoites (midgut sporozoites) of *P. falciparum* are putatively membrane-bound, based on the presence of a signal peptide (SP) and transmembrane (TM) domains [51]. Out of 482 proteins detected in both these parasite life cycle stages, 96 have a SP and 139 have at least one TM domain; 63 contain both SP and TM domains (PlasmoDB version 11.1). Correct permanent targeting of such proteins into the membrane of newly formed organelles requires the presence of TM domains, while temporary membrane association can also be achieved through PTMs such as prenylation, glypiation, cholesteroylation and fatty acid acylation [228, 229]. These PTMs are collectively known as lipidation and increase the affinity of a modified protein to membranes.

Fatty acid acylation is the addition of fatty acids to specific amino acids. Two processes of fatty acid acylation can be distinguished, myristoylation and palmitoylation; the latter is the reversible addition of long chain (16-carbon) saturated fatty acids to cysteine residues via a thioester bond or less frequently to N-terminal amino acids via amide bonds [229]. The most common added lipid moiety in palmitoylation reactions is palmitic acid (also known as palmitate or hexadecanoic acid), although stearic acid can also be used [230]. This PTM is also responsible for changing the subcellular localization of its protein targets [231, 232]. Being the sole known reversible lipidation PTM, palmitoylation enables a dynamic regulation of protein localisation and stability, influencing protein interactions and function, as well as gene expression [227, 229, 230, 233]. For example, reversible palmitoylation/depalmitoylation was shown to fine tune host cell invasion by the apicomplexan parasite *Toxoplasma gondii* [234].

Palmitoylation is catalysed by TM-spanning enzymes called palmitoyl-S-acyl-transferases (PATs) but rare events of spontaneous palmitoylation are also reported [229]. PATs are divided into two families: DHHC and MBOAT. DHHC-PATs are characterised by a highly conserved inter-TM cysteine-rich domain (CRD) domain comprehending the Asp-His-His-Cys (DHHC) motif, normally facing the cytosol, and are responsible for the palmitoylation of intracellular proteins, while membrane-bound *O*-acyl-transferases (MBOAT-PATs) modify secreted proteins and are mostly involved in the N-terminal-linked palmitoylation. Both families share an even number of TM domains, ranging from four to six in the case of DHHC-PATs [227,

229, 230]. DHHC-PAT-driven palmitoylation is highly conserved throughout evolution with 25 human and 7 *Saccharomyces cerevisiae* factors known; 12 are described in *P. falciparum* and 18 in *T. gondii* [227, 233]. Regardless of the organism in question, DHHC-PATs are essential for key biological processes. For example, *Saccharomyces cerevisiae* Pfa3 is responsible for the palmitoylation of the armadillo repeat protein Vac8. This event leads to Vac8 recruitment to the yeast vacuole, facilitating vacuolar fusion [235, 236]. In *T. gondii*, the activity of TgDHHC7 (homologue of yeast Pfa3), which localises to rhoptries, is necessary for invasion but not egress from host cells [233, 237], and tachyzoites treated with 2-bromopalmitate (2-BMP), an irreversible inhibitor of PATs [238, 239], show altered motility, invasion, replication and morphology [240].

The global extent of palmitoylation in asexual blood stages of *P. falciparum* comprises several hundred proteins; they include factors involved in gliding motility, invasion, adhesion, IMC function, signalling (kinases) and proteolytic activity (rhomboid proteases), but also chaperones, proteins targeted to the surface of an iRBC, transporters and factors within the secretory pathway [227]. Treatment of *P. falciparum in vitro* cultures with the PAT inhibitor 2-BMP causes schizont developmental defects and subsequent inhibition of RBC invasion by newly released merozoites through the destabilisation of the gliding motor components GAP45 and MTIP [227].

VII – MOTILITY AND INVASION OF MALARIA PARASITES

While proteins involved in invasion by the merozoite and sporozoite (and in gliding by the sporozoite as well) are believed to be transcribed and translated when needed, continuous studies highlight mRNAs encoding known motility and invasion proteins of the ookinete to be stored and translationally repressed in the female gametocytes by the RNA binding proteins DOZI and CITH. These include gliding molecular motor proteins such as MyoA and MTIP but possibly also alveolins and microneme proteins [107, 108]. Translational activation of these transcripts takes place during ookinete development and is dependent on the protein kinase CDPK1 [134].

Plasmodium parasites rely on gliding motility for migration through, and invasion of diverse host cells in two fundamentally different host species [204]. Ookinetes and sporozoites, the migrating forms of the malaria parasite, are morphologically distinct but share essential components of the gliding motility apparatus (**Figure 4**). Briefly, this machinery is composed of an actin-myosin motor (or glideosome) consisting of Myosin A (MyoA) molecules bound to actin filaments. MyoA is secured via association with a light chain called MyoA tail domain interacting protein (MTIP) to the glideosome-associated proteins (GAP) 45 and 50. GAP45 and GAP50 in their turn link the molecular motor to the IMC, while alveolins are the bridges that connect the IMC to the underlying cytoskeleton subpellicular microtubules. Towards the surface of the parasite, the glideosome is connected to surface adhesins on the PM that allow interaction with the substrate. For example, the membrane-spanning protein

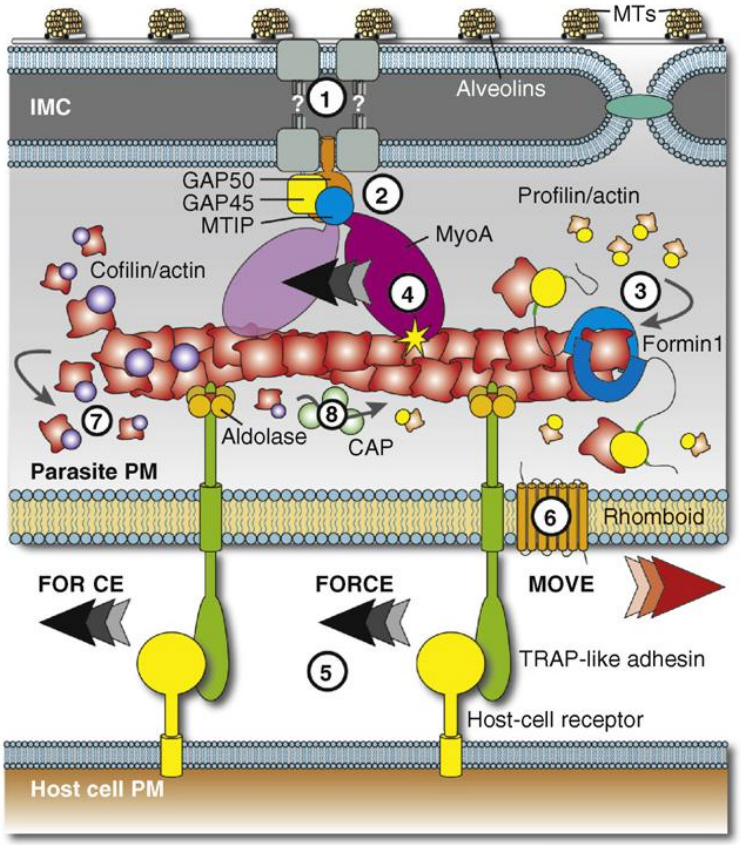

Figure 4 – Model for the *Plasmodium* gliding motility apparatus. (1) A direct link between the motor complex and the cytoskeleton may exist. (2) MyoA is stabilized by MTIP and interacts with GAP45 and GAP50. (3) Formin1 and profilin initiate actin polymerization. (4) MyoA drives ATP-dependent directed force through F-actin. (5) TRAP adhesin moves rear-wards through the parasite PM and its attachment to the host cell surface propels the parasite forwards. (6) Adhesin disentangle involves the shedding activity of , for example, rhomboid proteases. (7-8) Depolymerisation of F-actin is likely to occur via cofilin and cyclase-associated protein (CAP). MTs: subpellicular microtubules; IMC: inner membrane complex; PM: plasma membrane. [Adapted from Baum et al., *Trends Parasitol* 2008, 24(12): 557-63]

TRAP (thrombospondin-related anonymous protein) is connected to the actin filaments via aldolase [204]. Controversially, a recent study using *T. gondii* aldolase (TgALD) KO parasites as well as mutants that disrupt its binding to adhesins showed that this enzyme is not necessary for motility or invasion [241]. In both ookinetes [242] and sporozoites [243] the IMC is a single inner vacuole below the PM, sealed by a prominent suture running obliquely to the longitudinal axis of the cell. Due to its flattened morphology, this structure is normally seen in electron microscopy studies as two apposed phospholipid membranes below the PM [204]. Uniquely among all other apicomplexan motile stages, the IMC of *Plasmodium* ookinetes presents large pores scattered throughout the cell that are thought to constitute an alternative pathway for the transport of molecules between the cortical and inner cytoplasmic compartments, namely surface and motor proteins [242].

Gliding motility is a unique type of locomotion used by apicomplexan parasites [244] (and also by some free living protists such as raphid diatoms and the green alga *Chlamydomonas* [245]) to migrate through cells and tissues and is characterised by the absence of any cell shape modification. It was long believed to be the driving force for host cell invasion [246] that, in contrast to most intracellular pathogens, does not depend on active uptake of the parasite by endocytosis or phagocytosis [247, 248]. Reverse genetics studies targeting components of the gliding machinery have however revealed that invasion is still possible when parasites have lost their ability to move or breach host cells, uncoupling these two fundamental cellular processes [249].

The invasive stages of *Plasmodium* parasites contain secretory vesicles that discharge their contents during gliding motility and host cell invasion. For example, micronemes and rhoptries assist each other in providing invasion-related proteins, such as adhesins and proteases, but at the same time rhoptries, together with dense granules, are primary contributors to the formation of the parasitophorous vacuole (PV) that surrounds the intracellular parasite stages. While micronemes and rhoptries deliver their contents during parasite motility and invasion, proteins contained within dense granules are released after the invasion process is concluded to remodel the host cell environment. It is worth noting that while sporozoites (as well as merozoites, the red blood cell invasive stage) bear all three types of organelles, ookinetes only harbour micronemes [204]. The lack of rhoptries and dense granules in ookinetes is biologically meaningful as ookinete-derived oocysts do not develop inside cells and thus do not need to form a PV upon midgut invasion [250]. Interestingly, sporozoites do not always develop a PV when penetrating host cells. For instance, during invasion of the mosquito salivary glands, the sporozoite is initially surrounded by a second membrane [251] but this is subsequently disintegrated by an unknown mechanism, allowing the sporozoite to exit the cell into the secretory cavities of the salivary gland [252]. Although the nature of this membrane is unclear, it has been postulated to be a transient PVM [253]. When at the liver, the sporozoite also traverses a few cells without the need of a PV until it finally invades a hepatocyte with concomitant establishment of a PV inside of which the parasite develops and multiplies [37, 38].

Another organelle of sporozoites and merozoites but not ookinetes are the exonemes, which release proteases into the PV prior to microneme secretion and initiate parasite egress from host cells [204].

During gliding and invasion, many proteins are secreted from micronemes through the parasite apical pore. For instance, micronemal secretion in *Toxoplasma* is upregulated when parasites make contact with host cells [254]. While some of these proteins are discharged into the extracellular milieu — for example SOAP [255] and WARP [172, 205] — others are inserted into the PM where they engage host receptors [256]. Translocated backwards along the cell surface during gliding these TM proteins are shed by rhomboid and subtilisin-like serine proteases [204, 257, 258] and deposited along the parasite gliding trails, as are the cases of TRAP and CelTOS [175, 259, 260].

The apical to rear redistribution of parasite surface molecules led researchers to propose a capping model of gliding and invasion by apicomplexans. In this model, parasite ligands would bind the substrate at the anterior pole of the zoite and be transported to the posterior pole, while propelling the cell body forward [261, 262]. The first *Plasmodium* protein shown to be subjected to this process was the circumsporozoite protein (CSP) [263], being released onto the substrate along the gliding trails of the parasite [264]. This is a feature that is used in assays to measure the gliding motility of *Plasmodium* sporozoites.

Micronemal proteins of the ookinete include CTRP, WARP, SOAP, CHT1 and MAOP; in the sporozoite they are AMA1, TRAP, MAEBL, SPECT, SPECT2 and P52; only CelTOS is present in both [204, 265]. If and how these factors interact with each other and with host receptors to coordinate efficient gliding motility and invasion is largely unknown. It is also very likely that additional proteins are required in these complex cellular processes. The individual functions of micronemal proteins have however been the subject of many studies and found to affect parasite motility, host cell traversal and invasion as well as transmission to and from the mosquito vector.

Disruption of *cht1* reduces ookinete infectivity to mosquitoes [266, 267]. On the other hand, deletion of *warp* did not result in obvious phenotypic difference from WT parasites [176]. However, antisera produced against PfWARP, PgCTRP and PgCHT1 significantly reduced the infectivity of *P. gallinaceum* to *Aedes aegypti* and *P. falciparum* to *Anopheles* mosquitoes [172]. This study showed that ookinete micronemal proteins are good malaria TB targets.

AMA1 (apical membrane antigen 1) is expressed in both merozoites and sporozoites [204]. Although anti-AMA1 antibodies were shown to inhibit hepatocyte invasion by sporozoites *in vitro* [268], disruption and conditional deletion studies of *ama1* indicate that it has no role in *P. berghei* sporozoite infectivity to liver cells as mutants showed normal hepatocyte traversal and invasion and develop normally into EEFs, both *in vitro* and i*n vivo* [269, 270]. AMA1 was however shown to play a major role in the attachment of erythrocytic and hepatic merozoites to RBCs, resulting in highly reduced RBC entry rates in one of the studies [270] and complete lack

of blood stage infection in the other [269]. This phenotype was similarly observed in *P. falciparum*, where the conditional KO of *Pfama1* affected erythrocyte invasion by merozoites and reduced parasite blood stage growth by 40% [271].

CTRP is required for normal ookinete motility [272-274] while MAOP (membrane-attack ookinete protein) is essential for midgut epithelial cell entry [275]. SOAP (secreted ookinete adhesive protein) has also been implicated in midgut invasion by ookinetes as well as differentiation into oocysts [255]. MAEBL (merozoite adhesive erythrocytic binding-like protein) is predominantly expressed in midgut sporozoites and is vital for attachment to and invasion of mosquito salivary glands but does not participate in sporozoite motility or infectivity to the vertebrate host [276, 277]. SPECT [278] (sporozoite microneme protein essential for cell traversal) and SPECT2 [279] are salivary gland sporozoite-specific proteins specifically involved in cell traversal ability that do not participate in gliding or invasion. P52 (also known as P36p) and its P36 counterpart are members of the *Plasmodium* 6-cysteine domain-containing protein family [280]. Similarly to SPECT proteins they are also exclusively expressed in salivary gland sporozoites and have been specifically implicated in hepatocyte invasion, more precisely in commitment to hepatocyte infection. Without shifting from a cell migrating to a hepatocyte invasive status, *P. berghei* disruptants for these genes showed increased cell traversal activity, both *in vitro* and *in vivo*. Whereas P52 is present in micronemes and translocated to the parasite surface upon gliding, the subcellular localisation of P36 could not be determined [265]. Curiously, another study using independently-generated Δ*p52 P. berghei* parasites describes a role for P52 in parasite development within the hepatocyte but not in hepatocyte invasion. Hepatocyte traversal was also not affected by the absence of P52 in this study [281]. Contradictory results were also found for P36, where another *P. berghei* line lacking expression of this protein showed no differences comparing to WT parasites throughout the entire life cycle [282]. In agreement with these ulterior studies on P36 and P52, *P. berghei* double KO parasites for P36 and P52 only showed a developmental defect within hepatocytes [283] but deletion of both these molecules in *P. yoelii* resulted in a 50% reduction in hepatocyte invasion apart from the expected developmental impairment [284]. The reasons for these discrepancies remain to be elucidated but it is likely that at least P52 plays a role in both invasion of host hepatocytes and intracellular development [38]. TRAP is expressed in both midgut and salivary gland sporozoites and is known to influence sporozoite gliding as well as invasion of both salivary glands and hepatocytes *in vitro*. Disruption and loss-of-function mutations of TRAP resulted in decreased levels of transmissibility to naïve hosts, and in some cases transmission was completely abolished [259, 260, 285-287]. CelTOS (cell-traversal protein for ookinetes and sporozoites) is shared between the ookinete and sporozoite stages and was shown to play a major role in midgut epithelium and liver sinusoidal cell traversal [175].

Proteins other than those secreted by micronemes have also been implicated in parasite motility and host cell invasion events, both in the mosquito vector and vertebrate host. Examples include, for instance, S6/TREP [288, 289] and TLP [290-292], two sporozoite TRAP

family members with predicted surface localisation. S6 (sporozoite-specific gene 6) or TREP (TRAP-related protein) is mostly detected in salivary gland sporozoites and, as MAEBL, plays a major role in salivary gland invasion, but also in gliding motility. The absence of S6/TREP also decreases the capacity of parasites to invade hepatoma cells *in vitro* while leaving cell adhesion unaltered. Transmission to naïve rodents is however still achievable [288, 289]. On the other hand, the role of TLP (TRAP-like protein) is not completely clear. While some authors have shown that disruption of *tlp* decreases the cell traversal and *in vivo* infectivity capacities of sporozoites and does not alter *in vitro* sporozoite motility or hepatocyte invasion [290], others claim that this protein is only implicated in gliding motility on glass surfaces and is redundant throughout the parasite life cycle [291]. A follow-up review on this subject suggests that most likely TLP is important for sporozoite infectivity when these are injected into the skin but mildly relevant when these are injected directly into the blood [292], an interpretation that links the gliding and traversal phenotypes.

TRSP (thrombospondin-related sporozoite protein) is also structurally related to TRAP and has been first found in *P. yoelii* midgut and salivary gland sporozoites. Immunofluorescence assays showed a distinct subcellular staining pattern regarding CSP and TRAP proteins and was suggested to indicate rhoptry localisation [293]. A follow-up work on *P. berghei* has shown that TRSP has no effect on sporozoite gliding motility but has a significant role in hepatocyte entry, both *in vitro* and *in vivo* [294].

On the other hand, members of the *Plasmodium* cysteine repeat modular protein (PCRMP) family are involved in salivary gland invasion. PCRMP1 and 2 are expressed in merozoites and PCRMP2 was also shown to localize at the surface of hemolymph and salivary gland sporozoites. Both these proteins are key players in sporozoite targeting into the mosquito salivary glands, as gene deletion parasites are rarely found in these organs [295].

RON4 (rhoptry neck protein 4), a rhoptry-resident protein that, together with other proteins, namely the micronemal AMA1, compose the tight junction (TJ) of invading *T. gondii* [296, 297] and *P. falciparum* [298] parasites was shown to play an important and likely essential role in hepatocyte invasion by *P. berghei* sporozoites [269]. The TJ is an electron-dense ring-like structure formed by the plasma membranes of both parasite and host cell that connects the parasite motor to the host cell actin, and through which the motile zoite glides into a PV [204, 299].

Finally, conflicting results were obtained for another the *Plasmodium* inhibitor of cysteine proteases (ICP). In *P. yoelii*, it was observed in sporozoite rhoptries and dispersed throughout the cytoplasm, but shown to be essential for asexual blood stage replication [300]. On the other hand, the *P. berghei* ortholog did not shown any growth defect in the blood but severely impairs sporozoite motility and completely blocks mosquito salivary gland and hepatocyte invasion, leading to transmission blockade to naïve hosts. Interestingly, the lack of PbICP led to increased CSP proteolytic processing in oocyst-derived but not in hemolymph sporozoites, which might be responsible for the salivary gland invasion defect [301].

The invasion of both mosquito salivary glands and vertebrate liver is thought to be mediated by specific molecular interactions, and both CSP and TRAP have long been implicated in binding to these organs [302]. Although not secreted through any of the secretory organelles present in sporozoites, competition experiments using recombinant CSP as well as CSP peptides have shown that these can bind to the mosquito salivary glands and consequently inhibit invasion of these organs by the sporozoite [303, 304]. The demonstration that CSP binds to mosquito heparan sulphate suggests that this could play a role in targeting sporozoites to the mosquito salivary glands [305]. Similarly, peptide competition assays, genetic mutations in TRAP and down-regulation of saglin suggest that TRAP directly interacts with saglin on the surface of the salivary gland, thus allowing for efficient invasion of this organ [306]. In the liver, heparan sulphate proteoglycans (HSPGs) on the surface of different resident cells (hepatocytes, Kupffer cells and stellate cells) but also on the extracellular matrix have been proposed to be the main receptors for sporozoites. While present in most tissues, the sulphation levels of HSPGs in liver cells are particularly high, possibly explaining how sporozoites successfully target this organ. Here as well, both CSP and TRAP seem to be key players in sporozoite sequestration by interacting with the organ's HSPGs [38, 307], but also with the glycoprotein fetuin-A on hepatocyte membranes in the case of TRAP [308]. TRAP recombinant protein and peptides were also shown to bind to human hepatoma Hep G2 cells [309-311].

AIMS OF THIS THESIS

In the present thesis we aimed at characterising the roles of novel *P. berghei* putative translationally repressed gene products during parasite transmission and development in the anopheline mosquito vector. We have restricted our candidate gene selection to those transcriptionally upregulated in gametocytes but downregulated in *Δdozi* and/or Δ*cith* parasites and absent from published blood stage proteomes. Such mRNAs are likely to be stored in a translationally quiescent form in female gametocytes in a DOZI- and CITH-dependent manner. From this list we have chosen those with orthologs in *P. falciparum* and *P. vivax* with the goal of providing insights into conserved mechanisms that *Plasmodium* species use for life cycle progression in the mosquito. A further selection criterion was the presence of few non-synonymous single nucleotide polymorphisms (SNPs) in different *P. falciparum* strains according to the *Plasmodium* genomics resource PlasmoDB (plasmodb.org). This feature may be an extra indication of translational repression (TR): genes under TR are not expressed as proteins while the parasite is in the mammalian host, and are therefore not exposed to the host's immune system; as a consequence there is no selective pressure on these genes to mutate. They are therefore attractive transmission blocking (TB) antibody targets. Indeed, translationally repressed genes that are also malaria transmission blocking vaccine (MTBV) candidates have been shown to bear few sequence polymorphisms [312-315]. Finally, we have chosen gene products with predicted surface targeting signals such as signal peptide and/or transmembrane domains as a suggestive signature of secreted or integral membrane proteins that could be developed as targets of TB strategies, namely by TB antibodies.

Specifically, we aimed to determine the mRNA expression profile of each selected gene and unequivocally demonstrate that these are indeed translationally repressed and present in translationally quiescent messenger ribonucleoproteins (mRNPs). For this purpose we performed reverse transcriptase-polymerase chain reactions (RT-PCRs) to detect the mRNAs of interest in different life cycle stages, as well as in DOZI and CITH immunoprecipitation (IP) eluates. Green fluorescent protein (GFP)-tagged lines were generated for each of the proteins to assess protein expression during the transition from the female gametocyte to the ookinete by live imaging and/or immunofluorescence assay. The same GFP reporter lines were also used to identify the expression patterns and subcellular locations of these proteins along the parasite life cycle.

The functional importance of these translationally repressed molecules during mosquito stage development was determined by generating gene deletion parasite lines that were phenotypically screened throughout the entire life cycle. More specifically, null mutants were analysed *in vitro* and *in vivo* for any defects at the ookinete, oocyst, sporozoite and liver stage levels. Experiments were performed to evaluate the consequence of gene deletion for parasite transmission to naïve hosts.

EPSF: A NOVEL CRYSTALLOID BODY PROTEIN WITH A CRITICAL ROLE FOR *PLASMODIUM* SPOROZOITE DEVELOPMENT

Jorge M. Santos[1], Neuza Duarte[1], Blandine Franke-Fayard[2], Chris J. Janse[2], Gunnar R. Mair[1]

[1] Instituto de Medicina Molecular, Faculdade de Medicina da Universidade de Lisboa, Edifício Egas Moniz, Av. Prof. Egas Moniz, 1649-028 Lisbon, Portugal

[2] Leiden Malaria Research Group, Department of Parasitology, Leiden University Medical Center, Albinusdreef 2, 2333 ZA Leiden, The Netherlands

AUTHOR CONTRIBUTIONS

JMS and GRM designed experiments. JMS performed multiple alignments, RT-PCRs on immunoprecipitation samples, generated gene deletion and GFP tagging plasmids, cloned mutant parasites, determined asexual multiplication rates and sporozoite numbers, executed transmission experiments, performed all imaging experiments, analysed all data sets, wrote the Abstract, Methods, Results and Discussion and generated all figures and tables. JMS, BF-F and CJJ performed parasite transfections. JMS and ND performed RT-PCRs across the parasite life cycle, genotyped mutant parasites, determined oocyst numbers and sizes and performed oocyst Western blots. GRM supervised the work and revised the text.

ABSTRACT

Malaria parasites transit from a vertebrate host and an invertebrate vector. *Plasmodium* ookinetes, the true mosquito-infective parasite forms, assemble an enigmatic organelle called crystalloid body (CB) that persists until the early, now sessile oocyst stage that develops below the midgut epithelium. While the exact function of this organelle is not understood, it is known that sporozoite formation requires proteins contained within and provided by the ookinete CB. At present, only the six members of the LCCL protein family are known to be targeted to CBs and the absence of any of these proteins invariably results in lack of oocyst sporulation. Here we describe a novel CB component from the rodent malaria parasite *Plasmodium berghei* which we call EPSF (Essential Protein for Sporozoite Formation) with a vital role for oocyst sporulation and progression of the parasite life cycle in the mosquito. *epsf* is transcribed in the female gametocyte, but kept translationally repressed until translated during ookinete formation. Δe*psf* mutants establish normal oocyst numbers but fail to develop sporozoites, remain vacuolated and continue to increase in size without concomitant DNA replication or circumsporozoite protein expression. Consequently, Δe*psf* parasites are completely blocked in transmission. Our data further establish an important function for CB-resident proteins in oocyst sporulation.

METHODS

Experimental animals

Female Balb/c ByJ and OF-1 (6–8 weeks bred at Charles River, France) mice were used. Animal experiments performed in Leiden University Medical Center (LUMC, Leiden, The Netherlands) were approved by the Animal Experiments Committee of the Leiden University Medical Center (DEC 10099; 12042; 12120). In Instituto de Medicina Molecular (IMM, Lisbon, Portugal) animal experimentation protocols were approved by the IMM Animal Ethics Committee (under authorisation AEC_2010_018_GM_Rdt_General_IMM), the Portuguese authorities (Direção Geral de Alimentação e Veterinária) and performed according to European Union regulations.

Reference *P. berghei* ANKA lines

Six reference *P. berghei* ANKA parasite lines were used. Details of most lines can be found in the RMgmDB database (www.pberghei.eu). Line 683cl1 (DOZI::GFP; RMgm-133) [107] expressing a C-terminally GFP-tagged version of *dozi* (PBANKA_121770); line 909cl1 (CITH::GFP; RMgm-358) [108] expressing a C-terminally GFP-tagged version of *cith* (PBANKA_130130); line HPE, a non-gametocyte producer clone [316]; line 820cl1m1cl1 (Fluo-frmg; RMgm-164) [108] expressing RFP under the control of a female gametocyte specific promoter and GFP under the control of a male gametocyte specific promoter; line 259cl1 (PbGFPcon; RMgm-5) expressing GFP under the control of the constitutive *eef1a* promoter; and line cl15cy1, which is the reference parental line of *P. berghei* ANKA [317]. Line Fluo-frmg contains the transgenes integrated into the silent *230p* gene *locus* (PBANKA_030600) and does not contain a drug-selectable marker.

Reverse Transcriptase-PCR (RT-PCR)

Immunoprecipitation (IP) of DOZI::GFP and CITH::GFP parasite lysates, and subsequent RNA extraction and RT-PCR were performed as described [108]. To investigate the transcription pattern of *epsf* by RT-PCR, RNA from different life cycle stages were obtained using TRIzol® Reagent (Ambion®, #15596). Reverse transcription was done with random primers and oligo-d(T) using SuperScript® II Reverse Transcriptase (Invitrogen™, #18064). RNA sample origins were as follows: asexual blood stages from line HPE; mixed blood stages (asexuals & gametocytes) and oocysts d12 post-infection (p.i.) from line Fluo-frmg; *in vitro*-cultured ookinetes at different time points from line cl15cy1; midgut sporozoites d20 p.i. and salivary gland sporozoites d20 p.i. from line PbGFPcon; and exoerythrocytic forms from line PbGFPcon at different time points after mouse infection. Primers used in RT-PCRs are shown in **Table S1a**.

Generation of *epsf* gene deletion mutants

To disrupt the gene encoding *epsf* (PBANKA_072090) we constructed a standard replacement construct [318] using plasmid pL0001 (www.mr4.com) which contains the pyrimethamine resistant *Toxoplasma gondii* (*tg*) *dhfr/ts* as a selectable marker cassette. See **Table S2** and **Figure S4A** for the name and details of the construct. Target sequences for homologous recombination were PCR amplified from *P. berghei* wild-type (WT) genomic DNA using primers specific for the 5′ or 3′ flanking regions of *epsf* (see **Table S1b** for the sequence of the different primers). The PCR–amplified target sequences were cloned in plasmid pL0001 either upstream or downstream of the selectable marker to allow for integration of the construct into the genomic target sequence by homologous recombination. DNA construct used for transfection was obtained after digestion of the replacement construct with the appropriate restriction enzymes (**Table S2**). Transfection, selection and cloning of mutant parasite lines were performed as described [318]; see **Table S2** for details of the transfection experiments performed. Correct deletion of the *epsf* gene was confirmed by diagnostic PCR (for primers see **Table S1c**) and Southern analysis of Field-Inversion Gel Electrophoresis (FIGE)-separated chromosomes (**Figure S4B**). Chromosomes were hybridized with a probe recognizing the *tgdhfr/ts* selectable marker cassette. Absence of *epsf* mRNA was determined by RT-PCR analysis (**Figure S4C**) using RNA collected from infected blood containing asexual blood stages and gametocytes (see **Table S1c** for primers used for RT-PCR). Two cloned lines were used for further phenotype analyses: 2099cl1m7 (Δ*epsf*-a) and 2100cl1m1 (Δ*epsf*-b), both in the Fluo-frmg background.

Generation of transgenic line expressing GFP-tagged EPSF

In situ C-terminal GFP tagging of *epsf* was performed by single cross-over homologous recombination into the corresponding *locus*. See **Table S2** and **Figure S3A** for the name and details of the construct. The construct contains the *tgdhfr/ts* selectable marker. Primers used to amplify the targeting region of *epsf*, corresponding to the 3' end of the open reading frame (ORF) excluding the stop codon are listed in **Table S1b**. The targeting region was cloned in frame with *gfp*. Linearised plasmid was transfected into cl15cy1 parasites using standard methods. Transfection, selection and cloning of resulting mutant parasite line was performed as described [318], resulting in the transgenic line 2182cl2m2 (*epsf*::*gfp*). See **Table S2** for details of the transfection experiment performed. Correct integration of the construct was confirmed by diagnostic PCR (for primers see **Table S1c**) and Southern analysis of FIGE-separated chromosomes using a probe for the *tgdhfr/ts* selectable marker cassette (**Figure S3B**). Transcription and processing (splicing) of the *gfp* fusion was confirmed by RT-PCR using RNA from mixed blood stage forms (**Figure S3C**). Primers used for RT-PCR are listed in **Table S1c**.

In vivo multiplication rate of asexual blood stages

The multiplication rate of asexual blood stages in mice is determined during the cloning procedure of gene-deletion/transgenic parasites [319] and is calculated as follows: the percentage of infected erythrocytes in OF-1 mice injected with a single parasite is quantified at days 8–11 on Giemsa-stained blood films. The mean asexual multiplication rate per 24 h is then calculated assuming a total of 1.2×10^{10} erythrocytes per mouse and a blood volume of 2 mL. The percentage of infected erythrocytes in mice infected with reference lines of the *P. berghei* ANKA strain consistently ranges between 0.5 and 2% at day 8 after infection, resulting in a mean multiplication rate of 10 per 24 h [319, 320].

Oocyst production, sporozoite production and transmission experiments

Oocyst and sporozoite production of the mutant parasites was analysed by performing standard mosquito infections. Naïve female Balb/c ByJ mice were infected intraperitoneally (i.p.) with 10^6 infected red blood cells (iRBCs) of each line. On days 4-5 p.i., these mice were anesthetised and *Anopheles stephensi* female mosquitoes allowed to feed for 30 min. Twenty-four hours after feeding, mosquitoes were anesthetised by cold shock and unfed mosquitoes were removed. Oocyst and sporozoite numbers were counted at days 11-13 and 20-22 after mosquito infection, respectively. Oocyst sizes over time were determined at days 12 and 21/22 p.i. Oocysts were counted after mercurochrome staining and measured using ImageJ 1.47n software (imagej.nih.gov/ij). Sporozoites were counted in pools of 3 to 24 mosquitoes. To test the infectivity of sporozoites, 10 infected mosquitoes were allowed to feed for 30 min on anesthetised naïve female Balb/c ByJ mice on days 20-21 p.i. Successful feeding was confirmed by the presence of blood in the abdomen of mosquitoes. Blood stage parasitaemias in these mice were followed up to 33 days post-bite.

Western analysis of CSP expression in Δ*epsf* oocysts

To determine circumsporozoite protein (CSP) expression, Fluo-frmg- and Δ*epsf*-a-infected midguts were dissected at day 13 p.i. and resuspended in 1X Laemmli buffer. Samples were adjusted to 200 mM DTT, boiled and loaded onto SDS-PAGE gels. Nitrocellulose membranes were blocked for 1 h at room temperature (RT) with 5% skim milk/PBS-Tween 20 (0.05%), probed overnight at 4 °C with 3D11 mouse anti-CSP [321], 0.17 µg/mL in blocking solution) or parasite-specific 2E6 mouse monoclonal anti-PbHSP70 [322], 7.5 µg/mL in blocking solution) as primary antibodies, and 1h at RT with goat anti-mouse IgG-HRP [Santa Cruz Biotechnology, Inc.®, #sc-2005, 1:5000-1:10000 in PBS-Tween 20 (0.05%)] as secondary antibody. Westerns were developed with Immobilon™ Western Chemiluminescent HRP Substrate (Millipore, #P36599). Staining with the antibody recognizing *P. berghei* HSP70 was used as loading control.

Live imaging of blood stages and ookinetes and immunofluorescence assays (IFAs) of oocysts

Live imaging of transgenic parasites expressing GFP-tagged EPSF was done by collecting tail blood samples from infected mice and mosquito blood meals at 16 h p.i. and staining with 1 µg/mL of Hoechst 33342/PBS. To detect CSP expression in Fluo-frmg and Δ*epsf*-a oocysts by IFA, parasites at day 14 p.i. were stained with 3D11 mouse anti-PbCSP [321] (10 µg/mL) as primary antibody and goat anti-mouse IgG-Cy™3 (Jackson ImmunoResearch Laboratories, Inc., #115-166-003; 1:400) as secondary antibody. In these IFAs, samples were fixed with 4% PFA/PBS for 10 min at RT and simultaneously permeabilised and blocked for 1h at RT with a mixture of 0.5% TritonX-100/PBS and 1% BSA/PBS. All antibody incubations were done in permeabilising/blocking solution for 1h at RT and 5 ug/mL of Hoechst-33342/PBS was used to stain nuclei. Images were taken with a Leica DM5000B or Zeiss Axiovert 200M fluorescence microscope and processed using ImageJ 1.47n software (imagej.nih.gov/ij).

Multiple sequence alignments

Protein sequences in **Figures 1A and S1** were retrieved from EuPathDB (eupathdb.org). Clustal W alignments were done at EMBnet server (embnet.vital-it.ch/software/ClustalW.html) and shaded according to protein similarity levels with BOXSHADE 3.21 (www.ch.embnet.org/software/BOX_form.html).

Statistical methods

Statistical analyses of oocyst and sporozoite numbers as well as oocyst sizes were performed using Mann-Whitney test as part of Prism software package 5 (GraphPad Software).

RESULTS

EPSF is conserved in Apicomplexan parasites

EPSF (PBANKA_072090) is present in all *Plasmodium* species sequenced to date, as well as in related apicomplexan parasites such as *Babesia bovis* and *Theileria parva* (EuPathDB version 20). The similarity between the proteins from the rodent and human malaria parasites is 68% (**Figure 1A**) and is also high when compared to many other orthologs (**Figure S1**). *Plasmodium berghei epsf* is a 1775 base pair-long gene composed of nine exons (conserved in *P. falciparum*) (**Figure 1B**), and codes for a protein with a 22 amino acid-long, N-terminal signal peptide, a transmembrane domain and a weak TPM-similar domain (Pfam:PF04536), previously known as DUF477 or Repair PSII domain (**Figures 1A and C**). In plants, this domain is involved in the photosystem II (PSII) repair cycle.

epsf mRNA is present in gametocytes and early ookinetes but absent from asexual stage parasites. Upon ookinete formation, the transcript is almost absent. mRNA is synthesised again in sporulating oocysts and, although less abundant, it is still detected in midgut and salivary gland sporozoites (**Figure 1D**). *epsf* transcripts were not detected in *in vivo*-developed exoerythrocytic forms (**Figure S2**) suggesting a role for the protein during parasite development within the mosquito vector. There is no documented protein expression for the *P. berghei*, *P. falciparum* or the avian parasite *P. gallinaceum* proteins at any parasite life cycle stage ([49, 323-326] and PlasmoDB version 11.0).

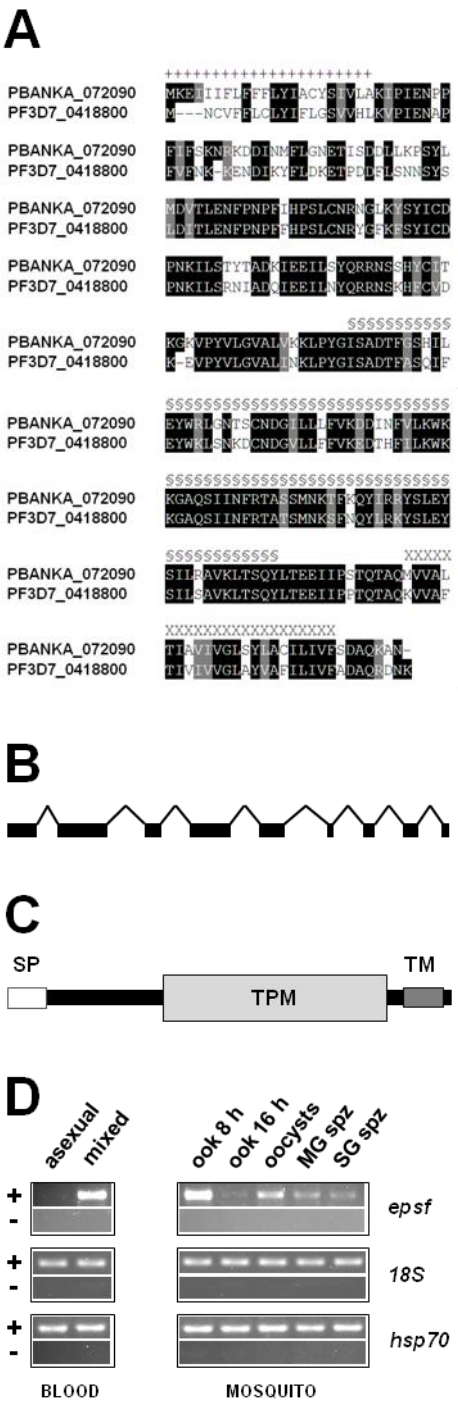

Figure 1 – Organisation of *epsf* gene and protein and its mRNA expression profile.
(A) Protein alignment of EPSF orthologs from *P. berghei* ANKA and *P. falciparum* 3D7 strains. "+" indicates the extent of the signal peptide (SignalP 4.0), "X" indicates the extent of the transmembrane domain (TMHMM 2.0) and § denotes a TPM similar domain (Pfam:PF04536) in *P. berghei* EPSF. **(B)** The *P. berghei epsf* gene (1775 bp) is composed of 9 exons (shaded bars) and 8 introns (lines); this organisation is conserved in *P. falciparum*. **(C)** Modular architecture of EPSF. SP: signal peptide; TPM: TPM similar domain; TM: transmembrane domain. **(D)** RT-PCRs of *epsf* along the life cycle. Asexual: asexual blood stages; mixed: asexuals and gametocytes; ook: ookinetes (8 and 16 hours after gametocyte activation); MG spz: midgut sporozoites; SG spz: salivary gland sporozoites. *18S* rRNA and *hsp70* serve as loading control genes. +: RT positive reaction; -: RT negative reaction.

epsf is transcribed in gametocytes and translationally repressed in DOZI/CITH-defined messenger ribonucleoproteins (mRNPs)

In the female gametocyte *epsf* has previously been found to rely for stability on the translational repressors DOZI [107] and CITH [108]; downregulation in the absence of these proteins reaches WT versus knock-out (KO) ratio $\log_2$ values higher than 2, similar to the hallmark mRNAs *p25* and *p28*. Using IP of DOZI::GFP and CITH::GFP followed by RT-PCR of bound RNAs we found *epsf* to interact, directly or indirectly, with repressors, suggesting storage of this mRNA for translation during ookinete formation in a manner similar to *p25* and *p28* (**Figure 2A**).

To test whether DOZI/CITH-bound *epsf* is indeed translationally repressed in gametocytes we generated a parasite line expressing a C-terminally GFP-tagged version of

EPSF (**Figure S3**). While the fusion transcript can be detected by RT-PCR in gametocytes (**Figure 2B**), we did not observe EPSF::GFP expression in live gametocytes. EPSF::GFP was however detected in mature ookinetes and was restricted to discrete foci that co-localised with haemozoin clusters visible under DIC microscopy (**Figure 2C**), suggesting CB localisation. In addition, *epsf*::*gfp* parasites completed the life cycle, including transmission to a naïve mouse host by mosquito bite, indicating no deleterious effect of the GFP tag for normal parasite life cycle progression (**Figure 2D and Table S3**). Although *epsf* is transcribed to a certain extent in sporulating oocysts, midgut sporozoites and salivary gland sporozoites (**Figure 1D**), we were unable to detect EPSF::GFP fusion protein in these developmental stages, either by live imaging or IFAs (data not shown).

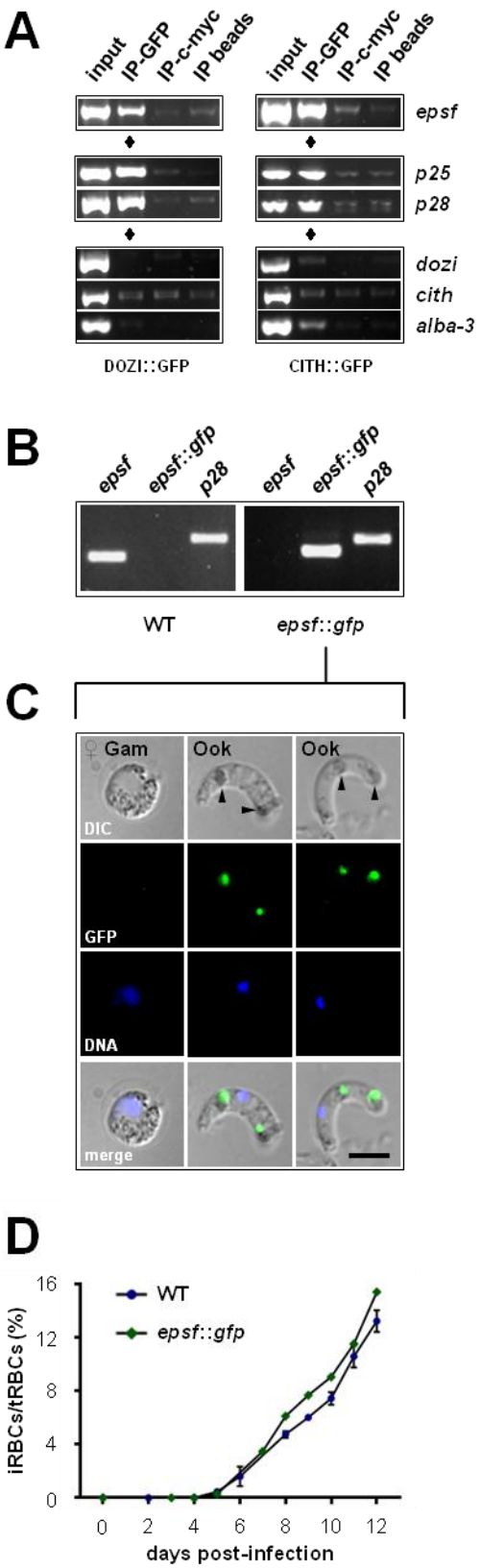

Figure 2 – *epsf* is translationally repressed in gametocytes and expressed in ookinetes.
(A) RT-PCR analysis on DOZI::GFP and CITH::GFP gametocyte immunoprecipitation (IP) eluates shows that *epsf* as well as *p25* and *p28* mRNAs (known to be translationally repressed) co-precipitate with DOZI and CITH. *dozi*, *cith* and *alba-3* are translated in gametocytes and are not enriched in the IP-GFP fractions. Input: total gametocyte mRNA; IP-GFP: IP with anti-GFP antibody; IP-c-myc: IP with anti-c-myc antibody; IP beads: no antibody used for IP. **(B)** RT-PCR analysis shows absence of WT *epsf* and presence of correctly spliced *epsf*::*gfp* mRNA in blood stages of *epsf*::*gfp* parasites. *p28* serves as control gene. **(C)** Live imaging of *epsf*::*gfp* parasites shows no EPSF expression in gametocytes while EPSF::GFP (in green) is localised to discrete foci in blood meal retrieved ookinetes. Arrowheads indicate DIC-visible haemozoin clusters. ♀ Gam: female gametocyte; Ook: ookinete. Scale bar = 5 µm. **(D)** Mice bitten by *epsf*::*gfp*-infected mosquitoes develop normal blood stage infection. Mean parasitaemias are shown by the dots, while SEM values are shown by the vertical lines. WT (2 independent experiments, *n*=2); *epsf*::*gfp* (1 experiment, *n*=1). iRBCs: infected red blood cells; tRBCs: total red blood cells.

EPSF is necessary for sporozoite formation

To dissect the function of EPSF, we generated two independent *epsf* gene deletion parasite lines: Δ*epsf*-a and Δ*epsf*-b (**Figure S4**). While Δ*epsf*-a showed a 30% reduction in oocyst burden compared to WT parasites (**Figure 3A**), the same analysis with the Δ*epsf*-b line did not corroborate this result (**Figure S5A**). Strikingly however, none of the lines showed midgut or salivary gland sporozoites as late as days 20-22 post-infection (p.i.) (**Figures 3B-C**

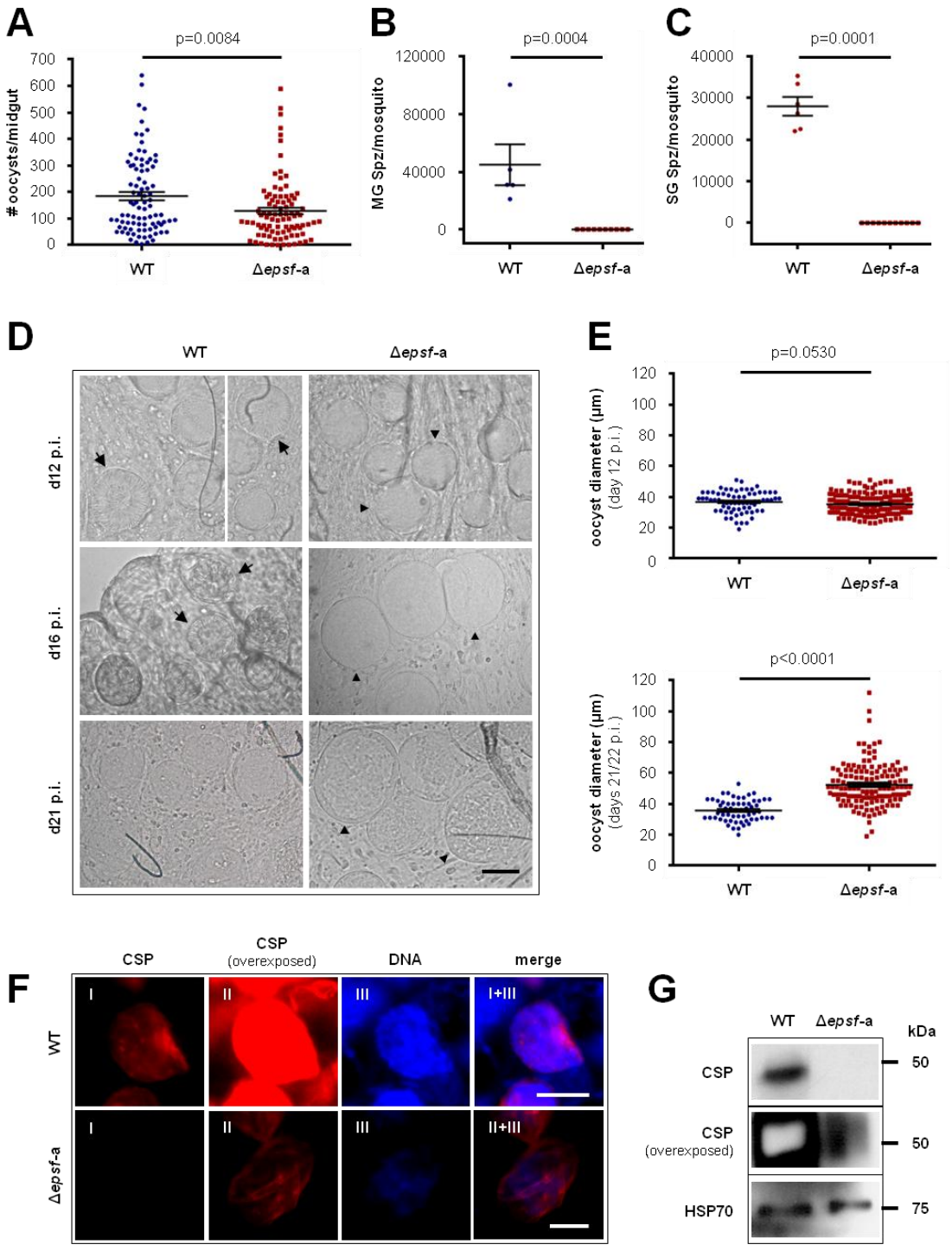

Figure 3 (legend next page) – Δ*epsf*-a oocysts do not sporulate and lack circumsporozoite protein.

and S5B-C).

WT oocysts sporulate as early as day 12 p.i. On the other hand, Δ*epsf* parasites showed no signs of sporozoite formation at this stage. Instead, mutant oocysts remain 'empty' and vacuolated up to day 21 p.i. (**Figure 3D**) and outgrow WT cysts in size (**Figure 3E**). Indeed, Δ*epsf* oocysts are significantly larger than WT parasites already at day 14 p.i. (data not shown).

CSP expression is normally detected soon following oocyst formation and is an essential factor for sporozoite development [327]. For these reasons, we analysed the expression of this sporozoite coat protein in WT and Δ*epsf* parasites by IFA (**Figure 3F**) and Western blot (**Figure 3G**). Both methodologies showed that CSP is barely expressed in mutant oocysts on days 13-14 p.i. Furthermore, DNA staining with the dye Hoechst-33342 revealed that DNA replication in Δ*epsf* parasites is reduced when compared with WT oocysts of the same age (**Figure 3F**).

Ultimately, the complete failure of Δ*epsf* parasites to colonise the salivary glands of their invertebrate host resulted in absence of transmission to naïve mice through the bite of infected female mosquitoes (**Figure S6**).

DISCUSSION

Many parasite genes important for ookinete formation and functionality (e.g., gliding motility and capacity to invade the mosquito midgut) are transcribed in blood stage female gametocytes but kept quiescent through binding to the translational repressors DOZI and CITH [107, 108]. Among these genes are those encoding the major ookinete surface proteins P25 and P28, alveolins, components of the gliding molecular motor and inner membrane complex (IMC) [108]. *Plasmodium* calcium-dependent protein kinase 1 (CDPK1) is then involved in the translational activation of these transcripts during ookinete development [134]. Interestingly, a large proportion of the transcripts bound by the RNA binding proteins DOZI and/or CITH, and thus thought to be subjected to translational repression (TR), encode for proteins with predicted

Figure 3 (previous page) – Δ*epsf*-a oocysts do not sporulate and lack circumsporozoite protein. **(A)** Δ*epsf*-a parasites show slightly reduced oocyst numbers on days 12 to 13 p.i. WT (6 independent experiments, *n*=88); Δ*epsf*-a (5 independent experiments, *n*=92). **(B)** Δ*epsf*-a parasites do not develop any midgut sporozoite (MG Spz). Absolute numbers of sporozoites per mosquito from 4 independent experiments are presented for both WT (*n*=5) and Δ*epsf*-a (*n*=10) parasites. **(C)** Δ*epsf*-a parasites do not develop any salivary gland sporozoite (SG Spz). Absolute numbers of sporozoites per mosquito from 5 independent experiments are presented for both WT (*n*=6) and Δ*epsf*-a (*n*=11) parasites. **(D)** Δ*epsf*-a oocysts lack signs of sporulation throughout time and appear 'empty' or vacuolated (arrowheads). On the contrary, most WT oocysts have already formed sporozoites by days 12 to 16 p.i. (arrows). Scale bar = 30 µm. **(E)** At day 12 p.i. Δ*epsf*-a oocysts have normal sizes (upper plot) but by days 21/22 p.i., KO oocysts are clearly enlarged when compared to WT oocysts (bottom plot). **(A-C, E)** Mean and SEM values are shown by the lines; p-values for Mann-Whitney test are shown above the data sets. **(F)** Immunofluorescence assay of oocyst-infected midguts at day 14 p.i. shows strongly reduced CSP expression (in red) in Δ*epsf*-a parasites. DNA replication in also decreased in KO oocysts, as seen by Hoechst-33342 staining (in blue). Scale bars = 20 µm. **(G)** Western blot analysis of oocyst-infected midguts at day 13 p.i. confirms diminished CSP expression in Δ*epsf*-a mutants. HSP70 serves as parasite loading control. **(F-G)** Note that when CSP is detected in Δ*epsf*-a oocysts, signal coming from WT oocysts is already saturated.

surface localisation signals, such as N-terminal signal peptides and/or transmembrane (TM) domains. For example, of the 114 mRNAs downregulated in both DOZI and CITH gene deletion mutants, 44 (approximately 38%) encode for known or putative surface molecules [107, 108]. Among these 44 transcripts one can find *epsf*, encoding for a protein with predicted signal peptide and C-terminal TM domain, but also those encoding for PbLAP4-6. Concordantly, *pblap4-6* have recently been shown to be translationally repressed [208].

Here we show that EPSF is also a target of TR in *P. berghei* macrogametocytes by interacting with both translational repressors DOZI and CITH, which is in agreement with previous studies from our group showing that *epsf* was downregulated in the absence of either protein [107, 108]. While not detected in gametocytes, the localisation of EPSF in ookinetes was restricted to one or two discrete cytoplasmic foci and greatly resembled that observed for the CB-resident proteins PbLAP1-6 [208, 211, 212]. Moreover, these foci co-localised with large haemozoin clusters easily recognisable under DIC microscopy. Therefore we concluded that EPSF is indeed targeted to CBs. EPSF represents an addition to the so far small repertoire of CB-associated proteins [208, 211, 212]. Besides being present in ookinetes, PbLAP1-3 are already scattered throughout the cytoplasm of female gametocytes, being later on recruited to the ookinete CBs [211, 212]; on the other hand, *epsf* is translationally repressed in gametocytes and thus behaves like *pblap4-6* [208].

The presence of a TPM-similar domain in EPSF is intriguing. In plants, the TPM domain-containing proteins TLP18.3 and Psb32 are implicated in the photosystem II (PSII) repair cycle. This domain may be involved in the regulation of synthesis/degradation of the D1 protein of the PSII core and in the assembly of PSII monomers into dimers in the grana stacks [328]. In the model nematode *Caenorhabditis elegans*, the MOLO-1 protein also contains a TPM domain and is an auxiliary subunit that positively modulates the gating of levamisole-sensitive acetylcholine receptors [329]. The function of this domain in other organisms is unknown. Given the highly distinct roles of the TPM domain-containing proteins in the two organisms mentioned above, it is at the moment difficult to understand how this domain could be implicated in the ascribed function of EPSF for parasite biology.

Our results show that EPSF is absolutely essential for the development of midgut sporozoites. The precise cellular function of this protein remains however unknown. Gene deletion studies have highlighted PbLAPs [176, 211, 224-226], plasmepsin VI [176], rhomboid 3 [330] and CSP [331] in the development of midgut sporozoites. The phenotypes of such mutant parasites include lack of DNA replication, highly vacuolated oocyst appearance (a sign of degeneration) and reduced CSP expression. It is known that CSP levels markedly influence the degree of sporozoite formation by affecting the development of inner membranes in the sporulating cyst [327]. All these phenotypes were also verified in Δ*epsf* parasites. Moreover, the oocyst enlargement reported here was also ascribed for KO parasites of PbSR, a *P. berghei* member of the LCCL protein family [224]. One particular contrasting feature of Δ*pbsr* parasites is the substantial DNA replication observed in KO oocysts [224]. It thus seems that the absence

of PbSR has an impact on cytokinesis rather than on nuclear division. Insterestingly, it was also shown that PbSR loss-of-function and gene deletion ookinetes are devoid of CBs [211]. Why exactly the lack of EPSF affects oocyst nuclear multiplication is not known and whether Δ*epsf* ookinetes present CBs remains to be determined.

Nonetheless, the present study reinforces the crucial role of *Plasmodium* CBs in parasite biology and in malaria transmission through the mosquito vector in particular. Additional studies on these peculiar organelles are therefore highly desirable to increase our current knowledge on CB biology, and are likely to highlight CBs as potential malaria intervention targets. By targeting CB proteins such as EPSF one could prevent the development of infectious sporozoites and consequently block malaria transmission.

SUPPLEMENTARY FIGURES AND TABLES

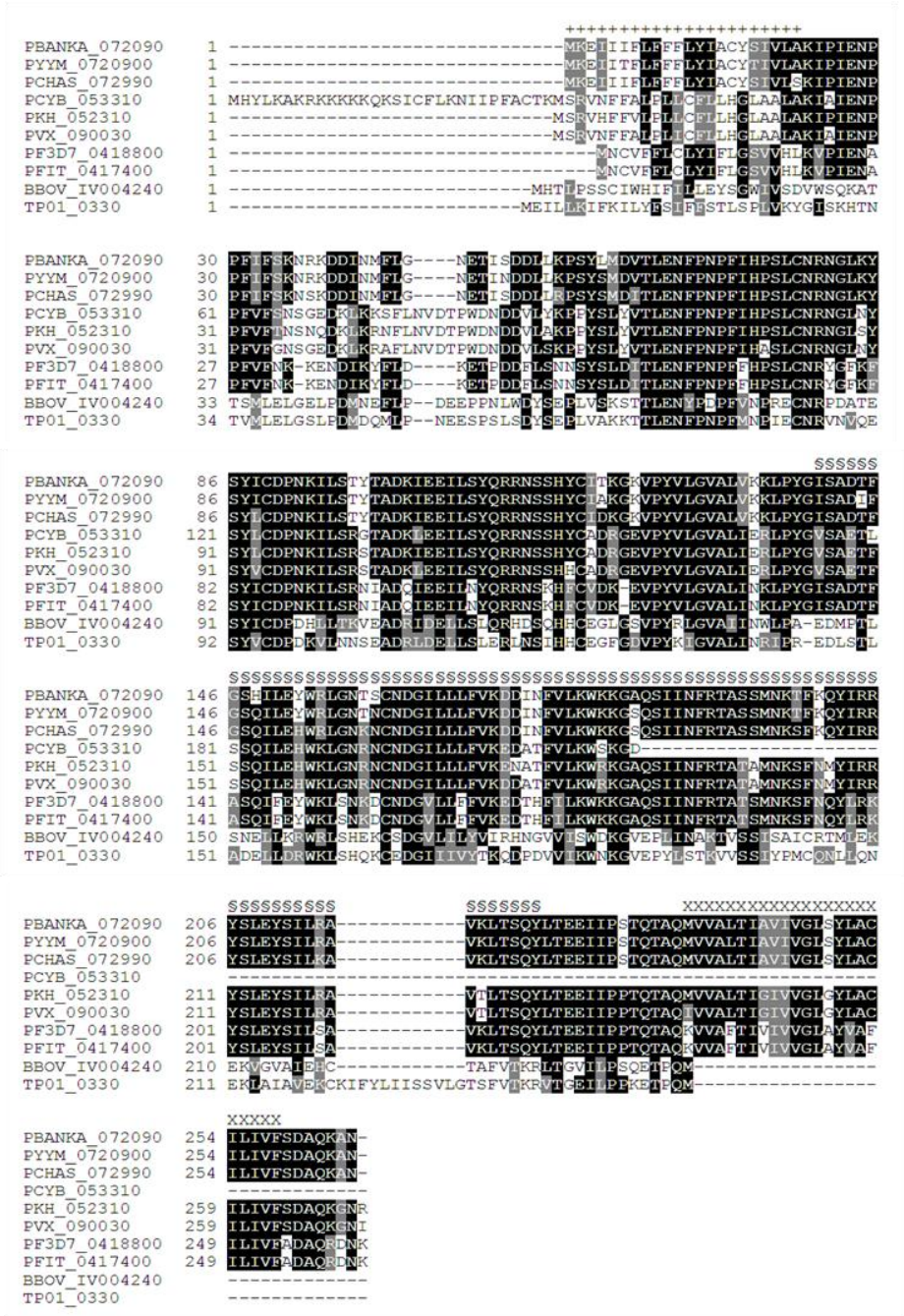

Figure S1 – EPSF is conserved in apicomplexan parasites.
Protein alignment of EPSF orthologs from 8 different *Plasmodium* species and strains as well as from the related apicomplexan parasites *Babesia bovis* and *Theileria parva*. "+" indicates the extent of the signal peptide (SignalP 4.0), "X" indicates the extent of the transmembrane domain (TMHMM 2.0) and § denotes a TPM similar domain (Pfam:PF04536) in *P. berghei* EPSF.

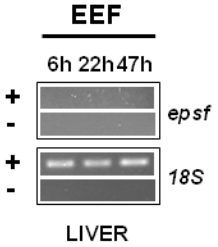

Figure S2 – *epsf* is not transcribed in liver stages.
RT-PCR analysis of *epsf* in *in vivo*-developed *P. berghei* exoerythrocytic forms (EEFs) at different time points after sporozoite injection. *18S* rRNA serves as loading control gene. +: RT positive reaction; -: RT negative reaction.

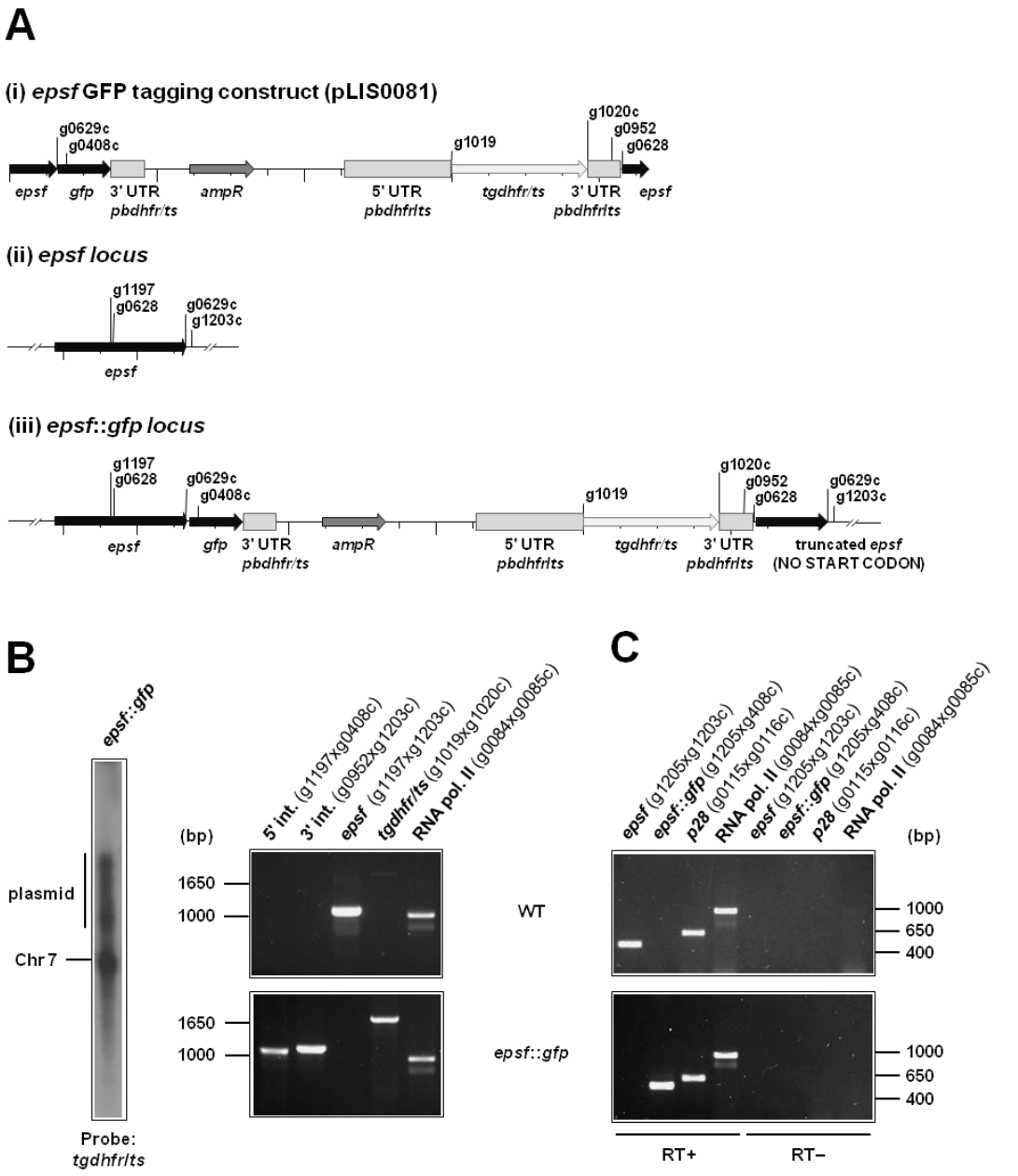

Figure S3 – Generation and genotyping of *epsf*::*gfp* parasite line.
(A) *epsf* GFP tagging construct pLIS0081 (i) was obtained by cloning the last 982 bp of *epsf* ORF excluding the stop codon upstream and in frame with the *gfp* gene. This construct includes the *Toxoplasma gondii dhfr/ts* selectable marker cassette under the control of *P. berghei dhfr/ts* 5' and 3' UTRs. The construct was integrated into the *epsf locus* (ii) of cl15cy1 by single homologous recombination, resulting in the fusion of *epsf* to *gfp* in *epsf*::*gfp* parasites (iii). **(B)** Correct tagging of *epsf* was shown by Southern analysis of separated chromosomes (left) and diagnostic PCR analyses (right). Hybridisation of separated chromosomes from uncloned *epsf*::*gfp* parasites with a probe against the *tgdhfr/ts* selectable marker cassette recognised integrated pLIS0081 into chromosome 7 and circular plasmid with higher molecular weight. PCR analyses confirm 5' and 3' integration (int.) of pLIS0081, absence of WT *epsf* ORF and presence of *tgdhfr/ts* gene. **(C)** Absence of WT *epsf* and presence of *epsf*::*gfp* mRNA was confirmed in cloned *epsf*::*gfp* mixed blood stages by RT-PCR. *p28* and RNA polymerase II serve as control genes. Primer g1205 only anneals with *epsf* cDNA.

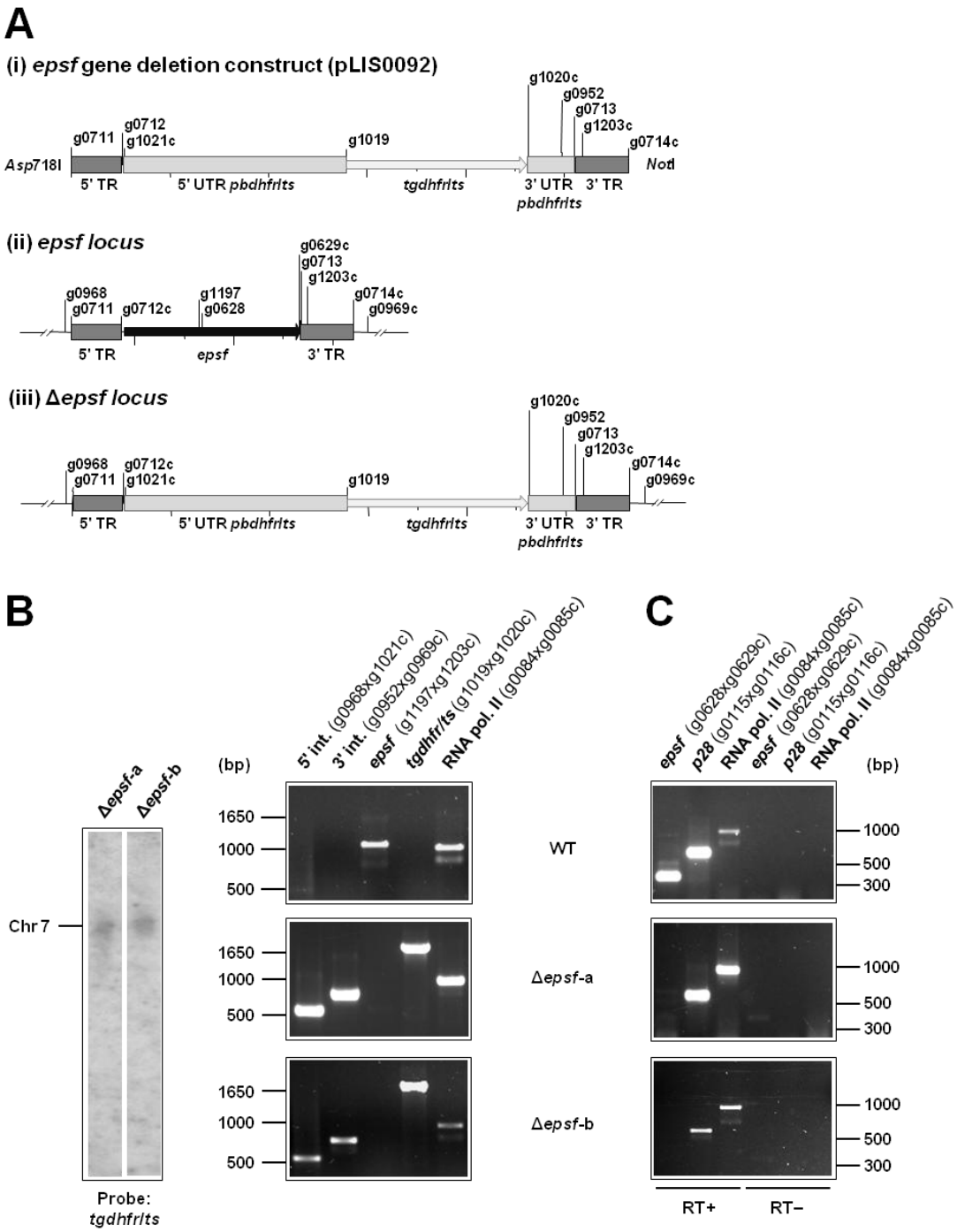

Figure S4 – Generation and genotyping of Δ*epsf* parasite lines.
(A) *epsf* gene deletion construct pLIS0092 (i) was obtained by cloning *epsf* 5' and 3' targeting regions (TR) upstream and downstream of the *Toxoplasma gondii dhfr/ts* selectable marker cassette, respectively. *tgdhfr/ts* gene is under the control of *P. berghei dhfr/ts* 5' and 3' UTRs. The construct was integrated into the *epsf locus* (ii) of Fluo-frmg WT line by double homologous recombination, resulting in the complete deletion of *epsf* ORF in Δ*epsf* parasites (iii). **(B)** Correct deletion of *epsf* was shown by Southern analysis of separated chromosomes (left) and diagnostic PCR analyses (right). Hybridisation of separated chromosomes with a probe against the *tgdhfr/ts* selectable marker cassette recognised integrated pLIS0092 into chromosome 7. PCR analyses confirm 5' and 3' integration (int.) of pLIS0092, absence of *epsf* ORF and presence of *tgdhfr/ts* gene. **(C)** Absence of *epsf* mRNA was confirmed in Δ*epsf* mixed blood stages by RT-PCR. *p28* and RNA polymerase II serve as control genes.

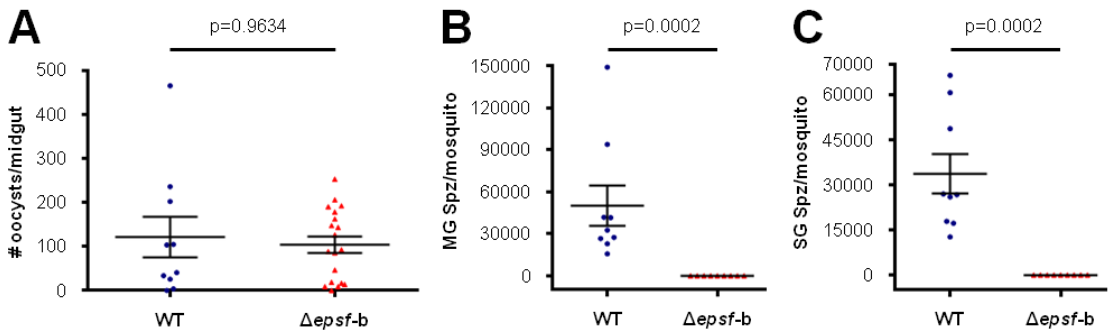

Figure S5 – Δ*epsf*-b oocysts do not sporulate.
(A) Δ*epsf*-b parasites show WT oocyst numbers on days 11 to 13 p.i. Absolute numbers of oocysts per midgut from 3 independent experiments are presented for both WT (*n*=10) and Δ*epsf*-b (*n*=19) parasites. **(B)** Δ*epsf*-b parasites do not develop any midgut sporozoite (MG Spz). **(C)** Δ*epsf*-b parasites do not develop any salivary gland sporozoite (SG Spz). **(B-C)** Absolute numbers of sporozoites per mosquito from 2 independent experiments are presented for both WT (*n*=9) and Δ*epsf*-b (*n*=9) parasites. **(A-C)** Mean and SEM values are shown by the lines; p-values for Mann-Whitney test are shown above the data sets.

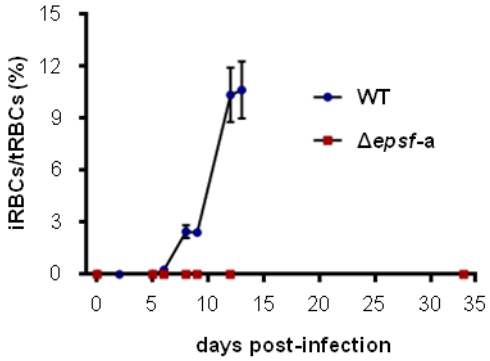

Figure S6 – Δ*epsf* mutants do not transmit to naïve mice.
Mice bitten by Δ*epsf*-a-infected mosquitoes do not develop blood stage infection. Mean parasitaemias from 3 independent experiments are shown by the dots while SEM values are shown by the vertical lines.

Table S1 - Primers used in the present work.

a) Primers used in life-cycle RT-PCRs and RT-PCRs of IP samples.

"c" or "Rev" at the end of primer names means they are antisense primers. All others are sense primers.

Nucleotide stretches in capital letter correspond to the complementary sequence to the respective gene. n.a.: not aplicable; ORF: open reading frame; UTR: untranslated region.

Gene name	Gene ID	Primer name	Sequence	Description	Product size gDNA (bp)	Product size cDNA (bp)	Across introns
epsf	PBANKA_072090	g0628	aaagaattcCATATATTAGAGTATTG	*epsf* ORF	1003	375	yes
		g0629c	aaagcggccgcAATTTGCCTTTTGTGCATC	*epsf* ORF			
***18S* rRNA**	n.a.	PbA18SFw	AAGCATTAAATAAAGCGAATACATCCTTAC	*18S* rRNA	134	134	no
		PbA18SRev	GGAGATTGGTTTTGACGTTTATGTG	*18S* rRNA			
hsp70	PBANKA_071190	g0258	AAAAGCAAAGCCAAACTTACC	*hsp70* ORF	139	139	no
		g0259c	GGATGGGGTTGTTCTATTACC	*hsp70* ORF			
p25	PBANKA_051500	g0385	CCGGAATTCATAAACAAATATACCTGG	*p25* 3' UTR	263	263	no
		g0476c	CGGGATCCTCATACGAATTTTATTG	*p25* 3' UTR			
p28	PBANKA_051490	g0115	TTCGATATCATGAATTTTAAATACAG	*p28* ORF	660	660	no
		g0116c	tccgcggccgcGCATTACTATCACGTAAATAAC	*p28* ORF			
dozi	PBANKA_121770	g0546	TAATTGTGTCGCTTCAAATG	*dozi* ORF	641	439	yes
		g0548c	TAATTCTTTTATCATAGCAG	*dozi* ORF			
cith	PBANKA_130130	g0549	GAAAAAAGCAAAGATGTATTATCTG	*cith* ORF	334	334	no
		g0550c	ATAGGCTGGGTATCTGTTAAATG	*cith* ORF			
alba3	PBANKA_120440	g0003	aaacccggggaattcCAAGAAAGAGCTGAAAAC	*alba3* ORF	641	324	yes
		g0004c	aaagcggccgctATTAGCAACAAAGTTTG	*alba3* ORF			

Table S1 - Primers used in the present work.

b) Primers used in the generation of gene deletion and GFP-tagging constructs.

"c" at the end of primer names means they are antisense primers. All others are sense primers.

Nucleotide stretches in capital letter correspond to the complementary sequence to the respective gene. Underlined are restriction site sequences.

ORF: open reading frame.

Gene name	Gene ID	Construct name	Primer name	Sequence	Restriction sites	Description
Gene deletion constructs						
epsf	PBANKA_072090	pLIS0092	g0711	aaaggtaccTTGTTATTCTTTGCAAG	*Asp* 718I	*epsf* 5' targeting region
			g0712c	aaaaagcttTGAATAATTAAAAAAAAGC	*Hin* dIII	*epsf* 5' targeting region
			g0713	aaagaattcTTATTTGATGATCAACC	*Eco* RI	*epsf* 3' targeting region
			g0714c	aaagcggccgcAATATATATAGTTATTTCC	*Not* I	*epsf* 3' targeting region
GFP-tagging constructs						
epsf	PBANKA_072090	pLIS0081	g0628	aaagaattcCATATATTAGAGTATTG	*Eco* RI	*epsf* ORF
			g0629c	aaagcggccgcAATTTGCCTTTTGTGCATC	*Not* I	*epsf* ORF

Table S1 - Primers used in the present work.

c) Primers used in genotyping and RT-PCR of mutant parasite lines (continues in next page).

"c" at the end of primer names means they are antisense primers. All others are sense primers.

Nucleotide stretches in capital letter correspond to the complementary sequence to the respective gene.

n.a.: not aplicable; *tg* : *Toxoplasma gondii* ; *dhfr*/*ts* : dihydrofolate reductase/thymidylate synthase; ORF: open reading frame; UTR: untranslated region.

Gene name/ mutant name	Gene ID	Primer name	Sequence	Description	Integration PCR pair	Product size (bp)
Primers for genotyping						
Δ*epsf*-a and Δ*epsf*-b	PBANKA_072090	g0968	TACATTGAAGTGTTGGTATG	*epsf* 5' integration	g1021c	600
		g0969c	TGCATGCACATATATGTCAC	*epsf* 3' integration	g0952	705
epsf::*gfp*		g1197	GCCTTATGGAATTAGTGC	*epsf* 5' integration	g0408c	1148
		g1203c	GTATTAATGCATGACTTG	*epsf* 3' integration	g0952	1202
epsf		g1197	GCCTTATGGAATTAGTGC	*epsf* ORF	n.a.	1097
		g1203c	GTATTAATGCATGACTTG	*epsf* 3' UTR	n.a.	
Primers for RT-PCR						
epsf	PBANKA_072090	g0628	aaagaattcCATATATTAGAGTATTG	*epsf* ORF	n.a.	375
		g0629c	aaagcggccgcAATTTGCCTTTTGTGCATC	*epsf* ORF	n.a.	
		g1205	AAGTTCCTTACGTATTAG	*epsf* ORF	n.a.	509
		g1203c	GTATTAATGCATGACTTG	*epsf* 3' UTR	n.a.	
epsf::*gfp*		g1205	AAGTTCCTTACGTATTAG	*epsf* ORF	g0408c	560

Table S1 - Primers used in the present work.

c) Primers used in genotyping and RT-PCR of mutant parasite lines (continuation).
"c" at the end of primer names means they are antisense primers. All others are sense primers.
Nucleotide stretches in capital letter correspond to the complementary sequence to the respective gene.
n.a.: not aplicable; *pb*: *Plasmodium berghei*; *tg*: *Toxoplasma gondii*; *dhfr/ts*: dihydrofolate reductase/thymidylate synthase; ORF: open reading frame;
UTR: untranslated region.

Gene name/ mutant name	Gene ID	Primer name	Sequence	Description	Integration PCR pair	Product size (bp)
General primers						
pbdhfr/ts	PBANKA_071930	g0952	GATTCATAAATAGTTGGACTTG	3' UTR *pbdhfr/ts*	n.a.	n.a.
		g1021c	ATTGTTGACCTGCAGGCATG	5' UTR *pbdhfr/ts*	n.a.	n.a.
tgdhfr/ts	n.a.	g1019	ATGCATAAACCGGTGTGTC	*tgdhfr/ts* ORF	n.a.	1866
		g1020c	AGCTTCTGTATTTCCGC	*tgdhfr/ts* ORF	n.a.	
RNA polymerase II subunit RPB1	PBANKA_080700	g0084	aaagaattcTGATGGTTTACAATCACC	RNA pol II ORF	n.a.	1015
		g0085c	aaagcggccgctTTCTTCCTGCATCTCCTC	RNA pol II ORF	n.a.	
p28	PBANKA_051490	g0115	TTCGATATCATGAATTTTAAATACAG	*p28* ORF	n.a.	660
		g0116c	tccgcggccgcGCATTACTATCACGTAAATAAC	*p28* ORF	n.a.	
gfp	n.a.	g0408c	GTATGTTGCATCACCTTC	*gfp* ORF	n.a.	n.a.

Table S2 - Parasite transfection experiments.

Gene name/ mutant name	Gene ID	DNA construct name	Restriction enzymes[1]	Experiment #/ mutant clone ID[2]	Parental line[3]
Gene deletion mutants					
Δ*epsf*-a	PBANKA_072090	pLIS0092	*Asp*718I and *Not*I	2099cl1m7	820cl1m1cl1
Δ*epsf*-b				2100cl1m1	820cl1m1cl1
GFP-tagged mutants					
epsf::*gfp*	PBANKA_072090	pLIS0081	*Afl*II	2182cl2m2	cl15cy1

[1] Restriction enzymes used for plasmid linearisation before transfection

[2] Experiment number for independent transfection experiments: experiment number/ID of the mutants clones

[3] Parental *P. berghei* ANKA line in which the transfection experiment was performed

Table S3 - Summary of phenotypes of the *P. berghei* mutants generated in the present study.

Mutant	Asexual multiplication rate[1] (s.d.)	Oocyst production[2] (s.d.)	MG Spz production[3] X10^4 (s.d.)	SG Spz production[4] X10^4 (s.d.)	Prepatent period[5]
Δ*epsf*-a	10 (0) *n* =3	128.6 (118.3) *n* =5	0 (0) *n* =4	0 (0) *n* =5	n.a.
Δ*epsf*-b	10 (0) *n* =7	104.7 (80.8) *n* =3	0 (0) *n* =2	0 (0) *n* =2	n.d.
epsf::*gfp*	10 (0) *n* =2	n.d.	n.d.	n.d.	4 *n* =1
WT[6]	10 (0) *n* >10	21-335 *n* =9	2.6-10 *n* =6	1.6-4.3 *n* =7	4-5 *n* =5

[1] The multiplication rate per 24 hours of blood stage parasites in mice infected with a single parasite

[2] The mean number of oocysts per mosquito (days 11–13)

[3] The mean number of midgut sporozoites (MG Spz) per mosquito (days 20–22)

[4] The mean number of salivary gland sporozoites (SG Spz) per mosquito (days 20–22)

[5] The prepatent period (measured in days post bite of 10 infected females per mouse) is defined as the day when parasites are detected in Giemsa-stained blood smears of mice

[6] The developmental data for wild type (WT) parasites are shown as the range of mean values

s.d.: standard deviation

n.d.: not determined

n.a.: not aplicable

PALMITOYLATION DEFINES KEY EVENTS DURING MALARIA LIFE CYCLE PROGRESSION IN THE MOSQUITO VECTOR

Jorge M. Santos[1], Neuza Duarte[1], Jessica Kehrer[2], Jai Ramesar[3], Cristina M. C. Avramut[4], Abraham J. Koster[4], Johannes T. Dessens[5], Friedrich Frischknecht[2], Chris J. Janse[3], Blandine Franke-Fayard[3], Gunnar R. Mair[1]

[1] Instituto de Medicina Molecular, Faculdade de Medicina da Universidade de Lisboa, Edifício Egas Moniz, Av. Prof. Egas Moniz, 1649-028 Lisbon, Portugal

[2] Parasitology, Department of Infectious Diseases, University of Heidelberg Medical School, Im Neuenheimer Feld 324, 69120 Heidelberg, Germany

[3] Leiden Malaria Research Group, Department of Parasitology, Leiden University Medical Center, Albinusdreef 2, 2333 ZA Leiden, The Netherlands

[4] Section Electron Microscopy (Molecular Cell Biology), Leiden University Medical Center, Leiden, The Netherlands

[5] Department of Pathogen Molecular Biology, Faculty of Infectious and Tropical Diseases, London School of Hygiene & Tropical Medicine, Keppel Street, London WC1E 7HT, United Kingdom

AUTHOR CONTRIBUTIONS

JMS and GRM designed experiments and generated gene deletion and GFP tagging plasmids. JMS performed RT-PCRs on immunoprecipitation samples, determined sporozoite numbers, executed transmission experiments, performed sporozoite traversal and invasion assays in the presence of palmitoylation inhibitor, analysed all data sets, wrote the Abstract, Methods, Results and Discussion and generated all figures and tables. JMS and ND performed RT-PCRs across the parasite life cycle, genotyped mutant parasites, determined oocyst numbers and sizes and performed oocyst Western blots. JMS, JR, CJJ, BF-F and GRM performed parasite transfections. JMS, JR and CJJ cloned mutant parasites and determined asexual multiplication rates. JMS, JK and BF-F performed light microscopy imaging experiments. JK performed sporozoite gliding assays in the presence of palmitoylation inhibitor. JR and CJJ performed gametocyte and ookinete development assays. CMCA and AJK performed electron microscopy experiments. JTD generated the LAP2 GFP tagging plasmid. BF-F and CJJ performed RNAseq experiments. FF contributed intellectually and finantially to the project. GRM supervised the work and revised the text.

ABSTRACT

Palmitoylation is an important, reversible protein modification that regulates multiple biological processes. The post-translational addition of C-16-long chain fatty acids to cysteine residues is catalysed by protein palmitoyl-S-acyl-transferases (PATs) and affects the affinity of a protein for membranes and therefore its subcellular localisation. In the human malaria parasite *Plasmodium falciparum* palmitoylation is implicated in asexual multiplication and host cell invasion. The role, if any, of palmitoylation for other stages within the complex *Plasmodium* life cycle remains elusive. Here we define the role of palmitoylation during several phases of mosquito stage infection, from the onset of sexual development in the erythrocyte to sporozoite formation and liver cell invasion in the rodent malaria model *P. berghei*. Using 2-BMP, an irreversible inhibitor of PATs, we reveal that palmitoylation is essential for developmental progression of zygotes into mature ookinetes. We show that certain PAT enzymes of *P. berghei* are transcriptionally up-regulated in sexual precursor cells (gametocytes) where they are bound by the translational repressors DOZI and CITH. One of these, DHHC10, activated translationally during ookinete formation is a key factor for sporogony through its central role in the formation of crystalloid bodies (CBs) and correct targeting of CB components in the ookinete. Finally we demonstrate that dynamic palmitoylation is not required for normal sporozoite gliding motility or hepatocyte traversal, but is necessary for optimal hepatocyte invasion. This is the first time that key functions are ascribed for a palmitoyl-S-acyl-transferase in mosquito stages of the malaria parasite; this report demonstrates the crucial nature of palmitoylation for transmission of the malaria parasite to the mosquito vector and its essential role for ookinete and sporozoite development.

METHODS

Experimental animals

Female Balb/c ByJ and OF-1 (6–8 weeks bred at Charles River, France) mice were used. Animal experiments performed in Leiden University Medical Center (LUMC, Leiden, The Netherlands) were approved by the Animal Experiments Committee of the Leiden University Medical Center (DEC 10099; 12042; 12120). In Instituto de Medicina Molecular (IMM, Lisbon, Portugal) animal experimentation protocols were approved by the IMM Animal Ethics Committee (under authorisation AEC_2010_018_GM_Rdt_General_IMM), the Portuguese authorities (Direção Geral de Alimentação e Veterinária) and performed according to European Union regulations. At the University of Heidelberg Medical School (Heidelberg, Germany) animal work was approved by the German Authorities (Regierungspräsidium Karlsruhe; Aktenzeichen 35-9185.81/G-3/11) and performed in compliance with FELASA guidelines and regulations.

Reference *P. berghei* ANKA lines

Seven reference *P. berghei* ANKA parasite lines were used. Details of most lines can be found in the RMgmDB database (www.pberghei.eu). Line 683cl1 (DOZI::GFP; RMgm-133) [107] expressing a C-terminally GFP-tagged version of *dozi* (PBANKA_121770); line 909cl1 (CITH::GFP; RMgm-358) [108] expressing a C-terminally GFP-tagged version of *cith* (PBANKA_130130); line HPE, a non-gametocyte producer clone [316]; line 820cl1m1cl1 (Fluo-frmg; RMgm-164) [108] expressing RFP under the control of a female gametocyte specific promoter and GFP under the control of a male gametocyte specific promoter; line 676m1cl1 (PbGFP-LUCcon; RMgm-29) expressing the fusion protein GFP-Luciferase under the control of the constitutive *eef1a* promoter; line 259cl1 (PbGFPcon; RMgm-5) expressing GFP under the control of the constitutive *eef1a* promoter; and line cl15cy1, which is the reference parental line of *P. berghei* ANKA [317]. Lines Fluo-frmg and PbGFP-LUCcon contain the transgenes integrated into the silent *230p* gene *locus* (PBANKA_030600) and do not contain a drug-selectable marker.

RNA sequencing (RNAseq) of separated asexual blood stages, gametocytes and ookinetes

RNA was collected from multiple synchronised blood stages: rings, trophozoites and schizonts [332], and purified gametocytes and ookinetes [332, 333] of *P. berghei* ANKA. RNA was isolated and sequenced as described [334]. To determine transcript abundance, FPKM values were calculated for all genes (FPKM: Fragments Per Kilobase of transcript per Million mapped reads) using Cuffdiff 2 algorithm [335]. A cut-off threshold of 21 FPKM was calculated; data below this value was considered absence of expression and is not shown. Data presented

is from two independent experiments for rings, trophozoites, schizonts, gametocytes and ookinetes 16 h, and from one experiment for ookinetes 24 h.

Reverse Transcriptase-PCR (RT-PCR)

Immunoprecipitation (IP) of DOZI::GFP and CITH::GFP parasite lysates, and subsequent RNA extraction and RT-PCR were performed as described [108]. To investigate the transcription patterns of the different *dhhc* genes by RT-PCR, RNA from different life cycle stages were obtained using TRIzol® Reagent (Ambion®, #15596). Reverse transcription was done with random primers and oligo-d(T) using SuperScript® II Reverse Transcriptase (Invitrogen™, #18064). RNA sample origins were as follows: asexual blood stages from line HPE; mixed blood stages (asexuals & gametocytes) and oocysts d12 post-infection (p.i.) from line Fluo-frmg; *in vitro*-cultured ookinetes at different time points from line cl15cy1; midgut sporozoites d20 p.i. and salivary gland sporozoites d20 p.i. from line PbGFPcon; and exoerythrocytic forms from line PbGFPcon at different time points after mouse infection. Primers used in RT-PCRs are shown in **Table S1a**.

Generation of *dhhc* gene deletion mutants

To disrupt genes encoding the three different DHHC members (*dhhc2,* PBANKA_010830; *dhhc3*, PBANKA_092730 and *dhhc10*, PBANKA_051200) we constructed standard replacement constructs [318] using plasmid pL0001 (www.mr4.com) which contains the pyrimethamine resistant *Toxoplasma gondii* (*tg*) *dhfr/ts* as a selectable marker cassette. See **Table S2** and **Figure S2A** for the names and details of the constructs. Target sequences for homologous recombination were PCR amplified from *P. berghei* wild-type (WT) genomic DNA using primers specific for the 5′ or 3′ flanking regions of the different *dhhc* genes (see **Table S1b** for the sequence of the different primers). The PCR–amplified target sequences were cloned in plasmid pL0001 either upstream or downstream of the selectable marker to allow for integration of the construct into the genomic target sequence by homologous recombination. DNA constructs used for transfection were obtained after digestion of the replacement constructs with the appropriate restriction enzymes (**Table S2**). Transfection, selection and cloning of mutant parasite lines were performed as described [318]; see **Table S2** for details of the transfection experiments performed. Correct deletion of the *dhhc10* gene was confirmed by diagnostic PCR (for primers see **Table S1c**) and Southern analysis of Field-Inversion Gel Electrophoresis (FIGE)-separated chromosomes (**Figure S2B**). Chromosomes were hybridized with a probe recognizing the 3' UTR of *pbdhfr/ts*. Absence of *dhhc10* mRNA was determined by RT-PCR analysis (**Figure S2C**) using RNA collected from infected blood containing asexual blood stages and gametocytes (see **Table S1c** for primers used for RT-PCR). Two cloned lines

were used for further phenotype analyses: 2097cl1 (Δ*dhhc10*-a, in the Fluo-frmg background) and 2365cl2 (Δ*dhhc10*-b, in the PbGFP-LUCcon background).

Generation of transgenic lines expressing GFP-tagged DHHC members

In situ C-terminal GFP tagging of *dhhc2*, *dhhc3* and *dhhc10* was performed by single cross-over homologous recombination into the corresponding *locus*. See **Table S2** and **Figures S3 and S5-S8, A** for the names and details of the constructs. All constructs contain the *tgdhfr*/*ts* selectable marker. Primers used to amplify the targeting regions of *dhhc2*, *dhhc3* and *dhhc10*, corresponding to the 3' end of each open reading frame (ORF) excluding the stop codon, as well as the 3' UTRs of *dhhc2* and *dhhc3* are listed in **Table S1b**. Targeting regions were cloned in frame with *gfp*. Linearised plasmids were transfected into cl15cy1 parasites using standard methods. Transfection, selection and cloning of mutant parasite lines were performed as described [318], resulting in the following transgenic lines: 2185cl1m1 (*dhhc2*::*gfp*), 192cl1m1 (*dhhc3*::*gfp*), 2187cl1m1 (*dhhc10*::*gfp*), 202cl1m1 (*dhhc2*::*gfp*-3'UTR) and 198cl1m1 (*dhhc3*::*gfp*-3'UTR). See **Table S2** for details of the transfection experiments performed. Correct integration of the constructs was confirmed by diagnostic PCR (for primers see **Table S1c**) and Southern analysis of FIGE-separated chromosomes using a probe for the 3' UTR of *pbdhfr*/*ts* (**Figures S3 and S5-S6, B**). Transcription and processing (splicing) of *gfp* fusions were confirmed by RT-PCR using RNA from mixed blood stage forms (**Figures S3 and S5-S8, C**). Primers used for RT-PCR are listed in **Table S1c**.

Generation of *dhhc10* gene deletion parasites expressing GFP-tagged PbLAP2

In situ C-terminal GFP tagging of *lap2* was performed by single cross-over homologous recombination into the corresponding *locus* using a construct published elsewhere [212]. This construct contains the human *dhfr*/*ts* selectable marker. Linearised plasmid was transfected into Δ*dhhc10*-a parasites using standard methods. Transfection was performed as described [318], and selection of mutant parasites was performed with the drug WR99210 [336], resulting in the following transgenic line: 2433 (Δ*dhhc10*;*lap2*::*gfp*). See **Table S2** for details of the transfection experiment performed. Correct integration of the construct was confirmed by Southern analysis of FIGE-separated chromosomes using a probe for the human *dhfr*/*ts* (**Figure 7A**).

In vivo multiplication rate of asexual blood stages

The multiplication rate of asexual blood stages in mice is determined during the cloning procedure of gene-deletion/transgenic parasites [319] and is calculated as follows: the percentage of infected erythrocytes in OF-1 mice injected with a single parasite is quantified at days 8–11 on Giemsa-stained blood films. The mean asexual multiplication rate per 24 h is then calculated assuming a total of 1.2×10^{10} erythrocytes per mouse and a blood volume of 2 mL. The percentage of infected erythrocytes in mice infected with reference lines of the *P. berghei*

ANKA strain consistently ranges between 0.5 and 2% at day 8 after infection, resulting in a mean multiplication rate of 10 per 24 h [319, 320].

Gametocyte production, *in vitro* fertilisation and ookinete formation assays

Gametocyte production of the different parasite lines was determined as described [333]. The gametocyte conversion rate is defined as the percentage of ring-forms that develop into gametocytes in standard synchronized *in vivo* infections in mice. *In vitro* fertilisation and ookinete formation assays were performed following published methods using gametocyte-enriched blood collected from mice treated with phenylhydrazine/NaCl [337]. Briefly, infected blood containing gametocytes was mixed in standard ookinete culture medium in 24-well plates and cultures were incubated for 18-24 h at 21-22 °C. The ookinete conversion rate is defined as the percentage of female gametes that develop into mature ookinetes determined by counting female gametes and mature ookinetes in Giemsa-stained blood smears 16-18 h after *in vitro* induction of gamete formation.

Palmitoyl-S-acyl-transferase inhibition during ookinete development, sporozoite gliding and liver cell traversal and invasion

To inhibit palmitoylation during ookinete development, 2-BMP (Sigma-Aldrich®, #21604) was added 1 h after adding *dhhc2*::*gfp* infected blood containing gametocytes to standard ookinete cultures as described above. 2-BMP was added at final concentrations of 0.01, 0.1, 0.25, 0.5, 1, 10, 25 and 100 µM. Since 2-BMP is prepared in dimethyl sulfoxide (DMSO), control cultures were set up in the presence (+) and absence (-) of DMSO. Eighteen hours after drug addition the different developmental stages (zygotes, developing ookinetes and mature ookinetes) were counted in Giemsa-stained slides according to the classification in [333]. Percentages from 2 independent experiments are presented for 0 (+), 0.01, 0.1, 0.25, 0.5, 25 and 100 µM 2-BMP, while data for 0 (-), 1 and 10 µM 2-BMP are from 4 independent experiments. To test the effect of palmitoylation inhibition on sporozoite gliding, parasites were dissected from infected mosquito salivary glands in PBS followed by incubation in RPMI/BSA containing 2-BMP for varying concentrations (0, 0.1, 1 and 100 µM) and times (15, 30 and 45 min). Movies were taken on a Zeiss Axiovert 200M widefield microscope (25X objective); frame-rate 3 sec for a duration of 4 min. The velocity was determined by using the manual tracking plug-in of ImageJ 1.47n software (imagej.nih.gov/ij). To evaluate the importance of palmitoylation in the sporozoite ability to traverse and invade hepatocytes *in vitro*, salivary gland sporozoites of line PbGFPcon were dissected and incubated with 100 µM of 2-BMP or equivalent volume of DMSO for 45 min on ice. 19000 sporozoites were then loaded, in the presence of 0.5 mg/mL of Dextran, Tetramethylrhodamine (Molecular Probes®, #D1817), onto 110000 Huh7 cells plated 16-20 h before in 24 well-plates and incubated for 1 h and 45 min at

37 °C. In each experiment, 2-3 replicate wells were analysed for both control (DMSO) and 2-BMP-treated sporozoites. Cells were then washed, trypsinised and analysed in a BD Biosciences® FACSCalibur flow cytometer. Percentage of traversal was quantified as the ratio of Dextran positive cells per live cells, while percentage of invasion was quantified as the ratio of GFP positive cells per live cells.

Transmission electron microscopy of ookinetes

WT (Fluo-frmg) and Δ*dhhc10*-b *in vitro* ookinete production followed by transmission electron microscopy was performed as previously described [330] with an additional post-staining step: prior to specimen imaging, 100 nm-thick sections were post-stained for 10 minutes at room temperature (RT) with 7% uranyl acetate in ultrapure water and 5 minutes at RT with lead citrate prepared according to Reynolds' method [338].

Oocyst production, sporozoite production and transmission experiments

Oocyst and sporozoite production of the mutant parasites was analysed by performing standard mosquito infections. Naïve female Balb/c ByJ mice were infected intraperitoneally (i.p.) with 10^6 infected red blood cells (iRBCs) of each line. On days 4-5 p.i., these mice were anesthetised and *Anopheles stephensi* female mosquitoes allowed to feed for 30 min. Twenty-four hours after feeding, mosquitoes were anesthetised by cold shock and unfed mosquitoes were removed. Oocyst and sporozoite numbers were counted at days 12-13 and 20-22 after mosquito infection, respectively. Oocyst sizes over time were determined at days 14 and 21/22 p.i. Oocysts were counted after mercurochrome staining and measured using ImageJ 1.47n software (imagej.nih.gov/ij). Sporozoites were counted in pools of 5 to 25 mosquitoes. To test the infectivity of sporozoites, 10 infected mosquitoes were allowed to feed for 30 min on anesthetised naïve female Balb/c ByJ mice on days 20-21 p.i. Successful feeding was confirmed by the presence of blood in the abdomen of mosquitoes. Blood stage parasitaemias in these mice were followed up to 32 days post-bite.

Western analysis of CSP expression in Δ*dhhc10* oocysts

To determine circumsporozoite protein (CSP) expression, Fluo-frmg- and Δ*dhhc10*-a-infected midguts were dissected at day 13 p.i. and resuspended in 1X Laemmli buffer. Samples were adjusted to 200 mM DTT, boiled and volumes equivalent to 2 midguts were loaded per SDS-PAGE gel lane for each parasite line. Nitrocellulose membranes were blocked for 1 h at RT with 5% skim milk/PBS-Tween 20 (0.05%), probed overnight at 4 °C with 3D11 mouse anti-CSP [321], 0.17 µg/mL in blocking solution) or parasite-specific 2E6 mouse monoclonal anti-PbHSP70 [322], 7.5 µg/mL in blocking solution) as primary antibodies, and 1h at RT with goat

anti-mouse IgG-HRP [Santa Cruz Biotechnology, Inc.®, #sc-2005, 1:5000-1:10000 in PBS-Tween 20 (0.05%)] as secondary antibody. Westerns were developed with Immobilon™ Western Chemiluminescent HRP Substrate (Millipore, #P36599). Staining with the antibody recognizing *P. berghei* HSP70 was used as loading control.

Live imaging and immunofluorescence assays (IFAs) of blood stages, ookinetes, oocysts and sporozoites

Live imaging of transgenic parasites expressing GFP-tagged DHHC-PATs and GFP-tagged LAP2 was done by collecting tail blood samples from infected mice, samples from ookinete cultures or mosquito blood meals at 16 h p.i., as well as dissected mosquito midguts, midgut sporozoites and salivary gland sporozoites and staining with 1 µg/mL of Hoechst 33342/PBS. DHHC2::GFP and DHHC3::GFP expression in live activated male and female gametocytes was visualized 10-15 minutes after adding infected blood to standard ookinete culture medium. To detect DHHC10::GFP expression in blood stages by IFA, mouse RBCs infected with *dhhc10*::*gfp* parasites were stained with rabbit polyclonal anti-GFP (Abcam®, #ab6556; 1:500) as primary antibody. As secondary antibody, goat anti-rabbit IgG-Alexa Fluor®488 (Jackson ImmunoResearch Laboratories, Inc., #111-545-003; 1:500) was used. To detect CSP expression in Fluo-frmg and Δ*dhhc10*-a oocysts, parasites at day 14 p.i. were stained with 3D11 mouse anti-PbCSP [321] (10 µg/mL) as primary antibody and goat anti-mouse IgG-Cy™3 (Jackson ImmunoResearch Laboratories, Inc., #115-166-003; 1:400) as secondary antibody. In all IFAs, samples were fixed with 4% PFA/PBS for 10 min at RT, permeabilised with 0.1-0.5% TritonX-100/PBS and blocked for 1h at RT with 1-3% BSA/PBS. All antibody incubations were done in blocking solution for 1h at RT and 1-5 ug/mL of Hoechst-33342/PBS was used to stain nuclei. Images were taken with a Leica DM5000B, Leica DM IRBE or Zeiss Axiovert 200M fluorescence microscope and processed using ImageJ 1.47n software (imagej.nih.gov/ij).

Statistical methods

Statistical analyses of oocyst and sporozoite numbers, oocyst sizes and *in vitro* hepatocyte traversal and invasion in the presence of the palmitoylation inhibitor 2-BMP were performed using Mann-Whitney test as part of Prism software package 5 (GraphPad Software).

RESULTS

Palmitoylation is essential for ookinete development

Palmitoylation is essential for schizogony, the ordered formation of 16-32 progeny from a single merozoite by asexual, mitotic division in the infected red blood cell [227]. Here we

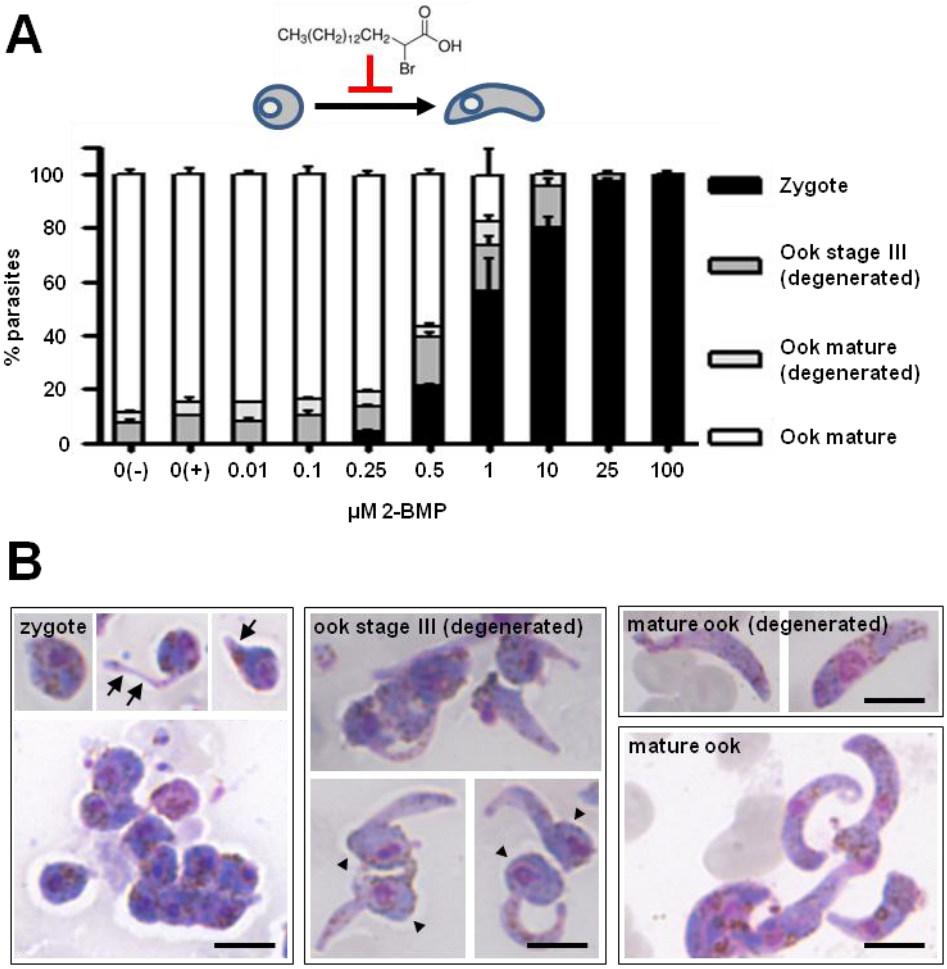

Figure 1 – Inhibition of protein palmitoylation arrests ookinete development.
(A) Effect of different 2-BMP concentrations on ookinete (ook) development; blockade of zygote-to-ookinete transformation is dose dependent. Control cultures were set up in the presence (+) and absence (-) of DMSO (vehicle). Bars and lines correspond to mean and SEM values, respectively. **(B)** Representative images of the Giemsa-stained developmental stages observed in cultures treated with 2-BMP. Stage I/II zygotes often show small protrusions (arrows), while degenerated stage III ookinetes are identified by long protrusions and a posterior bulb containing the nucleus (arrowheads). Scale bars = 5 µm.

investigated the role of palmitoylation during transmission of the rodent malaria *P. berghei* parasite to the mosquito vector. Following fertilization, the round zygote stage develops into the mature, banana-shaped ookinete within 24 hours. To test whether palmitoylation is required for this transformation process we used the inhibitor 2-bromopalmitate (2-BMP). 2-BMP was added in a 0.01 to 100 µM range to standard *in vitro* ookinete cultures [333] one hour after activation of gametocytes, the time point when gamete formation and fertilisation are completed. The development of ookinetes was determined 18 hours later. In control cultures without drug

(vehicle only) a mean of 77% (range 68-89%, *n*=3) of female gametocytes were fertilised and developed into mature ookinetes with WT morphology. We observed a clear dose-dependent effect of 2-BMP on the transition of zygotes into ookinetes (**Figure 1A**). Ookinete development was completely blocked soon after fertilization at concentrations of 100, 25 and 10 µM resulting in the presence of large clusters of stage I/II zygotes (round zygotes or such with small, thin protrusions) (**Figure 1B**). At 1 µM more than 50% of the parasites were arrested at the zygote I/II stage; only a small percentage of parasites was able to form mature ookinetes. As little as 0.25 µM of 2-BMP was effective in interfering with ookinete formation.

A characteristic feature of the inhibition effect is the small protrusions seen to emanate from zygotes; these are normally formed in the transformation from zygotes to ookinetes and the developmental arrest at these stage could indicate a membrane and protein trafficking defect associated with the inner membrane complex (IMC) or the plasma membrane (PM). Overall, these experiments prove that palmitoylation is an essential process for ookinete development and morphogenesis.

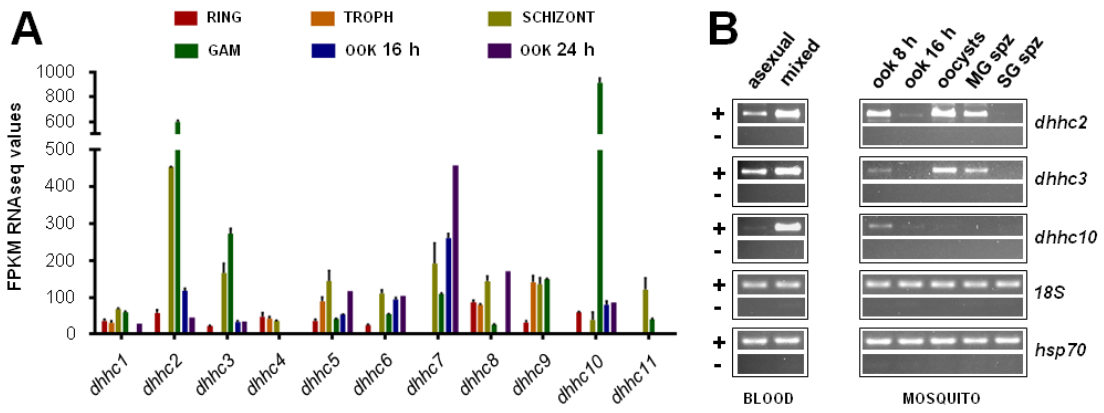

Figure 2 – mRNA expression of *P. berghei dhhc* genes.
(A) RNA sequencing (RNAseq) data from blood and early mosquito stages for all 11 *P. berghei dhhc* genes. *dhhc2*, *dhhc3* and *dhhc10* are upregulated in gametocytes. Bars and lines correspond to mean and SEM values, respectively. Troph: trophozoite; Gam: gametocyte; Ook: ookinete (16 and 24 hours after gametocyte activation); FPKM: Fragments Per Kilobase of transcript per Million mapped reads. **(B)** RT-PCRs of *dhhc2*, *dhhc3* and *dhhc10* along the life cycle. Asexual: asexual blood stages; mixed: asexuals and gametocytes; ook: ookinetes (8 and 16 hours after gametocyte activation); MG spz: midgut sporozoites; SG spz: salivary gland sporozoites. *18S* rRNA and *hsp70* serve as loading control genes. +: RT positive reaction; -: RT negative reaction.

Candidate palmitoyl-S-acyl-transferases involved in *P. berghei* mosquito stage development

Having established a crucial role for palmitoylation during ookinete formation we sought to identify the DHHC-PATs involved. With 11 described *P. berghei* DHHC-PATs we reviewed published RNA and protein expression data focussing on gametocytes, since many proteins and translationally repressed mRNAs are provided by the female gametocyte for post-

fertilization development [50, 108]. The immediate inhibitory effect of 2-BMP for ookinete development supported the involvement of one (or several) PATs with such transcriptional and translational profile.

Three *dhhc-pat* mRNAs (*dhhc2*, *3* and *10* according to *P. falciparum* nomenclature) had already been identified with reduced transcript levels in cells that lack the translational repressor DOZI [107] (**Table S3**) pointing towards a possible role of translationally repressed DHHC-PATs for ookinete development. Genome-wide RNAseq analysis of gametocytes and ookinetes (T.D. Otto, M. Berriman, A. Religa, A.P. Waters W.A.M. Hoeijmakers, H.G. Stunnenberg and C.J. Janse, unpublished data) highlighted the same three DHHC-PATs to be transcriptionally upregulated in gametocytes compared to asexual blood stages (**Figure 2A**). We confirmed the RNAseq data by RT-PCR and performed additional expression profiling of the three genes across the life cycle of *P. berghei* (**Figure 2B**). This revealed *dhhc2* and *dhhc3* expression in asexual blood stage forms and young (but not mature) ookinetes with an apparent second wave of transcription in oocysts and midgut sporozoites. *dhhc10* on the other hand was specifically transcribed in gametocytes and immature ookinetes. None of the transcripts could be detected in salivary gland sporozoites or liver stage parasites (**Figure 2B and Figure S1**).

Five *P. berghei* DHHC-PATs have recently been detected in blood stage parasites using an haemagglutinin (HA) tagging approach [233]; of these, three *P. falciparum* orthologs were known from proteome studies of intraerythrocytic forms and salivary gland sporozoites [339-341].

Out of the 11 *P. berghei* DHHC-PATs, only two (DHHC1 and DHHC4) were reported in proteome studies from gametocytes, albeit in 'mixed gametocyte proteome' rather than the highly purified male- or female-specific proteomes [50] and none were detected in zygote or ookinete proteomes [49, 325, 326]. Seven were found to be redundant for blood stage development in a gene deletion screen [233] (**Table S3**).

DHHC2 and DHHC3, but not DHHC10 are required for asexual *Plasmodium* development

To investigate whether any of the three DHHC-PATs identified above is essential for development of the ookinete we attempted to generate null mutants for each gene. Using standard methods of *P. berghei* genetic modification [318] we targeted each gene for deletion by double cross-over homologous recombination of a plasmid containing a *T. gondii* dihydrofolate reductase/thymidylate synthase (*tgdhfr*/*ts*) selectable marker. Three independent transfection experiments for *dhhc2* and *dhhc3* were unsuccessful (**Table S2**) suggesting a vital role for both proteins during asexual blood stage development; perhaps not surprising given the expression profile revealed by RT-PCR (**Figure 2B**).

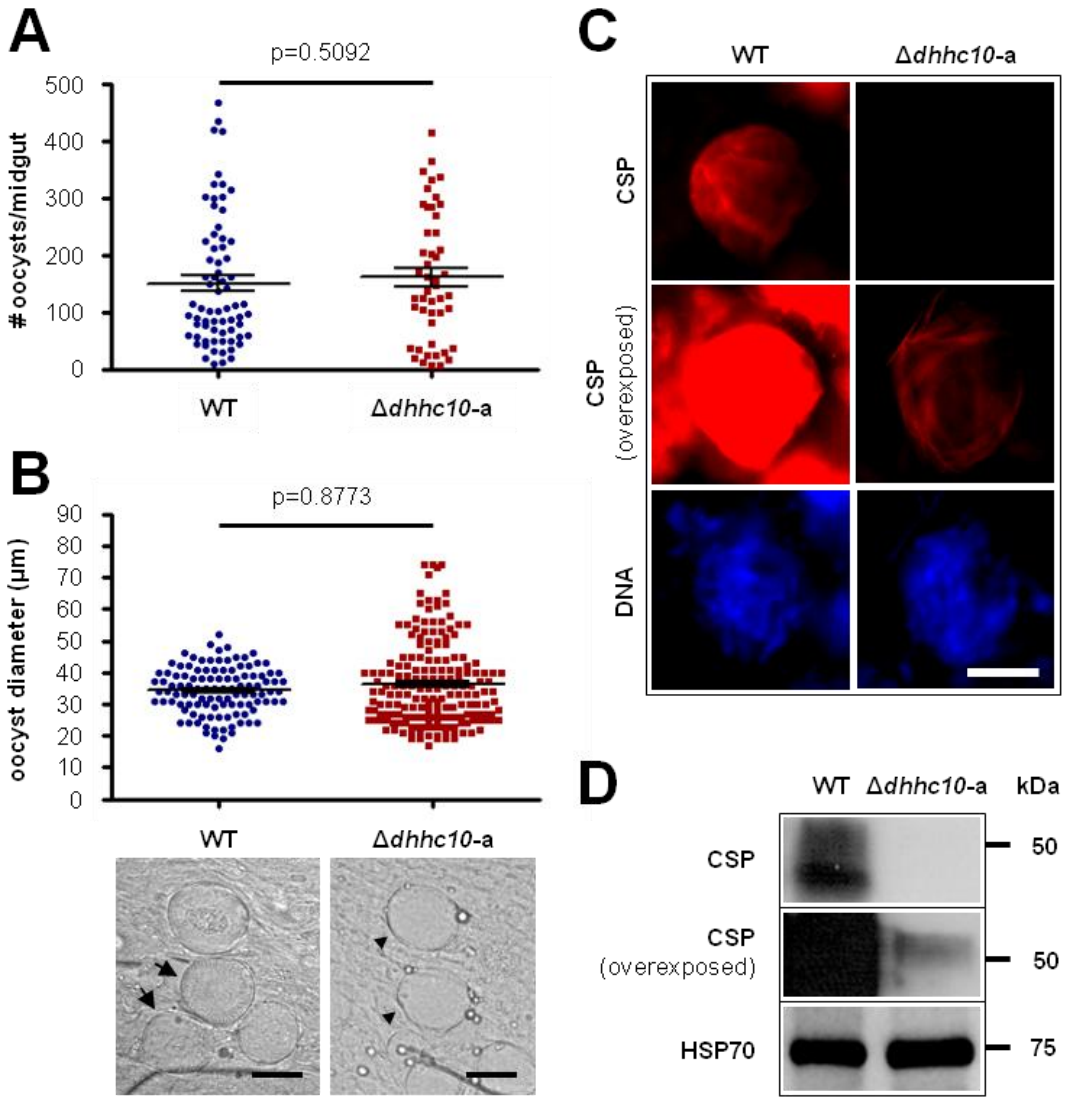

Figure 3 – Δ*dhhc10* oocysts do not sporulate and lack circumsporozoite protein.
(A) Δ*dhhc10*-a parasites show WT oocyst numbers on days 12 to 13 p.i. Absolute numbers of oocysts per midgut from 5 independent experiments are presented for both WT (*n*=70) and Δ*dhhc10*-a (*n*=48) parasites. **(B)** At day 14 p.i. Δ*dhhc10*-a oocysts have normal sizes (upper plot) but lack signs of sporulation and appear 'empty' (bottom pictures, arrowheads). On the contrary, most WT oocysts have already formed sporozoites inside (arrows). Scale bars = 20 µm. **(A-B)** Mean and SEM values are shown by the lines; p-values for Mann-Whitney test are shown above the data sets. **(C)** Immunofluorescence assay of oocyst-infected midguts at day 14 p.i. shows strongly reduced CSP expression (in red) in Δ*dhhc10*-a parasites. DNA replication in both parasite lines is comparable, as seen by Hoechst-33342 staining (in blue). Scale bar = 20 µm. **(D)** Western blot analysis of oocyst-infected midguts at day 13 p.i. confirms diminished CSP expression in Δ*dhhc10*-a mutants. HSP70 serves as parasite loading control. **(C-D)** Note that when CSP is detected in Δ*dhhc10*-a oocysts, signal coming from WT oocysts is already saturated.

On the other hand, we were able to select gene deletion mutants for *dhhc10* in two independent experiments (**Table S2**). Genotyping by diagnostic PCR and Southern analyses confirmed correct disruption of the *dhhc10* gene (**Figure S2**). Phenotype analyses of the two independent *dhhc10* null mutants, Δ*dhhc10*-a and Δ*dhhc10*-b, during blood stage development revealed normal asexual growth/multiplication and gametocyte production rates (**Table S4**).

DHHC10 is an essential factor for *P. berghei* sporozoite development

To establish a possible role for DHHC10 during mosquito infection (ookinete formation, midgut invasion and establishment of oocysts) and sporogony, we allowed *Anopheles stephensi* mosquitoes to feed on mice infected with Δ*dhhc10* parasites. Null mutants produced oocyst numbers that were comparable to those after infection with WT parasites (**Figure 3A**). Δ*dhhc10* mutants were thus not compromised in their ability to form infection-competent, motile ookinetes and establish oocysts that resist elimination by the invertebrate host's immune system. Following the development of these oocysts up to 22 days post-infection (p.i.) however revealed a complete failure in sporulation. Although similar in size to WT oocysts at day 14 p.i., mutants displayed an 'empty' appearance (**Figure 3B**) and lacked expression of CSP, the major sporozoite surface protein. While CSP is strongly expressed in WT oocysts of the same age, neither IFAs (**Figure 3C**) nor Western analysis (**Figure 3D**) of protein extracts from pooled infected midguts showed persuasive expression of this marker in Δ*dhhc10* parasites. On the other hand, labelling of cells with the DNA-specific dye (Hoechst-33342) revealed extensive staining throughout the mutant oocysts, suggesting that DNA replication was not affected in the absence of DHHC10 (**Figure 3C**).

At days 21/22 p.i. mutant oocysts were still present in mosquito midguts; they were enlarged compared to WT oocysts with the same 'empty', vacuolated appearance (**Figure 4A**). Indeed, Δ*dhhc10* oocysts were already significantly enlarged at day 19 p.i. (data not shown). Mosquitoes from the same cohort were unable to infect naïve mice (**Figure 4B**) and both midguts (**Figure 4C**) and salivary glands (**Figure 4D**) finally revealed a complete absence of sporozoites in both Δ*dhhc10*-a and Δ*dhhc10*-b mutants.

GFP tagging of DHHC10 reveals translational repression and highlights localisation to the ookinete CB

The ability of Δ*dhhc10* mutants to generate normal numbers of oocysts but failure to produce sporozoites was unexpected in view of the tight period of transcription observed by RT-PCR and RNAseq analyses; mRNA was only detected in gametocytes and young ookinetes but absent from all other stages examined (**Figures 2A and B**). The normal development of gametocytes, zygotes and ookinetes suggested that translation of *dhhc10* mRNA provided by the gametocyte could be postponed as late as oocyst formation. Alternatively, protein translated

in the ookinete may simply be redundant for ookinete development and stored for later use in the oocyst. In recent papers we [330] and others [208] had identified genes transcribed in the gametocyte to be key factors for sporogony.

In order to analyse DHHC10 protein expression we generated a mutant that expresses a GFP-tagged version of the protein. Tagging was performed using a construct that integrates by single cross-over recombination resulting in a C-terminal fusion under the transcriptional control of the endogenous promoter and absence of WT gene expression. We were able to select a line (*dhhc10*::*gfp*) with correct tagging of the gene *locus* (**Figure S3**). This mutant showed normal progression throughout the life cycle, including ookinete production and transmission to mice via mosquito bite (**Table S4**). GFP tagging of DHHC10 did thus not affect

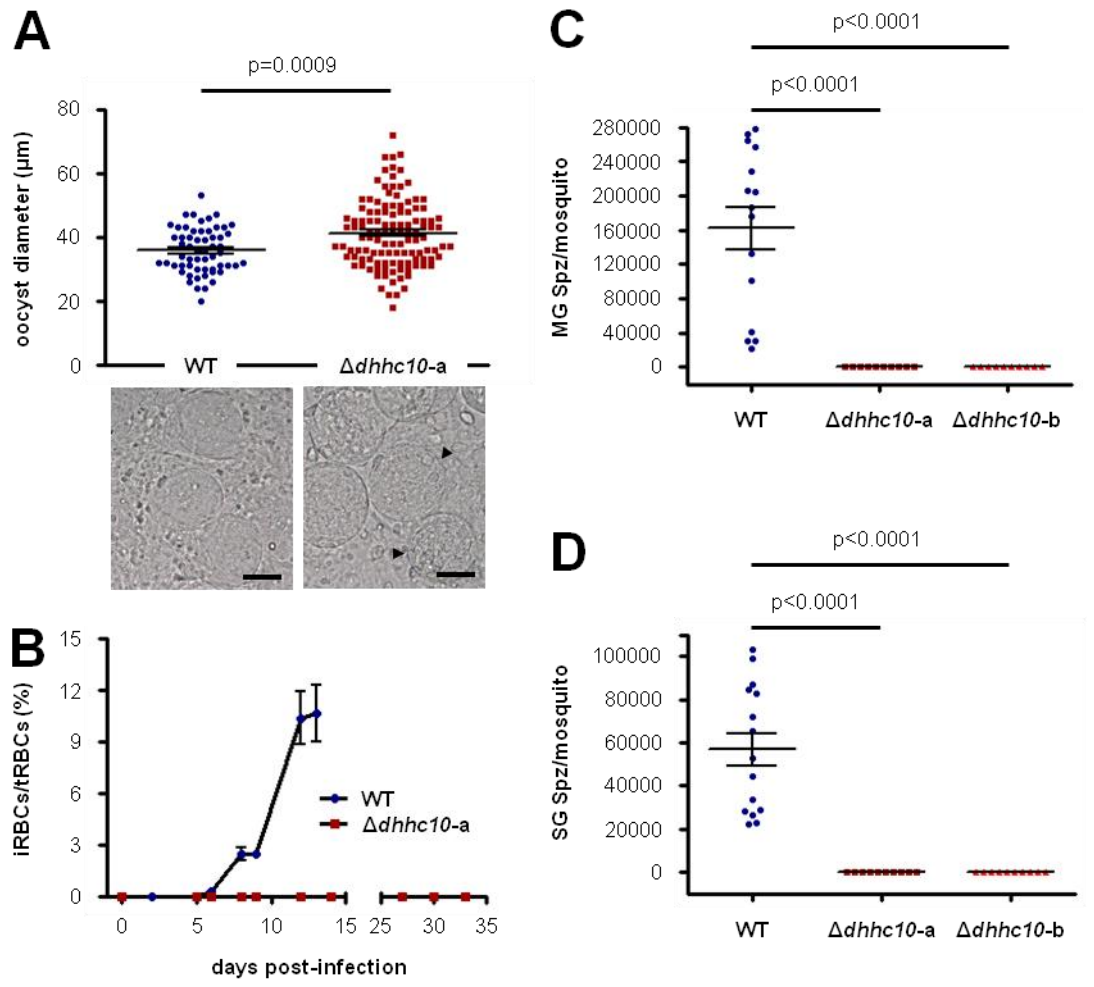

Figure 4 – Δ*dhhc10* mutants are impaired in sporozoite development and do not transmit to naïve mice.
(A) At days 21/22 p.i. Δ*dhhc10*-a oocysts are clearly enlarged when compared to WT oocysts (upper plot) and often show an 'empty', vacuolated aspect (bottom pictures, arrowheads). Scale bars = 20 µm. **(B)** Mice bitten by Δ*dhhc10*-a-infected mosquitoes do not develop blood stage infection. Mean parasitaemias from 3 independent experiments are shown by the dots while SEM values are shown by the vertical lines. **(C)** Neither Δ*dhhc10*-a nor Δ*dhhc10*-b parasites develop any midgut sporozoite (MG Spz). **(D)** Δ*dhhc10*-a and Δ*dhhc10*-b parasites do not develop any salivary gland sporozoite (SG Spz). **(C-D)** WT (5 independent experiments, *n*=15); Δ*dhhc10*-a (4 independent experiments, *n*=10); Δ*dhhc10*-b (1 experiment, *n*=10). **(A, C-D)** Mean and SEM values are shown by the lines; p-values for Mann-Whitney test are shown above the data sets.

protein function or parasite viability.

Although transcribed in gametocytes and therefore matching WT *dhhc10* transcription (**Figure 5A**), DHHC10::GFP was not detected until ookinete formation (**Figure 5B**). Consistent with translational repression (TR) and storage of this transcript in DOZI/CITH-defined messenger ribonucleoproteins (mRNPs) for translation in the ookinete, *dhhc10* co-immunoprecipitated with DOZI::GFP and CITH::GFP [107, 108] in a fashion similar to *p25* and *p28*, known translationally repressed mRNAs (**Figure 5C**).

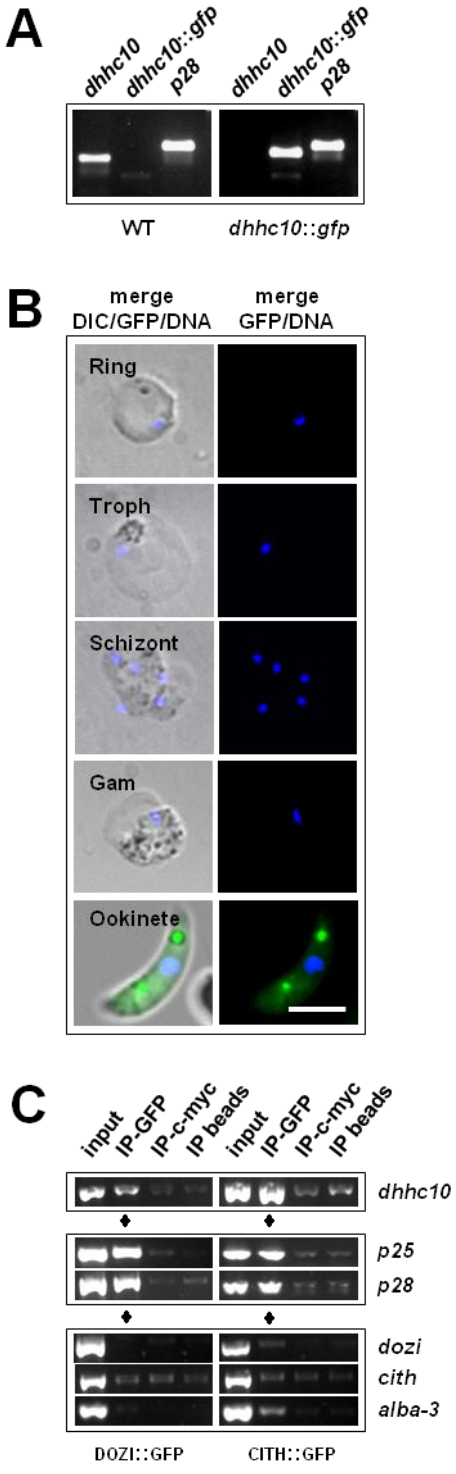

In live ookinetes DHHC10::GFP highlighted distinct cytoplasmic foci (**Figure 5B**) known for members of the LAP/CCp protein family and thus typical for CBs [208, 212]. These transient organelles are specific to ookinetes and early oocysts and thought to act as a reservoir for proteins necessary for oocyst development [210, 215]. Focal localisation in one or two spots was observed in 70% of the ookinetes (*n*=60), and these co-localised with haemozoin (malaria pigment) clusters as seen by DIC microscopy. The remaining 30% showed a somewhat diffuse GFP signal throughout the ookinete cytoplasm; dim and diffuse fluorescence was also present in the ookinetes that presented clear DHHC10::GFP foci (**Figure S4**). GFP fluorescence was not observed in live oocysts or sporozoites (data not shown), consistent with our RT-PCR data. The tagging experiments establish DHHC10 as the first enzyme localised to CBs.

Figure 5 – *dhhc10* is translationally repressed in gametocytes and expressed in ookinetes.
(A) RT-PCR analysis shows absence of WT *dhhc10* and presence of correctly spliced *dhhc10*::*gfp* mRNA in blood stages of *dhhc10*::*gfp* parasites. *p28* serves as control gene. **(B)** Immunofluorescence of *dhhc10*::*gfp* blood stage parasites shows no DHHC10 expression in asexual or sexual blood stages while live imaging of *in vitro*-cultured ookinetes shows DHHC10::GFP localisation (in green) in discrete foci. DNA was stained with Hoechst-33342 (in blue). Troph: trophozoite; Gam: gametocyte. Scale bar = 5 µm. **(C)** RT-PCR analysis on DOZI::GFP and CITH::GFP gametocyte immunoprecipitation (IP) eluates shows that *dhhc10* as well as *p25* and *p28* mRNAs (known to be translationally repressed) co-precipitate with DOZI and CITH. *dozi*, *cith* and *alba-3* are translated in gametocytes and are not enriched in the IP-GFP fractions. Input: total gametocyte mRNA; IP-GFP: IP with anti-GFP antibody; IP-c-myc: IP with anti-c-myc antibody; IP beads: no antibody used for IP.

Δ*dhhc10* ookinetes lack CBs

In vivo, Δ*dhhc10* mutants produced WT numbers of oocysts. *In vitro*, these mutants showed normal macrogametocyte to ookinete conversion rates (**Table S4**). Mutant ookinetes displayed a shape consistent with WT development and functionality and efficiently invaded mosquito midguts.

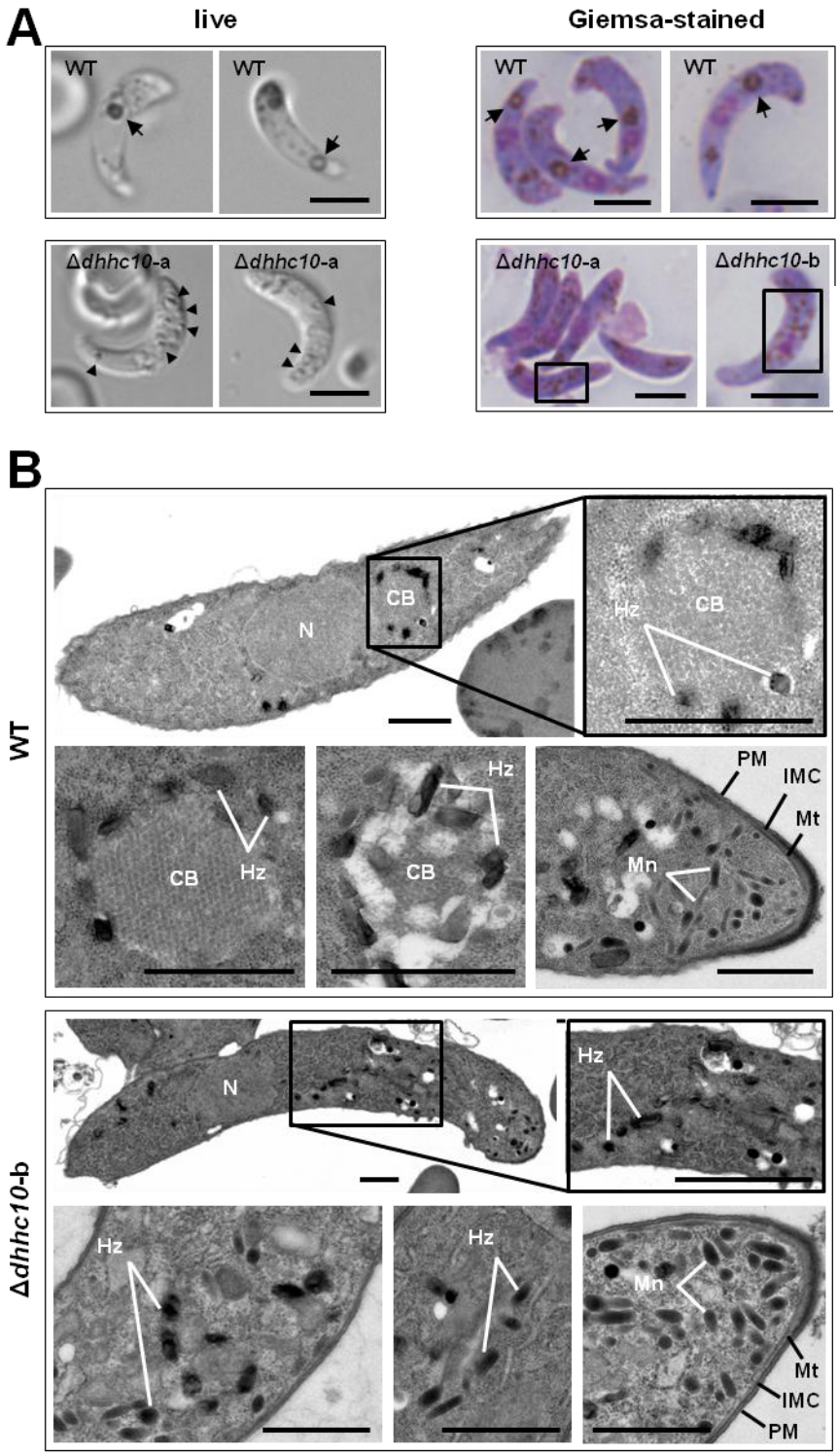

Figure 6 – Δ*dhhc10* ookinetes lack crystalloid bodies and associated haemozoin clusters. **(A)** WT ookinetes (top) show clear haemozoin clusters under live DIC microscopy or Giemsa-stained specimens (arrows). On the other hand, both Δ*dhhc10*-a and Δ*dhhc10*-b ookinetes (bottom) show haemozoin crystals dispersed in the cytoplasm (arrowheads and boxes). Scale bars = 5 µm. **(B)** Transmission electron microscopy confirms the absence of crystalloid bodies (CB) and CB-associated haemozoin (Hz) clusters in Δ*dhhc10*-b ookinetes. No differences were observed in the nucleus (N) nor in the apical complex which has a similar distribution and localization of micronemes (Mn) and arrangement of subpellicular microtubules (Mt), inner membrane complex (IMC) and plasma membrane (PM). Scale bars = 1 µm.

However, haemozoin clusters that typically surround and highlight CBs in WT *P. berghei* ookinetes [215, 216] (**Figure 6A, top**) were absent or dispersed throughout the cytoplasm of the mutants (**Figure 6A, bottom**) in live and Giemsa-stained specimens. This suggested that DHHC10 and palmitoylation are required for the formation and maintenance of CBs as well as the aggregation of haemozoin. However, this clearly did not affect invasion of the mosquito vector.

In transmission electron microscopy of WT ookinetes (**Figure 6B, top**) CBs appear highly ordered and surrounded by specks of haemozoin, the remnant of haemoglobin digestion by the intraerythrocytic, female gametocyte. WT parasites also show abundant micronemes at the apical complex, which are necessary for gliding motility and midgut epithelium invasion. Numerous micronemes can also be seen in the knock-out (KO) mutant (**Figure 6B, bottom**) explaining its WT invasion behaviour in the *in vivo* transmission experiments (**Figure 3A**). In 30 Δ*dhhc10*-b ookinetes analysed however we never observed characteristic CBs; instead, haemozoin crystals were scattered throughout the ookinete cytoplasm.

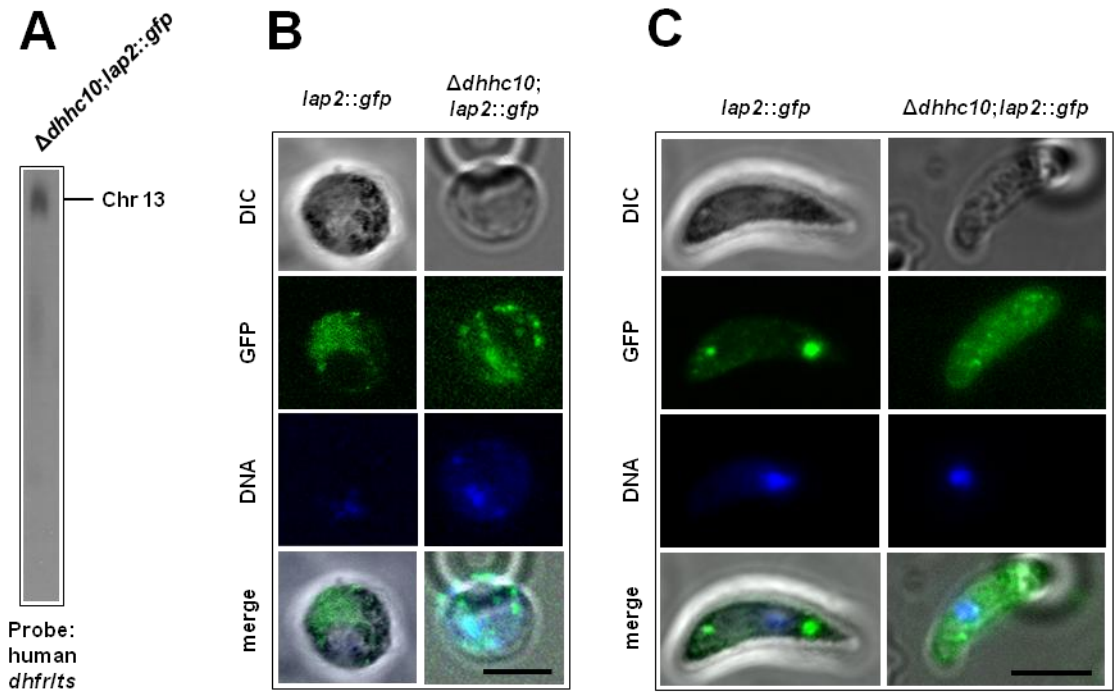

Figure 7 – Absence of crystalloid bodies in Δ*dhhc10* parasites leads to mislocalisation of LAP2. **(A)** Correct genomic integration of LAP2 GFP tagging construct into chromosome 13 of Δ*dhhc10*-a parasites was confirmed by Field-Inversion Gel Electrophoresis (FIGE) of separated whole chromosomes in uncloned Δ*dhhc10*;*lap2*::*gfp* parasite line. FIGE was developed using a probe for the human *dhfr*/*ts*. **(B)** Live imaging of WT and Δ*dhhc10*;*lap2*::*gfp* female gametocytes shows LAP2::GFP expression (in green) throughout the gametocyte cytoplasm in both parasite lines. **(C)** Live imaging of WT and Δ*dhhc10*;*lap2*::*gfp in vitro*-cultured ookinetes shows typical LAP2::GFP localisation (in green) in crystalloid bodies in WT parasites, while localisation in Δ*dhhc10*;*lap2*::*gfp* parasites is scattered throughout the ookinete cytoplasm. **(B-C)** DNA was stained with Hoechst-33342 (in blue). Scale bars = 5 µm.

To independently confirm CB absence in Δ*dhhc10* ookinetes and assess the consequences for CB-resident protein localisation we transfected the null mutant with a PbLAP2::GFP fusion construct [212]. The resulting Δ*dhhc10*;*lap2*::*gfp* parasites (**Figure 7A**) presented PbLAP2::GFP-positive female gametocytes (**Figure 7B**) where LAP2 is scattered throughout the cytoplasm as shown previously. While in WT ookinetes LAP2 is targeted and concentrated in CBs [212], the absence of DHHC10 resulted in LAP2::GFP protein remaining spread throughout the cytoplasm (**Figure 7C**), highlighting the importance of palmitoylation for CB formation and correct localisation of this known CB component. These experiments establish DHHC10 and palmitoylation as essential factors for CB biogenesis and function.

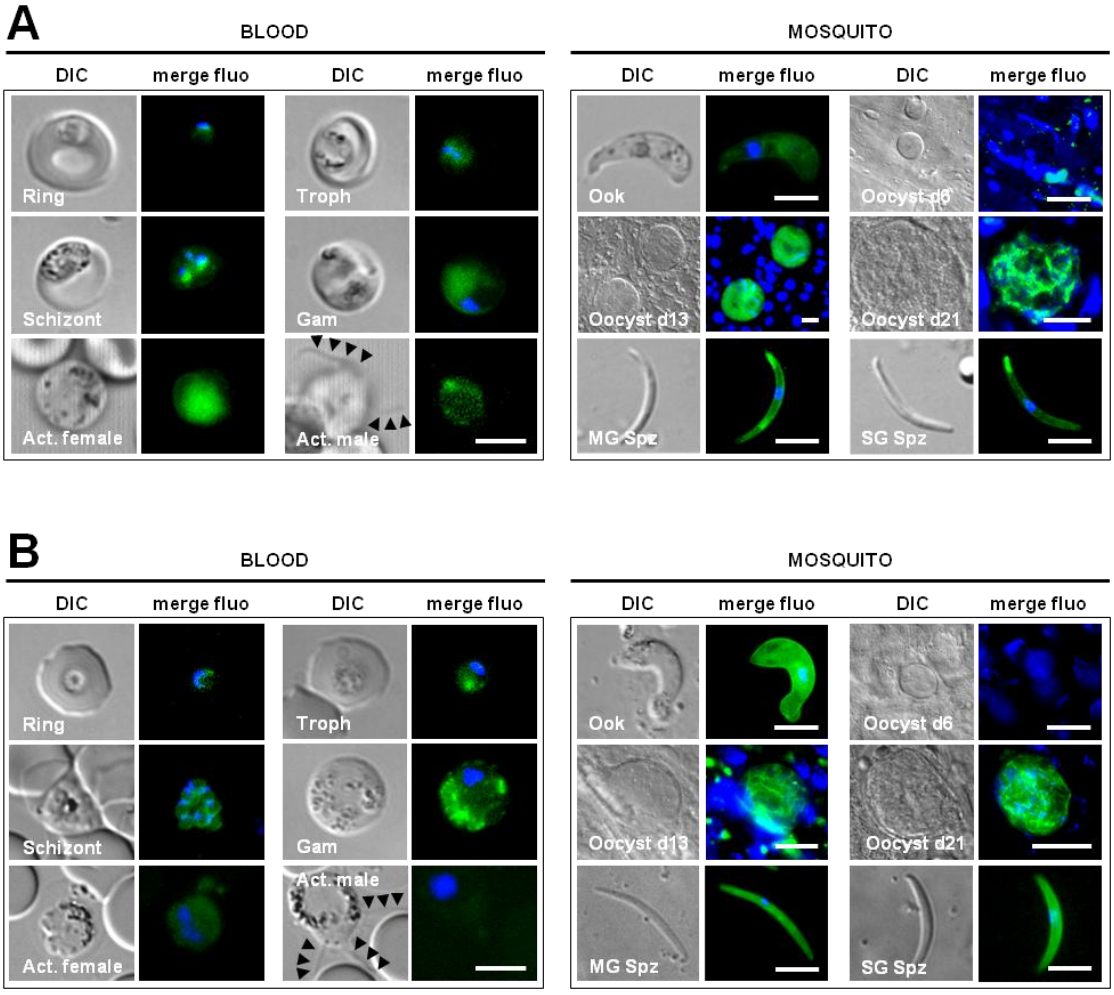

Figure 8 – DHHC2 and DHHC3 are expressed in blood and mosquito stages.
(A) Expression of DHHC2::GFP in live *dhhc2*::*gfp* parasites. **(B)** Expression of DHHC3::GFP in live *dhhc3*::*gfp* parasites. **(A-B)** DHHC2::GFP and DHHC3::GFP expression is shown in green while DNA was stained with Hoechst-33342 (in blue). Troph: trophozoite; Gam: gametocyte; Act. female: activated female gametocyte; Act. male: activated male gametocyte (male gametes projected from the male gametocyte are identified by the arrowheads); Ook: ookinete; Oocyst d6, d13 and d21: oocyst at days 6, 13 and 21 p.i.; MG Spz: midgut sporozoite at day 21 p.i.; SG Spz: salivary gland sporozoite at day 21 p.i. Scale bars = 5 µm (blood stages, ookinetes and sporozoites) or 20 µm (oocysts).

DHHC2 and DHHC3 GFP tagging reveals constitutive expression patterns

Since we were unable to delete *dhhc2* and *dhhc3*, we could not determine their potential functions in mosquito stage development. The unsuccessful attempts suggested an essential role during asexual blood stage development or perhaps a reduced accessibility of these *loci* for genetic modification. Therefore we targeted both genes for GFP tagging with constructs that integrate by single cross-over recombination resulting in a C-terminal fusion. For both genes we were able to select mutants (*dhhc2*::*gfp* and *dhhc3*::*gfp*) with correct tagging of the genomic *loci* proving that both *loci* are amenable to genetic modification (**Figures S5 and S6**). Both mutants showed normal blood and mosquito stages with WT morphology (**Figure 8 and Table S4**), indicating that the GFP tagging did not affect the function of these proteins.

Expression of DHHC2::GFP and DHHC3::GFP in different life cycle stages was determined by live fluorescence microscopy and displayed a similar pattern. Both DHHC2::GFP (**Figure 8A**) and DHHC3::GFP (**Figure 8B**) were detected in all asexual blood stages as well as in gametocytes and ookinetes. No expression was observed in young oocysts while oocysts undergoing sporogony expressed the fusion proteins. Sporozoites showed clear DHHC2::GFP signal, especially towards the apex, reminiscent of microneme or rhoptry localisation. On the other hand, DHHC3::GFP was evenly distributed throughout the sporozoite cytoplasm. In *dhhc3*::*gfp* schizonts, the GFP signal distribution towards the edges of the newly formed merozoites is indicative of IMC localisation. Localisation of DHHC3::GFP in ookinetes is also suggestive of association with the parasite PM or IMC.

In *dhhc2*::*gfp* and *dhhc3*::*gfp* parasites, the endogenous 3' untranslated regions (UTRs) have been replaced by that of *pbdhfr*/*ts*, a gene that does not undergo TR in female gametocytes [132]. TR of certain mRNAs in female gametocytes can be exerted through motifs found in their 3' UTRs, as in the case of *p28* [132]. To be certain that DHHC2::GFP and DHHC3::GFP expression in gametocytes reflects the true expression pattern of these proteins and rule out that TR-targeting motifs reside within the 3' UTRs of *dhhc2* and *dhhc3*, we generated C-terminally GFP-tagged mutants (*dhhc2*::*gfp*-3'UTR and *dhhc3*::*gfp*-3'UTR) that express these genes under the control of their own 5' and 3' UTRs (**Figures S7 and S8**). In these parasites, expression of DHHC2 and DHHC3 throughout the life cycle was confirmed to be the same as in lines *dhhc2*::*gfp* and *dhhc3*::*gfp* (**Figures S9A and B**).

Altogether, failure to delete *dhhc2* and *dhhc3* and successful tagging experiments, indicated that both proteins have an essential role in growth and/or multiplication of asexual blood stages. The observations of expression of the tagged proteins in mosquito stages, namely in oocysts and sporozoites, indicate that these proteins may also play a role in palmitoylation during sporogony or sporozoite function.

Palmitoylation influences sporozoite infectivity

The expression of both DHHC2 and DHHC3 in sporozoites suggested a possible role for these proteins and therefore for palmitoylation in sporozoite function. More specifically, the apical GFP distribution in *dhhc2*::*gfp* sporozoites, resembling micronemal or rhoptry localisation, pinpointed to a possible role for palmitoylation in parasite motility and/or invasion. To test this hypothesis we analysed gliding motility of salivary gland sporozoites in the presence of increasing concentrations of the PAT inhibitor 2-BMP for varying periods of time. Gliding motility

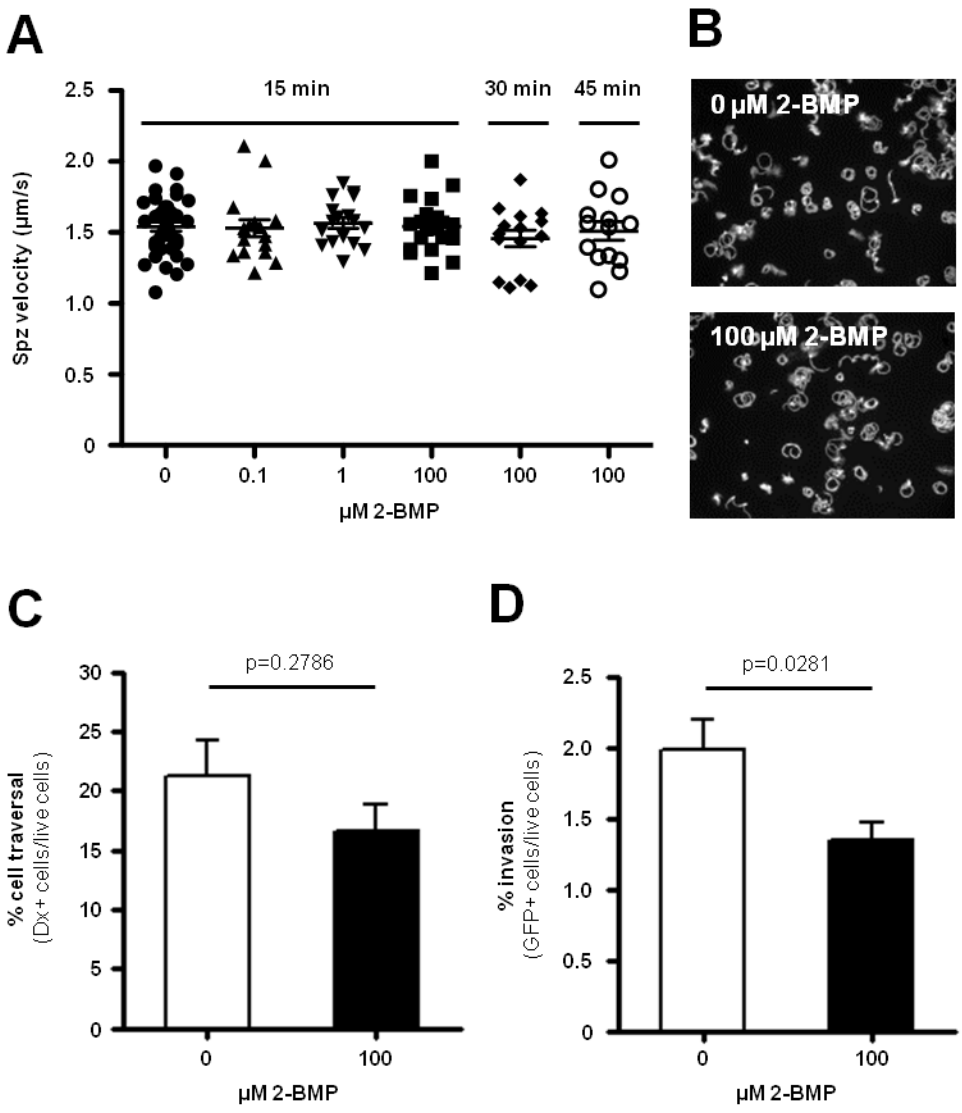

Figure 9 – Sporozoite invasion but not motility is dependent on protein palmitoylation.
(A) Live gliding motility movies of sporozoites (Spz) taken at different time points after 2-BMP addition in different concentrations did not show any differences in comparison with non-treated sporozoites (0 µM). Average speed of parasites was approximately 1.5 µm/s. **(B)** Maximum projections of gliding sporozoites in the absence (0 µM) and presence (100µM) of 2-BMP. **(C)** *In vitro* hepatocyte traversal is not affected by the presence (100µM) of 2-BMP. Dx+ cells: Dextran, Tetramethylrhodamine positive cells. **(D)** *In vitro* hepatocyte invasion levels are significantly reduced by drug inhibition of palmitoylation (100µM 2-BMP). **(C-D)** Mean percentages are shown by the bars while SEM values are shown by the vertical lines. Data corresponds to 3 independent experiments (*n*=8) for both treated and non-treated sporozoites; p-values for Mann-Whitney test are shown above the bars.

was assayed by generating 4-minute movies (frame-rate 3 seconds) followed by manual tracking of individual parasites. None of the experimental setups revealed any change in the number of moving parasites or in the speed or trajectories of treated sporozoites when compared to non-treated controls (**Figures 9A and B**).

Concordantly, when dissected salivary gland sporozoites were incubated for 45 min with 100 µM of 2-BMP, corresponding to the harshest condition tested in the above mentioned gliding assays, their *in vitro* hepatocyte traversal ability was not significantly altered (**Figure 9C**). On the other hand, hepatocyte invasion was significantly inhibited when sporozoites were treated with 2-BMP in the same way (**Figure 9D**). Altogether, this data clearly defines a functional role for palmitoylation in hepatocyte invasion by sporozoites, while not affecting gliding motility or liver cell traversal.

DISCUSSION

Post-translational modifications play an important role in protein function, localisation, trafficking, stability, conformation, interactions and signalling. The lipidation post-translational modification (PTM) designated palmitoylation has been the focus of much study in the last years. Being a reversible lipidation reaction, palmitoylation is now emerging as a key regulatory PTM in known and potentially novel molecular networks [342].

Our studies highlight for the first time the essential nature of protein palmitoylation for malaria parasite life cycle progression in the mosquito vector. Through the global inhibition of PATs and genetic studies we show that S-acylation is essential for zygote to ookinete development and sporozoite formation. The key finding of this study is the discovery of a single PAT (DHHC10) as an essential factor for the biogenesis of ookinete CBs. In the absence of this protein CBs fail to form and the CB-resident protein LAP2 mislocalises. While ookinete functionality remains unaffected, Δ*dhhc10* oocysts fail to undergo sporogony. Furthermore, we demonstrate that palmitoylation is required for optimal invasion of hepatocytes by sporozoites but redundant for parasite gliding motility. Finally, we provide strong evidence for the essential nature of two PATs (DHHC2 and DHHC3) for asexual blood stage development. On one hand this work establishes the universal role of palmitoylation as a regulator of key biological events during the entire *Plasmodium* life cycle; on the other hand the expression pattern and essential nature of DHHC10 emphasises the evolution of a specific PAT whose function is restricted to a very specific, narrowly timed phenomenon (CB biogenesis) that is, in its turn, crucial for sporogony.

We found ookinete formation to be extremely sensitive to the drug 2-BMP, a non-metabolisable palmitate analogue that blocks palmitate incorporation into proteins [343]. It is known that 2-BMP may exert metabolic pleiotropic effects [239]. However, zygote-to-ookinete transformation (ZOT) was inhibited at a concentration as low as 0.25 µM, corresponding to 400

times less drug than the concentration typically used to inhibit palmitoylation in other systems [239], and 200 to 400 times less than the concentrations known to affect *P. falciparum* blood stage schizogony [227]. As palmitoylation is a PTM known to alter protein localization and trafficking, the nature of the developmental abnormalities in zygotes/ookinetes following 2-BMP exposure suggests that defects in protein and membrane trafficking are responsible for the arrest in morphogenesis. While 2-BMP was previously shown to inhibit schizogony, it did not block nuclear division [227]. Similarly, we report that absence of sporozoite formation in Δ*dhhc10* oocysts takes place with no apparent arrest in DNA replication.

The shape of several *Plasmodium* life cycle stages (merozoite, ookinete and sporozoite) depends on the ordered arrangement of the subpellicular network and the IMC beneath the PM. At least 23 proteins are known to localise to the subpellicular network or are associated or inserted into the IMC (PlasmoDB version 11.0). Fourteen of those were found to be palmitoylated in *P. falciparum* asexual blood stage parasites [227] (**Table S5**); whether these proteins are present and post-translationally modified in the developing zygote/ookinete is not known. Of the 13 annotated alveolin/IMC/IMC sub-compartment proteins, 8 were part of the global *P. falciparum* blood stage palmitome. IMC sub-compartment proteins ISP1 and ISP3 (PF3D7_1011000 and PF3D7_1460600, respectively), which are clearly detected in stage I/II ookinetes [344], are palmitoylated [227] as well as myristoylated [344] in blood stage parasites; these proteins define and highlight apical polarity in the developing ookinete [344]. In addition, glideosome associated protein with multiple membrane spans (GAPM) 2 and 3 (PF3D7_0423500 and PF3D7_1406800, respectively) (but not 1) as well as glideosome-associated proteins (GAP) 40, 45 and 50 (PF3D7_0515700, PF3D7_1222700 and PF3D7_0918000, respectively) and myosin A tail domain interacting protein (MTIP) (PF3D7_1246400) are known palmitoylation substrates. The palmitoylated status of the recently identified subpellicular network protein G2 (PF3D7_0929600), subpellicular microtubule proteins (SPM) 1 and 2 (PF3D7_0909500 and PF3D7_1230300, respectively), IMC1a (PF3D7_0304000), IMC1b (PF3D7_1141900), IMC1h (PF3D7_1221400) and ALV7 (PF3D7_0621400) was however not reported.

Only few of these proteins have been shown experimentally to be involved in ookinete morphogenesis. Six gene deletion mutants have been generated for four of these targets: IMC1b, IMC1h, G2 and ISP3. Among these, two have targeted IMC1h and one is an IMC1b/h double KO (RMgmDB, www.pberghei.eu). The phenotypes of these mutants included shortened/stunted ookinete morphology and reduced gliding motility leading to lowered mosquito infectivity. However, a strong developmental defect as the one observed in our global palmitoylation inhibition studies was never reported. It is likely that the global inhibition of several (yet unknown) PATs in this study resulted in an additive effect leading to the early growth defects.

Which specific PAT (or PATs) is required for ZOT remains elusive. Previous work from our group identified three *pbdhhc-pats* (*dhhc2*, *dhhc3* and *dhhc10*) to rely on the RNA helicase DOZI for RNA stability in gametocytes, thus suggesting a role for these three genes/proteins during post-fertilization development of the zygote [107]. Such mRNAs are typically subject to TR in the female gametocyte; translation and protein function occur after fertilisation within the mosquito host allowing successful colonization of the vector [71, 137]. The RNAseq as well as RT-PCR data presented here identified each of these three genes to be upregulated in gametocytes, and the RNA-immunoprecipitation (RNA-IP) experiments supported a physical interaction of DOZI and CITH (a second translational repressor) with *dhhc10* (**Figure 5C**) as well as with *dhhc2* and *dhhc3* (**Figure S10**). However, only *dhhc10* behaves as a typical, gametocyte-specific and translationally repressed gene with absence of protein in gametocytes and translation of the stored mRNA only in the zygote/ookinete. The GFP tagging experiments showed the presence of DHHC2 and DHHC3 in gametocytes. It is possible that both these proteins are required during early gametocytogenesis. As a result, mature gametocytes contain both protein and translationally repressed mRNAs that are produced in the late gametocyte. The clear association of *dhhc2* and *dhhc3* mRNAs with DOZI and CITH supports this interpretation.

At the transcript level, and based on RNAseq data, *P. falciparum dhhc2* is particularly upregulated in schizonts, while *pfdhhc3* and *pfdhhc10* are upregulated in gametocytes [84]. The blood stage translational profiles reported herein for DHHC2::GFP and DHHC3::GFP together with published observations on expression in *P. falciparum* blood stages (DHHC2 in rings [345] and schizonts [340] and DHHC3 in schizonts [340, 341]; see **Table S3**) suggest a role for these proteins in asexual development and/or red blood cell invasion, and likely explains our failure to delete these genes. DHHC10, on the other hand, has not been reported in any of these proteomics studies. All three DHHC-PATs analysed here were however absent from the datasets of asexual blood stages, as well as mixed and separated male and female gametocyte proteomes of *P. berghei* ([50] and **Table S3**). The inability to KO *dhhc2* and *dhhc3* did not allow us to assess the contribution of these PATs, if any, to ookinete development. Previous attempts to delete these genes have been reported; while *dhhc2* deletion failed, *dhhc3* deletion was reported to be successful [233]. However, this study used a different gene targeting approach (*Plasmo*GEM, plasmogem.sanger.ac.uk, [346]) and lacks detailed genotype and phenotype analyses of the selected mutants to confirm correct deletion of *dhhc3*. Our failure to delete both *dhhc2* and *dhhc3* indicate that these proteins have an essential and non-redundant function in blood stage parasites. Further insight into the exact role of these proteins for both asexual and sexual stages of *Plasmodium* will require methodologies for conditional knock-out/down of expression in defined life cycle stages through promoter swap (e.g., [134, 347]).

Analyses of the transgenic parasites expressing GFP-tagged DHHC2 and DHHC3 showed expression of these proteins in ookinetes and sporozoites. Translation of both genes was low (if any) in immature oocysts but was upregulated during sporogony and maintained in

midgut and salivary gland sporozoites, matching their “waving” mRNA expression profile throughout the parasite’s life cycle. DHHC2 and DHHC3 have also been detected in salivary gland sporozoites by mass-spectrometry analyses ([339] and **Table S3**) in addition to four other DHHC-PATs (DHHC1, 4, 7 and 9).

Our observations showed localisation of DHHC2::GFP at the apex of the sporozoite, perhaps in micronemes or rhoptries. DHHC3::GFP protein on the other hand is distributed throughout the sporozoite. In blood stages the protein distributes towards the edges of newly formed merozoites. This localisation is in agreement with recently reported localisation of HA-tagged PbDHHC3 in merozoites which co-localised with merozoite surface protein 1 (MSP1), suggesting an IMC localisation [233]. In ookinetes, DHHC3::GFP signal is stronger at the surface of the parasite, suggesting that DHHC3 could also be localised to the IMC at this stage.

Based on the expression in merozoites, ookinetes and sporozoites and on their subcellular localisation, both DHHC2 and DHHC3 were candidate factors for gliding motility and invasion-related events. The absence of an effect of 2-BMP on gliding motility and hepatocyte traversal by sporozoites indicate that, in contrast to palmitoylation of GAP45 in *T. gondii* tachyzoites [234], dynamic PAT-mediated protein palmitoylation is not required for motility of *Plasmodium* sporozoites. In contrast, hepatocyte invasion by sporozoites was significantly reduced in the presence of 2-BMP indicating that palmitoylation is important for liver cell invasion. Together with published data on *P. falciparum* [227] and *T. gondii* [234, 237, 240], our results confirm palmitoylation of parasite proteins as an important factor for general host cell invasion by Apicomplexans.

For the first time we link a specific PAT to a specific cell biological role during parasite development inside the mosquito. We show that DHHC10 is dispensable for normal development of asexual blood stages. Concordantly, *dhhc10* has previously been targeted for deletion and its non essential nature for blood stage parasites was reported [233]. Although transcribed in the gametocyte, *dhhc10* is a target of TR and plays no immediate role in the development of gametocytes or ookinetes as well. DHHC10-deficient parasites produce gametocytes that are able to differentiate into fertile gametes, which, in turn mate and form zygotes that develop into ookinetes capable of establishing normal number of oocysts. The protein has thus no role in ZOT, nor affects traversal or invasion of the midgut wall by the ookinete. Oocysts show DNA replication but sporogony is completely aborted in DHHC10-deficient parasites, resulting in ‘empty’, vacuolated oocysts that outgrow WT oocysts in size. Our results show that DHHC10 is essential for the normal formation of CBs, transient organelles formed in the ookinete that exert their function in the oocyst. In the absence of DHHC10 no typical CBs could be detected at light- and electron-microscopy levels and the CB-resident protein LAP2 showed an aberrant localisation. The phenotype of vacuolated oocysts showing reduced CSP expression and lacking sporozoite formation has been observed in several other gene deletion mutants, some of which are deficient in proteins that associate with CBs. These

include members of LCCL protein family, also called LAP proteins in *P. berghei* [176, 211, 224-226]. Like *dhhc10*, certain *lap* mRNAs, namely *pblap4-6* [208], are translationally repressed in gametocytes while in ookinetes the proteins become associated with the CB [208]. The aberrant oocyst phenotypes described above have also been ascribed to mutant parasites lacking expression of plasmepsin VI [176], rhomboid 3 [330] and CSP itself [331]. Interestingly, the absence of CBs has only been reported so far for one specific member of the LAP family, PbSR [211], making DHHC10 the second protein (and the first enzyme) with vital role in CB formation to be reported in *P. berghei*. Moreover, other phenotypic similarities between PbSR and DHHC10 null mutants include the oocyst enlargement while DNA replication continues [224], suggesting that the basic expansion program of the oocyst is thus operational while morphogenesis and cellularisation depend on the presence of these two CB-resident proteins. Based on the notion that CSP levels markedly influence the degree of sporozoite formation by affecting the development of inner membranes in the sporulating cyst [327], we analysed CSP expression in Δ*dhhc10* oocysts by Western blot as well as IFA. We concluded by both methods that CSP is almost absent from KO cysts, further corroborating the abortive nature of the gene deletion cysts.

Our observations provide additional evidence to support the proposed function of CBs as ookinete protein storage organelles [210, 215] and corroborate the importance of CB and CB-associated proteins for formation of sporozoites inside the oocyst. Studies on mutants lacking LAP proteins and now DHHC10 provide strong support for a central role of CBs in sporozoite formation. However, since disruption of the LAP protein PbSR and DHHC10 affects correct formation of CB it is not clear whether these proteins have a direct function in sporozoite formation or their absence affects the correct storage and transport of other (lipo)proteins or lipids that are essential for sporogony.

Sporogony in the mosquito midgut oocyst involves a several thousand-fold replication step that is followed by the generation of individual, motile sporozoites that are capable of invading the mosquito's salivary glands, traverse human/rodent skin, capillaries and liver cells, and invade hepatocytes. This step, as well as the formation of the motile banana-shaped ookinete from the round zygote, most likely necessitate proper protein trafficking and localisation, something that can be achieved for instance through the action of DHHC-PATs. The localisation of such PATs within the parasitic cell will of course determine the proteins they can modify. A common feature of all PATs is that they are inserted into membranes [229]. Indeed, several *Plasmodium* and *Toxoplasma* DHHC-PATs have been localized to distinct subcellular compartments including the PM, IMC, rhoptries, endoplasmic reticulum and Golgi [233, 348], suggesting roles for motility, host cell invasion and protein trafficking. While DHHC10 localises to CBs in ookinetes, DHHC10::GFP was not detectable by live imaging in immature or mature oocysts. Co-localisation IFAs with known organelle markers and immuno-electron microscopy on *dhhc10*::*gfp* oocysts could be done to further elucidate this question.

The targets of protein palmitoylation in ookinetes, oocysts or developing midgut sporozoites are at the moment unknown. However, the published *P. berghei* and *P. gallinaceum* zygote and ookinete proteomes comprehend 277 out of 1368 (20%) *P. falciparum* orthologs found to be palmitoylated in *P. falciparum* schizonts. A comparison of published oocyst and oocyst-derived (midgut) sporozoite proteome data from *P. falciparum* [51] with the recently identified palmitome of *P. falciparum* schizonts [227] showed that 54 out of the 134 proteins detected in 7-8 days old oocysts were targets of palmitoylation in blood stages, while of the 453 proteins detected in 13-14 days old midgut sporozoites, 176 were also present in the schizont palmitome. Of the 5398 protein coding genes in the genome of *P. falciparum* 3D7 strain, 3689 have protein evidence in blood stage parasites, including asexual and sexual stages (PlasmoDB version 11.0); only 475 of those (13%) were identified to be palmitoylated in the above mentioned study [227]. The total number of proteins detected in oocysts and oocyst-derived sporozoites is low when compared to those identified in blood stage parasites; the fraction shown to be potential target of palmitoylation is however extremely high: 40% for oocysts, and 39% for midgut sporozoites. These large proportions (if true and not simply the result of preferential detection of membrane-bound proteins in midgut-associated parasites) could explain the severe developmental failure in the *dhhc10* null mutant and the essential role of DHHC10 in the modification and trafficking of such proteins prior to and during sporogony.

Cysteines are the canonical target residues for palmitoylation. However, *in silico* prediction of palmitoylation sites from primary protein sequences is difficult to achieve since there are only few poorly defined palmitoylation motifs known to date [349]. Therefore, the identification of palmitoylated proteins in different organisms has been done using proteomic strategies [227]. One such strategy is called Acyl-Biotin Exchange (ABE), in which the thioester-linked palmitoyl groups are substituted by biotin, allowing for a streptavidin-based purification of palmitoylated proteins, followed by mass-spectrometry [350]. This method has already been used to identify the palmitome of *P. falciparum* schizonts, comprehending over 400 proteins [227]. A similar approach could be employed not only to determine the palmitome of *P. berghei* ookinetes and oocysts but also to identify the enzymatic targets of DHHC10 by comparing the pool of palmitoylated proteins in Δ*dhhc10* versus WT parasites.

The results obtained in the present study clearly show the critical role of PTMs, namely protein palmitoylation, in the life cycle progression of malaria parasites within the mosquito vector. Although the DHHC-containing domain of DHHC-PATs is highly conserved between phylogenetically divergent taxa, their N- and C-termini are usually quite distinct and thought to determine substrate specificity [229]. Affecting parasite development in both vertebrate and invertebrate hosts, the development of parasite-specific DHHC-PAT inhibitors could be of extreme interest in the fight against malaria.

SUPPLEMENTARY FIGURES AND TABLES

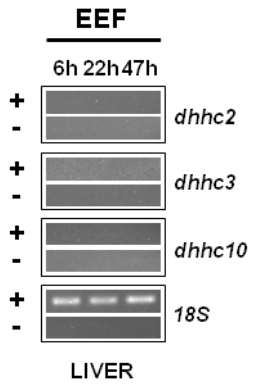

Figure S1 – *dhhc2*, *dhhc3* and *dhhc10* are not transcribed in liver stages. RT-PCR analyses of *dhhc2*, *dhhc3* and *dhhc10* in *in vivo*-developed *P. berghei* exoerythrocytic forms (EEFs) at different time points after sporozoite injection. *18S* rRNA serves as loading control gene. +: RT positive reaction; -: RT negative reaction.

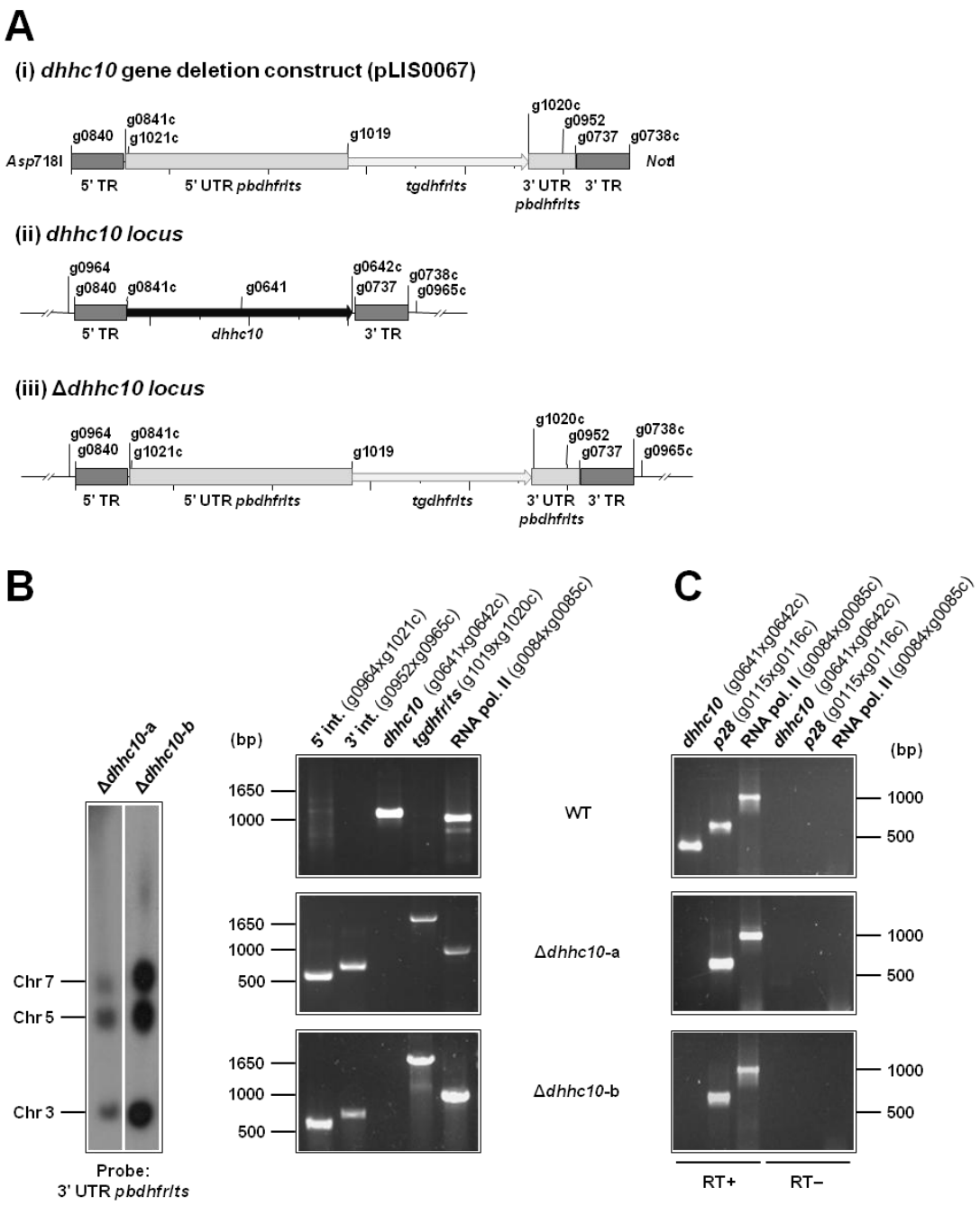

Figure S2 – Generation and genotyping of Δ*dhhc10* parasite lines.
(A) *dhhc10* gene deletion construct pLIS0067 (i) was obtained by cloning *dhhc10* 5' and 3' targeting regions (TR) upstream and downstream of the *Toxoplasma gondii dhfr/ts* selectable marker cassette, respectively. *tgdhfr/ts* gene is under the control of *P. berghei dhfr/ts* 5' and 3' UTRs. The construct was integrated into the *dhhc10 locus* (ii) of Fluo-frmg and PbGFP-LUCcon WT lines by double homologous recombination, resulting in the complete deletion of *dhhc10* ORF in Δ*dhhc10* parasites (iii). **(B)** Correct deletion of *dhhc10* was shown by Southern analysis of separated chromosomes (left) and diagnostic PCR analyses (right). Hybridisation of separated chromosomes with a probe against the 3' UTR of *pbdhfr/ts* recognised integrated pLIS0067 into chromosome 5, the endogenous *pbdhfr/ts locus* in chromosome 7 and reporter gene constructs (GFP/RFP or GFP-Luciferase) in chromosome 3. PCR analyses confirm 5' and 3' integration (int.) of pLIS0067, absence of *dhhc10* ORF and presence of *tgdhfr/ts* gene. **(C)** Absence of *dhhc10* mRNA was confirmed in Δ*dhhc10* mixed blood stages by RT-PCR. *p28* and RNA polymerase II serve as control genes.

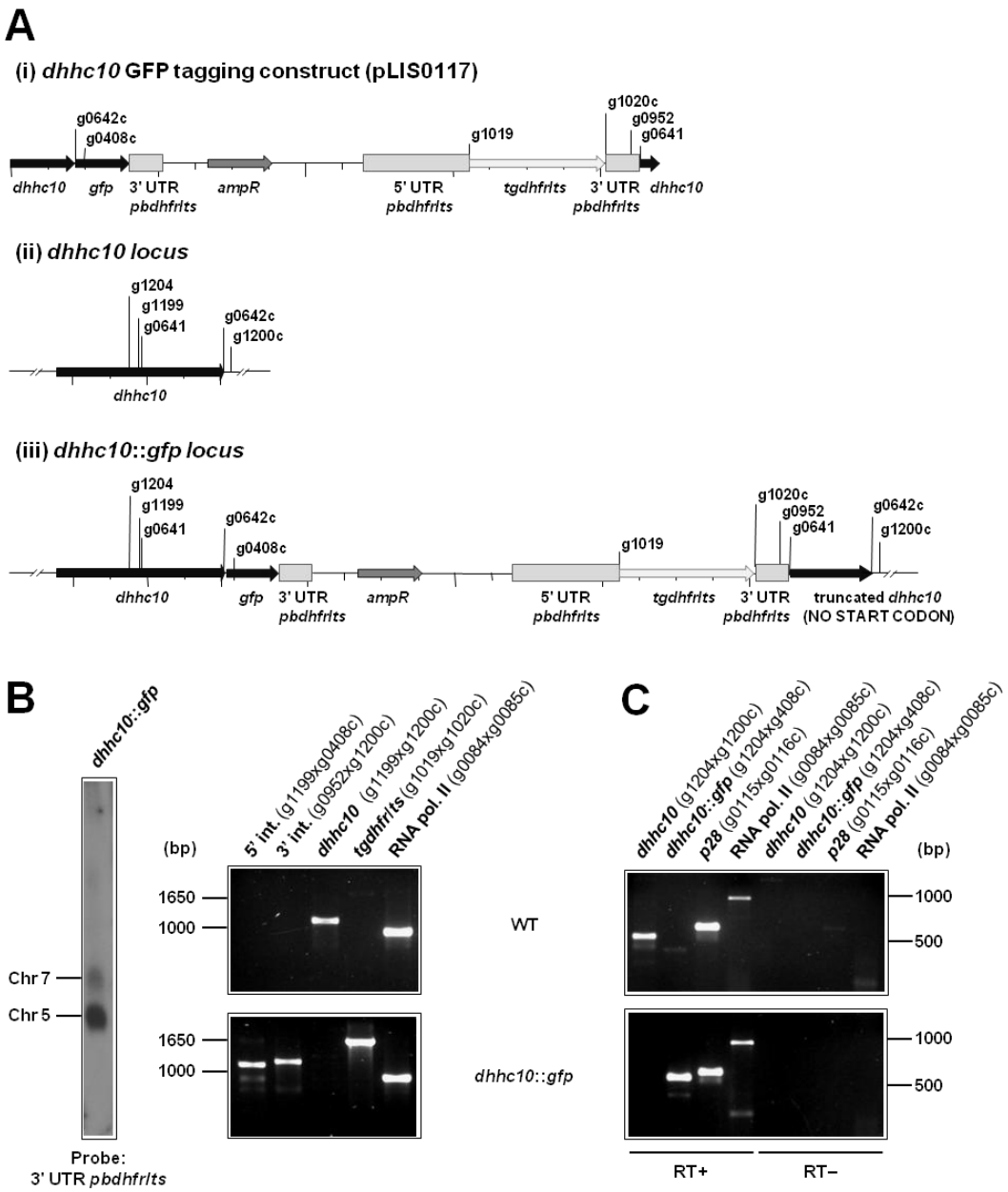

Figure S3 – Generation and genotyping of *dhhc10*::*gfp* parasite line.
(A) *dhhc10* GFP tagging construct pLIS0117 (i) was obtained by cloning the last 1116 bp of *dhhc10* ORF excluding the stop codon upstream and in frame with the *gfp* gene. This construct includes the *Toxoplasma gondii dhfr/ts* selectable marker cassette under the control of *P. berghei dhfr/ts* 5' and 3' UTRs. The construct was integrated into the *dhhc10 locus* (ii) of cl15cy1 by single homologous recombination, resulting in the fusion of *dhhc10* to *gfp* in *dhhc10*::*gfp* parasites (iii). **(B)** Correct tagging of *dhhc10* was shown by Southern analysis of separated chromosomes (left) and diagnostic PCR analyses (right). Hybridisation of separated chromosomes with a probe against the 3' UTR of *pbdhfr/ts* recognised integrated pLIS0117 into chromosome 5 and the endogenous *pbdhfr/ts locus* in chromosome 7. PCR analyses confirm 5' and 3' integration (int.) of pLIS0117, absence of WT *dhhc10* ORF and presence of *tgdhfr/ts* gene. **(C)** Absence of WT *dhhc10* and presence of *dhhc10*::*gfp* mRNA was confirmed in cloned *dhhc10*::*gfp* mixed blood stages by RT-PCR. *p28* and RNA polymerase II serve as control genes.

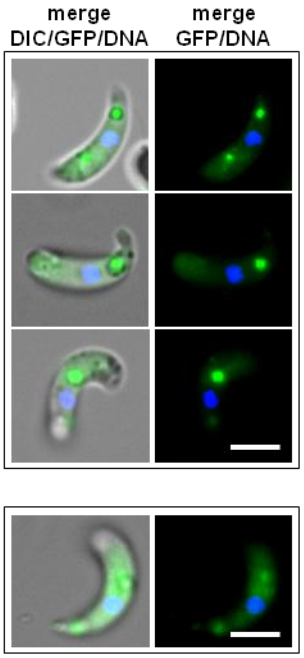

Figure S4 – DHHC10 localisation in ookinetes.
Live imaging of *in vitro*-cultured *dhhc10*::*gfp* ookinetes shows DHHC10::GFP localisation (in green) in discrete foci in approximately 75% of the ookinetes (upper pannel). Remaining parasites only showed diffuse cytoplasmic GFP signal (lower pannel) (*n*=60). DNA was stained with Hoechst-33342 (in blue). Scale bars = 5 µm.

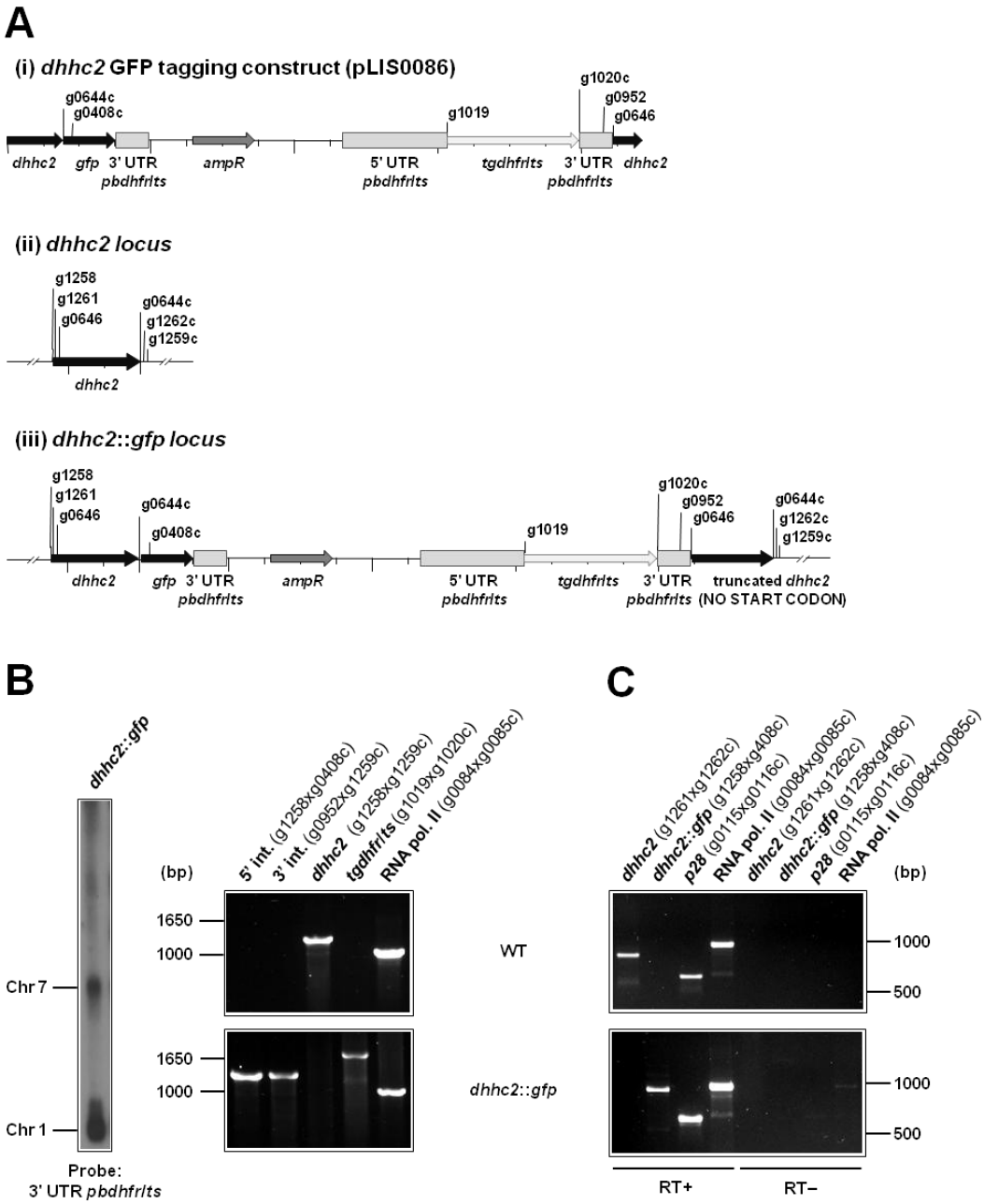

Figure S5 – Generation and genotyping of *dhhc2*::*gfp* parasite line.
(A) *dhhc2* GFP tagging construct pLIS0086 (i) was obtained by cloning the last 1167 bp of *dhhc2* ORF excluding the stop codon upstream and in frame with the *gfp* gene. This construct includes the *Toxoplasma gondii dhfr/ts* selectable marker cassette under the control of *P. berghei dhfr/ts* 5' and 3' UTRs. The construct was integrated into the *dhhc2 locus* (ii) of cl15cy1 by single homologous recombination, resulting in the fusion of *dhhc2* to *gfp* in *dhhc2*::*gfp* parasites (iii). **(B)** Correct tagging of *dhhc2* was shown by Southern analysis of separated chromosomes (left) and diagnostic PCR analyses (right). Hybridisation of separated chromosomes with a probe against the 3' UTR of *pbdhfr/ts* recognised integrated pLIS0086 into chromosome 1 and the endogenous *pbdhfr/ts locus* in chromosome 7. PCR analyses confirm 5' and 3' integration (int.) of pLIS0086, absence of WT *dhhc2* ORF and presence of *tgdhfr/ts* gene. **(C)** Absence of WT *dhhc2* and presence of *dhhc2*::*gfp* mRNA was confirmed in cloned *dhhc2*::*gfp* mixed blood stages by RT-PCR. *p28* and RNA polymerase II serve as control genes.

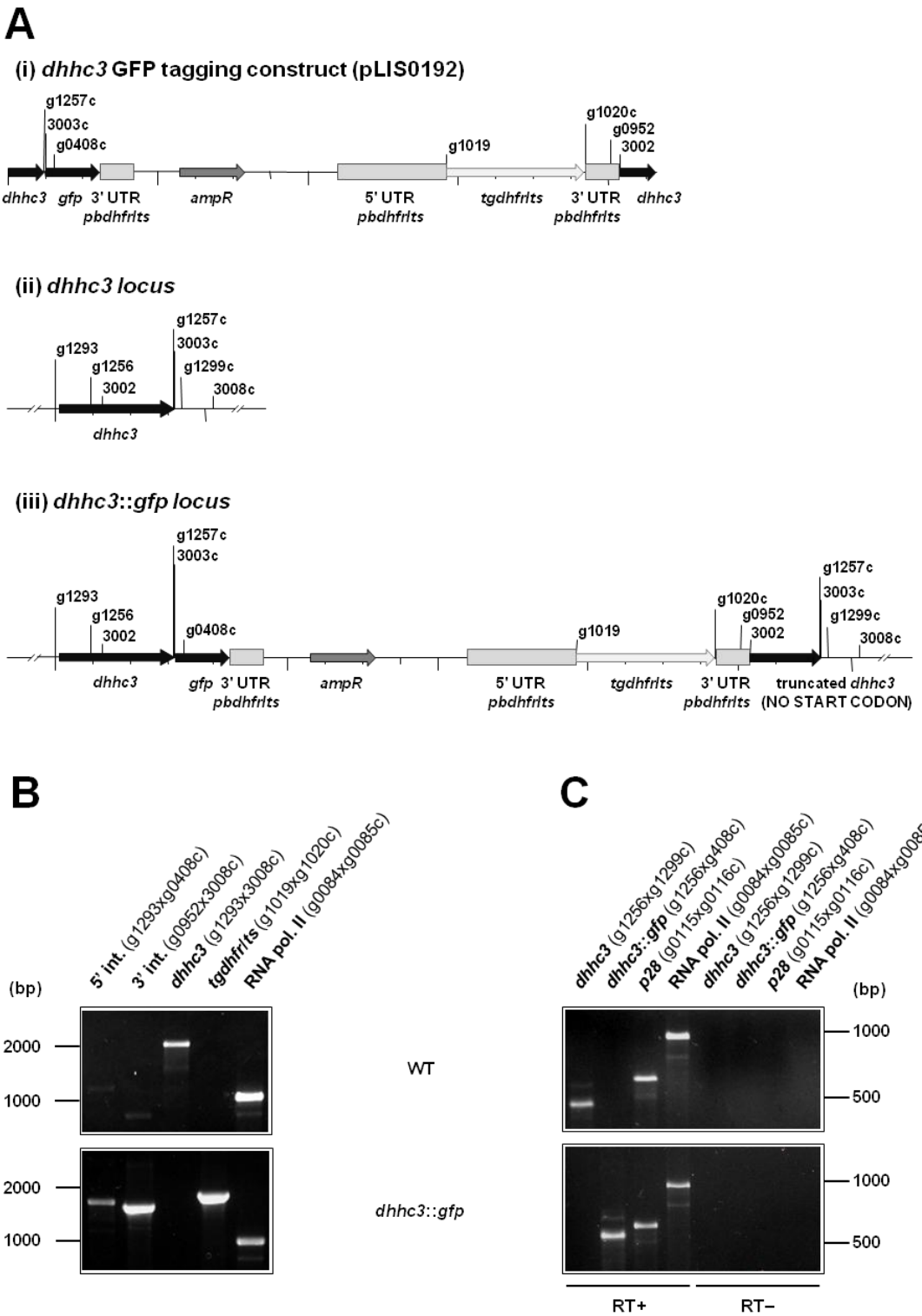

Figure S6 – Generation and genotyping of *dhhc3*::*gfp* parasite line.
(A) *dhhc3* GFP tagging construct pLIS0192 (i) was obtained by cloning the last 968 bp of *dhhc3* ORF excluding the stop codon upstream and in frame with the *gfp* gene. This construct includes the *Toxoplasma gondii dhfr/ts* selectable marker cassette under the control of *P. berghei dhfr/ts* 5' and 3' UTRs. The construct was integrated into the *dhhc3 locus* (ii) of cl15cy1 by single homologous recombination, resulting in the fusion of *dhhc3* to *gfp* in *dhhc3*::*gfp* parasites (iii). **(B)** Correct tagging of *dhhc3* was shown by diagnostic PCR analyses, confirming 5' and 3' integration (int.) of pLIS0192 into chromosome 9, absence of WT *dhhc3* ORF and presence of *tgdhfr/ts* gene. **(C)** Absence of WT *dhhc3* and presence of *dhhc3*::*gfp* mRNA was confirmed in cloned *dhhc3*::*gfp* mixed blood stages by RT-PCR. *p28* and RNA polymerase II serve as control genes.

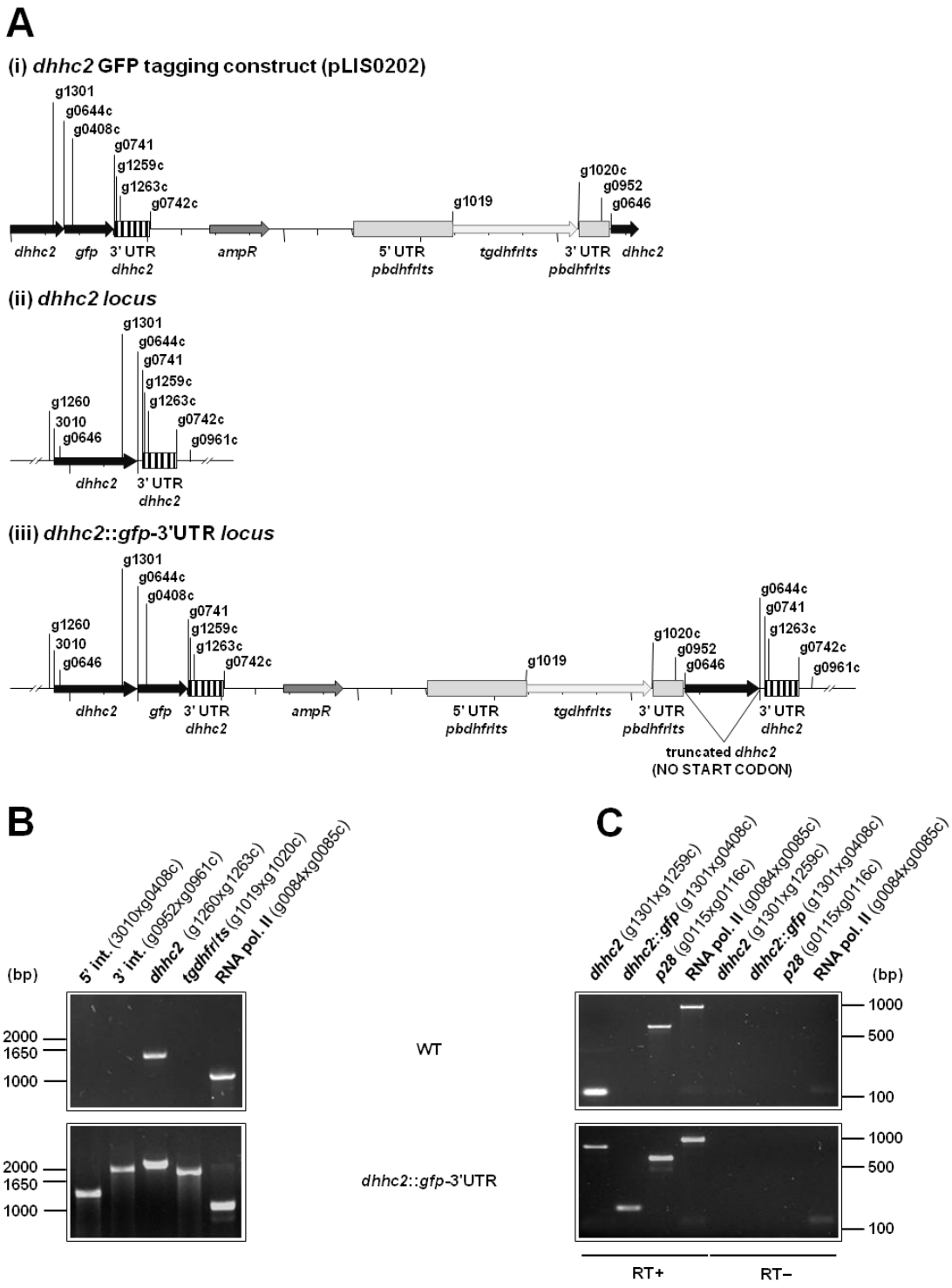

Figure S7 – Generation and genotyping of *dhhc2*::*gfp*-3'UTR parasite line.
(A) *dhhc2* GFP tagging construct pLIS0202 (i) was obtained by cloning the last 1167 bp of *dhhc2* ORF excluding the stop codon upstream and in frame with the *gfp* gene and nucleotide positions 36 to 541 of *dhhc2* 3' UTR downstream of *gfp*. This construct includes *Toxoplasma gondii dhfr/ts* selectable marker cassette under the control of *P. berghei dhfr/ts* 5' and 3' UTRs. The construct was integrated into the *dhhc2 locus* (ii) of cl15cy1 by single homologous recombination, resulting in the fusion of *dhhc2* to *gfp* and maintaining the endogenous *dhhc2* 3' UTR in *dhhc2*::*gfp*-3'UTR parasites (iii). **(B)** Correct tagging of *dhhc2* was shown by diagnostic PCR analyses, confirming 5' and 3' integration (int.) of pLIS0202 into chromosome 1, absence of WT *dhhc2* ORF and presence of *tgdhfr/ts* gene. **(C)** Absence of WT *dhhc2* and presence of *dhhc2*::*gfp* mRNA was confirmed in cloned *dhhc2*::*gfp*-3'UTR mixed blood stages by RT-PCR. *p28* and RNA polimerase II serve as control genes.

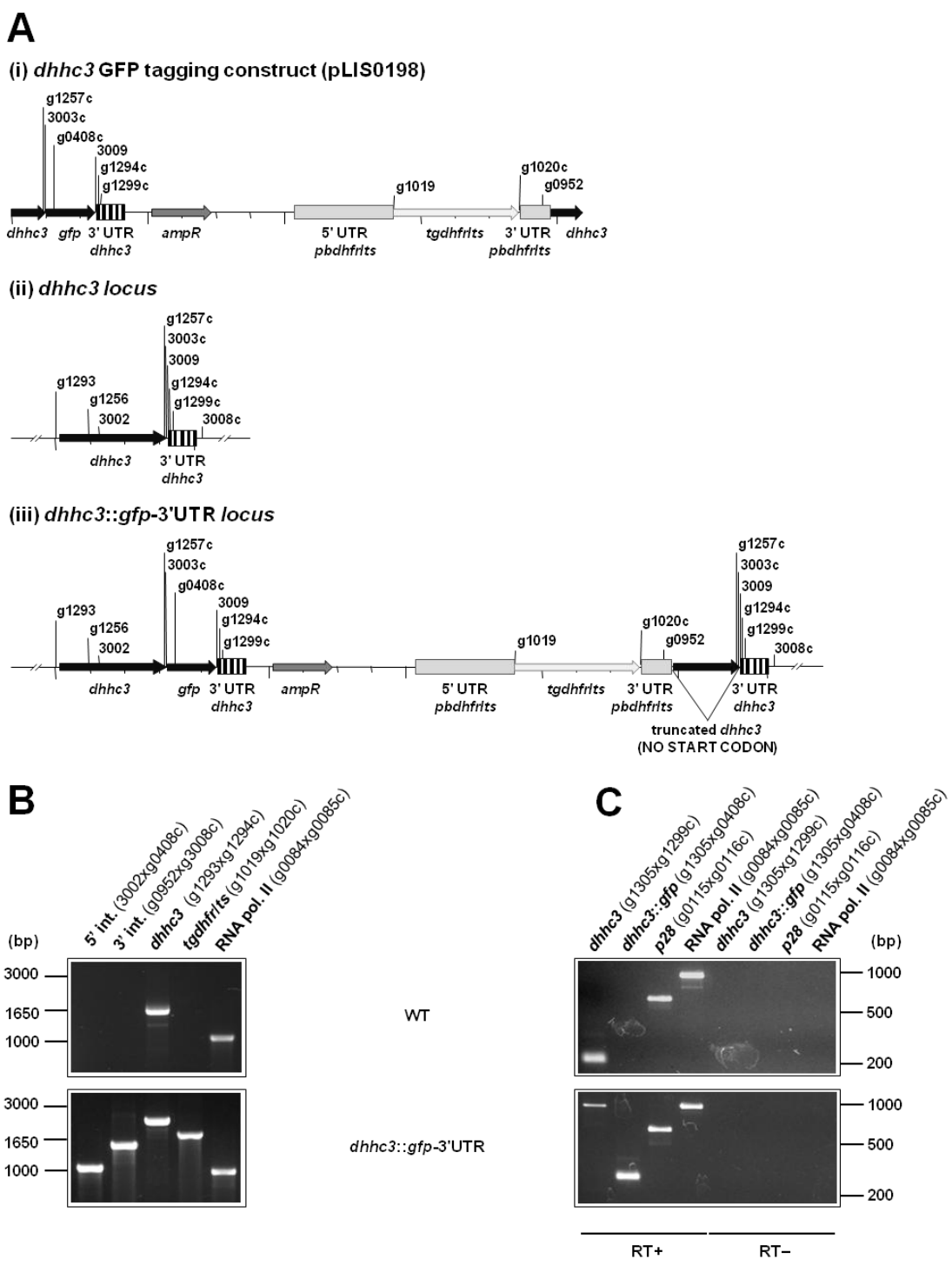

Figure S8 – Generation and genotyping of *dhhc3*::*gfp*-3'UTR parasite line.
(A) *dhhc3* GFP tagging construct pLIS0198 (i) was obtained by cloning the last 948 bp of *dhhc3* ORF excluding the stop codon upstream and in frame with the *gfp* gene and the first 391 bp of *dhhc3* 3' UTR downstream of *gfp*. This construct includes *Toxoplasma gondii dhfr/ts* selectable marker cassette under the control of *P. berghei dhfr/ts* 5' and 3' UTRs. The construct was integrated into the *dhhc3 locus* (ii) of cl15cy1 by single homologous recombination, resulting in the fusion of *dhhc3* to *gfp* and maintaining the endogenous *dhhc3* 3' UTR in *dhhc3*::*gfp*-3'UTR parasites (iii). **(B)** Correct tagging of *dhhc3* was shown by diagnostic PCR analyses, confirming 5' and 3' integration (int.) of pLIS0198 into chromosome 9, absence of WT *dhhc3* ORF and presence of *tgdhfr/ts* gene. **(C)** Absence of WT *dhhc3* and presence of *dhhc3*::*gfp* mRNA was confirmed in cloned *dhhc3*::*gfp*-3'UTR mixed blood stages by RT-PCR. *p28* and RNA polymerase II serve as control genes. Primer g1305 only anneals with *dhhc3* cDNA.

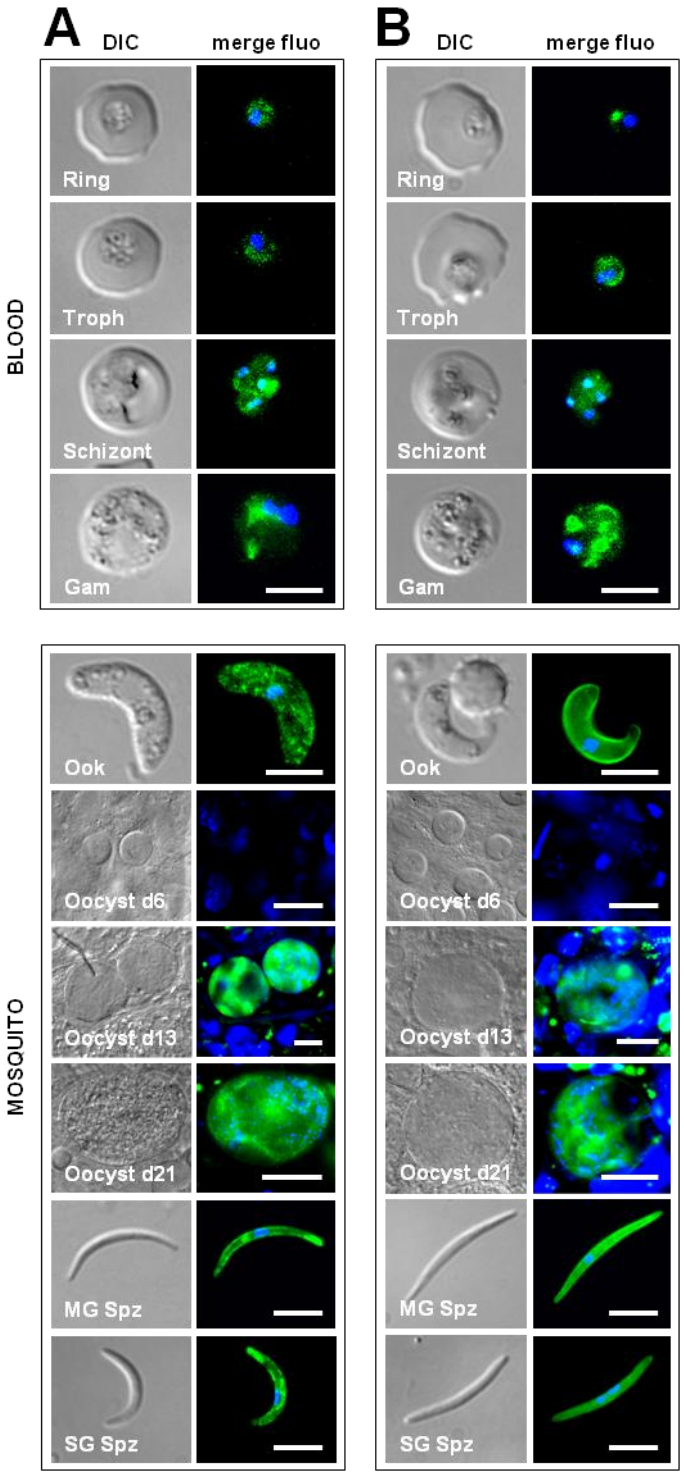

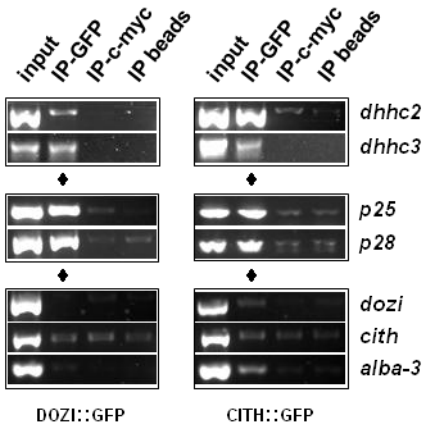

Figure S10 – *dhhc2* and *dhhc3* transcripts are bound by DOZI/CITH-defined mRNPs.
RT-PCR analysis on DOZI::GFP and CITH::GFP gametocyte immunoprecipitation (IP) eluates shows that *dhhc2*, *dhhc3* as well as *p25* and *p28* mRNAs (known to be translationally repressed) co-precipitate with DOZI and CITH. *dozi*, *cith* and *alba-3* are translated in gametocytes and are not enriched in the IP-GFP fractions. Input, total gametocyte mRNA; IP-c-myc, IP with anti-c-myc antibody; IP beads, no antibody used for IP.

Figure S9 – DHHC2 and DHHC3 are expressed in blood and mosquito stages.
(A) Expression of DHHC2::GFP in live *dhhc2*::*gfp*-3'UTR parasites. **(B)** Expression of DHHC3::GFP in live *dhhc3*::*gfp*-3'UTR parasites. **(A-B)** DHHC2::GFP and DHHC3::GFP expression is shown in green while DNA was stained with Hoechst-33342 (in blue). Troph: trophozoite; Gam: gametocyte; Ook: ookinete; Oocyst d6, d13 and d21: oocyst at days 6, 13 and 21 p.i.; MG Spz: midgut sporozoite at day 21 p.i.; SG Spz: salivary gland sporozoite at day 21 p.i. Scale bars = 5 µm (blood stages, ookinetes and sporozoites) or 20 µm (oocysts).

Table S1 - Primers used in the present work.

a) Primers used in life-cycle RT-PCRs and RT-PCRs of IP samples.

"c" or "Rev" at the end of primer names means they are antisense primers. All others are sense primers.
Nucleotide stretches in capital letter correspond to the complementary sequence to the respective gene. n.a.: not aplicable; ORF: open reading frame; UTR: untranslated region.

Gene name	Gene ID	Primer name	Sequence	Description	Product size gDNA (bp)	Product size cDNA (bp)	Across introns
dhhc2	PBANKA_010830	g0646	aaagaattcTCGATATTCATATTTATTG	*dhhc2* ORF	1188	816	yes
		g0644c	aaagcggccgcATATATTACTTCCATGTG	*dhhc2* ORF			
dhhc3	PBANKA_092730	g1256	TGGGTTAATAATTGCATAGG	*dhhc3* ORF	1118	456	yes
		g1257c	ATATTTTATAGACCTTTCAGCTTC	*dhhc3* ORF			
dhhc10	PBANKA_051200	g0641	aaagaattcAAAACTGTTTTAAAGATG	*dhhc10* ORF	1137	459	yes
		g0642c	aaagcggccgcATAATGTTTTATAAAATAGCC	*dhhc10* ORF			
***18S* rRNA**	n.a.	PbA18SFw	AAGCATTAAATAAAGCGAATACATCCTTAC	*18S* rRNA	134	134	no
		PbA18SRev	GGAGATTGGTTTTGACGTTTATGTG	*18S* rRNA			
hsp70	PBANKA_071190	g0258	AAAAGCAAAGCCAAACTTACC	*hsp70* ORF	139	139	no
		g0259c	GGATGGGGTTGTTCTATTACC	*hsp70* ORF			
p25	PBANKA_051500	g0385	CCGGAATTCATAAACAAATATACCTGG	*p25* 3' UTR	263	263	no
		g0476c	CGGGATCCTCATACGAATTTTATTG	*p25* 3' UTR			
p28	PBANKA_051490	g0115	TTCGATATCATGAATTTTAAATACAG	*p28* ORF	660	660	no
		g0116c	tccgcggccgcGCATTACTATCACGTAAATAAC	*p28* ORF			
dozi	PBANKA_121770	g0546	TAATTGTGTCGCTTCAAATG	*dozi* ORF	641	439	yes
		g0548c	TAATTCTTTTATCATAGCAG	*dozi* ORF			
cith	PBANKA_130130	g0549	GAAAAAAGCAAAGATGTATTATCTG	*cith* ORF	334	334	no
		g0550c	ATAGGCTGGGTATCTGTTAAATG	*cith* ORF			
alba3	PBANKA_120440	g0003	aaacccggggaattcCAAGAAAGAGCTGAAAAC	*alba3* ORF	641	324	yes
		g0004c	aaagcggccgctATTAGCAACAAAGTTTG	*alba3* ORF			

Table S1 - Primers used in the present work.

b) Primers used in the generation of gene deletion and GFP-tagging constructs.

"c" at the end of primer names means they are antisense primers. All others are sense primers.

Nucleotide stretches in capital letter correspond to the complementary sequence to the respective gene. Underlined are restriction site sequences.

n.a.: not aplicable; ORF: open reading frame; UTR: untranslated region.

Gene name	Gene ID	Construct name	Primer name	Sequence	Restriction sites	Description
Gene deletion constructs						
dhhc2	PBANKA_010830	pLIS0065	g0739	aaaggtaccTTTATTATTTGAGTGTTG	*Asp* 718I	*dhhc2* 5' targeting region
			g0740c	aaaaagcttTTTATATTGATTTTGATTG	*Hin* dIII	*dhhc2* 5' targeting region
			g0741	aaagaattcTTGAGTTTATAATATGTC	*Eco* RI	*dhhc2* 3' targeting region
			g0742c	aaagcggccgcATATCCTAAAAACTATTG	*Not* I	*dhhc2* 3' targeting region
dhhc3	PBANKA_092730	pLIS0190	3000	aaaggtaccATATAGTATATTCCTTGCGC	*Asp* 718I	*dhhc3* 5' targeting region
			3001c	aaaaagcttAATTATAGTATGTGATATGC	*Hin* dIII	*dhhc3* 5' targeting region
			3002	TATAGCTATTTTTAATATAC	*Sna* BI	*dhhc3* 3' targeting region
			3003c	aaagcggccgcAATATTTTATAGACCTTTC	*Not* I	*dhhc3* 3' targeting region
dhhc10	PBANKA_051200	pLIS0067	g0735	aaaggtaccTTTTTCTCCAAATTTTTG	*Asp* 718I	*dhhc10* 5' targeting region
			g0736c	aaaaagcttCGTTAATATATAATAATAG	*Hin* dIII	*dhhc10* 5' targeting region
			g0737	aaagaattcGAAATATTTATTCTATTTG	*Eco* RI	*dhhc10* 3' targeting region
			g0738c	aaagcggccgcTTAATCTATATGCATTTC	*Not* I	*dhhc10* 3' targeting region
GFP-tagging constructs						
dhhc2	PBANKA_010830	pLIS0086	g0646	aaagaattcTCGATATTCATATTTATTG	*Eco* RI	*dhhc2* ORF
			g0644c	aaagcggccgcATATATTACTTCCATGTG	*Not* I	*dhhc2* ORF
		pLIS0202	g0646	aaagaattcTCGATATTCATATTTATTG	*Eco* RI	*dhhc2* ORF
			g0644c	aaagcggccgcATATATTACTTCCATGTG	*Not* I	*dhhc2* ORF
			g0741	aaagaattcTTGAGTTTATAATATGTC	*Eco* RI	*dhhc2* 3' UTR
			g0742c	aaagcggccgcATATCCTAAAAACTATTG	*Not* I	*dhhc2* 3' UTR
dhhc3	PBANKA_092730	pLIS0192	3002	TATAGCTATTTTTAATATAC	n.a.	*dhhc3* ORF
			3003c	aaagcggccgcAATATTTTATAGACCTTTC	*Not* I	*dhhc3* ORF
		pLIS0198	3002	TATAGCTATTTTTAATATAC	*Sna* BI	*dhhc3* ORF
			3003c	aaagcggccgcAATATTTTATAGACCTTTC	*Not* I	*dhhc3* ORF
			3009	aaatctagaTAAAAAAAAGTTATTAAACAAAT	*Xba* I	*dhhc3* 3' UTR
			3008c	CTAACAAAACGATTGAG	*Hpy* 8I	*dhhc3* 3' UTR
dhhc10	PBANKA_051200	pLIS0117	g0641	aaagaattcAAAACTGTTTTAAAGATG	*Eco* RI	*dhhc10* ORF
			g0642c	aaagcggccgcATAATGTTTTATAAAATAGCC	*Not* I	*dhhc10* ORF

Table S1 - Primers used in the present work.

c) Primers used in genotyping and RT-PCR of mutant parasite lines (continues in next page).

"c" at the end of primer names means they are antisense primers. All others are sense primers.

Nucleotide stretches in capital letter correspond to the complementary sequence to the respective gene.

n.a.: not aplicable; ORF: open reading frame; UTR: untranslated region.

Gene name/ mutant name	Gene ID	Primer name	Sequence	Description	Integration PCR pair	Product size (bp)
Primers for genotyping						
Δ*dhhc10*-a and Δ*dhhc10*-b	PBANKA_051200	g0964	AACGAATTTGACTTGCATTC	*dhhc10* 5' integration	g1021c	626
		g0965c	GGTATGAACTCATACATGTC	*dhhc10* 3' integration	g0952	643
dhhc10		g0641	aaagaattcAAAACTGTTTTAAAGATG	*dhhc10* ORF	n.a.	1137
		g0642c	aaagcggccgcATAATGTTTTATAAAATAGCC	*dhhc10* ORF	n.a.	
dhhc2::*gfp*	PBANKA_010830	g1258	ACACATAAATATATGCAG	*dhhc2* 5' integration	g0408c	1353
		g1259c	ATGACATATTATAAACTC	*dhhc2* 3' integration	g0952	1364
dhhc2::*gfp*-3'UTR		3010	ATGACACATAAATATATGCAGATAT	*dhhc2* 5' integration	g0408c	1365
		g0961c	GAGAATTAAGCCTATATATAC	*dhhc2* 3' integration	g0952	2041
dhhc2		g1260	TGAGGAGAATATTATAAG	*dhhc2* 5' UTR	n.a.	2175
		g1263c	AATGCTATTGCATATTTG	*dhhc2* 3' UTR	n.a.	
		g1258	ACACATAAATATATGCAG	*dhhc2* ORF	n.a.	1279
		g1259c	ATGACATATTATAAACTC	*dhhc2* 3' UTR	n.a.	
		g1260	TGAGGAGAATATTATAAG	*dhhc2* 5' UTR	n.a.	1460
		g1263c	AATGCTATTGCATATTTG	*dhhc2* 3' UTR	n.a.	
dhhc3::*gfp*	PBANKA_092730	g1293	ATTAAGCATATCACATAC	*dhhc3* 5' integration	g0408c	1713
		3008c	CTAACAAAACGATTGAG	*dhhc3* 3' integration	g0952	1611
dhhc3::*gfp*-3'UTR		3002	TATAGCTATTTTTAATATAC	*dhhc3* 5' integration	g0408c	1100
		3008c	CTAACAAAACGATTGAG	*dhhc3* 3' integration	g0952	1591
dhhc3		g1293	ATTAAGCATATCACATAC	*dhhc3* 5' UTR	n.a.	2367
		g1294c	ATTATTGATCATATTTCG	*dhhc3* 3' UTR	n.a.	
		g1293	ATTAAGCATATCACATAC	*dhhc3* 5' UTR	n.a.	2097
		3008c	CTAACAAAACGATTGAG	*dhhc3* 3' UTR	n.a.	
		g1293	ATTAAGCATATCACATAC	*dhhc3* 5' UTR	n.a.	1630
		g1294c	ATTATTGATCATATTTCG	*dhhc3* 3' UTR	n.a.	
dhhc10::*gfp*	PBANKA_051200	g1199	ATTTTTGGGGGTTTTCAG	*dhhc10* 5' integration	g0408c	1276
		g1200c	GTTTTCAACACAAGTGTG	*dhhc10* 3' integration	g0952	1362
dhhc10		g1199	ATTTTTGGGGGTTTTCAG	*dhhc10* ORF	n.a.	1251
		g1200c	GTTTTCAACACAAGTGTG	*dhhc10* 3' UTR	n.a.	

Table S1 - Primers used in the present work.

c) Primers used in genotyping and RT-PCR of mutant parasite lines (continuation).

"c" at the end of primer names means they are antisense primers. All others are sense primers.

Nucleotide stretches in capital letter correspond to the complementary sequence to the respective gene.

n.a.: not aplicable; *pb*: *Plasmodium berghei*; *tg*: *Toxoplasma gondii*; *dhfr/ts*: dihydrofolate reductase/thymidylate synthase; ORF: open reading frame; UTR: untranslated region.

Gene name/ mutant name	Gene ID	Primer name	Sequence	Description	Integration PCR pair	Product size (bp)
Primers for RT-PCR						
dhhc2	PBANKA_010830	g1261	AATATATGCAGATATCAC	*dhhc2* ORF	n.a.	879
		g1262c	AAAAAAATATACTTGTGC	*dhhc2* 3' UTR	n.a.	
		g1301	CATTGTATTTCAAATAGACC	*dhhc2* ORF	n.a.	130
		g1259c	ATGACATATTATAAACTC	*dhhc2* 3' UTR	n.a.	
dhhc2::*gfp*		g1258	ACACATAAATATATGCAG	*dhhc2* ORF	g0408c	981
		g1301	CATTGTATTTCAAATAGACC	*dhhc2* ORF	g0408c	204
dhhc2::*gfp*-3'UTR		g1301	CATTGTATTTCAAATAGACC	*dhhc2* ORF	n.a.	845
		g1259c	ATGACATATTATAAACTC	*dhhc2* 3' UTR	n.a.	
dhhc3	PBANKA_092730	g1256	TGGGTTAATAATTGCATAGG	*dhhc3* ORF	n.a.	531
		g1299c	ATATTTTTGATGGATTCTCC	*dhhc3* 3' UTR	n.a.	
		g1305	ATAATTAACCGATCTAACTC	*dhhc3* ORF	n.a.	234
		g1299c	ATATTTTTGATGGATTCTCC	*dhhc3* 3' UTR	n.a.	
dhhc3::*gfp*		g1256	TGGGTTAATAATTGCATAGG	*dhhc3* ORF	g0408c	588
		g1305	ATAATTAACCGATCTAACTC	*dhhc3* ORF	g0408c	291
dhhc3::*gfp*-3'UTR		g1305	ATAATTAACCGATCTAACTC	*dhhc3* ORF	n.a.	971
		g1299c	ATATTTTTGATGGATTCTCC	*dhhc3* 3' UTR	n.a.	
dhhc10	PBANKA_051200	g0641	aaagaattcAAAACTGTTTTAAAGATG	*dhhc10* ORF	n.a.	459
		g0642c	aaagcggccgcATAATGTTTTATAAAATAGCC	*dhhc10* ORF	n.a.	
		g1204	ATACAAACCAGACAGATC	*dhhc10* ORF	n.a.	585
		g1200c	GTTTTCAACACAAGTGTG	*dhhc10* 3' UTR	n.a.	
dhhc10::*gfp*		g1204	ATACAAACCAGACAGATC	*dhhc10* ORF	g0408c	610
General primers						
pbdhfr/ts	PBANKA_071930	g0952	GATTCATAAATAGTTGGACTTG	3' UTR *pbdhfr/ts*	n.a.	n.a.
		g1021c	ATTGTTGACCTGCAGGCATG	5' UTR *pbdhfr/ts*	n.a.	n.a.
tgdhfr/ts	n.a.	g1019	ATGCATAAACCGGTGTGTC	*tgdhfr/ts* ORF	n.a.	1866
		g1020c	AGCTTCTGTATTTCCGC	*tgdhfr/ts* ORF	n.a.	
RNA polymerase II subunit RPB1	PBANKA_080700	g0084	aaagaattcTGATGGTTTACAATCACC	RNA pol II ORF	n.a.	1015
		g0085c	aaagcggccgctTTCTTCCTGCATCTCCTC	RNA pol II ORF	n.a.	
p28	PBANKA_051490	g0115	TTCGATATCATGAATTTTAAATACAG	*p28* ORF	n.a.	660
		g0116c	tccgcggccgcGCATTACTATCACGTAAATAAC	*p28* ORF	n.a.	
gfp	n.a.	g0408c	GTATGTTGCATCACCTTC	*gfp* ORF	n.a.	n.a.

Table S2 - Parasite transfection experiments.

Gene name/ mutant name	Gene ID	DNA construct name	Restriction enzymes[1]	Experiment #/ mutant clone ID[2]	Parental line[3]
Unsussessful gene deletion attempts					
dhhc2	PBANKA_010830	pLIS0065	*Asp* 718I and *Not* I	2095 (LUMC)	820cl1m1cl1
				2362, 2363 (LUMC)	676m1cl1
dhhc3	PBANKA_092730	pLIS0190	*Asp* 718I and *Not* I	2359, 2360, 2361 (LUMC)	676m1cl1
Gene deletion mutants					
Δ*dhhc10* -a	PBANKA_051200	pLIS0067	*Asp* 718I and *Not* I	2097cl1 (LUMC)	820cl1m1cl1
Δ*dhhc10* -b				2365cl2 (LUMC)	676m1cl1
GFP-tagged mutants					
dhhc2 ::*gfp*	PBANKA_010830	pLIS0086	*Fsp* AI	2185cl1m1 (LUMC)	cl15cy1
dhhc3 ::*gfp*	PBANKA_092730	pLIS0192	*Bsi* WI	192cl1m1 (Heidelberg)	cl15cy1
dhhc10 ::*gfp*	PBANKA_051200	pLIS0117	*Sna* BI	2187cl1m1 (LUMC)	cl15cy1
dhhc2 ::*gfp* -3'UTR	PBANKA_010830	pLIS0202	*Fsp* AI	202cl1m1 (Heidelberg)	cl15cy1
dhhc3 ::*gfp* -3'UTR	PBANKA_092730	pLIS0198	*Bsi* WI	198cl1m1 (Heidelberg)	cl15cy1
Δ*dhhc10* ;*lap2* ::*gfp*	PBANKA_130070	[1]	[1]	2433 (LUMC)	Δ*dhhc10* -a

[1] Restriction enzymes used for plasmid linearisation before transfection

[2] Experiment number for independent transfection experiments:
the unsuccessful attempts and the experiment number/ID of the mutants clones

[3] Parental *P. berghei* ANKA line in which the transfection experiment was performed

[1] Saeed et al., *Mol Biochem Parasitol* 2010 170(1): p. 49-53

Table S3 - Summary of *Plasmodium* DHHC-PAT expression data (continues in next page).

				P. berghei gam proteome [1]			*P. berghei* asexual	zygote/ook
Pf gene ID	Pb gene ID	gene name	annotation	mixed	male	female	expression [2]	proteomes [3-5]
PF3D7_0303400	PBANKA_040200	DHHC1	palmitoyl transferase (AnkDHHC)	2	n.detec.	n.detec.	not deter.	n.detec.
PF3D7_0609800	PBANKA_010830	DHHC2	zinc finger protein, putative	n.detec.	n.detec.	n.detec.	not deter.	n.detec.
PF3D7_1121000	PBANKA_092730	DHHC3	zinc finger, DHHC-type, putative	n.detec.	n.detec.	n.detec.	IMC	n.detec.
PF3D7_0714300	PBANKA_142090	DHHC4	zinc finger protein, putative (ERF2)	1	n.detec.	n.detec.	n.detec.	n.detec.
PF3D7_1322500	PBANKA_133780	DHHC5	DHHC-type zinc finger protein, putative	n.detec.	n.detec.	n.detec.	ER	n.detec.
PF3D7_0932500	PBANKA_083330	DHHC6	DHHC-type zinc finger protein, putative	n.detec.	n.detec.	n.detec.	n.detec.	n.detec.
PF3D7_0528400	PBANKA_124300	DHHC7	cell cycle regulator with zn-finger domain	n.detec.	n.detec.	n.detec.	Rhoptry	n.detec.
PF3D7_1321400	PBANKA_141970	DHHC8	DHHC-type zinc finger protein, putative	n.detec.	n.detec.	n.detec.	punctuate, not Golgi	n.detec.
PF3D7_1115900	PBANKA_093210	DHHC9	conserved Plasmodium membrane protein	n.detec.	n.detec.	n.detec.	IMC	n.detec.
PF3D7_1027900	PBANKA_051200	DHHC10	DHHC-type zinc finger protein, putative	n.detec.	n.detec.	n.detec.	n.detec.	n.detec.
PF3D7_0215900	PBANKA_031260	DHHC11	zinc finger protein, putative	n.detec.	n.detec.	n.detec.	n.detec.	n.detec.

			plasmodb	*P. berghei*	LUMC RNAseq	Δ*dozi*	own RIP-Chip#	own lines	
Pf gene ID	Pb gene ID	gene name	*P. falciparum* proteome	KO line [2]	up regulated in	microarrays [11]*	DOZI/CITH	KO	GFP
PF3D7_0303400	PBANKA_040200	DHHC1	SG Spz [6]	not deter.	n.a.	n.d.r.	not detec./not detec.	not deter.	not deter.
PF3D7_0609800	PBANKA_010830	DHHC2	Ring [7] / Schizont [8] / SG Spz [6]	not deter.	gam	1.45	+/+	failed	OK
PF3D7_1121000	PBANKA_092730	DHHC3	Schizont [8-9] / SG Spz [6]	OK	gam	1.38	+/+	failed	OK
PF3D7_0714300	PBANKA_142090	DHHC4	Schizont [8] / SG Spz [10]	failed	n.a.	n.d.r.	not detec./not detec.	not deter.	not deter.
PF3D7_1322500	PBANKA_133780	DHHC5	n.detec.	OK	n.a.	n.d.r.	not detec./not detec.	not deter.	not deter.
PF3D7_0932500	PBANKA_083330	DHHC6	n.detec.	OK	n.a.	n.d.r.	not detec./not detec.	not deter.	not deter.
PF3D7_0528400	PBANKA_124300	DHHC7	Schizont [8] / SG Spz [6]	OK	ook	n.d.r.	not detec./not detec.	not deter.	not deter.
PF3D7_1321400	PBANKA_141970	DHHC8	n.detec.	failed	n.a.	n.d.r.	not detec./not detec.	not deter.	not deter.
PF3D7_1115900	PBANKA_093210	DHHC9	SG Spz [6]	OK	n.a.	n.d.r.	-/-	not deter.	not deter.
PF3D7_1027900	PBANKA_051200	DHHC10	n.detec.	OK	gam	1.75	+/+	OK	OK
PF3D7_0215900	PBANKA_031260	DHHC11	n.detec.	OK	n.a.	n.d.r.	not detec./not detec.	not deter.	not deter.

Table S3 - Summary of *Plasmodium* DHHC-PAT expression data (continuation).

			closest orthologs		
Pf gene ID	**Pb gene ID**	**gene name**	**yeast**	***A. thaliana***	**metazoa**
PF3D7_0303400	PBANKA_040200	DHHC1	SWF1, ERF2	At3g26935	*Xenopus* ZDHHC15
PF3D7_0609800	PBANKA_010830	DHHC2	PFA3	At3g09320	mouse ZDHHC20
PF3D7_1121000	PBANKA_092730	DHHC3	SWF1, ERF2	At4g15080	human ZDHHC11
PF3D7_0714300	PBANKA_142090	DHHC4	ERF2	At3g26935	human ZDHHC14
PF3D7_1322500	PBANKA_133780	DHHC5	ERF2	At2g14255	mouse ZDHHC17
PF3D7_0932500	PBANKA_083330	DHHC6	SWF1	At3g04970	mouse ZDHHC14
PF3D7_0528400	PBANKA_124300	DHHC7	PFA3	At4g00840	mouse ZDHHC20
PF3D7_1321400	PBANKA_141970	DHHC8	ERF2	At5g41060	human ZDHHC14
PF3D7_1115900	PBANKA_093210	DHHC9	PFA3	At4g22750	*Xenopus* ZDHHC15
PF3D7_1027900	PBANKA_051200	DHHC10	PFA3	At4g22750	mouse ZDHHC20
PF3D7_0215900	PBANKA_031260	DHHC11	PFA3	At3g60800	mouse ZDHHC3

n.detec.	not detected
n.deter.	not determined
n.a.	not applicable
n.d.r.	not differentially regulated
gam	gametocyte
ook	ookinete
*	Microarray log2 ratios of wild-type compared to Δ*dozi* gametocytes. Positive values indicate downregulation in Δ*dozi* parasites.
#	unpublished data; +: enriched; -: not enriched

[1] Khan et al., *Cell* 2005 121(5): p. 675-87; number of peptide hits are shown for each protein
[2] Frenal et al., *Traffic* 2013 14(8): p. 895-911
[3] Hall et al., *Science* 2005 307: p. 82-6
[4] Patra et al., *Proteomics* 2008 8: p. 2492–9
[5] Lal et al., *Proteomics* 2009 9: p. 1142–51
[6] Lindner et al., *Mol Cell Proteomics* 2013 12(5): p. 1127-43
[7] Oehring et al., *Genome Biol* 2012 13(11): p. R108
[8] Treeck et al., *Cell Host Microbe* 2011 10(4): p. 410-9
[9] Solyakov et al., *Nat Commun* 2011 2: p. 565
[10] Florens et al., *Nature* 2002 419: p. 520-6
[11] Mair et al., *Science* 2006 313(5787): p. 667-9

Table S4 - Summary of phenotypes of the *P. berghei* mutants generated in the present study.

Mutant	Asexual multiplication rate[1] (s.d.)	Gametocyte production[2] % (s.d.)	Ookinete production[3] % (s.d.)	Oocyst production[4] (s.d.)	MG Spz production[5] X10^4 (s.d.)	SG Spz production[6] X10^4 (s.d.)	Prepatent period[7]
Δ*dhhc10*-a	10 (0) *n* =2	19.7 (1.2) *n* =3	69.0 (5.4) *n* =4	161.4 (112.5) *n* =5	0 (0) *n* =4	0 (0) *n* =4	n.a.
Δ*dhhc10*-b	10 (0) *n* =4	17.7 (1.5) *n* =3	62.5 (6.6) *n* =4	n.d.	0 (0) *n* =1	0 (0) *n* =1	n.d.
dhhc2::*gfp*	n.d.	17.6 (1.5) *n* =3	76.7 (11.0) *n* =3	n.d.	n.d.	n.d.	4 *n* =1
dhhc3::*gfp*	10 (0) *n* =6	n.d.	n.d.	n.d.	n.d.	n.d.	4 *n* =1
dhhc10::*gfp*	10 (0) *n* =4	18.3 (2.5) *n* =3	82.0 (8.8) *n* =4	n.d.	n.d.	n.d.	5 *n* =1
dhhc2::*gfp*-3'UTR	10 (0) *n* =8	n.d.	n.d.	n.d.	n.d.	n.d.	4 *n* =1
dhhc3::*gfp*-3'UTR	10 (0) *n* =2	n.d.	n.d.	n.d.	n.d.	n.d.	4 *n* =1
Δ*dhhc10*;*lap2*::*gfp*	n.d.	n.d.	n.d.	n.d.	n.d.	n.d.	n.d.
WT[8]	10 (0) *n* >10	15-25 *n* >10	50-90 *n* >10	112-249 *n* =5	2.6-22 *n* =5	2.2-7.2 *n* =5	4-5 *n* =5

[1] The multiplication rate per 24 hours of blood stage parasites in mice infected with a single parasite

[2] The mean percentage of blood stage parasites developing into gametocytes *in vivo*

[3] The mean percentage of female gametes developing into mature ookinetes *in vitro*

[4] The mean number of oocysts per mosquito (days 12–13)

[5] The mean number of midgut sporozoites (MG Spz) per mosquito (days 20–22)

[6] The mean number of salivary gland sporozoites (SG Spz) per mosquito (days 20–22)

[7] The prepatent period (measured in days post bite of 10 infected females per mouse) is defined as the day when parasites are detected in Giemsa-stained blood smears of mice

[8] The developmental data for wild type (WT) parasites are shown as the range of mean values

s.d.: standard deviation

n.d.: not determined

n.a.: not aplicable

Table S5 - Identification of subpellicular network and IMC-associated proteins shown to be palmitoylated in [1].

Palmitoylated proteins are shaded.

Pf Gene ID	*Pf* Product Description	*Pb* Gene ID	*Pb* Product Description
PF3D7_0304000	inner membrane complex protein 1a, putative (IMC1a)	PBANKA_040260	inner membrane complex protein 1a (IMC1a)
PF3D7_0304100	membrane skeletal protein IMC1-related (ALV2)	PBANKA_040270	membrane skeletal protein, putative
PF3D7_0423500	glideosome associated protein with multiple membrane spans 2 (GAPM2)	PBANKA_052390	glideosome associated protein with multiple membrane spans 2, putative (GAPM2)
PF3D7_0515700	glideosome-associated protein 40, putative (GAP40)	PBANKA_111530	glideosome-associated protein 40, putative (GAP40)
PF3D7_0522600	inner membrane complex protein	PBANKA_123730	inner membrane complex protein, putative
PF3D7_0525800	membrane skeletal protein IMC1-related	PBANKA_124060	membrane skeletal protein, putative
PF3D7_0621400	Pf77 protein (ALV7)	PBANKA_112040	Pfs77 homologue, putative
PF3D7_0823500	membrane skeletal protein IMC1-related	PBANKA_070710	membrane skeletal protein, putative
PF3D7_0909500	subpellicular microtubule protein 1, putative (SPM1)	PBANKA_081070	subpellicular microtubule protein 1, putative (SPM1)
PF3D7_0918000	secreted acid phosphatase (GAP50)	PBANKA_081900	secreted acid phosphatase, putative,glideosome-associated protein 50, putative (GAP50)
PF3D7_0929600	conserved Plasmodium protein, unknown function	PBANKA_083040	G2 protein, putative
PF3D7_1003600	membrane skeletal protein IMC1-related (ALV5)	PBANKA_120200	membrane skeletal protein, putative
PF3D7_1011000	inner membrane complex protein, putative	PBANKA_120940	inner membrane complex sub-compartment protein 1
PF3D7_1141900	inner membrane complex protein 1b, putative (IMC1b)	PBANKA_090710	inner membrane complex protein 1b (IMC1b)
PF3D7_1221400	inner membrane complex protein 1h, putative (IMC1h)	PBANKA_143660	inner membrane complex protein 1h (IMC1h)
PF3D7_1222700	glideosome-associated protein 45 (GAP45)	PBANKA_143760	glideosome-associated protein 45, putative
PF3D7_1230300	subpellicular microtubule protein 2, putative (SPM2)	PBANKA_144500	subpellicular microtubule protein 2, putative (SPM2)
PF3D7_1246400	myosin light chain 1,myosin A tail domain interacting protein (MTIP)	PBANKA_145950	myosin light chain 1, putative,myosin A tail domain interacting protein MTIP, putative (MTIP)
PF3D7_1323700	glideosome associated protein with multiple membrane spans 1 (GAPM1)	PBANKA_133890	glideosome associated protein with multiple membrane spans 1, putative (GAPM1)
PF3D7_1345600	inner membrane complex protein	PBANKA_135850	inner membrane complex protein, putative
PF3D7_1351700	alveolin, putative (ALV6)	PBANKA_136440	conserved Plasmodium protein, unknown function
PF3D7_1406800	glideosome associated protein with multiple membrane spans 3 (GAPM3)	PBANKA_103540	glideosome associated protein with multiple membrane spans 3, putative (GAPM3)
PF3D7_1460600	inner membrane complex protein, putative	PBANKA_132430	inner membrane complex sub-compartment protein 3

[1] Jones et al., *Cell Host & Microbe* 2012 12: p. 246-258

LIMP: A SURFACE PROTEIN ESSENTIAL FOR MALARIA PARASITE MOTILITY AND INVASION THROUGH REGULATION OF ADHESION SITE TURNOVER

Jorge M. Santos[1], Vanessa Zuzarte-Luís[1], Catherine Moreau[2], Andreia Pinto[1], Mário da Costa[1], Blandine Franke-Fayard[3], Chris J. Janse[3], Friedrich Frischknecht[2], Gunnar R. Mair[1]

[1] Instituto de Medicina Molecular, Faculdade de Medicina da Universidade de Lisboa, Edifício Egas Moniz, Av. Prof. Egas Moniz, 1649-028 Lisbon, Portugal

[2] Parasitology, Department of Infectious Diseases, University of Heidelberg Medical School, Im Neuenheimer Feld 324, 69120 Heidelberg, Germany

[3] Leiden Malaria Research Group, Department of Parasitology, Leiden University Medical Center, Albinusdreef 2, 2333 ZA Leiden, The Netherlands

AUTHOR CONTRIBUTIONS

JMS, VZ-L and GRM designed experiments. JMS performed multiple alignments, RT-PCRs on immunoprecipitation samples and across the parasite life cycle, generated gene deletion and GFP tagging plasmids, cloned and genotyped mutant parasites, analysed blood stage development, determined asexual multiplication rates, oocyst and sporozoite numbers, analysed all data sets, wrote the Abstract, Methods, Results and Discussion and generated all figures and tables. JMS and VZ-L performed sporozoite traversal, adhesion and invasion assays, EEF development assays, executed transmission experiments and performed light microscopy imaging experiments. JMS and CM performed sporozoite gliding motility assays. JMS, BF-F and CJJ performed parasite transfections. AP performed electron microscopy experiments. MdC produced mosquitoes. CJJ performed ookinete development assays. FF contributed intellectually and finantially to the project. GRM supervised the work and revised the text.

ABSTRACT

Gliding motility is a type of locomotion used by malaria parasites and related apicomplexans such as *Toxoplasma* to migrate across tissues and invade cells in diverse host species. Powered by an actin-myosin motor that is anchored to the inner membrane complex, gliding motility requires the secretion of soluble and plasma membrane-resident proteins that provide adhesion with the substrate. Here, we highlight a novel *Plasmodium berghei* surface protein, LIMP, with an essential role in gliding motility and host cell adhesion, traversal and invasion. The absence of this protein reduces transmission to the mosquito vector by half, salivary gland invasion 10-fold and renders parasites unable to infect naïve mice by mosquito bite or when injected intravenously. Translationally repressed in gametocytes, LIMP is targeted to the ookinete crystalloids, transcriptionally activated a second time during sporogony and localized to the sporozoite plasma membrane. While LIMP-depleted parasites display no gliding motility, *in situ* GFP tagging of this 13 kDa (110 amino acids) protein resulted in a limping movement characterised by reduced speed and frequent stretching, which has been correlated with reduced turnover of parasite-substrate adhesion sites. Our results suggest that LIMP plays a critical role in regulating parasite attachment/detachment cycles that supports productive gliding motility and invasion of host target cells.

METHODS

Experimental animals

Animal experiments performed in Leiden University Medical Center (LUMC, Leiden, The Netherlands) were approved by the Animal Experiments Committee of the Leiden University Medical Center (DEC 10099; 12042; 12120). In Instituto de Medicina Molecular (IMM, Lisbon, Portugal) animal experimentation protocols were approved by the IMM Animal Ethics Committee (under authorisation AEC_2010_018_GM_Rdt_General_IMM) and the Portuguese authorities (Direção Geral de Alimentação e Veterinária). At the University of Heidelberg Medical School (Heidelberg, Germany) animal work was approved by the German Authorities (Regierungspräsidium Karlsruhe; Aktenzeichen 35-9185.81/G-3/11) and performed in compliance with FELASA guidelines and regulations. All animal work was in accordance with European Union regulations.

Reference *P. berghei* ANKA lines

Seven reference *P. berghei* ANKA parasite lines were used. Details of most lines can be found in the RMgmDB database (www.pberghei.eu). Line 683cl1 (DOZI::GFP; RMgm-133) [107] expressing a C-terminally GFP-tagged version of *dozi* (PBANKA_121770); line 909cl1 (CITH::GFP; RMgm-358) [108] expressing a C-terminally GFP-tagged version of *cith* (PBANKA_130130); line HPE, a non-gametocyte producer clone [316]; line 820cl1m1cl1 (Fluo-frmg; RMgm-164) [108] expressing RFP under the control of a female gametocyte specific promoter and GFP under the control of a male gametocyte specific promoter; line 259cl1 (PbGFPcon; RMgm-5) expressing GFP under the control of the constitutive *eef1a* promoter; and line cl15cy1, which is the reference parental line of *P. berghei* ANKA [317]. Line Fluo-frmg contains the transgenes integrated into the silent *230p* gene *locus* (PBANKA_030600) and does not contain a drug-selectable marker.

Reverse Transcriptase-PCR (RT-PCR)

Immunoprecipitation (IP) of DOZI::GFP and CITH::GFP parasite lysates, and subsequent RNA extraction and RT-PCR were performed as described [108]. To investigate the transcription pattern of *limp* by RT-PCR, RNA from different life cycle stages were obtained using TRIzol® Reagent (Ambion®, #15596). Reverse transcription was done with random primers and oligo-d(T) using SuperScript® II Reverse Transcriptase (Invitrogen™, #18064). RNA sample origins were as follows: asexual blood stages from line HPE; mixed blood stages (asexuals & gametocytes) and oocysts d12 post-infection (p.i.) from line Fluo-frmg; *in vitro*-cultured ookinetes at different time points from line cl15cy1; midgut sporozoites d20 p.i. and salivary gland sporozoites d20 p.i. from line PbGFPcon; and exoerythrocytic forms from line

PbGFPcon at different time points after mouse infection. Primers used in RT-PCRs are shown in **Table S1a**.

Generation of *limp* gene deletion mutants

To disrupt the gene encoding *limp* (PBANKA_060580) we constructed a standard replacement construct [318] using plasmid pL0001 (www.mr4.com) which contains the pyrimethamine resistant *Toxoplasma gondii* (*tg*) *dhfr/ts* as a selectable marker cassette. See **Table S2** and **Figure S2A** for the name and details of the construct. Target sequences for homologous recombination were PCR amplified from *P. berghei* wild-type (WT) genomic DNA using primers specific for the 5′ or 3′ flanking regions of *limp* (see **Table S1b** for the sequence of the different primers). The PCR–amplified target sequences were cloned in plasmid pL0001 either upstream or downstream of the selectable marker to allow for integration of the construct into the genomic target sequence by homologous recombination. DNA construct used for transfection was obtained after digestion of the replacement construct with the appropriate restriction enzymes (**Table S2**). Transfection, selection and cloning of mutant parasite lines were performed as described [318]; see **Table S2** for details of the transfection experiments performed. Correct deletion of the *limp* gene was confirmed by diagnostic PCR (for primers see **Table S1c**) and Southern analysis of Field-Inversion Gel Electrophoresis (FIGE)-separated chromosomes (**Figure S2B**). Chromosomes were hybridized with a probe recognizing the 3' UTR of *pbdhfr*/*ts*. Absence of *limp* mRNA was determined by RT-PCR analysis (**Figure S2C**) using RNA collected from infected blood containing asexual blood stages and gametocytes (see **Table S1c** for primers used for RT-PCR). Two cloned lines were used for further phenotype analyses: 2091cl2m5 (Δ*limp*-a) and 2090cl2m6 (Δ*limp*-b), both in the Fluo-frmg background.

Generation of transgenic line expressing GFP-tagged LIMP

In situ C-terminal GFP tagging of *limp* was performed by single cross-over homologous recombination into the corresponding *locus*. See **Table S2** and **Figure S1A** for the name and details of the construct. The construct contains the *tgdhfr*/*ts* selectable marker. Primers used to amplify the targeting region of *limp*, corresponding to the 3' end of the open reading frame (ORF) excluding the stop codon are listed in **Table S1b**. The targeting region was cloned in frame with *gfp*. Linearised plasmid was transfected into cl15cy1 parasites using standard methods. Transfection, selection and cloning of resulting mutant parasite line was performed as described [318], resulting in the transgenic line 2180cl1m4 (*limp*::*gfp*). See **Table S2** for details of the transfection experiment performed. Correct integration of the construct was confirmed by diagnostic PCR (for primers see **Table S1c**) and Southern analysis of FIGE-separated chromosomes using a probe for the 3' UTR of *pbdhfr*/*ts* (**Figure S1B**). Transcription and

processing (splicing) of the *gfp* fusion was confirmed by RT-PCR using RNA from mixed blood stage forms (**Figure S1C**). Primers used for RT-PCR are listed in **Table S1c**.

In vivo multiplication rate of asexual blood stages

The multiplication rate of asexual blood stages in mice is determined during the cloning procedure of gene-deletion/transgenic parasites [319] and is calculated as follows: the percentage of infected erythrocytes in OF-1 mice injected with a single parasite is quantified at days 8–11 on Giemsa-stained blood films. The mean asexual multiplication rate per 24 h is then calculated assuming a total of 1.2×10^{10} erythrocytes per mouse and a blood volume of 2 mL. The percentage of infected erythrocytes in mice infected with reference lines of the *P. berghei* ANKA strain consistently ranges between 0.5 and 2% at day 8 after infection, resulting in a mean multiplication rate of 10 per 24 h [319, 320].

Analysis of Δ*limp* blood stage development

Naïve BALB/c mice were infected intravenously (i.v.) with 10^4 infected red blood cells (iRBCs) of either WT (Fluo-frmg) or Δ*limp*-a parasites. Total parasitaemia as well female and male gametocytaemias were determined daily by fluorescence-activated cell sorting (FACS). Total parasitaemia was determined using the vital DNA dye Vybrant® DyeCycle™ Ruby stain (Molecular Probes®, #V10273). Given that both WT and Δ*limp*-a parasite lines express RFP in female gametocytes and GFP in male gametocytes, female gametocytaemias were calculated as RFP+ RBCs/total RBCs, while male gametocytaemias were calculated as GFP+ RBCs/total RBCs.

Ookinete formation assays

Ookinete formation assays were performed following published methods using gametocyte-enriched blood collected from mice treated with phenylhydrazine/NaCl [337]. Briefly, infected blood containing gametocytes was mixed in standard ookinete culture medium in 24-well plates and cultures were incubated for 18-24 h at 21-22 ºC. The ookinete conversion rate is defined as the percentage of female gametes that develop into mature ookinetes determined by counting female gametes and mature ookinetes in Giemsa-stained blood smears 16-18 h after *in vitro* induction of gamete formation.

Oocyst and sporozoite production

Oocyst and sporozoite production of the mutant parasites was analysed by performing standard mosquito infections. Naïve female Balb/c ByJ mice were infected intraperitoneally (i.p.)

with 10^6 infected red blood cells (iRBCs) of each line. On days 4-5 p.i., these mice were anesthetised and *Anopheles stephensi* female mosquitoes allowed to feed for 30 min. Twenty-four hours after feeding, mosquitoes were anesthetised by cold shock and unfed mosquitoes were removed. Oocyst and sporozoite numbers were counted at days 12 and 20-21 after mosquito infection, respectively. Oocysts were counted after mercurochrome staining. Sporozoites were counted in pools of 4-10 mosquitoes.

Transmission experiments

To test the infectivity of sporozoites, 10 infected mosquitoes were allowed to feed for 30 min on anesthetised naïve female Balb/c ByJ mice on days 20-22 p.i. Successful feeding was confirmed by the presence of blood in the abdomen of mosquitoes. Blood stage parasitaemia in these mice were followed up to 34 days post-bite. Transmission of Δ*limp*-a parasites was also assessed by injecting i.v. 3500 salivary gland sporozoites dissected at day 20 p.i. into naïve female Balb/c ByJ mice. Livers were extracted at 44 h p.i. and parasite load determined by quantitative real-time PCR (qPCR) using specific primers for *P. berghei* ANKA *18S* rRNA gene. Mouse hypoxanthine-guanine phosphoribosyltransferase (HPRT) was used as host tissue control gene. Primers used for qPCR are listed in **Table S1a**. Absolute number of mRNA copies was determined for each gene using standard curves. Blood stage parasitaemias in littermate mice were followed up to 34 days post-bite. Similar experiments were performed with WT (Fluo-frmg) for comparison purposes.

***In vitro* sporozoite gliding motility assays**

WT (Fluo-frmg or cl15cy1), Δ*limp*-a and *limp*::*gfp* salivary gland sporozoites were dissected at days 20-21 p.i. and their gliding motility assessed in a standard gliding assay [351]. Briefly, glass coverslips were coated overnight at room temperature (RT) with a 10 µg/mL suspension of 3D11 mouse anti-*P. berghei* circumsporozoite protein (CSP) monoclonal antibody [321]. On the following day, 10000-20000 salivary gland sporozoites of each line were loaded per coverslips and incubated for 1 h at 37 ºC, 5% CO_2, in the presence of 10% FBS. In the case of *limp*::*gfp*, sporozoites were also pre-incubated for 1 h on ice in the presence of rabbit polyclonal anti-GFP (Abcam®, #ab6556; 10 µg/mL) or control rabbit IgGs (Abcam®, #ab37415; 10 µg/mL) to evaluate possible gliding blockade. Sporozoites were then fixed with 4% PFA/PBS and an anti-PbCSP immunofluorescence assay (IFA) was performed to detect CSP trails (see below for IFA details). Coverslips were analysed in a Leica DM5000B fluorescence microscope. Each sporozoite was categorised according to the number of trails it formed. Percentages of sporozoites in each category for each line were calculated as the ratio between the number of sporozoites in each category and the total number of sporozoites analysed. Live motility of WT (Fluo-frmg) and *limp*::*gfp* parasites was assessed by imaging

dissected salivary gland sporozoites in a Nunc™ MicroWell™ 96-well plate with optical bottom (Thermo Scientific™) as described before [352, 353], using an inverted Zeiss Axiovert 200M widefield microscope with an XBO75 xenon lamp, the AxioVision 4.7.2 software, a 25X objective (LCI Plan-NEOFLUAR ImmKorr NA 0.8, water) (all Zeiss) and a CoolSNAP™ HQ^2 high resolution CCD camera (Photometrics). Bright field images were acquired every 3 seconds for 5 minutes (101 frames per movie). Sporozoite speed was assessed using the manual tracking plug-in of ImageJ 1.44o software (imagej.nih.gov/ij). The imaged sporozoites were clustered into three different categories according to [353]: 'moving' sporozoites (consistently gliding with a speed of at least 0.2 µm/s over a minimum of 150 seconds); 'partially moving' sporozoites (displaying circular gliding motility, but failing to meet the 'moving' requirements); and 'attached/waving' sporozoites (not showing any circular gliding but attached at either one or both ends).

In vitro sporozoite traversal, adhesion and invasion assays

WT (Fluo-frmg or cl15cy1), Δ*limp*-a, Δ*limp*-b and *limp*::*gfp* salivary gland sporozoites were dissected at day 21 p.i. To test the parasite capacity to traverse human hepatoma cells *in vitro*, 5000 salivary gland sporozoites of the different parasite lines were loaded, in the presence of 0.5 mg/mL of Dextran, Tetramethylrhodamine (Molecular Probes®, #D1817), onto 110000 Huh7 cells plated 16-20 h before in 24 well-plates and incubated for 2 h at 37 ºC, 5% CO_2. Equivalent amounts of non-infected mosquito salivary gland debris were also loaded onto the same number of cells to serve as negative control. Cells were then washed, trypsinised and analysed in a BD Biosciences® FACSCalibur flow cytometer. Percentage of traversal was quantified as the ratio of Dextran positive cells per live cells. To test the parasite capacity to adhere to and invade human hepatoma cells *in vitro*, 5000 WT (Fluo-frmg or cl15cy1), Δ*limp*-a, Δ*limp*-b or *limp*::*gfp* salivary gland sporozoites were loaded onto 25000 Huh7 cells plated 16-20 h before in black-walled 96 well-plates and incubated for 2 h at 37 ºC, 5% CO_2. In the case of *limp*::*gfp*, sporozoites were also pre-incubated for 1 h on ice in the presence of rabbit polyclonal anti-GFP (Abcam®, #ab6556; 10 µg/mL) or control rabbit IgGs (Abcam®, #ab37415; 10 µg/mL) to evaluate possible invasion blockade. Cells were then fixed with 4% PFA/PBS and a dual colour anti-PbCSP IFA was performed to distinguish between sporozoites that invaded from those that didn´t, following adapted published methods [354]. Briefly, external sporozoites were detected before cell permeabilisation using a 10 µg/mL suspension of 3D11 mouse anti-PbCSP [321] followed by goat anti-mouse IgG-Cy™3 (Jackson ImmunoResearch Laboratories, Inc., #115-166-003; 1:500). Cells were then permeabilised with 0.1% TritonX-100/PBS and total sporozoites detected by a second incubation with the same 3D11 mouse anti-PbCSP dilution followed by goat anti-mouse IgG-Alexa Fluor®488 (Jackson ImmunoResearch Laboratories, Inc., #115-546-006; 1:500). Cells were imaged under a Zeiss Axiovert 200M fluorescence

microscope. Adhesion was quantified as the ratio of imaged sporozoites per number of Huh7 cells in the same optical fields.

In vitro exoerythrocytic form (EEF) development assays

WT (Fluo-frmg or cl15cy1), Δ*limp*-a, Δ*limp*-b and *limp*::*gfp* salivary gland sporozoites were dissected at day 21 p.i. and tested for their ability to transform into EEFs inside Huh7 cells in culture. 5000 salivary gland sporozoites of the different parasite lines were loaded onto 10000 Huh7 cells plated 16-20 h before in black-walled 96 well-plates and incubated for 45 h at 37 ºC, 5% CO_2. Cells were then fixed with 4% PFA/PBS and an IFA performed to detect parasite HSP70 and UIS4 (see below for IFA details). The area of cl15cy1 and *limp*::*gfp* EEFs were calculated based on HSP70 staining using ImageJ 1.47n software (imagej.nih.gov/ij).

Live imaging and IFAs of blood stages, ookinetes, oocysts and sporozoites

Live imaging of transgenic *limp*::*gfp* parasites was done by retrieving ookinetes from mosquito blood meals at 16 h p.i. as well as dissecting infected mosquito midguts at days 13 and 21 p.i. To detect LIMP::GFP expression by IFA in blood stages, as well as in midgut and salivary gland sporozoites, mouse RBCs infected with *limp*::*gfp* parasites or dissected midgut and salivary gland sporozoites were stained with rabbit polyclonal anti-GFP (Abcam®, #ab6556; 1:500) or mouse monoclonal anti-GFP (Abcam®, #ab1218; 1:250) as primary antibody. As secondary antibody, goat anti-rabbit IgG-Alexa Fluor®488 (Jackson ImmunoResearch Laboratories, Inc., #111-545-003; 1:500) or goat anti-mouse IgG-Alexa Fluor®488 (Jackson ImmunoResearch Laboratories, Inc., #115-546-006; 1:500) was used. IFAs to detect CSP or TRAP in *limp*::*gfp* salivary gland sporozoites were done using 3D11 mouse anti-PbCSP [321] (10 µg/mL) or rabbit polyclonal anti-PbTRAP repeats antiserum [260] (1:100) as primary antibodies and goat anti-mouse IgG-Cy™3 (Jackson ImmunoResearch Laboratories, Inc., #115-166-003; 1:500) or goat anti-rabbit IgG-Alexa Fluor®594 (Jackson ImmunoResearch Laboratories, Inc., #111-586-047; 1:500) as secondary antibodies, respectively. IFAs to detect HSP70 and UIS4 in *in vitro*-developed EEFs were done using parasite-specific 2E6 mouse monoclonal anti-PbHSP70 [322] at 18.75 µg/mL and polyclonal goat anti-PbUIS4 (SICGEN, #AB0042; 2 µg/mL), respectively, followed by donkey anti-mouse IgG-DyLight®549 (Jackson ImmunoResearch Laboratories, Inc., #745-506-150; 1:500) and donkey anti-goat IgG-Alexa Fluor®488 (Jackson ImmunoResearch Laboratories, Inc., #705-546-147; 1:500). In all IFAs, samples were fixed with 4% PFA/PBS for 10 min at RT, permeabilised with 0.1% TritonX-100/PBS (or cold absolute methanol in the case of anti-TRAP IFA [260]) and blocked for 1h at RT with 1-3% BSA/PBS. All antibody incubations were done in blocking solution for 1h at RT and 1-5 ug/mL of Hoechst-33342/PBS was used to stain nuclei. All images were taken with a

Leica DM5000B or Zeiss Axiovert 200M fluorescence microscope and processed using ImageJ 1.47n software (imagej.nih.gov/ij).

Transmission electron microscopy (TEM) and immuno-gold electron microscopy (EM) of sporozoites

Infected mosquito midguts and salivary glands were dissected on days 20-27 p.i and fixed for 3 h at 4 ºC in 0.1 M cacodylate buffer, pH 7.4, containing 2.5% (v/v) glutaraldehyde. Following 1 h of post-fixation with 1% (w/v) osmium tetroxide and 30 min of staining in 1% (w/v) uranyl acetate, samples were dehydrated in ethanol gradient (70-95-100%), transferred to propylene oxide and embedded in EPON™ resin. Semi-thin sections (300-400 nm) were stained with toluidine blue for light microscope evaluation. Ultra-thin sections (70 nm) were collected in copper slot grids and then stained with 2% uranyl acetate and lead citrate (Reynolds recipe). For immuno-gold EM, ultra-thin sections (70 nm) collected in Nickel 150 mesh grids were blocked for 30 min at RT with 0.8% BSA, 0.1% cold water fish skin gelatine, and incubated overnight at 4 ºC with rabbit polyclonal anti-GFP (Abcam®, #ab6556; 1:50). After a new blocking step of 15 min at RT, sections were incubated for 1 h at RT with Protein A conjugated to 15 nm gold particles (obtained from Cell Microscopy Center, University Medical Center Utrecht, The Netherlands; 1:50). Sections were finally stained with 2% uranyl acetate and lead citrate (Reynolds recipe). Antibody and Protein A incubations were done in blocking solution. All grids were examined in a Hitachi H-7650 transmission electron microscope at 100kV acceleration.

Multiple sequence alignments

Protein sequences in **Figure 1B** were retrieved from PlasmoDB (plasmodb.org). Clustal W alignments were done at EMBnet server (embnet.vital-it.ch/software/ClustalW.html) and shaded according to protein similarity levels with BOXSHADE 3.21 (www.ch.embnet.org/software/BOX_form.html).

Statistical methods

Statistical analyses were performed using Prism software package 5 (GraphPad Software).

RESULTS

limp is translationally repressed in *P. berghei* gametocytes and translated during ookinete development

Recent studies on DOZI and CITH gene deletion mutants identified more than 100 known and putative surface proteins to be under the translational control during transmission of *P. berghei* gametocytes from the rodent to the mosquito host [107, 108]. One of these proteins, PBANKA_060580 (LIMP) is conserved among *Plasmodium* species but lacks homologs outside the genus. BlastP and tblastn searches (www.ncbi.nlm.nih.gov) failed to identify *T. gondii* or any other apicomplexan Expressed Sequence Tags (ESTs) with homology to *Plasmodium limp*. An identical search at ToxoDB (www.toxodb.org) that included *Toxoplasma*, *Eimeria*, *Gregarina* and *Neospora* was also negative. A secondary structure prediction [355] indicated that the protein consists of an N-terminal signal peptide, a coil domain and a C-terminal alpha-helical domain. LIMP is encoded on an 1194 base pair-long gene in the *P. berghei* ANKA genome with syntenic orthologs in the human parasites *P. falciparum* and *P. vivax*. The gene comprises 6 exons and 5 introns and encodes a protein of 110 amino acids with a predicted molecular weight of approximately 13 kDa, including a 22 amino acid-long signal peptide (**Figure 1**).

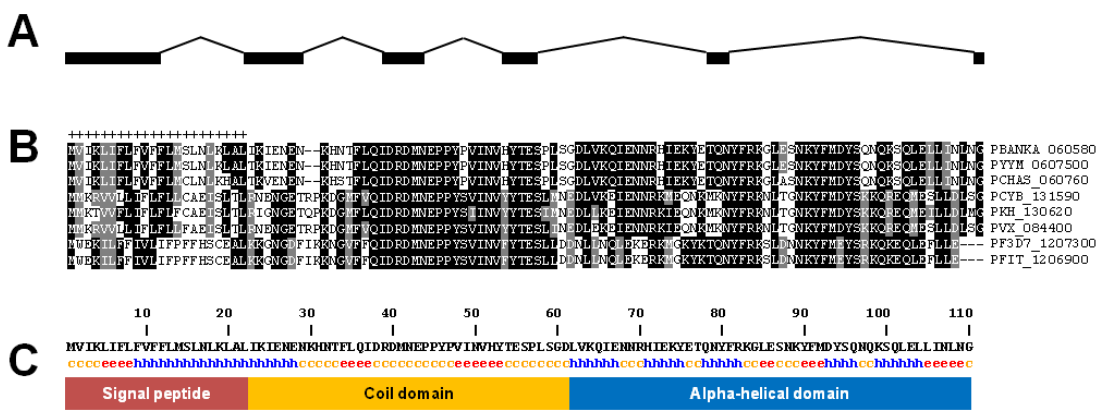

Figure 1 – Gene and protein structure of *limp*.
(A) The *P. berghei limp* gene (1194 bp) is composed of 6 exons (shaded bars) and 5 introns (lines); this organisation is conserved in all other *Plasmodium* species. **(B)** Protein alignment of LIMP orthologs from 8 different *Plasmodium* species and strains. "+" indicates the extent of the signal peptide in *P. berghei*. **(C)** Secondary structure prediction of *P. berghei* LIMP according to NPS@ (npsa-pbil.ibcp.fr). c: random coil; h: alpha helix; e: extended strand.

limp mRNA was found downregulated in Δ*dozi* parasites, suggesting that it might be transcribed preferentially in female gametocytes but kept translationally repressed until activated during ookinete development [107]. IP of DOZI::GFP- and CITH::GFP-expressing parasite lines [107, 108] clearly demonstrated that *limp* mRNA, like *p25* and *p28*, is bound directly or indirectly by DOZI and CITH (**Figure 2A**). Control transcripts known to be translated (*dozi*, *cith* and *alba-3*) did not co-immunoprecipitate with DOZI or CITH.

To confirm unequivocally that *limp* is translationally repressed in female gametocytes but activated during ookinete formation, we GFP-tagged LIMP at the C-terminus leaving the gene under the control of its endogenous transcriptional promoter (**Figure S1**). In this mutant parasite line, blood stage parasites only transcribe the tagged *limp* mRNA (**Figure 2B and S1C**). An IFA confirmed that, as expected, LIMP::GFP is not expressed in asexual stage parasites (not shown) or gametocytes (**Figure 2C**). *limp* is only translated in the ookinete stage and its expression is clearly visible in discrete foci resembling crystalloid bodies (CBs) (**Figure 2C**).

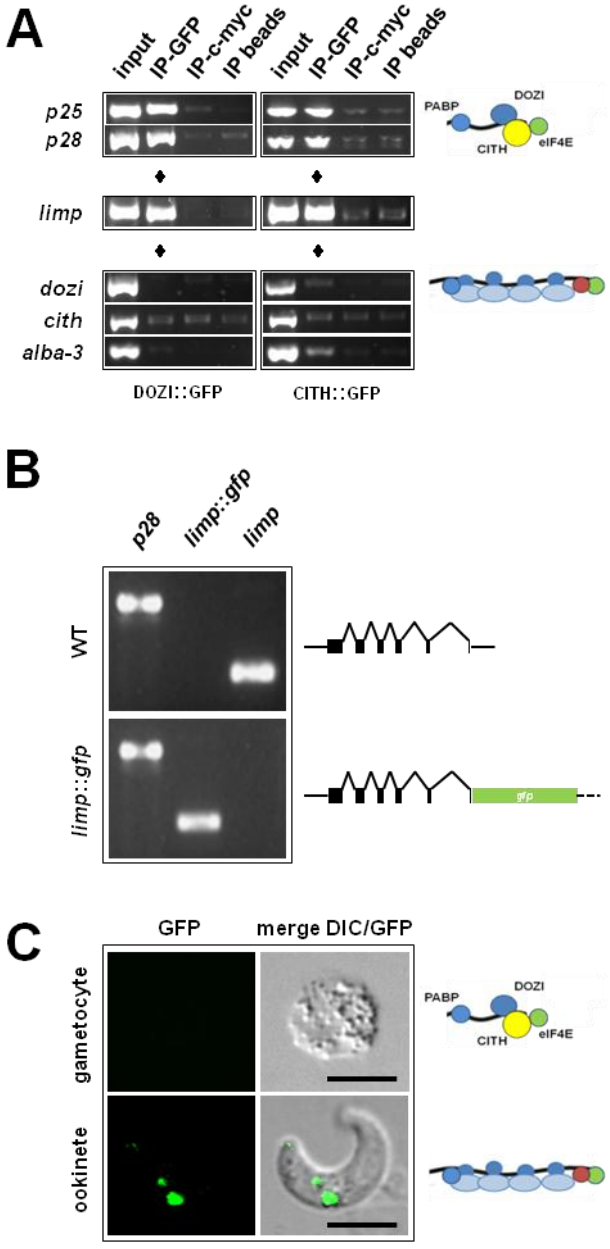

Figure 2 – *limp* is translationally repressed in gametocytes and expressed in ookinetes.
(A) RT-PCR analysis on DOZI::GFP and CITH::GFP gametocyte immunoprecipitation (IP) eluates shows that *limp* as well as *p25* and *p28* mRNAs (known to be translationally repressed) co-precipitate with DOZI and CITH. *dozi*, *cith* and *alba-3* are translated in gametocytes and are not enriched in the IP-GFP fractions. Input: total gametocyte mRNA; IP-GFP: IP with anti-GFP antibody; IP-c-myc: IP with anti-c-myc antibody; IP beads: no antibody used for IP. **(B)** RT-PCR analysis shows absence of WT *limp* and presence of correctly spliced *limp*::*gfp* mRNA in blood stages of *limp*::*gfp* parasites. *p28* serves as control gene. **(C)** Immunofluorescence of *limp*::*gfp* blood stages shows no LIMP expression in gametocytes while live imaging of blood meal-retrieved ookinetes shows LIMP::GFP localisation (in green) in discrete foci. Scale bar = 5 µm.

***limp* gene deletion mutants suffer cumulative population loss during mosquito passage**

In order to understand the function of LIMP for early mosquito stage development we generated two independent knock-out (KO) mutant lines, Δ*limp*-a and Δ*limp*-b, in the reference line Fluo-frmg [108] by deleting the entire *limp* ORF (**Figure S2**). These parasites showed normal asexual blood stage development over time as well as gametocyte numbers and female/male ratios (**Figure S3 and Table S3**). The capacity of Δ*limp* parasites to develop into ookinetes was comparable to that of WT lines, as determined by *in vitro* ookinete conversion

rates ranging from 55 to 91% (**Figure 3A**). KO ookinetes showed normal WT morphology, including the presence of haemozoin clusters suggesting correctly formed CBs (**Figure S4**) [215, 216]. When we characterised Δ*limp* parasites during mosquito passage we consistently found lower oocyst numbers per mosquito when compared to its genetic background WT line (**Figure 3B**); on average, KO parasites developed 52% less oocysts than its WT counterpart. Still, the number of oocyst-derived sporozoites (midgut sporozoites) per oocyst was not significantly changed in KO-infected mosquitoes (**Figure 3C**), showing that development and sporulation proceeded normally in the absence of LIMP once oocysts had been established. Rather, Δ*limp* sporozoites showed a tendency to accumulate in the hemolymph (**Figure 3D**), a feature that was accompanied by an almost complete failure to invade the salivary glands. The number of salivary gland-resident sporozoites per mosquito was reduced 10-fold (**Figure 3E**). A striking reduction was still evident when numbers of salivary gland sporozoites

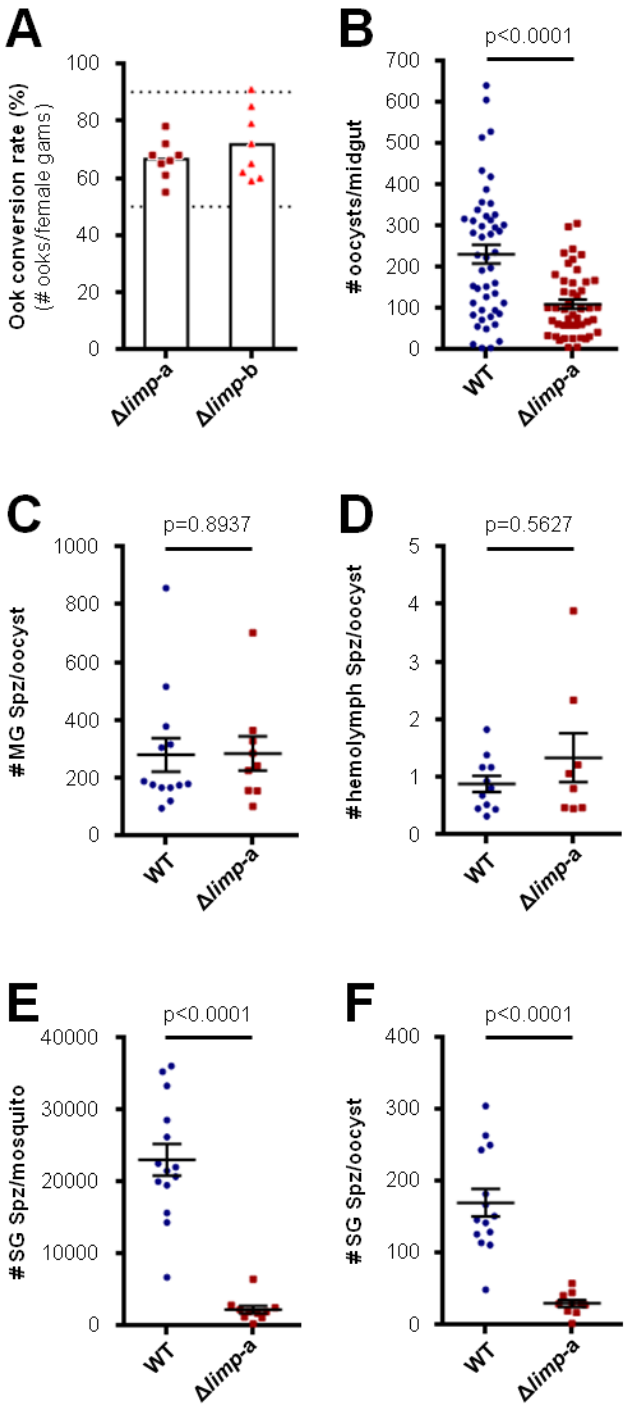

Figure 3 – Δ*limp* parasites suffer cumulative population loss during mosquito passage.
(A) Ookinete (Ook) conversion rates of both Δ*limp*-a and Δ*limp*-b parasites fall within the expected range for a WT parasite line (50-90%, dashed horizontal lines). Mean values are shown by the bars, while dots represent individual conversion rates. Δ*limp*-a and Δ*limp*-b (4 independent experiments, *n*=8). **(B)** Δ*limp*-a parasites show reduced numbers of oocysts per mosquito midgut on day 12 p.i. WT (4 independent experiments, *n*=48); Δ*limp*-a (6 independent experiments, *n*=46). **(C)** Sporozoite development is unaffected in Δ*limp*-a parasites, as seen by the similar number of midgut sporozoites (MG Spz) per oocyst in WT and Δ*limp*-a lines. WT (3 independent experiments, *n*=13); Δ*limp*-a (5 independent experiments, *n*=9). **(D)** Sporozoite (Spz) release to the mosquito hemolymph is comparable between WT and Δ*limp*-a parasites. WT (3 independent experiments, *n*=11); Δ*limp*-a (4 independent experiments, *n*=8). **(E-F)** Δ*limp*-a sporozoites are severely impaired in salivary gland invasion, as seen by the lower number of salivary gland sporozoites (SG Spz) per mosquito (E) and per oocyst (F) in the KO line. WT (4 independent experiments, *n*=14); Δ*limp*-a (6 independent experiments, *n*=10). **(B-F)** Mean and SEM values are shown by the lines; p-values for Mann-Whitney test are shown above the data sets.

were normalised by the number of pre-existing oocysts (**Figure 3F**). Overall, these results clearly suggested a defect in salivary gland invasion by Δ*limp* parasites but no effect of LIMP depletion on sporogony.

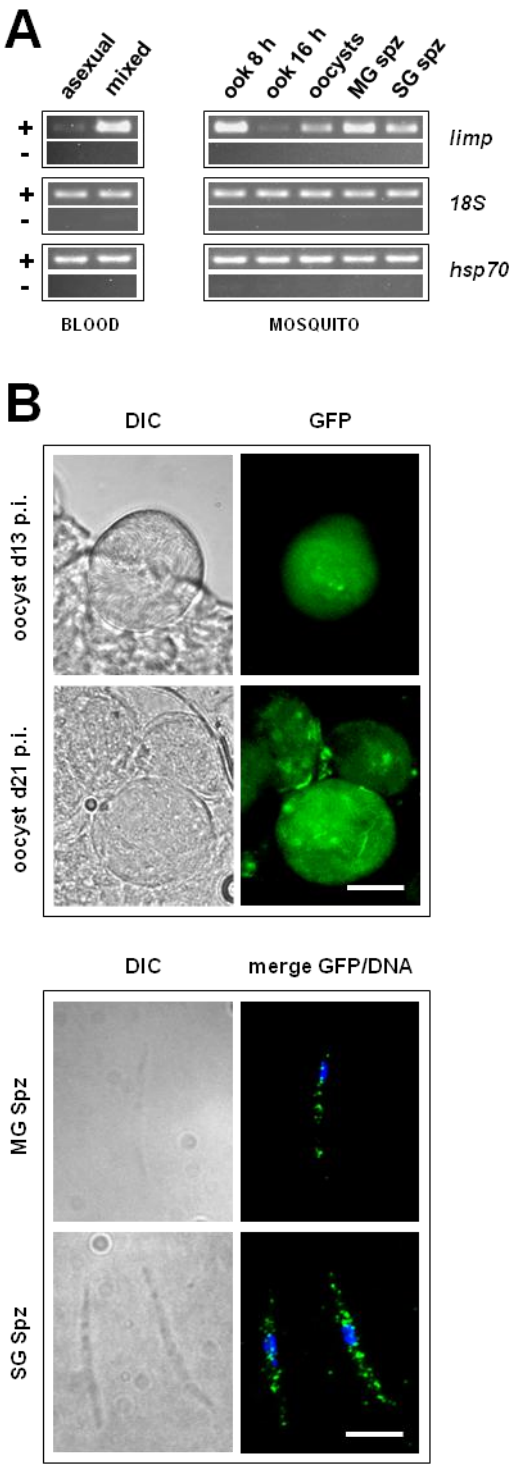

Figure 4 – *limp* mRNA and protein expression profiles.
(A) RT-PCR of *limp* along the parasite life cycle. Asexual: asexual blood stages; mixed: asexuals and gametocytes; ook: ookinetes (8 and 16 hours after gametocyte activation); MG spz: midgut sporozoites; SG spz: salivary gland sporozoites. *18S* rRNA and *hsp70* serve as loading control genes. +: RT positive reaction; -: RT negative reaction. **(B)** Live imaging of *limp*::*gfp* oocysts at days 13 and 21 p.i. (upper panel) shows LIMP expression (in green) in sporulating oocysts. Immunofluorescence assay of *limp*::*gfp* parasites (lower panel) shows LIMP expression (in green) in both midgut sporozoites (MG Spz) at day 24 p.i. and salivary gland sporozoites (SG Spz) at day 21 p.i. DNA was stained with Hoechst-33342 (in blue). Scale bars = 20 µm (oocysts) or 5 µm (sporozoites).

The sporozoite stage phenotype is in agreement with the expression profile found for *limp* mRNA. While high in gametocytes, transcription of the gene is reduced in mature ookinetes, but activated again during sporogony where it persists at least until day 20 post-infection (p.i.) in salivary gland sporozoites (**Figure 4A**). *limp* transcripts could not be detected in liver stage parasites (**Figure S5**).

This transcription profile correlated with LIMP::GFP expression across the parasite's life cycle; apart from expression in ookinetes protein was also detected in sporulating oocysts, as well as midgut and salivary gland sporozoites (**Figure 4B**).

In light of the invasion defect observed for Δ*limp* sporozoites, we tested whether this was mosquito-specific or also extended to invasion of the mammalian host. To this end naïve mice were infected by two different routes with WT- or KO-infected mosquitoes: (i) mosquito bite (**Figure 5A**) or (ii) i.v. injection of dissected sporozoites (**Figure 5B**). In both cases, WT-infected mice developed normal blood stage parasitemia while KO-infected mice never showed parasites in the blood. Moreover, mice injected i.v. with Δ*limp* salivary gland

sporozoites showed no parasite load in the liver at 44 hours p.i. as determined by qPCR of the *P. berghei* ANKA *18S* gene (**Figure 5C**), suggesting an inability of KO parasites to invade and establish an infection inside hepatocytes.

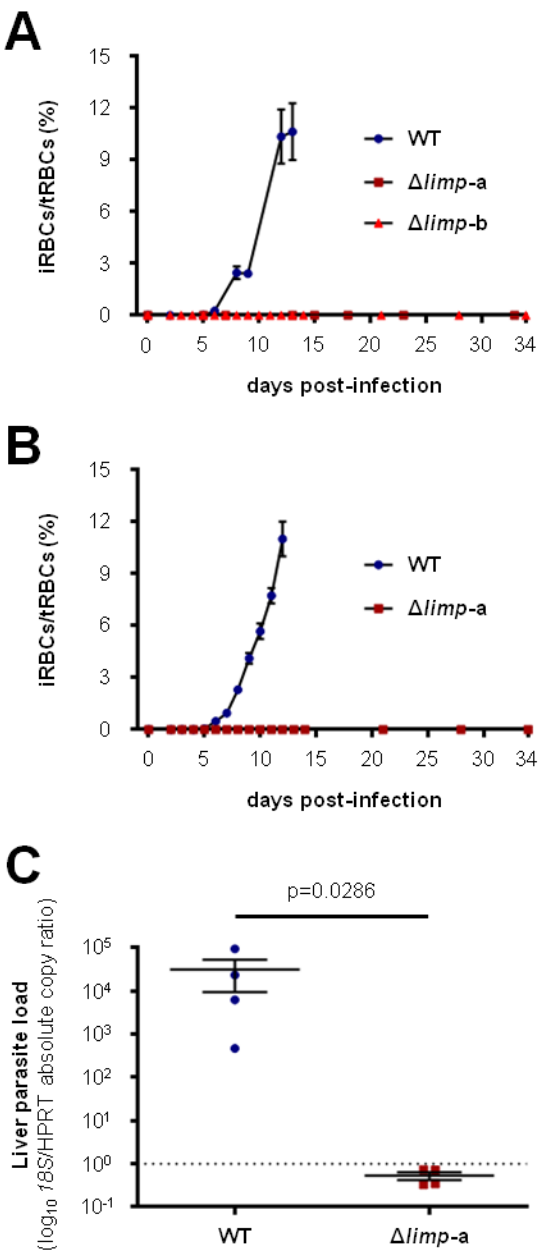

Figure 5 – Δ*limp* parasites do not transmit to naïve mice.
(A) Mice bitten by Δ*limp*-a- or Δ*limp*-b-infected mosquitoes do not develop blood stage infection. Mean parasitaemias are shown by the dots, while SEM values are shown by the vertical lines. WT and Δ*limp*-a (3 independent experiments, *n*=3); Δ*limp*-b (1 experiment, *n*=1). **(B)** Mice injected i.v. with Δ*limp*-a salivary gland sporozoites also do not develop blood stage infection. Mean parasitaemias are shown by the dots, while SEM values are shown by the vertical lines. WT and Δ*limp*-a (3 independent experiments, *n*=4). **(A-B)** iRBCs: infected red blood cells; tRBCs: total red blood cells. **(C)** Mice injected i.v. with Δ*limp*-a salivary gland sporozoites do not present any parasite load in the liver. Mean $\log_{10}$ *18S*/HPRT absolute copy ratio from 2 technical replicates for each mouse is represented by the dots. Overall mean and SEM values are shown by the lines; p-value for Mann-Whitney test is shown above the data sets. Note that the number of *18S* copies per copy of HPRT in all Δ*limp*-a-infected mice was estimated as being below 1 (dashed line), meaning that Δ*limp*-a parasites do not establish a successful liver infection.

Δ*limp* parasites are impaired in hepatocyte transmigration, adhesion and invasion and do not develop into exoerythrocytic forms

Corroborating *in vivo* data, Δ*limp* salivary gland sporozoites were unable to develop into EEFs inside Huh7 human hepatoma cells *in vitro* (**Figure 6A**), suggesting either an invasion or developmental defect. When we assessed hepatocyte invasion at 2 hours p.i. we observed that Δ*limp* parasites are strongly impaired in their capacity to invade Huh7 cells *in vitro* (**Figure 6B**), explaining the complete absence of Δ*limp* EEFs at 45 hours p.i. mentioned above. Moreover, KO sporozoites showed a complete inability to traverse cells as determined by FACS analysis; it is not different from background levels obtained from cells incubated with non-infected mosquito salivary gland material (**Figure 6C**). In addition, Δ*limp* sporozoites also showed reduced adhesion to Huh7 cells in culture (**Figure 6D**).

limp::*gfp* sporozoites on the other hand were not affected in their host cell traversal capability (**Figure S6A**) and transformed (**Figure S6B**) and developed (**Figure S6C**) normally into EEFs with WT morphology and clear expression of cytoplasmic heat shock protein 70 (HSP70) and UIS4 (in the parasitophorous vacuole membrane) (**Figure S6D**). Concordantly, mice bitten by *limp*::*gfp*-infected mosquitoes developed blood stage parasitaemia with the same prepatent period as WT-infected animals (**Figure S6E**).

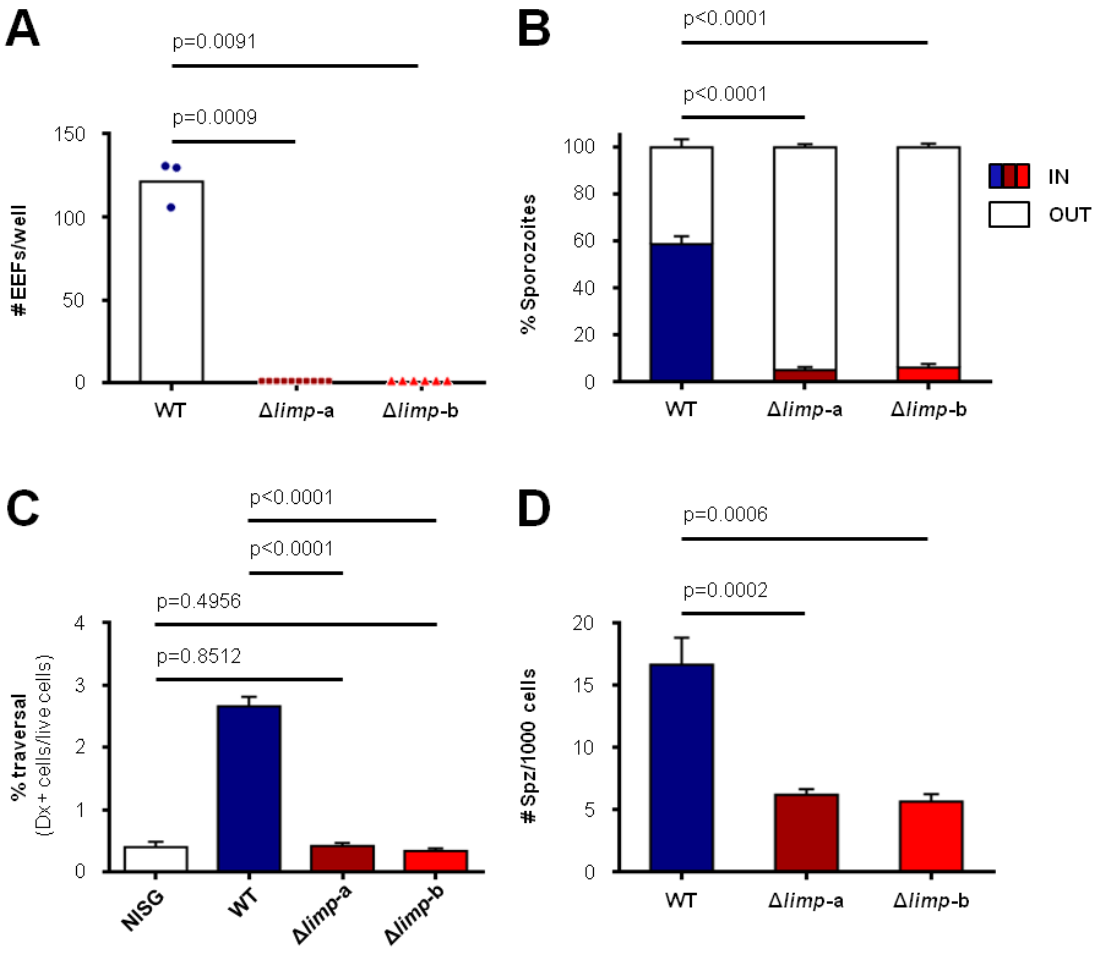

Figure 6 – Δ*limp* parasites are severely impaired in establishing liver infection *in vitro*.
(A) Δ*limp* parasites do not form any exoerythrocytic form (EEF) *in vitro*. Mean numbers of EEFs per well are shown by the bars, while dots represent individual data points; p-values for Mann-Whitney test are shown above the data sets. WT (1 experiment, *n*=3); Δ*limp*-a (4 independent experiments, *n*=10); Δ*limp*-b (2 independent experiments, *n*=6). **(B)** Δ*limp* parasites are impaired in their hepatocyte invasion capacity. WT (4 independent experiments; *n* = 12; 1292 sporozoites analysed); Δ*limp*-a (5 independent experiments; *n* = 12; 806 sporozoites analysed); Δ*limp*-b (2 independent experiments; *n* = 6; 381 sporozoites analysed). **(C)** Δ*limp* parasites are impaired in their hepatocyte traversal capacity. NISG: cells incubated with non-infected salivary gland material. WT (4 independent experiments, *n*=12); Δ*limp*-a (5 independent experiments, *n*=10); Δ*limp*-b (2 independent experiments, *n*=6). Dx+ cells: Dextran, Tetramethylrhodamine positive cells. **(D)** Δ*limp* sporozoites (Spz) are impaired in their cell adhesion capacity. WT (3 independent experiments, *n*=6); Δ*limp*-a (3 independent experiments, *n*=8); Δ*limp*-b (2 independent experiments, *n*=6). **(B-D)** Mean values are shown by the bars, while SEM values are shown by the vertical lines; p-values for Student´s *t*-test are shown above the bars.

Δ*limp* parasites are severely impaired in gliding motility

Escape from the blood meal and traversal of the mosquito midgut epithelium by the ookinete and invasion of salivary glands by the sporozoite, as well as escape from the host's

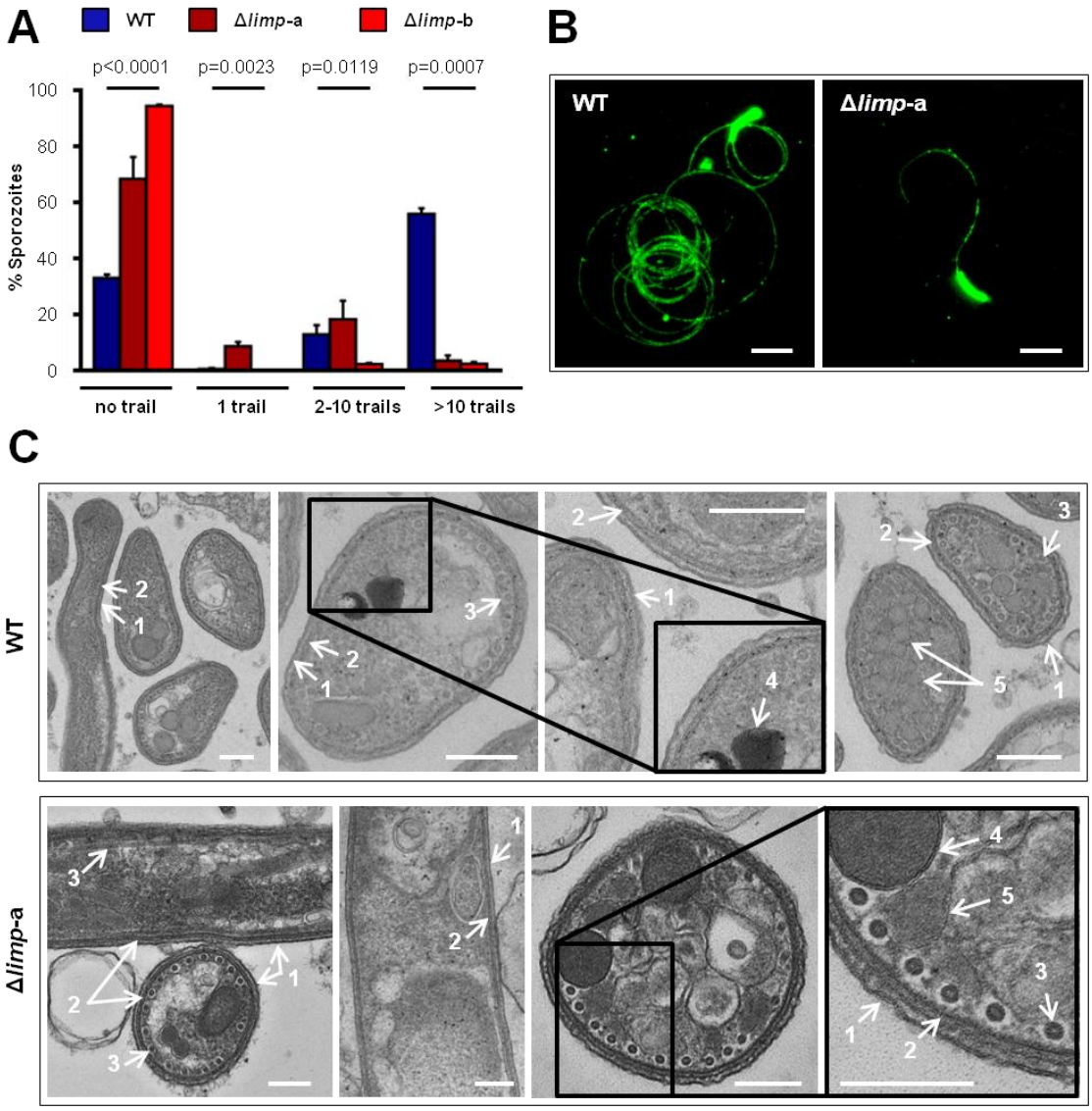

Figure 7 – Δ*limp* parasites are greatly impaired in gliding motility but do not show altered cellular ultrastructure.
(A) Both Δ*limp*-a and Δ*limp*-b parasites show significantly reduced gliding motility. Mean percentages of sporozoites within each gliding category are shown by the bars, while SEM values are shown by the vertical lines; p-value for Kruskal-Wallis test is shown above the bars. WT (4 independent experiments; *n*= 7; 820 sporozoites analysed); Δ*limp*-a (4 independent experiments; *n*= 4; 477 sporozoites analysed); Δ*limp*-b (1 experiment; *n*= 3; 299 sporozoites analysed). **(B)** Representative images of WT and Δ*limp*-a gliding trails. Scale bars = 10 µm. **(C)** Detailed cellular ultrastructure of Δ*limp*-a sporozoites is not altered when compared to WT parasites. 1: plasma membrane; 2: inner membrane complex; 3: subpellicular microtubules; 4: rhoptries; 5: micronemes. Scale bars = 200 nm.

skin and traversal/invasion of liver cells require gliding motility. The reduced numbers of oocysts and near absence of salivary gland sporozoites in the Δ*limp* strain suggested that LIMP could be involved in gliding motility. Therefore, we performed a standard gliding motility assay to detect CSP trails deposited on microscope slides by moving sporozoites. KO parasites were

severely impaired in gliding motility, evident both by the large number of completely immotile parasites as well as the number and length of gliding trails of the few moving parasites (**Figures 7A and B**).

Morphologically, KO parasites appeared normal. TEM studies of Δ*limp* sporozoites revealed no ultrastructural defects. The arrangement of the plasma membrane (PM), inner membrane complex (IMC), subpellicular microtubules as well as micronemes and rhoptries (the organelles involved in protein secretion during parasite motility and invasion [252, 254, 356]) appeared not different from WT parasites (**Figure 7C**).

LIMP::GFP localisation and motility and invasion by *limp*::*gfp* parasites

In ookinetes, LIMP::GFP localised to CBs (**Figure 2C**). When we performed IFAs on sporozoites from midguts and salivary glands from the same mutant line, fluorescence was found in a speckle-like distribution throughout the entire length of the parasite (**Figure 4B**), most likely on or at the cell surface as indicated by staining in the absence of permeabilisation. LIMP::GFP did not co-localise with CSP or the micronemal protein TRAP in these assays (**Figure 8A**).

Consistent with such a surface localisation we found LIMP::GFP to be predominantly localised to the parasite PM in an immuno-EM approach using anti-GFP antibody and gold-conjugated Protein A (**Figure 8B**). In three independent staining experiments done with three different samples, an average of 75.4% of gold particles (from a total of 281 particles) were associated with the parasite PM, 11.4% were observed outside of the parasites and 13.2% intracellularly though not associated with any specific organelle. In *limp*::*gfp* negative control preparations where incubation with primary antibody was omitted or in an additional negative control where WT parasites (these do not express GFP in sporozoites) were incubated with both primary antibody and Protein A-gold, gold particles were few and didn't show any preferential localisation (**Table S4**).

Given the surface localisation of LIMP::GFP, we explored the possibility that the protein might be secreted or shed from the parasite surface during gliding. We therefore performed a gliding assay with *limp*::*gfp* salivary gland sporozoites by coating the parasite substrate with the same commercial anti-GFP antibody as used for sporozoite IFAs and immuno-EM. No gliding trails were detected in this assay, suggesting that the GFP-tagged protein is not shed from the parasite surface or is shed at levels below the detection limit of this assay. *limp*::*gfp* salivary gland sporozoites produced normal numbers and shapes of CSP gliding trails. Moreover, the presence of high concentrations of either anti-GFP antibodies or unspecific control immunoglobulins (IgGs) did not affect the overall gliding nor CSP shedding in these parasites (**Figures 9A and B**). Similarly, *in vitro* hepatocyte invasion by *limp*::*gfp* sporozoites was

comparable to WT parasites and was also not affected by the presence of anti-GFP or control antibodies (**Figure 9C**).

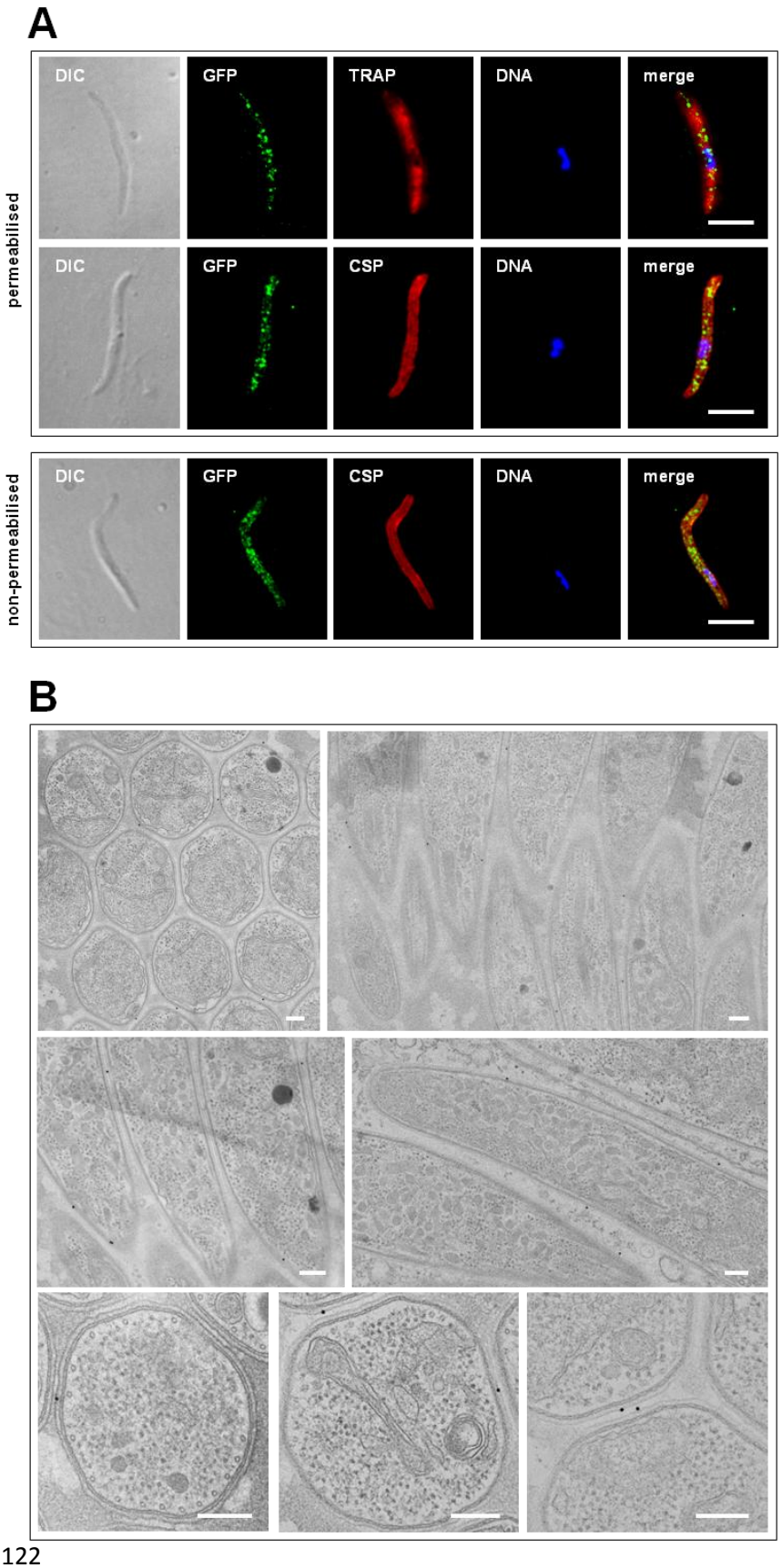

Figure 8 – LIMP::GFP is localised to the parasite plasma membrane. **(A)** Immunofluorescence assays of day 21 p.i. *limp*::*gfp* salivary gland sporozoites with the surface marker CSP and the surface/microneme marker TRAP (in red) pinpoints to a LIMP surface localisation (in green), as suggested by the detection of LIMP::GFP in the absence of cell permeabilisation. DNA was stained with Hoechst-33342 (in blue). Scale bars = 5 µm. **(B)** Immuno-electron microscopy of longitudinal and transversal *limp*::*gfp* salivary gland sporozoite sections with anti-GFP antibodies identifies LIMP::GFP (black, circular dots) at the parasite plasma membrane. Scale bars = 200 nm.

While CSP trail-based motility analyses did not highlight significant differences between WT and *limp*::*gfp* parasites, live motility assays of *limp*::*gfp* sporozoites revealed a peculiar feature. Compared to the WT line the number of moving parasites was identical (**Figure 10A**); the velocity of these parasites was however reduced by more than 20% (**Figure 10B**). Maximum projections of gliding paths highlighted higher number of parasites with irregular trails and wider circumferences instead of tight concentric rings typical for WT parasites (**Figure 10C**). While WT parasites continuously move in a circular fashion following their crescent cell shape, *limp*::*gfp* sporozoites moved with a limp, hence the gene designation *limp*: the movement of *limp*::*gfp* parasites is characterised by an accentuated frequency of cell stretching events (**Figures 10D and E**), which result in a transient increase of sporozoite front-to-rear end distance termed a limp (**Figure 10F**). While more than 50% of WT sporozoites did not exhibit a limp during 100 seconds of gliding, 50% of *limp*::*gfp* sporozoites limped at least four times during the same period. This suggests that a functional impairment of LIMP through GFP leads to a deficit in detachment at the rear end of the parasite.

DISCUSSION

Here we have identified a novel and unique *Plasmodium* protein with a function in the transition from the ookinete to the oocyst and salivary gland sporozoite gliding motility, cell traversal, adhesion and invasion.

limp was readily deleted, leaving blood stage parasitaemia and gametocytaemias unaffected while being detrimental to mosquito and liver infection. *limp* mRNA is under translational control in female gametocytes and de-repressed in the ookinete, where it seems to play a role in mosquito midgut invasion and/or efficient oocyst development. The gene is transcriptionally activated a second time during sporozoite formation to promote salivary gland and hepatocyte invasion processes. Parasite mutants that lack LIMP are deficient in salivary gland invasion and are completely incapable of establishing an infection in hepatocytes, both *in vitro* and *in vivo*. This 'waving' expression pattern translates into successive steps where the absence of LIMP results in significant parasite population losses.

LIMP has not been detected in any proteomics study published so far in *P. berghei*, *P. yoelii* (rodent malaria species), *P. falciparum*, *P. vivax* (human malaria species) or even *P. gallinaceum* (avian malaria species), covering the entire parasite life cycle (PlasmoDB version 11.1 and [49, 323-326]). It was also not detected in a recent study on translational de-repression in the ookinete where proteins translated *de novo* during ookinete development were assessed by mass-spectrometry [134]. However, we clearly demonstrate that *limp* is subjected to translational repression (TR) in *P. berghei* gametocytes and translated in mature ookinetes. In our *limp*::*gfp* parasite line the endogenous 3' untranslated region (UTR) of *limp* had been substituted with that of *P. berghei* dihydrofolate reductase/thymidylate synthase (*dhfr*/*ts*), known to lack TR-targeting motifs [132]. This however did not lead to precocious mRNA translation in

gametocytes, indicating that TR of *limp* is mechanistically similar to *p25*, which is dependent on RNA motifs located within its 5' UTR [132].

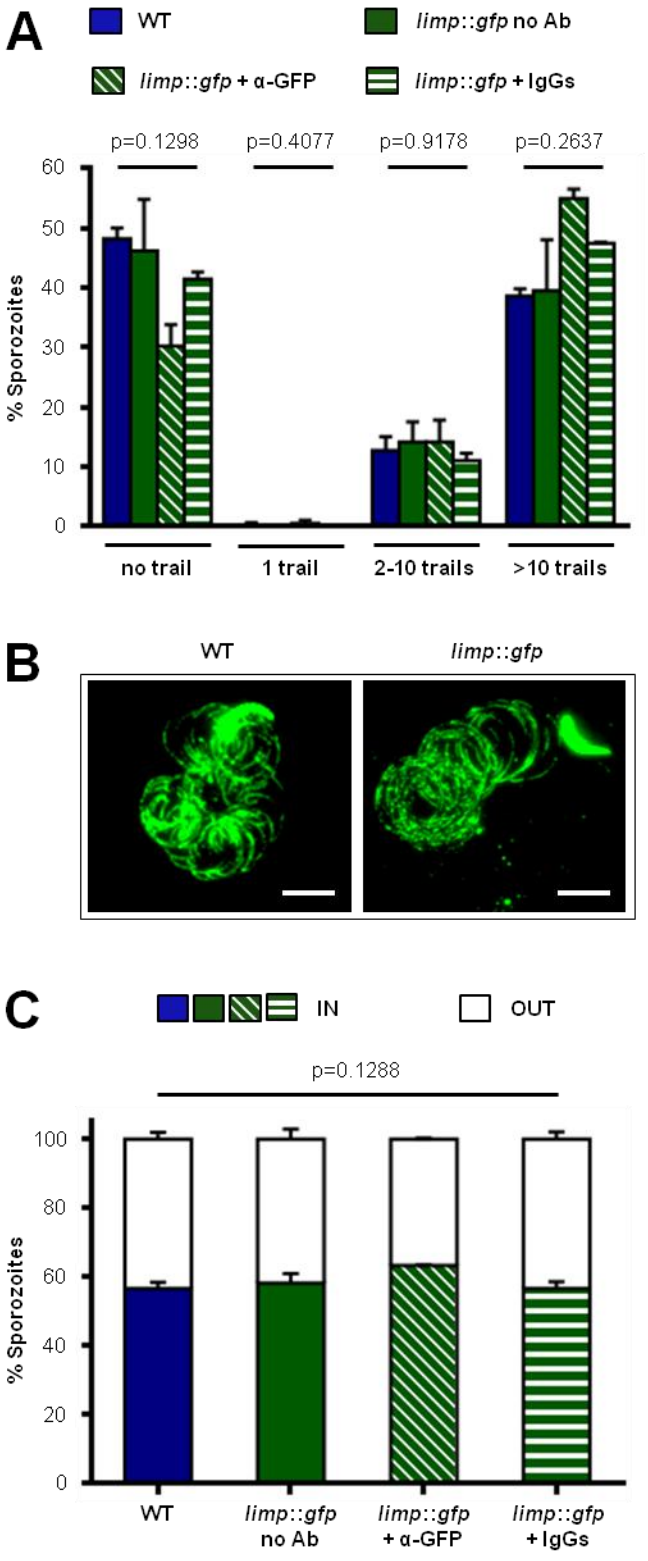

Figure 9 – *limp*::*gfp* parasites present productive gliding and invasion.
(A) *limp*::*gfp* salivary gland sporozoites produce normal numbers of CSP gliding trails and motility is not affected by the presence of anti-GFP antibodies. Mean percentages of sporozoites within each gliding category are shown by the bars, while SEM values are shown by the vertical lines. WT (1 experiment; *n* = 3; 280 sporozoites analysed); *limp*::*gfp* with no antibody (Ab) (2 independent experiments; *n* = 5; 492 sporozoites analysed); *limp*::*gfp* + anti(α)-GFP (1 experiment; *n* = 3; 197 sporozoites analysed); *limp*::*gfp* + IgGs (1 experiment; *n* = 3; 234 sporozoites analysed). **(B)** Representative images of WT and *limp*::*gfp* (no antibody) gliding trails. Scale bars = 10 µm. **(C)** *limp*::*gfp* salivary gland sporozoites invade hepatocytes at WT levels and host cell invasion is not affected by the presence of anti-GFP antibodies. Mean percentages of invading (IN) and non-invading (OUT) parasites are shown by the bars, while SEM values are shown by the vertical lines. Data is from 1 experiment (*n* = 3) for all parasite lines and conditions. Numbers of sporozoites analysed: WT = 346, *limp*::*gfp* with no antibody (Ab) = 763, *limp*::*gfp* + anti(α)-GFP = 807, *limp*::*gfp* + IgGs = 742. **(A,C)** p-values for Kruskal-Wallis test are shown above the bars.

Several translationally repressed genes are known to be necessary for normal ookinete development and consequently to the establishment of oocysts in the mosquito midgut basal lamina. This is the case, for example, of the ookinete surface antigens *p25* and *p28* [137] and the ookinete-specific transcription factor *ap2-o* [71]. On the other hand, ookinete invasion-related genes have been shown to be transcribed *de novo* after fertilisation [357], including SOAP [255] and CTRP [272, 273]. It is thought that the transcriptional activation of such genes is mediated by AP2-O [71]. Interestingly, the absence of *limp* did not lead to reduced numbers of ookinetes or ookinetes with abnormal morphology. Instead, a reduction in oocyst numbers to half of WT levels was observed which, in light of the phenotype of Δ*limp* sporozoites, is most likely explained by a midgut invasion defect.

The localisation of LIMP in ookinetes is consistent with CB localization, as observed for proteins of the LCCL (LAP, CCp) protein family [208, 211, 212]. Curiously, the LCCL protein family members LAP4, LAP5 and LAP6 have been shown to be translationally repressed in gametocytes [208]. Regardless of being translationally repressed or not, all CB-associated proteins that have been functionally analysed so far are solely necessary for oocyst sporulation. This makes LIMP the first *Plasmodium* CB protein with a function other than formation of oocyst-derived sporozoites.

Furthermore, Δ*limp* sporozoites are severely impaired in their gliding motility and invasion capacities. Both ookinetes and sporozoites present numerous micronemes concentrated in the apical end of the cell that are responsible for protein secretion during both motility and invasion processes [204, 256], as well as subpellicular microtubules that aid in microneme mobilisation and secretion [358, 359]. When we investigated these subcellular structures by TEM we could not find any differences between Δ*limp* and WT parasites that could explain the phenotype of Δ*limp* parasites. Thus, the absence of LIMP seems not to affect subcellular structures involved in gliding motility and invasion such as the IMC, the subpellicular microtubules, rhoptries or micronemes.

In situ tagging of LIMP with GFP identified the protein at the sporozoite PM. We cannot however assert that LIMP is completely absent from other subcellular compartments, specifically the cytosol, as sample processing methodologies employed here could lead to cytosolic protein extraction. Nonetheless, in light of LIMP's mode of action and the phenotypes of Δ*limp* parasites, the PM is the most plausible location for this protein.

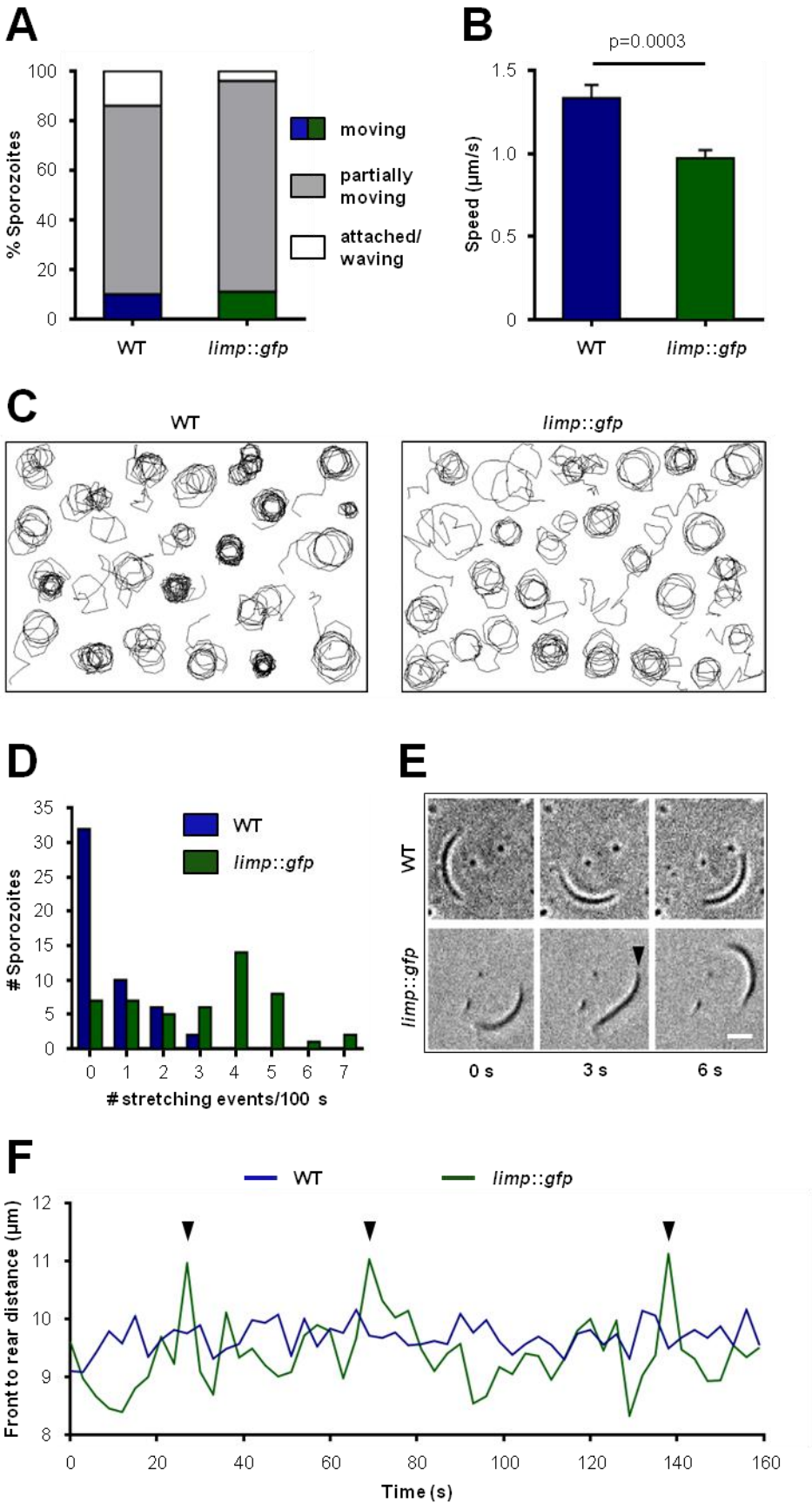

Figure 10 (legend next page) – *limp*::*gfp* salivary gland sporozoites glide with a limp.

In our immuno-EM experiments, the distribution of gold particles along the parasite PM was relatively sparse. This can partially be explained by the osmium tetroxide post-fixation step used in our protocol. This compound is known to create cross-links with sample molecules which can render epitopes inaccessible to antibodies. However, it is particularly useful at preserving membranes. Another possible explanation is the use of an epoxy resin (more specifically EPON™) for sample embedding. Despite of its good sample impregnation, elasticity and stability during sectioning, this resin polymerizes at high temperatures (slow process) and this can be harmful to proteins. Nevertheless, the overall protocol employed here is better at preserving subcellular structures than conventional immuno-gold procedures, namely lipid membranes. It allowed us to detect LIMP::GFP (albeit at low levels) while unequivocally identifying it at the parasite PM. This sparse distribution is also in agreement with the staining pattern obtained in our IFAs. In these assays, where the overall LIMP::GFP signal along the entire parasite is observed, LIMP is not uniformly spread and appears speckled. Consequently, when looking at a 70 nm-thick transversal or longitudinal section of a parasite (as was the case of the immuno-EM micrographs), one could expect to see just a few gold dots.

LIMP plays a role in gliding motility, cell traversal, adhesion and invasion, and ultimately in overall *in vivo* infectivity. Several other secreted proteins of parasite origin are known to play a role in one or more of these processes: CTRP [272-274], MAOP [275] and SOAP [255] in the ookinete; MAEBL [276, 277], SPECT [278], SPECT2 [279], P52 [265, 284] and TRAP [259, 260, 285-287] in the sporozoite; and CelTOS [175] in both the ookinete and the sporozoite. For detailed description of protein functions please see **Introduction - MOTILITY AND INVASION OF MALARIA PARASITES**.

A common feature to all of these proteins is that they localise to the micronemes. In contrast, LIMP does not localise to these organelles and unlike the above mentioned proteins, it plays vital roles in all of the cellular processes on which sporozoites rely to successfully infect their hosts. Moreover, LIMP is also necessary for efficient ookinete-to-oocyst transformation most likely by influencing ookinete gliding and midgut epithelium invasion and traversal. These results highlight LIMP as a parasite protein with unique features and crucial impact at several steps of the *Plasmodium* life cycle.

The underlying requirement for gliding, cell traversal and invasion is that the sporozoite

---

Figure 10 (previous page) – *limp*::*gfp* salivary gland sporozoites glide with a limp.
(A) Percentage of moving *limp*::*gfp* sporozoites is comparable to WT parasites. WT (260 sporozoites analysed); *limp*::*gfp* (228 sporozoites analysed). **(B)** 'Moving' *limp*::*gfp* salivary gland sporozoites show significantly reduced gliding speed. Mean values are shown by the bars, while SEM values are shown by the vertical lines; p-value for Student´s *t*-test is shown above the bars. WT and *limp*::*gfp* (*n*=23). **(C)** Maximum projections of WT and *limp*::*gfp* 'moving' sporozoites tracked in (B). **(D)** Gliding *limp*::*gfp* sporozoites show higher frequency of stretching events than WT parasites. Absolute numbers of sporozoites within each stretching frequency category are shown by the bars. WT and *limp*::*gfp* (50 sporozoites analysed). **(A-D)** WT and *limp*::*gfp* data is from 3 independent experiments. **(E)** Consecutive bright filed images of representative gliding WT and *limp*::*gfp* sporozoites. Arrowhead indicates a stretched sporozoite. Scale bar = 5 µm. **(F)** Distance between front and rear ends of WT and *limp*::*gfp* sporozoites shown in (E) over 159 seconds. Arrowheads indicate stretching events.

adheres to its substrate, whether it is an artificial one such as glass or plastic, or biological as in the case of cells (skin, liver sinusoidal or hepatocytes) [360]. Adhesion of eukaryotic cells is a complex cellular mechanism by which surface receptors interact with extracellular ligands thereby modulating cytoskeleton organisation within the cell [361, 362]. For motility, adhesion sites have to assemble at the leading end of the cell and disassemble at the trailing end [363, 364]. In the case of *Plasmodium* sporozoites, adhesion is a stepwise process divided into three steps: an initial adhesion occurs at either the apical or proximal (rear) end, followed by a secondary adhesion with the opposite end; the apical end then moves slightly forward and the sporozoite flips over on one of its sides, thus increasing the area of contact between the sporozoite body and the substrate; finally a tertiary adhesion is made at centre of the parasite. It is also known that the primary step of adhesion is dependent on the parasite's actin dynamics, as the induction of actin polymerisation leads to weaker adhesion [365]. Not many proteins have been reported to play a role in sporozoite adhesion. TRAP and S6/TREP were reported to be important for initial *in vitro* adhesion. It was suggested that this function was associated with the interaction of their predicted von Willebrand A extracellular adhesive domains with the substrate [365]. Interestingly, TRAP-deficient parasites adhere preferentially with their front end, while sporozoites lacking S6/TREP show no preference for apical or rear end initial adhesion. Moreover, their differential spatial interaction with cytoskeleton actin filaments suggests these proteins cannot compensate for one another during adhesion and motility [360]. TRAP was also shown to play a role in detachment of sporozoite adhesion sites. On one hand TRAP-deficient sporozoites adhere less well but once attached they fail completely to detach, suggesting that TRAP coordinates continuous gliding motility through deadhesion of contact sites [366].

On the other hand, the structurally related protein TLP appears to stabilise newly formed adhesion sites and/or to increase the speed of adhesion formation, thereby augmenting continued adhesion formation during gliding [365]. Finally, parasite HSP20 (heat shock protein 20) has been implicated in the regulation of the dynamics of parasite adhesion site formation and rupture with KO parasites for this protein showing slower and unidirectional gliding motility while leaving *in vitro* cell traversal and invasion unaffected [367].

The turnover of adhesion sites is known to be necessary for continuous parasite motility. Strong adhesion forces at the rear (but also at the centre) of the sporozoite during gliding have been shown to lead to temporary movement arrest and parasite stretching when the parasite still tries to pull forward [366]. The phenotype of our *limp*::*gfp* parasites may thus suggest that LIMP is important for efficient and timely detachment of the sporozoite from the substrate, allowing for fast and uninterrupted gliding. This hypothesis could also explain why in the complete absence of LIMP, parasites rarely present any motility. On the other hand, the observation that Δ*limp* parasites adhere less to hepatoma cells *in vitro* implies that LIMP is not only necessary for adhesion site turnover but also important for the establishment of initial adhesion contacts with the substrate, thereby affecting the subsequent events of motility and invasion. In that sense it is a protein with an equivalent function to TRAP. It is possible that

LIMP is a regulator of TRAP or acts in conjunction with TRAP and/or other TRAP family member. Alternatively, LIMP could be acting completely independently of TRAP. Both scenarios highlight how little we understand about formation of adhesion sites, their turnover and the generation of force within the parasite. LIMP is currently the most enigmatic and thus interesting protein involved in sporozoite motility. As it contains a coil domain and these are known to often serve to interact with other proteins, finding LIMP binding partners will constitute the next step to unravel its function.

In summary, LIMP plays an essential role in parasite transmission by facilitating productive gliding motility that results in traversal of various mosquito and mammalian tissues and invasion of the mosquito salivary glands and liver cells in the vertebrate host. This makes LIMP a unique protein with crucial impact on multiple biologically relevant steps that are vital for the completion of the parasite's life cycle. Moreover, LIMP is exclusive to malaria parasites. Altogether, these properties highlight LIMP as an exciting target for malaria intervention strategies, should we be able to interfere with its function by perhaps the use of small molecules, while underlying the importance of interfering with malaria parasite transmission by targeting its gliding motility machinery.

SUPPLEMENTARY FIGURES AND TABLES

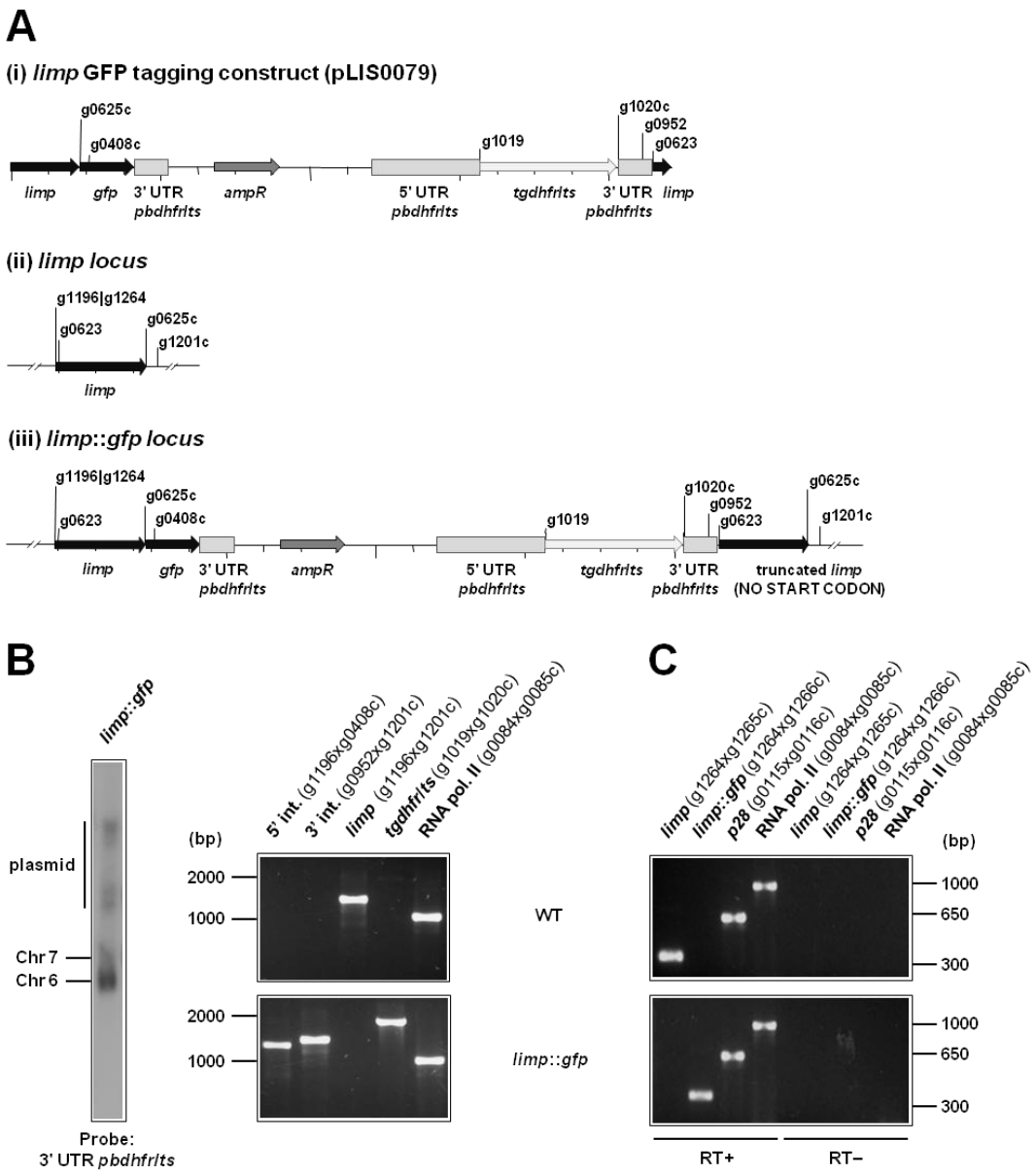

Figure S1 – Generation and genotyping of *limp*::*gfp* parasite line.
(A) *limp* GFP tagging construct pLIS0079 (i) was obtained by cloning the last 1149 bp of the *limp* ORF excluding the stop codon upstream and in frame with the *gfp* gene. This construct includes *Toxoplasma gondii dhfr/ts* selectable marker cassette under the control of *P. berghei dhfr/ts* 5' and 3' UTRs. The construct was integrated into the *limp locus* (ii) of cl15cy1 by single homologous recombination, resulting in the fusion of *limp* to *gfp* in *limp*::*gfp* parasites (iii). **(B)** Correct tagging of *limp* was shown by Southern analysis of separated chromosomes (left) and diagnostic PCR analyses (right). Hybridisation of separated chromosomes from uncloned *limp*::*gfp* parasites with a probe against the 3' UTR of *pbdhfr/ts* recognised integrated pLIS0079 into chromosome 6, the endogenous *pbdhfr/ts locus* in chromosome 7 and circular plasmid with higher molecular weight. PCR analyses confirm 5' and 3' integration (int.) of pLIS0079, absence of WT *limp* ORF and presence of *tgdhfr/ts* gene. **(C)** Absence of WT *limp* and presence of *limp*::*gfp* mRNA was confirmed in cloned *limp*::*gfp* mixed blood stages by RT-PCR. *p28* and RNA polymerase II serve as control genes. Primer g1265c only binds to *limp* WT cDNA while primer g1266c only anneals with *limp*::*gfp* cDNA.

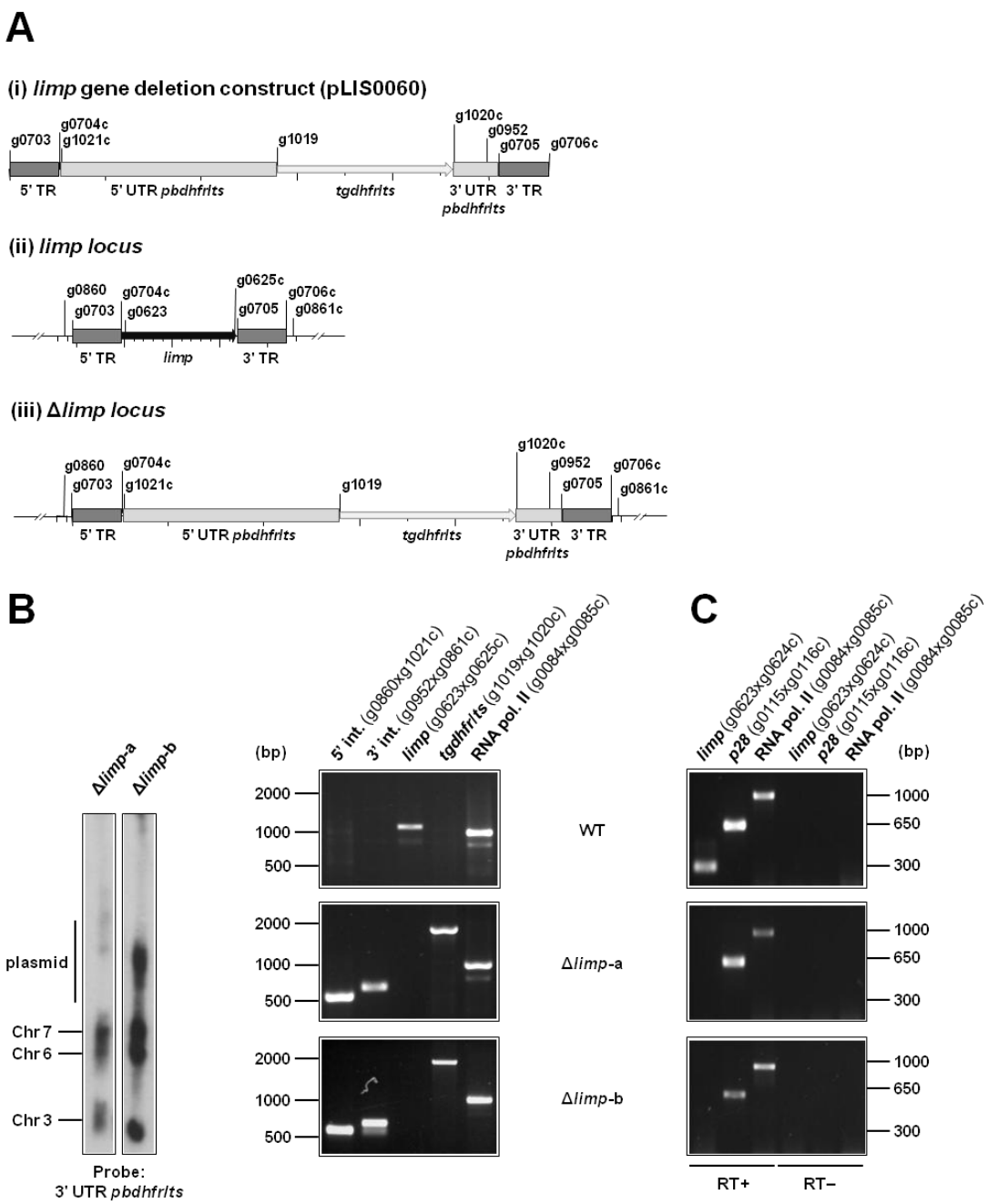

Figure S2 – Generation and genotyping of Δ*limp* parasite lines.
(A) *limp* gene deletion construct pLIS0060 (i) was obtained by cloning *limp* 5' and 3' targeting regions (TR) upstream and downstream of the *Toxoplasma gondii dhfr/ts* selectable marker cassette, respectively. *tgdhfr/ts* gene is under the control of *P. berghei dhfr/ts* 5' and 3' UTRs. The construct was integrated into the *limp locus* (ii) of Fluo-frmg by double homologous recombination, resulting in the complete deletion of *limp* ORF in Δ*limp* parasites (iii). **(B)** Correct deletion of *limp* was shown by Southern analysis of separated chromosomes (left) and diagnostic PCR analyses (right). Hybridisation of separated chromosomes from uncloned Δ*limp* parasites with a probe against the 3' UTR of *pbdhfr/ts* recognised integrated pLIS0060 into chromosome 6, the endogenous *pbdhfr/ts locus* in chromosome 7, reporter gene constructs (GFP/RFP or GFP-Luciferase) in chromosome 3 and circular plasmid with higher molecular weight. PCR analyses confirm 5' and 3' integration (int.) of pLIS0060, absence of *limp* ORF and presence of *tgdhfr/ts* gene. **(C)** Absence of *limp* mRNA was confirmed in cloned Δ*limp* mixed blood stages by RT-PCR. *p28* and RNA polymerase II serve as control genes. Primer g0624c only anneals with *limp* cDNA.

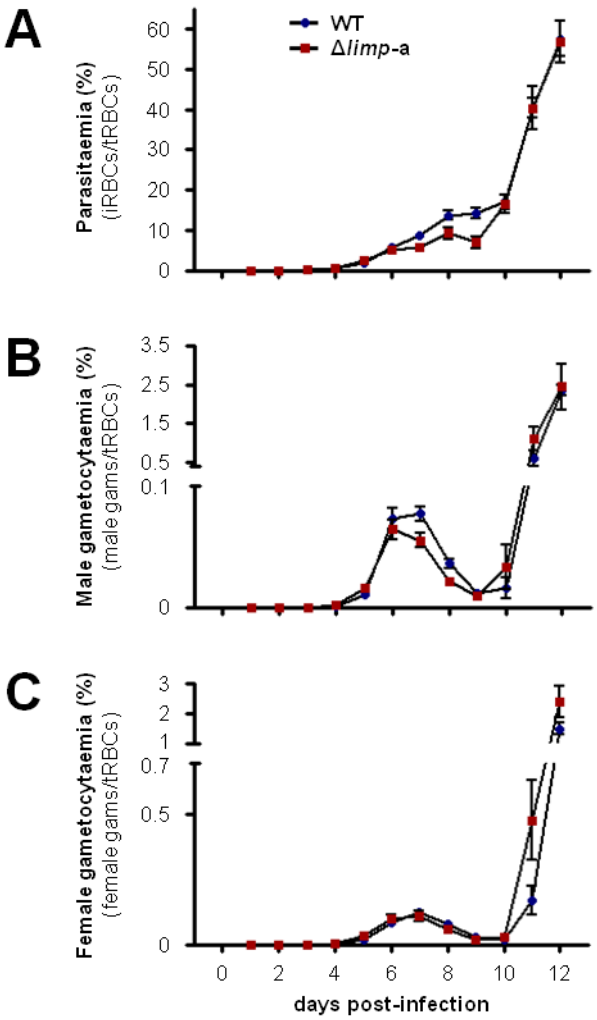

Figure S3 – Δ*limp* parasites develop normal blood stage parasitaemia and gametocytaemias over the course of infection.
(A) WT and Δ*limp*-a total parasitaemias over time. **(B)** WT and Δ*limp*-a male gametocytaemias over time. **(C)** WT and Δ*limp*-a female gametocytaemias over time. **(A-C)** Mean values are shown by the dots, while SEM values are shown by the vertical lines. WT and Δ*limp*-a (*n*=6). gams: gametocytes; iRBCs: infected red blood cells; tRBCs: total red blood cells.

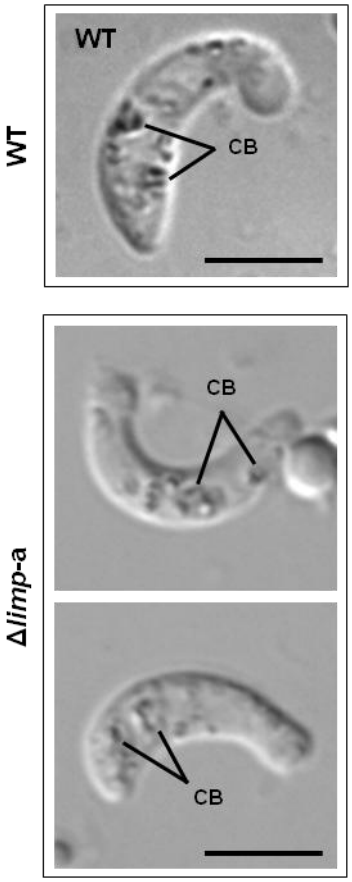

Figure S4 – Δ*limp* ookinetes show WT morphology.
WT and Δ*limp*-a blood meal-retrieved ookinetes were imaged under DIC microscopy and showed similar overall morphology, including the presence of crystalloid bodies (CB) identified by the associated haemozoin clusters. Scale bars = 5 µm.

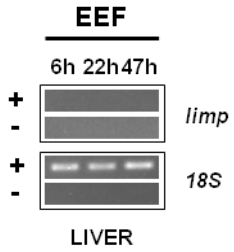

Figure S5 – *limp* is not transcribed in liver stages.
RT-PCR analysis of *limp* in *in vivo*-developed *P. berghei* exoerythrocytic forms (EEFs) at different time points after sporozoite injection. *18S* rRNA serves as loading control gene. +: RT positive reaction; -: RT negative reaction.

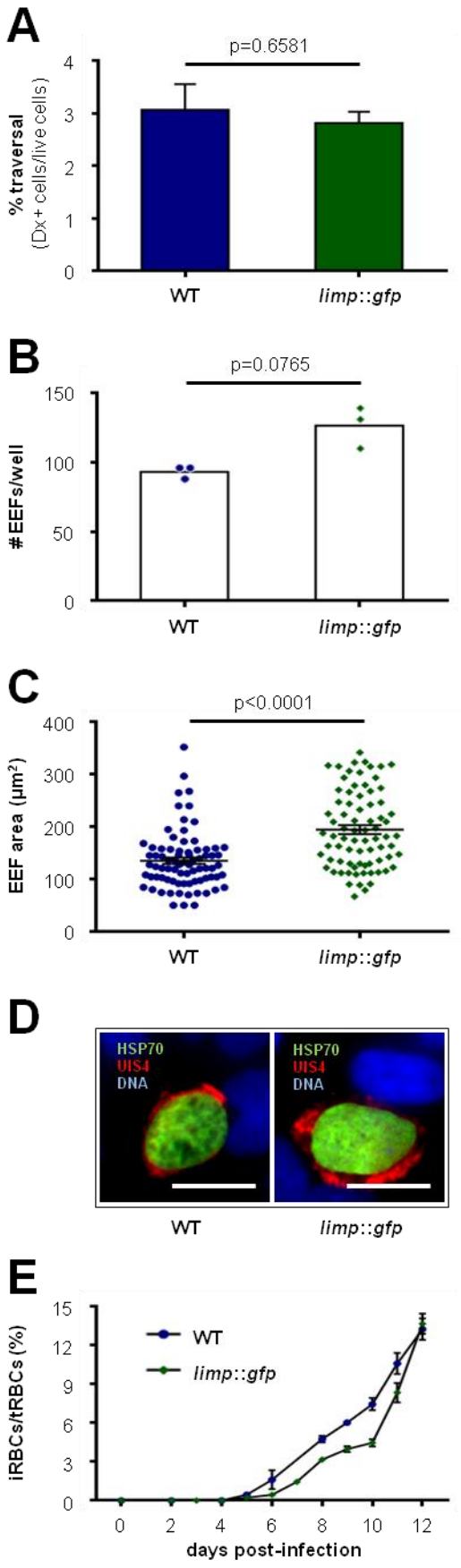

Figure S6 – *limp*::*gfp* parasites establish normal liver infection.
(A) Hepatocyte traversal ability of *limp*::*gfp* sporozoites is comparable to WT parasites. Mean percentages of cell traversal are shown by the bars, while SEM values are shown by the vertical lines; p-value for Student´s *t*-test is shown above the bars. WT and *limp*::*gfp* (1 experiment, *n*=3). Dx+ cells: Dextran, Tetramethylrhodamine positive cells. **(B)** *limp*::*gfp* sporozoites transform normally into exoerythrocytic forms (EEFs). Mean numbers of EEFs per well are shown by the bars, while dots represent individual data points. WT and *limp*::*gfp* (1 experiment, *n*=3). **(C)** *limp*::*gfp* parasites develop into normally sized exoerythrocytic forms (EEFs). Mean and SEM values are shown by the lines. WT (1 experiment, *n*=79); *limp*::*gfp* (1 experiment, *n*=77). **(B-C)** p-values for Mann-Whitney test are shown above the data sets. **(D)** Representative images of WT and *limp*::*gfp* exoerythrocytic forms. Scale bars = 20 µm. **(E)** Mice bitten by *limp*::*gfp*-infected mosquitoes develop normal blood stage infection. Mean parasitaemias are shown by the dots, while SEM values are shown by the vertical lines. WT (2 independent experiments, *n*=2); *limp*::*gfp* (3 independent experiments, *n*=3). iRBCs: infected red blood cells; tRBCs: total red blood cells.

Table S1 - Primers used in the present work.

a) Primers used in life-cycle RT-PCRs, RT-PCRs of IP samples and qPCR of RNA extracts from infected livers.
"c" or "Rev" at the end of primer names means they are antisense primers. All others are sense primers.
Nucleotide stretches in capital letter correspond to the complementary sequence to the respective gene. n.a.: not aplicable; ORF: open reading frame; UTR: untranslated region.

Gene name	Gene ID	Primer name	Sequence	Description	Product size gDNA (bp)	Product size cDNA (bp)	Across introns
limp	PBANKA_060580	g0623	aaagaattcTCTCTTAATTTAAAACTTG	*limp* ORF	n.a.	309	yes
		g0624c	aaagcggccgcATCCATTTAAATTAATTAGC	*limp* ORF			
***18S* rRNA**	n.a.	PbA18SFw	AAGCATTAAATAAAGCGAATACATCCTTAC	*18S* rRNA	134	134	no
		PbA18SRev	GGAGATTGGTTTTGACGTTTATGTG	*18S* rRNA			
hsp70	PBANKA_071190	g0258	AAAAGCAAAGCCAAACTTACC	*hsp70* ORF	139	139	no
		g0259c	GGATGGGGTTGTTCTATTACC	*hsp70* ORF			
p25	PBANKA_051500	g0385	CCGGAATTCATAAACAAATATACCTGG	*p25* 3' UTR	263	263	no
		g0476c	CGGGATCCTCATACGAATTTTATTG	*p25* 3' UTR			
p28	PBANKA_051490	g0115	TTCGATATCATGAATTTTAAATACAG	*p28* ORF	660	660	no
		g0116c	tccgcggccgcGCATTACTATCACGTAAATAAC	*p28* ORF			
dozi	PBANKA_121770	g0546	TAATTGTGTCGCTTCAAATG	*dozi* ORF	641	439	yes
		g0548c	TAATTCTTTTATCATAGCAG	*dozi* ORF			
cith	PBANKA_130130	g0549	GAAAAAAGCAAAGATGTATTATCTG	*cith* ORF	334	334	no
		g0550c	ATAGGCTGGGTATCTGTTAAATG	*cith* ORF			
alba3	PBANKA_120440	g0003	aaacccggggaattcCAAGAAAGAGCTGAAAAC	*alba3* ORF	641	324	yes
		g0004c	aaagcggccgctATTAGCAACAAAGTTTG	*alba3* ORF			
mouse *hprt*	n.a.	HPRT-1Fw	CATTATGCCGAGGATTTGGA	*hprt* ORF	3053	163	yes
		HPRT-1Rev	AATCCAGCAGGTCAGCAAAG	*hprt* ORF			

Table S1 - Primers used in the present work.

b) Primers used in the generation of gene deletion and GFP-tagging constructs.

"c" at the end of primer names means they are antisense primers. All others are sense primers.

Nucleotide stretches in capital letter correspond to the complementary sequence to the respective gene. Underlined are restriction site sequences.

ORF: open reading frame.

Gene name	Gene ID	Construct name	Primer name	Sequence	Restriction sites	Description
Gene deletion constructs						
limp	PBANKA_060580	pLIS0060	g0703	aaaggtaccATTTTAATTTCTCGTAAG	*Asp* 718I	*limp* 5' targeting region
			g0704c	aaaaagcttTTTTTCTCTTTTTAAAAAG	*Hin* dIII	*limp* 5' targeting region
			g0705	aaagaattcATAAAAATATATACTTTCC	*Eco* RI	*limp* 3' targeting region
			g0706c	aaagcggccgcTTCATTTCAAAAGAAATG	*Not* I	*limp* 3' targeting region
GFP-tagging constructs						
limp	PBANKA_060580	pLIS0079	g0623	aaagaattcTCTCTTAATTTAAAACTTG	*Eco* RI	*limp* ORF
			g0625c	aaagcggccgcATCCATTTAAATCTAATG	*Not* I	*limp* ORF

Table S1 - Primers used in the present work.

c) Primers used in genotyping and RT-PCR of mutant parasite lines.

"c" at the end of primer names means they are antisense primers. All others are sense primers.

Nucleotide stretches in capital letter correspond to the complementary sequence to the respective gene.

n.a.: not aplicable; *pb*: *Plasmodium berghei*; *tg*: *Toxoplasma gondii*; *dhfr/ts*: dihydrofolate reductase/thymidylate synthase; ORF: open reading frame; UTR: untranslated region.

Gene name/ mutant name	Gene ID	Primer name	Sequence	Description	Integration PCR pair	Product size (bp)
Primers for genotyping						
Δ*limp*-a and Δ*limp*-b	PBANKA_060580	g0860	AAACACATTGTGAATTGCAC	*limp* 5' integration	g1021c	629
		g0861c	CTAAGGATATATCCTTTTGC	*limp* 3' integration	g0952	638
limp		g0623	aaagaattcTCTCTTAATTTAAAACTTG	*limp* ORF	n.a.	1170
		g0625c	aaagcggccgcATCCATTTAAATCTAATG	*limp* ORF	n.a.	
limp::*gfp*		g1196	AAAAGAGAAAAAATGGTG	*limp* 5' integration	g0408c	1335
		g1201c	GTAAAAAAGGCATTATAG	*limp* 3' integration	g0952	1447
limp		g1196	AAAAGAGAAAAAATGGTG	*limp* 5' UTR|ORF	n.a.	1362
		g1201c	GTAAAAAAGGCATTATAG	*limp* 3' UTR	n.a.	
Primers for RT-PCR						
limp	PBANKA_060580	g0623	aaagaattcTCTCTTAATTTAAAACTTG	*limp* ORF	n.a.	309
		g0624c	aaagcggccgcATCCATTTAAATTAATTAGC	*limp* ORF	n.a.	
		g1264	TTTACTTTTTAAAAAGAGAAAAAATGGTG	*limp* 5' UTR|ORF	n.a.	370
		g1265c	CTTTATAATAAAGGCTATCCATTTAAATTAA	*limp* 3' UTR|ORF	n.a.	
limp::*gfp*		g1264	TTTACTTTTTAAAAAGAGAAAAAATGGTG	*limp* 5' UTR|ORF	n.a.	360
		g1266c	GGCCGCATCCATTTAAATTAA	*gfp* linker|*limp* ORF	n.a.	
General primers						
pbdhfr/ts	PBANKA_071930	g0952	GATTCATAAATAGTTGGACTTG	3' UTR *pbdhfr/ts*	n.a.	n.a.
		g1021c	ATTGTTGACCTGCAGGCATG	5' UTR *pbdhfr/ts*	n.a.	n.a.
tgdhfr/ts	n.a.	g1019	ATGCATAAACCGGTGTGTC	*tgdhfr/ts* ORF	n.a.	1866
		g1020c	AGCTTCTGTATTTCCGC	*tgdhfr/ts* ORF	n.a.	
RNA polymerase II subunit RPB1	PBANKA_080700	g0084	aaagaattcTGATGGTTTACAATCACC	RNA pol II ORF	n.a.	1015
		g0085c	aaagcggccgctTTCTTCCTGCATCTCCTC	RNA pol II ORF	n.a.	
p28	PBANKA_051490	g0115	TTCGATATCATGAATTTTAAATACAG	*p28* ORF	n.a.	660
		g0116c	tccgcggccgcGCATTACTATCACGTAAATAAC	*p28* ORF	n.a.	
gfp	n.a.	g0408c	GTATGTTGCATCACCTTC	*gfp* ORF	n.a.	n.a.

Table S2 - Parasite transfection experiments.

Gene name/ mutant name	Gene ID	DNA construct name	Restriction enzymes[1]	Experiment #/ mutant clone ID[2]	Parental line[3]
Gene deletion mutants					
Δ*limp*-a	PBANKA_060580	pLIS0060	*Asp*718I and *Not*I	2091cl2m5	820cl1m1cl1
Δ*limp*-b				2090cl2m6	820cl1m1cl1
GFP-tagged mutants					
limp::*gfp*	PBANKA_060580	pLIS0079	*Afl*II	2180cl1m4	cl15cy1

[1] Restriction enzymes used for plasmid linearisation before transfection

[2] Experiment number for independent transfection experiments: experiment number/ID of the mutants clones

[3] Parental *P. berghei* ANKA line in which the transfection experiment was performed

Table S3 - Summary of phenotypes of the *P. berghei* mutants generated in the present study.

Mutant	Asexual multiplication rate[1] (s.d.)	Ookinete production[2] % (s.d.)	Oocyst production[3] (s.d.)	MG Spz production[4] X10^4 (s.d.)	Hemolymph Spz counts[5] (s.d.)	SG Spz production[6] X10^3 (s.d.)	Prepatent period[7]
Δ*limp*-a	10 (0) *n* =4	66.6 (6.9) *n* =4	110.1 (77.6) *n* =6	2.3 (1.8) *n* =5	93.8 (95.0) *n* =4	2.2 (1.7) *n* =6	n.a.
Δ*limp*-b	10 (0) *n* =9	71.6 (12.2) *n* =4	n.d.	n.d.	n.d.	n.d.	n.a.
limp::*gfp*	10 (0) *n* =3	n.d.	n.d.	n.d.	n.d.	n.d.	4 *n* =3
WT[8]	10 (0) *n* >10	50-90 *n* >10	112-319 *n* =4	2.6-4.2 *n* =3	80-165 *n* =3	21.4-35.2 *n* =4	4-5 *n* =8

[1] The multiplication rate per 24 hours of blood stage parasites in mice infected with a single parasite

[2] The mean percentage of female gametes developing into mature ookinetes *in vitro*

[3] The mean number of oocysts per mosquito (day 12)

[4] The mean number of midgut sporozoites (MG Spz) per mosquito (day 21)

[5] The mean number of hemolymph sporozoites (Spz) per mosquito (day 21)

[6] The mean number of salivary gland sporozoites (SG Spz) per mosquito (days 20–21)

[7] The prepatent period (measured in days post bite of 10 infected females per mouse) is defined as the day when parasites are detected in Giemsa-stained blood smears of mice

[8] The developmental data for wild type (WT) parasites are shown as the range of mean values

s.d.: standard deviation

n.d.: not determined

n.a.: not aplicable

Table S4 - Quantification of gold particles in the immuno-EM specimens analysed in the present work.

Absolute counts	***limp*::*gfp* sample 1**	***limp*::*gfp* sample 1 (negative control)**	***limp*::*gfp* sample 2**	***limp*::*gfp* sample 2 (negative control)**	***limp*::*gfp* sample 3**	***limp*::*gfp* sample 3 (negative control)**	**WT**
Plasma membrane	50	1	66	2	96	2	3
Extracellular	7	0	19	1	6	7	4
Intracellular	5	2	26	1	6	3	1
TOTAL	62	3	111	4	108	12	8
Percentages							
Plasma membrane	80,6	33,3	59,5	50,0	88,9	16,7	37,5
Extracellular	11,3	0,0	17,1	25,0	5,6	58,3	50,0
Intracellular	8,1	66,7	23,4	25,0	5,6	25,0	12,5

Absolute counts	**pool of *limp*::*gfp* samples 1-3**	**pool of *limp*::*gfp* negative control samples 1-3**	**WT**
Plasma membrane	212	5	3
Extracellular	32	8	4
Intracellular	37	6	1
TOTAL	281	19	8
Percentages			
Plasma membrane	75,4	26,3	37,5
Extracellular	11,4	42,1	50,0
Intracellular	13,2	31,6	12,5

GENERAL DISCUSSION

Translational repression (TR) in *P. berghei* is particularly important during the phases of transmission of the parasites: from the vertebrate host to the mosquito vector and back to a new host. By accumulating hundreds of mRNAs in a 'stand-by' mode, the parasite is in a state of molecular preparedness that allows it to quickly adapt to new, distinct environments (blood to midgut and salivary glands to liver) and rapidly transform into the next life cycle form, but only at the right time, when the right environmental cues are in place. In the mosquito midgut, for example, fertilisation of the female by the male gamete takes place within one hour after the blood meal, and complete ookinete formation and midgut invasion is accomplished within a day [36]. In the rodent host, sporozoites are found inside hepatocytes as fast as two minutes after they have entered the bloodstream [368]. Many proteins necessary for these crucial transitions are synthesised from repressed mRNAs and therefore independent from *de novo* transcription.

The mRNA loss in Δ*dozi* and Δ*cith* gametocytes can be regarded as a foolproof mechanism that malaria parasites employ to ensure that certain antigens are not expressed before time when they cannot be properly translationally silenced. By doing so, the parasites warrant the encoded proteins are not present to be detected by the mammalian host's immune system and therefore prevent adaptive immune responses resulting in the generation of potential transmission blocking (TB) antibodies. Such antibodies could block the function of the target proteins while inside the mosquito midgut and hence could prevent transmission of the current and future parasite populations. Indeed, several rodent and human malaria translationally repressed genes in gametocytes are known targets of TB antibodies.

In the present study we have characterised three genes of previously unknown or putative function in the rodent malaria parasite *P. berghei*: *epsf*, *dhhc10* and *limp*. Each gene revealed an essential or important function during mosquito stage infection. All three genes have conserved orthologs in the human malaria parasite species *P. falciparum* and *P. vivax* that perhaps are equally crucial for life cycle progression. The use of *P. berghei* for the functional characterisation of novel gene products has several advantages: first it is the genetically most amenable species easily allowing for the deletion, tagging or conditional knock-out (using the site-specific recombination FLP-FRT system [369-371]) and knock-down (by stage-specific promoter swap strategies [134] or the tetracycline-repressible transactivator system [372]) of specific genes of interest; secondly it is the most tractable parasite throughout the entire life cycle, permitting the follow-up of any genetic modification in life cycle stages where *P. falciparum* and *P. vivax* are not so easily manipulated, namely during development within the mosquito vector and *in vivo* in the vertebrate host's liver.

Despite distinct in their structure and function, each of the three genes are subjected to TR in female gametocytes. Upon gametocyte activation and ookinete formation, the encoded proteins are targeted to a unique ookinete organelle, the crystalloid body (CB). Our data on EPSF and DHHC10 support the hypothesis raised by studies on LAP proteins suggesting that

CBs act as storage organelles for proteins that are used during oocyst/sporozoite development, as the corresponding null phenotypes were only observable during sporogony in the mosquito midgut. It is nonetheless worth noting that proteins that are produced within 24 hours after fertilisation will only exert their functions several days after mosquito infection. It is even more striking to recognize that the corresponding mRNAs are targets of a repressor molecular mechanism taking place in blood stage parasites, a process that can be initiated some days before the gametocyte is taken up during a blood meal. Alternatively, EPSF and/or DHHC10 act early on during mosquito infection leaving a molecular footprint that sets the basis for future morphological events. In their absence, the lack of such molecular landscape will only have a detrimental impact for parasite survival later in development. Indeed, the lack of CBs in Δ*dhhc10* ookinetes suggests that this might be the case at least for DHHC10.

While all CB-associated proteins studied so far are indeed involved in oocyst sporogony [176, 211, 224-226], the absence of LIMP does not result in abortive oocysts. In fact, Δ*limp* oocysts develop wild-type (WT) numbers of midgut sporozoites. Instead, LIMP has a role in the transition from the ookinete to the oocyst and thus challenges the current paradigm of malaria CBs acting as mere storage compartments. Alternatively, LIMP does not exert its functions while present in the CBs but is rather redistributed to other sites within the cell, possibly the ookinete plasma membrane (PM) as suggested by its localisation in sporozoites, but at lower levels than those detectable in crystalloids.

From nine CB components identified to date (LAP1-6 [208, 211, 212] as well as EPSF, DHHC10 and LIMP), six are translationally repressed in female gametocytes, including LAP4-6 [208] and those studied here. As many more uncharacterised gene products are likely to be subjected to this mechanism in the transition from host to vector, it will be interesting to know how many more of these proteins are targeted to this organelle, and what their roles are during parasite development in the mosquito. Such studies would not only expand our understanding of the biological relevance of TR but also increase our knowledge on this poorly understood subcellular compartment.

Together with published data on *P. falciparum* and *T. gondii*, the present findings highlight the impact of post-translational modifications (PTMs), namely palmitoylation, for parasite biology. The importance of protein S-palmitoylation has also been studied in a highly divergent pathogen, the gut parasitic protozoan *Giardia lamblia*, the principal cause of non-viral/non-bacterial diarrheal disease worldwide [373]. In this organism, palmitoylation of the C-terminal cytoplasmic tails of variant-specific surface proteins (VSPs) is linked to the segregation of these proteins to plasma membrane *rafts* and detection by host antibodies. This antibody recognition contributes to antigenic variation in these parasites, a process in which the trophozoite continuously changes its surface antigen coat to avoid being detected and eliminated by the host's immune system; by binding to the surface of the parasites, the antibodies trigger the elimination of parasite populations expressing the recognised VSPs,

which are then replaced by cells expressing unrecognised counterparts. Mutations in the palmitoylation site of VSPH7 render parasites resistant to cell death by this complement-independent, antibody-mediated cytotoxicity without a simultaneous switching of the active VSP [374]. A recent study identified nine putative DHHC-PATs in *Giardia* and showed that the developmental transition from the gut-colonising trophozoite to the disseminating, environmental-resistant and infectious cyst, a process that depends on *de novo* generation of endomembrane compartments, protein sorting and vesicle fusion, involves substantial palmitoylation of parasite proteins. Conversely, drug inhibition of palmitoylation yielded fewer numbers of cysts [375]. Like in *Giardia*, our results support the idea that S-acylation is a PTM with major impact in parasite life cycle progression, namely during the formation of the infectious and transmissible parasite stages, the cyst in the case of *Giardia*, and the sporozoite in the case of *Plasmodium*.

Another reversible PTM, phosphorylation, is also extremely important for mosquito stage development of *Plasmodium* parasites. Just like palmitoylation, the complex, dynamic and coordinated addition and removal of phosphate groups to specific amino acid residues by kinases and phosphatases, respectively, allows for tight regulation of protein function, hence strongly influencing many cellular processes such as sexual and sporogonic development [376]. This is the case, for instance, of the activation of the arrested gametocytes by the cyclic guanosine monophosphate (cGMP)-dependent protein kinase PKG [377], the initiation of male genome replication by the calcium-dependent protein kinase 4 (CDPK4) [378] and the egress of male microgametes through the action of the mitogen-activated protein kinase 2 (MAP-2) [379]. Moreover, the meiotic division occurring after fertilisation necessitates the function of the Never in Mitosis Gene A (NIMA)-related protein kinases, Nek-2 and Nek-4 [380]. While the absence of any of these kinases results in parasites that are severely affected in their ability to produce ookinetes *in vitro*, subsequent work identified a serine/arginine (SR)-rich protein kinase (SRPK) as an absolute requirement for the completion of this developmental transition in the parasite life cycle [376]. On the other hand, ookinete motility relies on CDPK3 [381, 382], and as a consequence, the absence of this protein leads to strongly reduced oocyst numbers *in vivo* (less than 10% of WT numbers) [376]. Another two kinase mutants are equally impaired in their capacity to develop oocysts: protein kinase 7 (*pk7*) and cyclin G-associated kinase (*gak*) gene deletion parasites. PK7 is a hybrid kinase with homology to mammalian MEK3/6 and fungal protein kinase A in the C- and N-termini of its kinase domain, respectively. GAK on the other hand resembles the Ark/Prk group of yeast kinases as well as the cyclin G-associated kinase/AP2-associated kinase 1 group in animals, which are involved in the uncoating of clathrin-coated vesicles [383]. The few Δ*pk7* and Δ*gak* oocysts that successfully established in mosquito midguts never formed sporoblasts or any sporozoites [376]. Together with our data, this observation indicates that PTMs, namely phosphorylation and palmitoylation are of vital relevance for *Plasmodium* sporogony. Interestingly, Δ*pk7* oocysts stopped growing by day 10 p.i., while Δ*gak* cysts continued growing and by day 21 p.i. had outgrown WT parasites but

remained unsporulated. In both mutants developmental arrest was accompanied by lack of DNA replication [376]. Curiously, this is in contrast to what we have observed in our Δ*dhhc10* oocysts but similar to Δ*epsf* parasites. Further studies will be necessary to dissect the pathways governing cell cycle progression in the still enigmatic process of sporozoite formation which represents one of the vastest mitotic division phases in the *Plasmodium* life cycle.

A recent genome-wide functional analysis of *Plasmodium* protein phosphatases (PPs) has also highlighted six PPs essential for sexual development and differentiation of mosquito-associated parasite stages. Metallo-dependent protein phosphatase 1 (PPM1) is crucial for microgametocyte exflagellation, PPM2, kelch-like motifs PP (PPKL) and Shewanella-like PP 1 (SHLP1) knock-out (KO) parasites are blocked in ookinete-to-oocyst transition, and PPM5 and protein tyrosine phosphatase-like A homolog (PTPLA) null mutants do not form midgut sporozoites. Some differences exist between Δ*ppm5* and Δ*ptpla* parasites. The former produces viable ookinetes similar to WT controls but shows markedly reduced numbers and sizes of oocysts, resembling the phenotype of Δ*pk7* parasites. Δ*ptpla* mutants on the other hand produced WT numbers of oocysts that do not undergo sporulation [384]. These later parasites therefore mimic the phenotype we report here for *dhhc10* but also *epsf* gene deletion mutants. The similarity between some kinase and phosphatase null phenotypes indicates that signal transduction pathways leading to morphological and functional alterations are not simply activated by kinases and silenced by PPs. They are rather controlled through a dynamic balance between both types of enzymes, with multiple kinases and PPs contributing to certain stage-specific pathways.

Two final interesting general observations can be made from the data presented herein on the gene *limp*. LIMP exerts its function in two very distinct phases of the *Plasmodium* life cycle. First, it is important for the establishment of the sessile oocyst in the basal lamina of the mosquito midgut. Later on, it is critical for salivary gland invasion, hepatocyte adhesion, traversal and also invasion. Examples of other dual functioning proteins exist in the malaria literature. CelTOS, for instance, plays the same fundamental role (host cell traversal) in both ookinetes and sporozoites [175]. On the other hand, PbGEST (gamete egress and sporozoite traversal) is a *Plasmodium*-specific conserved protein that is targeted to osmiophilic bodies (gametocyte-specific secretory organelles) and the sporozoite micronemes from which it is secreted shortly after gametocyte activation and during sporozoite migration, respectively. PbGEST is necessary for gametocyte egress from the RBC and for sporozoite cell traversal in the skin of the mammalian host [385]. The fact that malaria parasites can use a single protein to play roles in distinct life cycle stages raises the possibility that the *Plasmodium* genome of just over 5,000 genes can be greatly potentiated by the addition of a supplementary layer of complexity to its proteome. As proteins can have pleiotropic roles and/or act in different developmental stages, the parasite is not limited to a 1:1 stoichiometric ration between protein coding genes and protein functional/temporal activities.

Another remarkable observation is that despite being expressed in gametocytes and sporozoites, *limp* is translationally repressed in the former and immediately translated in the latter. This observation suggests that TR mechanisms in place in these two developmental stages of the parasite do not target the same transcripts, even when these are present in both. This could be due to at least three reasons: (i) the TR machinery is distinct in the two parasite forms and *limp* mRNA possesses motifs that are recognised by the repressor complexes in female gametocytes but not in sporozoites, (ii) alternative transcription initiation and/or termination sites exist on *limp* gene that are used differently in gametocytes and sporozoites or (iii) alternative splicing events occur in the untranslated regions (UTRs) of *limp* in these two parasite stages. It the latter two hypotheses, TR-targeting motifs could be present in *limp* mRNA while expressed in gametocytes but not in sporozoites. Follow-up studies will be necessary to fully dissect these questions.

Being specifically transcribed in gametocytes and not in asexual blood stages, it is pertinent to emphasise that *epsf*, *dhhc10* and *limp* were found significantly downregulated in KO parasites for the sexual commitment major regulators AP2-G and AP2-G2, together with known gametocyte-specific genes. In the absence of these transcription factors, gametocyte production is completely abolished (in the case of AP2-G) or highly reduced (AP2-G2) [67, 70]. More precisely, mRNA levels of all three genes are diminished in the *P. berghei* Δ*pbap2-g* line. Moreover, *epsf* transcripts are reduced more than 2-fold in the absence of *P. falciparum* PfAP2-G, while *limp* is also negatively affected in Δ*pbap2-g2* parasites, although less markedly than upon depletion of PbAP2-G. Additionally, microarray analyses of three *P. berghei* gametocyte non-producer lines obtained by successive asexual mechanical passage over 52 weeks showed that all genes were strongly downregulated in these parasites when compared to their WT counterpart, equally or more than in the Δ*pbap2-g* parasite line. It is thus reasonable to hypothesise that *epsf*, *dhhc10* and *limp* are transcribed at some point during gametocyte differentiation by either AP2-G, AP2-G2 or both, and that they may constitute true gametocyte signature genes.

The present essay contributes to increase our knowledge on the relevance of TR and its target mRNAs for parasite biology. At the same time it also highlights how little we actually know about how this molecular mechanism works and opens many new questions that need to be addressed. Unlike several other *Plasmodium* translationally repressed genes studied to date, the three that were the major focus of this work are unlikely to represent attractive malaria transmission blocking vaccine candidates. Two main reasons are behind this conclusion. First, the encoded proteins are not localised to the ookinete PM and are thus inaccessible to TB antibodies. Secondly, interfering with their function only has deleterious effects for the parasites at later stages of mosquito infection, namely at the oocyst and sporozoite levels, moments at which potentially effective antibodies generated by the mammalian host are no longer available inside the mosquito. Nevertheless, this work is a clear further demonstration that interfering with TR itself or with its targets can be a powerful tool in the quest against malaria. By inhibiting the

function of either EPSF, DHHC10 or LIMP, perhaps by the use of small molecules, but also of several other published translationally repressed genes, malaria transmission to and from the mosquito vector can be completely blocked, which will certainly represent a strong component of our endeavour to eradicate malaria [386, 387].

REFERENCES

1. MORRISON, D.A., *EVOLUTION OF THE APICOMPLEXA: WHERE ARE WE NOW?* TRENDS PARASITOL, 2009. **25**(8): P. 375-82.
2. MORRISSETTE, N.S. AND L.D. SIBLEY, *CYTOSKELETON OF APICOMPLEXAN PARASITES.* MICROBIOL MOL BIOL REV, 2002. **66**(1): P. 21-38; TABLE OF CONTENTS.
3. RUSSELL, D.G. AND R.G. BURNS, *THE POLAR RING OF COCCIDIAN SPOROZOITES: A UNIQUE MICROTUBULE-ORGANIZING CENTRE.* J CELL SCI, 1984. **65**: P. 193-207.
4. HU, K., D.S. ROOS, AND J.M. MURRAY, *A NOVEL POLYMER OF TUBULIN FORMS THE CONOID OF TOXOPLASMA GONDII.* J CELL BIOL, 2002. **156**(6): P. 1039-50.
5. LEMGRUBER, L., ET AL., *CRYO-ELECTRON TOMOGRAPHY REVEALS FOUR-MEMBRANE ARCHITECTURE OF THE PLASMODIUM APICOPLAST.* MALAR J, 2013. **12**: P. 25.
6. LIM, L. AND G.I. MCFADDEN, *THE EVOLUTION, METABOLISM AND FUNCTIONS OF THE APICOPLAST.* PHILOS TRANS R SOC LOND B BIOL SCI, 2010. **365**(1541): P. 749-63.
7. *WORLD MALARIA REPORT 2012*, WORLD HEALTH ORGANIZATION: GENEVA, SWITZERLAND.
8. MILLER, L.H., M.F. GOOD, AND G. MILON, *MALARIA PATHOGENESIS.* SCIENCE, 1994. **264**(5167): P. 1878-83.
9. EPIPHANIO, S., ET AL., *VEGF PROMOTES MALARIA-ASSOCIATED ACUTE LUNG INJURY IN MICE.* PLOS PATHOG, 2010. **6**(5): P. E1000916.
10. BAPTISTA, F.G., ET AL., *ACCUMULATION OF PLASMODIUM BERGHEI-INFECTED RED BLOOD CELLS IN THE BRAIN IS CRUCIAL FOR THE DEVELOPMENT OF CEREBRAL MALARIA IN MICE.* INFECT IMMUN, 2010. **78**(9): P. 4033-9.
11. FLICK, K. AND Q. CHEN, *VAR GENES, PFEMP1 AND THE HUMAN HOST.* MOL BIOCHEM PARASITOL, 2004. **134**(1): P. 3-9.
12. KRAEMER, S.M. AND J.D. SMITH, *A FAMILY AFFAIR: VAR GENES, PFEMP1 BINDING, AND MALARIA DISEASE.* CURR OPIN MICROBIOL, 2006. **9**(4): P. 374-80.
13. CLAUSEN, T.M., ET AL., *STRUCTURAL AND FUNCTIONAL INSIGHT INTO HOW THE PLASMODIUM FALCIPARUM VAR2CSA PROTEIN MEDIATES BINDING TO CHONDROITIN SULFATE A IN PLACENTAL MALARIA.* J BIOL CHEM, 2012. **287**(28): P. 23332-45.
14. MOLINA-CRUZ, A., T. LEHMANN, AND J. KNOCKEL, *COULD CULICINE MOSQUITOES TRANSMIT HUMAN MALARIA?* TRENDS PARASITOL, 2013. **29**(11): P. 530-7.
15. WANG, R., J.D. SMITH, AND S.H. KAPPE, *ADVANCES AND CHALLENGES IN MALARIA VACCINE DEVELOPMENT.* EXPERT REV MOL MED, 2009. **11**: P. E39.
16. COX-SINGH, J., ET AL., *PLASMODIUM KNOWLESI MALARIA IN HUMANS IS WIDELY DISTRIBUTED AND POTENTIALLY LIFE THREATENING.* CLIN INFECT DIS, 2008. **46**(2): P. 165-71.
17. COLLINS, W.E. AND J.W. BARNWELL, *PLASMODIUM KNOWLESI: FINALLY BEING RECOGNIZED.* J INFECT DIS, 2009. **199**(8): P. 1107-8.
18. FONTENILLE, D. AND F. SIMARD, *UNRAVELLING COMPLEXITIES IN HUMAN MALARIA TRANSMISSION DYNAMICS IN AFRICA THROUGH A COMPREHENSIVE KNOWLEDGE OF VECTOR POPULATIONS.* COMP IMMUNOL MICROBIOL INFECT DIS, 2004. **27**(5): P. 357-75.
19. LAVERAN, A., *NOTE SUR UN NOUVEAU PARASITE TROUVÉ DANS LE SANG DE PLUSIEURS MALADES ATTEINTS DE FIÈVRE PALUSTRE.* BULL ACAD MÉD PARIS, 1880. **9**: P. 1235-6.
20. MARCHIAFAVA, E. AND A. CELLI, *NOUVE RICERCHE SULLA INFEZIONE MALARICA.* ARCH SCINZE MED TORINI, 1885. **9**: P. 311-40.
21. ROSS, R., *ON SOME PECULIAR PIGMENTED CELLS FOUND IN TWO MOSQUITOES FED ON MALARIAL BLOOD.* BR MED J, 1897. **2**: P. 1786-8.
22. ROSS, R., *REPORT ON THE CULTIVATION OF PROTEOSOMA, LABBÉ IN GREY MOSQUITOES*. 1898: GOVT PRESS CALCUTTA.
23. GARNHAM, P.C., *EXOERTHROCYTIC SCHIZOGONY IN PLASMODIUM KOCHI LAVERAN; A PRELIMINARY NOTE.* TRANS R SOC TROP MED HYG, 1947. **40**(5): P. 719-22.
24. SHORTT, H.E. AND P.C. GARNHAM, *PRE-ERYTHROCYTIC STAGE IN MAMMALIAN MALARIA PARASITES.* NATURE, 1948. **161**(4082): P. 126.
25. SHORTT, H.E. AND P.C. GARNHAM, *DEMONSTRATION OF A PERSISTING EXO-ERYTHROCYTIC CYCLE IN PLASMODIUM CYNOMOLGI AND ITS BEARING ON THE PRODUCTION OF RELAPSES.* BR MED J, 1948. **1**(4564): P. 1225-8.
26. SHORTT, H.E. AND P.C. GARNHAM, *THE PRE-ERYTHROCYTIC DEVELOPMENT OF PLASMODIUM CYNOMOLGI AND PLASMODIUM VIVAX.* TRANS R SOC TROP MED HYG, 1948. **41**(6): P. 785-95.

27. SHORTT, H.E., P.C. GARNHAM, AND ET AL., *THE PRE-ERYTHROCYTIC STAGE OF HUMAN MALARIA, PLASMODIUM VIVAX.* BR MED J, 1948. **1**(4550): P. 547.
28. SHORTT, H.E., ET AL., *THE PRE-ERYTHROCYTIC STAGE OF PLASMODIUM FALCIPARUM.* TRANS R SOC TROP MED HYG, 1951. **44**(4): P. 405-19.
29. GARNHAM, P.C., ET AL., *THE PRE-ERYTHROCYTIC STAGE OF PLASMODIUM OVALE.* TRANS R SOC TROP MED HYG, 1955. **49**(2): P. 158-67.
30. GARNHAM, P.C.C., ET AL., *THE LATE PRIMARY EXOERYTHROCYTIC STAGES OF PLASMODIUM MALARIAE.* TRANS R SOC TROP MED HYG, 1967. **61**: P. 482-9.
31. BANNISTER, L. AND G. MITCHELL, *THE INS, OUTS AND ROUNDABOUTS OF MALARIA.* TRENDS PARASITOL, 2003. **19**(5): P. 209-13.
32. JANSE, C.J. AND A.P. WATERS, *SEXUAL DEVELOPMENT OF MALARIA PARASITES*, IN *MALARIA PARASITES: GENOMES AND MOLECULAR BIOLOGY*, A.P. WATERS AND C.J. JANSE, EDITORS. 2004, CAISTER ACADEMIC PRESS.
33. TALMAN, A.M., ET AL., *GAMETOCYTOGENESIS: THE PUBERTY OF PLASMODIUM FALCIPARUM.* MALAR J, 2004. **3**: P. 24.
34. SIEBER, K.P., ET AL., *THE PERITROPHIC MEMBRANE AS A BARRIER: ITS PENETRATION BY PLASMODIUM GALLINACEUM AND THE EFFECT OF A MONOCLONAL ANTIBODY TO OOKINETES.* EXP PARASITOL, 1991. **72**(2): P. 145-56.
35. BEIER, J.C., *MALARIA PARASITE DEVELOPMENT IN MOSQUITOES.* ANNU REV ENTOMOL, 1998. **43**: P. 519-43.
36. BATON, L.A. AND L.C. RANFORD-CARTWRIGHT, *SPREADING THE SEEDS OF MILLION-MURDERING DEATH: METAMORPHOSES OF MALARIA IN THE MOSQUITO.* TRENDS PARASITOL, 2005. **21**(12): P. 573-80.
37. MOTA, M.M., ET AL., *MIGRATION OF PLASMODIUM SPOROZOITES THROUGH CELLS BEFORE INFECTION.* SCIENCE, 2001. **291**(5501): P. 141-4.
38. PRUDENCIO, M., A. RODRIGUEZ, AND M.M. MOTA, *THE SILENT PATH TO THOUSANDS OF MEROZOITES: THE PLASMODIUM LIVER STAGE.* NAT REV MICROBIOL, 2006. **4**(11): P. 849-56.
39. KROTOSKI, W.A., ET AL., *DEMONSTRATION OF HYPNOZOITES IN SPOROZOITE-TRANSMITTED PLASMODIUM VIVAX INFECTION.* AM J TROP MED HYG, 1982. **31**(6): P. 1291-3.
40. COGSWELL, F.B., *THE HYPNOZOITE AND RELAPSE IN PRIMATE MALARIA.* CLIN MICROBIOL REV, 1992. **5**(1): P. 26-35.
41. JANSE, C.J., ET AL., *DNA SYNTHESIS IN PLASMODIUM BERGHEI DURING ASEXUAL AND SEXUAL DEVELOPMENT.* MOL BIOCHEM PARASITOL, 1986. **20**(2): P. 173-82.
42. NEWBOLD, C.I., ET AL., *STAGE SPECIFIC PROTEIN AND NUCLEIC ACID SYNTHESIS DURING THE ASEXUAL CYCLE OF THE RODENT MALARIA PLASMODIUM CHABAUDI.* MOL BIOCHEM PARASITOL, 1982. **5**(1): P. 33-44.
43. CONKLIN, K.A., ET AL., *DNA AND RNA SYNTHESES BY INTRAERYTHROCYTIC STAGES OF PLASMODIUM KNOWLESI.* J PROTOZOOL, 1973. **20**(5): P. 683-8.
44. INSELBURG, J. AND H.S. BANYAL, *SYNTHESIS OF DNA DURING THE ASEXUAL CYCLE OF PLASMODIUM FALCIPARUM IN CULTURE.* MOL BIOCHEM PARASITOL, 1984. **10**(1): P. 79-87.
45. GRITZMACHER, C.A. AND R.T. REESE, *PROTEIN AND NUCLEIC ACID SYNTHESIS DURING SYNCHRONIZED GROWTH OF PLASMODIUM FALCIPARUM.* J BACTERIOL, 1984. **160**(3): P. 1165-7.
46. WAKI, S., I. YONOME, AND M. SUZUKI, *X-RAY SENSITIVITY AND DNA SYNTHESIS IN SYNCHRONOUS CULTURE OF PLASMODIUM FALCIPARUM.* Z PARASITENKD, 1985. **71**(2): P. 213-8.
47. JIN, Y., C. KEBAIER, AND J. VANDERBERG, *DIRECT MICROSCOPIC QUANTIFICATION OF DYNAMICS OF PLASMODIUM BERGHEI SPOROZOITE TRANSMISSION FROM MOSQUITOES TO MICE.* INFECT IMMUN, 2007. **75**(11): P. 5532-9.
48. BLAGBOROUGH, A.M., ET AL., *TRANSMISSION-BLOCKING INTERVENTIONS ELIMINATE MALARIA FROM LABORATORY POPULATIONS.* NAT COMMUN, 2013. **4**: P. 1812.
49. HALL, N., ET AL., *A COMPREHENSIVE SURVEY OF THE PLASMODIUM LIFE CYCLE BY GENOMIC, TRANSCRIPTOMIC, AND PROTEOMIC ANALYSES.* SCIENCE, 2005. **307**(5706): P. 82-6.
50. KHAN, S.M., ET AL., *PROTEOME ANALYSIS OF SEPARATED MALE AND FEMALE GAMETOCYTES REVEALS NOVEL SEX-SPECIFIC PLASMODIUM BIOLOGY.* CELL, 2005. **121**(5): P. 675-87.
51. LASONDER, E., ET AL., *PROTEOMIC PROFILING OF PLASMODIUM SPOROZOITE MATURATION IDENTIFIES NEW PROTEINS ESSENTIAL FOR PARASITE DEVELOPMENT AND INFECTIVITY.* PLOS PATHOG, 2008. **4**(10): P. E1000195.

52. Baum, J., et al., *Molecular genetics and comparative genomics reveal RNAi is not functional in malaria parasites.* Nucleic Acids Res, 2009. **37**(11): p. 3788-98.
53. Duffy, M.F., et al., *Epigenetic regulation of the Plasmodium falciparum genome.* Brief Funct Genomics, 2014. **13**(3): p. 203-16.
54. Gupta, A.P., et al., *Dynamic epigenetic regulation of gene expression during the life cycle of malaria parasite Plasmodium falciparum.* PLoS Pathog, 2013. **9**(2): p. e1003170.
55. Vembar, S.S., A. Scherf, and T.N. Siegel, *Noncoding RNAs as emerging regulators of Plasmodium falciparum virulence gene expression.* Curr Opin Microbiol, 2014. **20**: p. 153-161.
56. Zhang, Q., et al., *Exonuclease-mediated degradation of nascent RNA silences genes linked to severe malaria.* Nature, 2014. **513**(7518): p. 431-5.
57. Llinas, M., K.W. Deitsch, and T.S. Voss, *Plasmodium gene regulation: far more to factor in.* Trends Parasitol, 2008. **24**(12): p. 551-6.
58. Ay, F., et al., *Three-dimensional modeling of the P. falciparum genome during the erythrocytic cycle reveals a strong connection between genome architecture and gene expression.* Genome Res, 2014. **24**(6): p. 974-88.
59. Balaji, S., et al., *Discovery of the principal specific transcription factors of Apicomplexa and their implication for the evolution of the AP2-integrase DNA binding domains.* Nucleic Acids Res, 2005. **33**(13): p. 3994-4006.
60. Iyer, L.M., et al., *Comparative genomics of transcription factors and chromatin proteins in parasitic protists and other eukaryotes.* Int J Parasitol, 2008. **38**(1): p. 1-31.
61. Altschul, S.F., et al., *The construction and use of log-odds substitution scores for multiple sequence alignment.* PLoS Comput Biol, 2010. **6**(7): p. e1000852.
62. Jofuku, K.D., et al., *Control of Arabidopsis flower and seed development by the homeotic gene APETALA2.* Plant Cell, 1994. **6**(9): p. 1211-25.
63. Le Roch, K.G., et al., *Global analysis of transcript and protein levels across the Plasmodium falciparum life cycle.* Genome Res, 2004. **14**(11): p. 2308-18.
64. Deitsch, K., et al., *Mechanisms of gene regulation in Plasmodium.* Am J Trop Med Hyg, 2007. **77**(2): p. 201-8.
65. Campbell, T.L., et al., *Identification and genome-wide prediction of DNA binding specificities for the ApiAP2 family of regulators from the malaria parasite.* PLoS Pathog, 2010. **6**(10): p. e1001165.
66. Flueck, C., et al., *A major role for the Plasmodium falciparum ApiAP2 protein PfSIP2 in chromosome end biology.* PLoS Pathog, 2010. **6**(2): p. e1000784.
67. Kafsack, B.F., et al., *A transcriptional switch underlies commitment to sexual development in malaria parasites.* Nature, 2014. **507**(7491): p. 248-52.
68. Brancucci, N.M., et al., *Heterochromatin protein 1 secures survival and transmission of malaria parasites.* Cell Host Microbe, 2014. **16**(2): p. 165-76.
69. Coleman, B.I., et al., *A Plasmodium falciparum Histone Deacetylase Regulates Antigenic Variation and Gametocyte Conversion.* Cell Host Microbe, 2014. **16**(2): p. 177-86.
70. Sinha, A., et al., *A cascade of DNA-binding proteins for sexual commitment and development in Plasmodium.* Nature, 2014. **507**(7491): p. 253-7.
71. Yuda, M., et al., *Identification of a transcription factor in the mosquito-invasive stage of malaria parasites.* Mol Microbiol, 2009. **71**(6): p. 1402-14.
72. Yuda, M., et al., *Transcription factor AP2-Sp and its target genes in malarial sporozoites.* Mol Microbiol, 2010. **75**(4): p. 854-63.
73. Iwanaga, S., et al., *Identification of an AP2-family protein that is critical for malaria liver stage development.* PLoS One, 2012. **7**(11): p. e47557.
74. Komaki-Yasuda, K., et al., *Identification of a Novel and Unique Transcription Factor in the Intraerythrocytic Stage of Plasmodium falciparum.* PLoS One, 2013. **8**(9): p. e74701.
75. Kawazu, S., et al., *Molecular cloning and characterization of a peroxiredoxin from the human malaria parasite Plasmodium falciparum.* Mol Biochem Parasitol, 2000. **109**(2): p. 165-9.
76. Yano, K., et al., *Expression of mRNAs and proteins for peroxiredoxins in Plasmodium falciparum erythrocytic stage.* Parasitol Int, 2005. **54**(1): p. 35-41.

77. GRISHIN, N.V., *KH DOMAIN: ONE MOTIF, TWO FOLDS.* NUCLEIC ACIDS RES, 2001. **29**(3): P. 638-43.
78. VALVERDE, R., L. EDWARDS, AND L. REGAN, *STRUCTURE AND FUNCTION OF KH DOMAINS.* FEBS J, 2008. **275**(11): P. 2712-26.
79. GARDNER, M.J., ET AL., *GENOME SEQUENCE OF THE HUMAN MALARIA PARASITE PLASMODIUM FALCIPARUM.* NATURE, 2002. **419**(6906): P. 498-511.
80. OTTO, T.D., ET AL., *NEW INSIGHTS INTO THE BLOOD-STAGE TRANSCRIPTOME OF PLASMODIUM FALCIPARUM USING RNA-SEQ.* MOL MICROBIOL, 2010. **76**(1): P. 12-24.
81. SORBER, K., M.T. DIMON, AND J.L. DERISI, *RNA-SEQ ANALYSIS OF SPLICING IN PLASMODIUM FALCIPARUM UNCOVERS NEW SPLICE JUNCTIONS, ALTERNATIVE SPLICING AND SPLICING OF ANTISENSE TRANSCRIPTS.* NUCLEIC ACIDS RES, 2011. **39**(9): P. 3820-35.
82. NARAYAN, A., ET AL., *REGULATION OF GENE EXPRESSION IN PLASMODIUM FALCIPARUM.* CURR SCI INDIA, 2012. **102**(5): P. 712-24.
83. BUNNIK, E.M., ET AL., *POLYSOME PROFILING REVEALS TRANSLATIONAL CONTROL OF GENE EXPRESSION IN THE HUMAN MALARIA PARASITE PLASMODIUM FALCIPARUM.* GENOME BIOL, 2013. **14**(11): P. R128.
84. LOPEZ-BARRAGAN, M.J., ET AL., *DIRECTIONAL GENE EXPRESSION AND ANTISENSE TRANSCRIPTS IN SEXUAL AND ASEXUAL STAGES OF PLASMODIUM FALCIPARUM.* BMC GENOMICS, 2011. **12**: P. 587.
85. SCHLAX, P.J. AND D.J. WORHUNSKY, *TRANSLATIONAL REPRESSION MECHANISMS IN PROKARYOTES.* MOL MICROBIOL, 2003. **48**(5): P. 1157-69.
86. BABITZKE, P., C.S. BAKER, AND T. ROMEO, *REGULATION OF TRANSLATION INITIATION BY RNA BINDING PROTEINS.* ANNU REV MICROBIOL, 2009. **63**: P. 27-44.
87. GEBAUER, F. AND M.W. HENTZE, *MOLECULAR MECHANISMS OF TRANSLATIONAL CONTROL.* NAT REV MOL CELL BIOL, 2004. **5**(10): P. 827-35.
88. MAZAN-MAMCZARZ, K., ET AL., *TRANSLATIONAL REPRESSION BY RNA-BINDING PROTEIN TIAR.* MOL CELL BIOL, 2006. **26**(7): P. 2716-27.
89. GU, S. AND M.A. KAY, *HOW DO MIRNAS MEDIATE TRANSLATIONAL REPRESSION?* SILENCE, 2010. **1**(1): P. 11.
90. WICKENS, M., ET AL., *A PUF FAMILY PORTRAIT: 3'UTR REGULATION AS A WAY OF LIFE.* TRENDS GENET, 2002. **18**(3): P. 150-7.
91. SPASSOV, D.S. AND R. JURECIC, *THE PUF FAMILY OF RNA-BINDING PROTEINS: DOES EVOLUTIONARILY CONSERVED STRUCTURE EQUAL CONSERVED FUNCTION?* IUBMB LIFE, 2003. **55**(7): P. 359-66.
92. WHARTON, R.P. AND A.K. AGGARWAL, *MRNA REGULATION BY PUF DOMAIN PROTEINS.* SCI STKE, 2006. **2006**(354): P. PE37.
93. OPPERMAN, L., ET AL., *A SINGLE SPACER NUCLEOTIDE DETERMINES THE SPECIFICITIES OF TWO MRNA REGULATORY PROTEINS.* NAT STRUCT MOL BIOL, 2005. **12**(11): P. 945-51.
94. MURATA, Y. AND R.P. WHARTON, *BINDING OF PUMILIO TO MATERNAL HUNCHBACK MRNA IS REQUIRED FOR POSTERIOR PATTERNING IN DROSOPHILA EMBRYOS.* CELL, 1995. **80**(5): P. 747-56.
95. SONODA, J. AND R.P. WHARTON, *RECRUITMENT OF NANOS TO HUNCHBACK MRNA BY PUMILIO.* GENES DEV, 1999. **13**(20): P. 2704-12.
96. KIM-HA, J., K. KERR, AND P.M. MACDONALD, *TRANSLATIONAL REGULATION OF OSKAR MRNA BY BRUNO, AN OVARIAN RNA-BINDING PROTEIN, IS ESSENTIAL.* CELL, 1995. **81**(3): P. 403-12.
97. CHEKULAEVA, M., M.W. HENTZE, AND A. EPHRUSSI, *BRUNO ACTS AS A DUAL REPRESSOR OF OSKAR TRANSLATION, PROMOTING MRNA OLIGOMERIZATION AND FORMATION OF SILENCING PARTICLES.* CELL, 2006. **124**(3): P. 521-33.
98. ZHANG, Y., ET AL., *SPATIALLY RESTRICTED TRANSLATION OF THE XCR1 MRNA IN XENOPUS EMBRYOS.* MOL CELL BIOL, 2009. **29**(13): P. 3791-802.
99. PADMANABHAN, K. AND J.D. RICHTER, *REGULATED PUMILIO-2 BINDING CONTROLS RINGO/SPY MRNA TRANSLATION AND CPEB ACTIVATION.* GENES DEV, 2006. **20**(2): P. 199-209.
100. PAILLARD, L., ET AL., *EDEN AND EDEN-BP, A CIS ELEMENT AND AN ASSOCIATED FACTOR THAT MEDIATE SEQUENCE-SPECIFIC MRNA DEADENYLATION IN XENOPUS EMBRYOS.* EMBO J, 1998. **17**(1): P. 278-87.
101. PATON, M.G., ET AL., *STRUCTURE AND EXPRESSION OF A POST-TRANSCRIPTIONALLY REGULATED MALARIA GENE ENCODING A SURFACE PROTEIN FROM THE SEXUAL STAGES OF PLASMODIUM BERGHEI.* MOL BIOCHEM PARASITOL, 1993. **59**(2): P. 263-75.

102. THOMPSON, J. AND R.E. SINDEN, *IN SITU DETECTION OF PBS21 MRNA DURING SEXUAL DEVELOPMENT OF PLASMODIUM BERGHEI.* MOL BIOCHEM PARASITOL, 1994. **68**(2): P. 189-96.
103. VERVENNE, R.A., ET AL., *DIFFERENTIAL EXPRESSION IN BLOOD STAGES OF THE GENE CODING FOR THE 21-KILODALTON SURFACE PROTEIN OF OOKINETES OF PLASMODIUM BERGHEI AS DETECTED BY RNA IN SITU HYBRIDISATION.* MOL BIOCHEM PARASITOL, 1994. **68**(2): P. 259-66.
104. ABRAHAM, E.G., ET AL., *ANALYSIS OF THE PLASMODIUM AND ANOPHELES TRANSCRIPTIONAL REPERTOIRE DURING OOKINETE DEVELOPMENT AND MIDGUT INVASION.* J BIOL CHEM, 2004. **279**(7): P. 5573-80.
105. NAKAMURA, A., ET AL., *ME31B SILENCES TRANSLATION OF OOCYTE-LOCALIZING RNAS THROUGH THE FORMATION OF CYTOPLASMIC RNP COMPLEX DURING DROSOPHILA OOGENESIS.* DEVELOPMENT, 2001. **128**(17): P. 3233-42.
106. COLEGROVE-OTERO, L.J., A. DEVAUX, AND N. STANDART, *THE XENOPUS ELAV PROTEIN ELRB REPRESSES VG1 MRNA TRANSLATION DURING OOGENESIS.* MOL CELL BIOL, 2005. **25**(20): P. 9028-39.
107. MAIR, G.R., ET AL., *REGULATION OF SEXUAL DEVELOPMENT OF PLASMODIUM BY TRANSLATIONAL REPRESSION.* SCIENCE, 2006. **313**(5787): P. 667-9.
108. MAIR, G.R., ET AL., *UNIVERSAL FEATURES OF POST-TRANSCRIPTIONAL GENE REGULATION ARE CRITICAL FOR PLASMODIUM ZYGOTE DEVELOPMENT.* PLOS PATHOG, 2010. **6**(2): P. E1000767.
109. CORDIN, O., ET AL., *THE DEAD-BOX PROTEIN FAMILY OF RNA HELICASES.* GENE, 2006. **367**: P. 17-37.
110. LADOMERY, M., E. WADE, AND J. SOMMERVILLE, *XP54, THE XENOPUS HOMOLOGUE OF HUMAN RNA HELICASE P54, IS AN INTEGRAL COMPONENT OF STORED MRNP PARTICLES IN OOCYTES.* NUCLEIC ACIDS RES, 1997. **25**(5): P. 965-73.
111. SMILLIE, D.A. AND J. SOMMERVILLE, *RNA HELICASE P54 (DDX6) IS A SHUTTLING PROTEIN INVOLVED IN NUCLEAR ASSEMBLY OF STORED MRNP PARTICLES.* J CELL SCI, 2002. **115**(PT 2): P. 395-407.
112. SHETH, U. AND R. PARKER, *DECAPPING AND DECAY OF MESSENGER RNA OCCUR IN CYTOPLASMIC PROCESSING BODIES.* SCIENCE, 2003. **300**(5620): P. 805-8.
113. DECKER, C.J. AND R. PARKER, *CAR-1 AND TRAILER HITCH: DRIVING MRNP GRANULE FUNCTION AT THE ER?* J CELL BIOL, 2006. **173**(2): P. 159-63.
114. LING, S.H., ET AL., *CRYSTAL STRUCTURE OF HUMAN EDC3 AND ITS FUNCTIONAL IMPLICATIONS.* MOL CELL BIOL, 2008. **28**(19): P. 5965-76.
115. DECKER, C.J., D. TEIXEIRA, AND R. PARKER, *EDC3P AND A GLUTAMINE/ASPARAGINE-RICH DOMAIN OF LSM4P FUNCTION IN PROCESSING BODY ASSEMBLY IN SACCHAROMYCES CEREVISIAE.* J CELL BIOL, 2007. **179**(3): P. 437-49.
116. KAWAHARA, H., ET AL., *NEURAL RNA-BINDING PROTEIN MUSASHI1 INHIBITS TRANSLATION INITIATION BY COMPETING WITH EIF4G FOR PABP.* J CELL BIOL, 2008. **181**(4): P. 639-53.
117. XUE, H., ET AL., *AN ABUNDANT DNA BINDING PROTEIN FROM THE HYPERTHERMOPHILIC ARCHAEON SULFOLOBUS SHIBATAE AFFECTS DNA SUPERCOILING IN A TEMPERATURE-DEPENDENT FASHION.* J BACTERIOL, 2000. **182**(14): P. 3929-33.
118. SANDMAN, K. AND J.N. REEVE, *ARCHAEAL CHROMATIN PROTEINS: DIFFERENT STRUCTURES BUT COMMON FUNCTION?* CURR OPIN MICROBIOL, 2005. **8**(6): P. 656-61.
119. ARAVIND, L., L.M. IYER, AND V. ANANTHARAMAN, *THE TWO FACES OF ALBA: THE EVOLUTIONARY CONNECTION BETWEEN PROTEINS PARTICIPATING IN CHROMATIN STRUCTURE AND RNA METABOLISM.* GENOME BIOL, 2003. **4**(10): P. R64.
120. MANI, J., ET AL., *ALBA-DOMAIN PROTEINS OF TRYPANOSOMA BRUCEI ARE CYTOPLASMIC RNA-BINDING PROTEINS THAT INTERACT WITH THE TRANSLATION MACHINERY.* PLOS ONE, 2011. **6**(7): P. E22463.
121. CHANDRAN, V. AND B.F. LUISI, *RECOGNITION OF ENOLASE IN THE ESCHERICHIA COLI RNA DEGRADOSOME.* J MOL BIOL, 2006. **358**(1): P. 8-15.
122. LO, S.C. AND M. HANNINK, *PGAM5 TETHERS A TERNARY COMPLEX CONTAINING KEAP1 AND NRF2 TO MITOCHONDRIA.* EXP CELL RES, 2008. **314**(8): P. 1789-803.
123. AUDHYA, A., ET AL., *A COMPLEX CONTAINING THE SM PROTEIN CAR-1 AND THE RNA HELICASE CGH-1 IS REQUIRED FOR EMBRYONIC CYTOKINESIS IN CAENORHABDITIS ELEGANS.* J CELL BIOL, 2005. **171**(2): P. 267-79.

124. GOMES-SANTOS, C.S., ET AL., *TRANSITION OF PLASMODIUM SPOROZOITES INTO LIVER STAGE-LIKE FORMS IS REGULATED BY THE RNA BINDING PROTEIN PUMILIO.* PLOS PATHOG, 2011. **7**(5): P. E1002046.
125. MULLER, K., K. MATUSCHEWSKI, AND O. SILVIE, *THE PUF-FAMILY RNA-BINDING PROTEIN PUF2 CONTROLS SPOROZOITE CONVERSION TO LIVER STAGES IN THE MALARIA PARASITE.* PLOS ONE, 2011. **6**(5): P. E19860.
126. MATUSCHEWSKI, K., ET AL., *INFECTIVITY-ASSOCIATED CHANGES IN THE TRANSCRIPTIONAL REPERTOIRE OF THE MALARIA PARASITE SPOROZOITE STAGE.* J BIOL CHEM, 2002. **277**(44): P. 41948-53.
127. LINDNER, S.E., ET AL., *PERTURBATIONS OF PLASMODIUM PUF2 EXPRESSION AND RNA-SEQ OF PUF2-DEFICIENT SPOROZOITES REVEAL A CRITICAL ROLE IN MAINTAINING RNA HOMEOSTASIS AND PARASITE TRANSMISSIBILITY.* CELL MICROBIOL, 2013. **15**(7): P. 1266-83.
128. MIAO, J., ET AL., *THE PUF-FAMILY RNA-BINDING PROTEIN PFPUF2 REGULATES SEXUAL DEVELOPMENT AND SEX DIFFERENTIATION IN THE MALARIA PARASITE PLASMODIUM FALCIPARUM.* J CELL SCI, 2010. **123**(PT 7): P. 1039-49.
129. FAN, Q., ET AL., *CHARACTERIZATION OF PFPUF2, MEMBER OF THE PUF FAMILY RNA-BINDING PROTEINS FROM THE MALARIA PARASITE PLASMODIUM FALCIPARUM.* DNA CELL BIOL, 2004. **23**(11): P. 753-60.
130. CUI, L., Q. FAN, AND J. LI, *THE MALARIA PARASITE PLASMODIUM FALCIPARUM ENCODES MEMBERS OF THE PUF RNA-BINDING PROTEIN FAMILY WITH CONSERVED RNA BINDING ACTIVITY.* NUCLEIC ACIDS RES, 2002. **30**(21): P. 4607-17.
131. ZHANG, M., ET AL., *THE PLASMODIUM EUKARYOTIC INITIATION FACTOR-2ALPHA KINASE IK2 CONTROLS THE LATENCY OF SPOROZOITES IN THE MOSQUITO SALIVARY GLANDS.* J EXP MED, 2010. **207**(7): P. 1465-74.
132. BRAKS, J.A., ET AL., *A CONSERVED U-RICH RNA REGION IMPLICATED IN REGULATION OF TRANSLATION IN PLASMODIUM FEMALE GAMETOCYTES.* NUCLEIC ACIDS RES, 2008. **36**(4): P. 1176-86.
133. SILVIE, O., ET AL., *POST-TRANSCRIPTIONAL SILENCING OF UIS4 IN PLASMODIUM BERGHEI SPOROZOITES IS IMPORTANT FOR HOST SWITCH.* MOL MICROBIOL, 2014. **91**(6): P. 1200-13.
134. SEBASTIAN, S., ET AL., *A PLASMODIUM CALCIUM-DEPENDENT PROTEIN KINASE CONTROLS ZYGOTE DEVELOPMENT AND TRANSMISSION BY TRANSLATIONALLY ACTIVATING REPRESSED MRNAS.* CELL HOST MICROBE, 2012. **12**(1): P. 9-19.
135. STITZEL, M.L. AND G. SEYDOUX, *REGULATION OF THE OOCYTE-TO-ZYGOTE TRANSITION.* SCIENCE, 2007. **316**(5823): P. 407-8.
136. SIDEN-KIAMOS, I., ET AL., *DISTINCT ROLES FOR PBS21 AND PBS25 IN THE IN VITRO OOKINETE TO OOCYST TRANSFORMATION OF PLASMODIUM BERGHEI.* J CELL SCI, 2000. **113 PT 19**: P. 3419-26.
137. TOMAS, A.M., ET AL., *P25 AND P28 PROTEINS OF THE MALARIA OOKINETE SURFACE HAVE MULTIPLE AND PARTIALLY REDUNDANT FUNCTIONS.* EMBO J, 2001. **20**(15): P. 3975-83.
138. RODRIGUEZ MDEL, C., ET AL., *THE SURFACE PROTEIN PVS25 OF PLASMODIUM VIVAX OOKINETES INTERACTS WITH CALRETICULIN ON THE MIDGUT APICAL SURFACE OF THE MALARIA VECTOR ANOPHELES ALBIMANUS.* MOL BIOCHEM PARASITOL, 2007. **153**(2): P. 167-77.
139. VLACHOU, D., ET AL., *ANOPHELES GAMBIAE LAMININ INTERACTS WITH THE P25 SURFACE PROTEIN OF PLASMODIUM BERGHEI OOKINETES.* MOL BIOCHEM PARASITOL, 2001. **112**(2): P. 229-37.
140. ARRIGHI, R.B. AND H. HURD, *THE ROLE OF PLASMODIUM BERGHEI OOKINETE PROTEINS IN BINDING TO BASAL LAMINA COMPONENTS AND TRANSFORMATION INTO OOCYSTS.* INT J PARASITOL, 2002. **32**(1): P. 91-8.
141. KOTSYFAKIS, M., ET AL., *PLASMODIUM BERGHEI OOKINETES BIND TO ANOPHELES GAMBIAE AND DROSOPHILA MELANOGASTER ANNEXINS.* MOL MICROBIOL, 2005. **57**(1): P. 171-9.
142. SAXENA, A.K., Y. WU, AND D.N. GARBOCZI, *PLASMODIUM P25 AND P28 SURFACE PROTEINS: POTENTIAL TRANSMISSION-BLOCKING VACCINES.* EUKARYOT CELL, 2007. **6**(8): P. 1260-5.
143. CARTER, R., *TRANSMISSION BLOCKING MALARIA VACCINES.* VACCINE, 2001. **19**(17-19): P. 2309-14.
144. HISAEDA, H., ET AL., *ANTIBODIES TO MALARIA VACCINE CANDIDATES PVS25 AND PVS28 COMPLETELY BLOCK THE ABILITY OF PLASMODIUM VIVAX TO INFECT MOSQUITOES.* INFECT IMMUN, 2000. **68**(12): P. 6618-23.
145. KASLOW, D.C., *TRANSMISSION-BLOCKING VACCINES: USES AND CURRENT STATUS OF DEVELOPMENT.* INT J PARASITOL, 1997. **27**(2): P. 183-9.

146. GOZAR, M.M., V.L. PRICE, AND D.C. KASLOW, *SACCHAROMYCES CEREVISIAE-SECRETED FUSION PROTEINS PFS25 AND PFS28 ELICIT POTENT PLASMODIUM FALCIPARUM TRANSMISSION-BLOCKING ANTIBODIES IN MICE.* INFECT IMMUN, 1998. **66**(1): P. 59-64.
147. COBAN, C., ET AL., *INDUCTION OF PLASMODIUM FALCIPARUM TRANSMISSION-BLOCKING ANTIBODIES IN NONHUMAN PRIMATES BY A COMBINATION OF DNA AND PROTEIN IMMUNIZATIONS.* INFECT IMMUN, 2004. **72**(1): P. 253-9.
148. STOWERS, A.W., ET AL., *A REGION OF PLASMODIUM FALCIPARUM ANTIGEN PFS25 THAT IS THE TARGET OF HIGHLY POTENT TRANSMISSION-BLOCKING ANTIBODIES.* INFECT IMMUN, 2000. **68**(10): P. 5530-8.
149. AREVALO-HERRERA, M., ET AL., *INDUCTION OF TRANSMISSION-BLOCKING IMMUNITY IN AOTUS MONKEYS BY VACCINATION WITH A PLASMODIUM VIVAX CLINICAL GRADE PVS25 RECOMBINANT PROTEIN.* AM J TROP MED HYG, 2005. **73**(5 SUPPL): P. 32-7.
150. SAUL, A., ET AL., *IMMUNOGENICITY IN RHESUS OF THE PLASMODIUM VIVAX MOSQUITO STAGE ANTIGEN PVS25H WITH ALHYDROGEL AND MONTANIDE ISA 720.* PARASITE IMMUNOL, 2007. **29**(10): P. 525-33.
151. TSUBOI, T., ET AL., *TRANSMISSION-BLOCKING VACCINE OF VIVAX MALARIA.* PARASITOL INT, 2003. **52**(1): P. 1-11.
152. WU, Y., ET AL., *PHASE 1 TRIAL OF MALARIA TRANSMISSION BLOCKING VACCINE CANDIDATES PFS25 AND PVS25 FORMULATED WITH MONTANIDE ISA 51.* PLOS ONE, 2008. **3**(7): P. E2636.
153. MALKIN, E.M., ET AL., *PHASE 1 VACCINE TRIAL OF PVS25H: A TRANSMISSION BLOCKING VACCINE FOR PLASMODIUM VIVAX MALARIA.* VACCINE, 2005. **23**(24): P. 3131-8.
154. SAUL, A., *EFFICACY MODEL FOR MOSQUITO STAGE TRANSMISSION BLOCKING VACCINES FOR MALARIA.* PARASITOLOGY, 2008. **135**(13): P. 1497-506.
155. SAUL, A., *MINIMAL EFFICACY REQUIREMENTS FOR MALARIAL VACCINES TO SIGNIFICANTLY LOWER TRANSMISSION IN EPIDEMIC OR SEASONAL MALARIA.* ACTA TROP, 1993. **52**(4): P. 283-96.
156. CARTER, R., *SPATIAL SIMULATION OF MALARIA TRANSMISSION AND ITS CONTROL BY MALARIA TRANSMISSION BLOCKING VACCINATION.* INT J PARASITOL, 2002. **32**(13): P. 1617-24.
157. GWADZ, R.W., *SUCCESSFUL IMMUNIZATION AGAINST THE SEXUAL STAGES OF PLASMODIUM GALLINACEUM.* SCIENCE, 1976. **193**(4258): P. 1150-1.
158. CARTER, R. AND D.H. CHEN, *MALARIA TRANSMISSION BLOCKED BY IMMUNISATION WITH GAMETES OF THE MALARIA PARASITE.* NATURE, 1976. **263**(5572): P. 57-60.
159. LAVAZEC, C. AND C. BOURGOUIN, *MOSQUITO-BASED TRANSMISSION BLOCKING VACCINES FOR INTERRUPTING PLASMODIUM DEVELOPMENT.* MICROBES INFECT, 2008. **10**(8): P. 845-9.
160. SAUL, A., *MOSQUITO STAGE, TRANSMISSION BLOCKING VACCINES FOR MALARIA.* CURR OPIN INFECT DIS, 2007. **20**(5): P. 476-81.
161. SAUERWEIN, R.W., *MALARIA TRANSMISSION-BLOCKING VACCINES: THE BONUS OF EFFECTIVE MALARIA CONTROL.* MICROBES INFECT, 2007. **9**(6): P. 792-5.
162. MILEK, R.L., ET AL., *IMMUNOLOGICAL PROPERTIES OF RECOMBINANT PROTEINS OF THE TRANSMISSION BLOCKING VACCINE CANDIDATE, PFS48/45, OF THE HUMAN MALARIA PARASITE PLASMODIUM FALCIPARUM PRODUCED IN ESCHERICHIA COLI.* PARASITE IMMUNOL, 1998. **20**(8): P. 377-85.
163. OUTCHKOUROV, N., ET AL., *EPITOPE ANALYSIS OF THE MALARIA SURFACE ANTIGEN PFS48/45 IDENTIFIES A SUBDOMAIN THAT ELICITS TRANSMISSION BLOCKING ANTIBODIES.* J BIOL CHEM, 2007. **282**(23): P. 17148-56.
164. OUTCHKOUROV, N.S., ET AL., *CORRECTLY FOLDED PFS48/45 PROTEIN OF PLASMODIUM FALCIPARUM ELICITS MALARIA TRANSMISSION-BLOCKING IMMUNITY IN MICE.* PROC NATL ACAD SCI U S A, 2008. **105**(11): P. 4301-5.
165. MILEK, R.L., ET AL., *PLASMODIUM FALCIPARUM: HETEROLOGOUS SYNTHESIS OF THE TRANSMISSION-BLOCKING VACCINE CANDIDATE PFS48/45 IN RECOMBINANT VACCINIA VIRUS-INFECTED CELLS.* EXP PARASITOL, 1998. **90**(2): P. 165-74.
166. MILEK, R.L., H.G. STUNNENBERG, AND R.N. KONINGS, *ASSEMBLY AND EXPRESSION OF A SYNTHETIC GENE ENCODING THE ANTIGEN PFS48/45 OF THE HUMAN MALARIA PARASITE PLASMODIUM FALCIPARUM IN YEAST.* VACCINE, 2000. **18**(14): P. 1402-11.
167. BUSTAMANTE, P.J., ET AL., *DIFFERENTIAL ABILITY OF SPECIFIC REGIONS OF PLASMODIUM FALCIPARUM SEXUAL-STAGE ANTIGEN, PFS230, TO INDUCE MALARIA TRANSMISSION-BLOCKING IMMUNITY.* PARASITE IMMUNOL, 2000. **22**(8): P. 373-80.
168. TACHIBANA, M., ET AL., *PLASMODIUM VIVAX GAMETOCYTE PROTEIN PVS230 IS A TRANSMISSION-BLOCKING VACCINE CANDIDATE.* VACCINE, 2012. **30**(10): P. 1807-12.

169. TACHIBANA, M., ET AL., *N-TERMINAL PRODOMAIN OF PFS230 SYNTHESIZED USING A CELL-FREE SYSTEM IS SUFFICIENT TO INDUCE COMPLEMENT-DEPENDENT MALARIA TRANSMISSION-BLOCKING ACTIVITY.* CLIN VACCINE IMMUNOL, 2011. **18**(8): P. 1343-50.
170. QUAKYI, I.A., ET AL., *THE 230-KDA GAMETE SURFACE PROTEIN OF PLASMODIUM FALCIPARUM IS ALSO A TARGET FOR TRANSMISSION-BLOCKING ANTIBODIES.* J IMMUNOL, 1987. **139**(12): P. 4213-7.
171. LANGER, R.C., ET AL., *MONOCLONAL ANTIBODY AGAINST THE PLASMODIUM FALCIPARUM CHITINASE, PFCHT1, RECOGNIZES A MALARIA TRANSMISSION-BLOCKING EPITOPE IN PLASMODIUM GALLINACEUM OOKINETES UNRELATED TO THE CHITINASE PGCHT1.* INFECT IMMUN, 2002. **70**(3): P. 1581-90.
172. LI, F., ET AL., *PLASMODIUM OOKINETE-SECRETED PROTEINS SECRETED THROUGH A COMMON MICRONEMAL PATHWAY ARE TARGETS OF BLOCKING MALARIA TRANSMISSION.* J BIOL CHEM, 2004. **279**(25): P. 26635-44.
173. SHAHABUDDIN, M., ET AL., *TRANSMISSION-BLOCKING ACTIVITY OF A CHITINASE INHIBITOR AND ACTIVATION OF MALARIAL PARASITE CHITINASE BY MOSQUITO PROTEASE.* PROC NATL ACAD SCI U S A, 1993. **90**(9): P. 4266-70.
174. GHOLIZADEH, S., ET AL., *CLONING, EXPRESSION AND TRANSMISSION-BLOCKING ACTIVITY OF ANTI-PVWARP, MALARIA VACCINE CANDIDATE, IN ANOPHELES STEPHENSI MYSORENSIS.* MALAR J, 2010. **9**: P. 158.
175. KARIU, T., ET AL., *CELTOS, A NOVEL MALARIAL PROTEIN THAT MEDIATES TRANSMISSION TO MOSQUITO AND VERTEBRATE HOSTS.* MOL MICROBIOL, 2006. **59**(5): P. 1369-79.
176. ECKER, A., ET AL., *REVERSE GENETICS SCREEN IDENTIFIES SIX PROTEINS IMPORTANT FOR MALARIA DEVELOPMENT IN THE MOSQUITO.* MOL MICROBIOL, 2008. **70**(1): P. 209-20.
177. KASLOW, D.C., *IMMUNOGENICITY OF PLASMODIUM FALCIPARUM SEXUAL STAGE ANTIGENS: IMPLICATIONS FOR THE DESIGN OF A TRANSMISSION BLOCKING VACCINE.* IMMUNOL LETT, 1990. **25**(1-3): P. 83-6.
178. BLAGBOROUGH, A.M., ET AL., *INTRANASAL AND INTRAMUSCULAR IMMUNIZATION WITH BACULOVIRUS DUAL EXPRESSION SYSTEM-BASED PVS25 VACCINE SUBSTANTIALLY BLOCKS PLASMODIUM VIVAX TRANSMISSION.* VACCINE, 2010. **28**(37): P. 6014-20.
179. MARTINEZ, A.P., ET AL., *THE ROLES OF THE GLYCOSYLPHOSPHATIDYLINOSITOL ANCHOR ON THE PRODUCTION AND IMMUNOGENICITY OF RECOMBINANT OOKINETE SURFACE ANTIGEN PBS21 OF PLASMODIUM BERGHEI WHEN PREPARED IN A BACULOVIRUS EXPRESSION SYSTEM.* PARASITE IMMUNOL, 2000. **22**(10): P. 493-500.
180. MIYATA, T., ET AL., *ADENOVIRUS-VECTORED PLASMODIUM VIVAX OOKINETE SURFACE PROTEIN, PVS25, AS A POTENTIAL TRANSMISSION-BLOCKING VACCINE.* VACCINE, 2011. **29**(15): P. 2720-6.
181. MLAMBO, G., N. KUMAR, AND S. YOSHIDA, *FUNCTIONAL IMMUNOGENICITY OF BACULOVIRUS EXPRESSING PFS25, A HUMAN MALARIA TRANSMISSION-BLOCKING VACCINE CANDIDATE ANTIGEN.* VACCINE, 2010. **28**(43): P. 7025-9.
182. CHOWDHURY, D.R., ET AL., *A POTENT MALARIA TRANSMISSION BLOCKING VACCINE BASED ON CODON HARMONIZED FULL LENGTH PFS48/45 EXPRESSED IN ESCHERICHIA COLI.* PLOS ONE, 2009. **4**(7): P. E6352.
183. KUMAR, R., E. ANGOV, AND N. KUMAR, *POTENT MALARIA TRANSMISSION-BLOCKING ANTIBODY RESPONSES ELICITED BY PLASMODIUM FALCIPARUM PFS25 EXPRESSED IN ESCHERICHIA COLI AFTER SUCCESSFUL PROTEIN REFOLDING.* INFECT IMMUN, 2014. **82**(4): P. 1453-9.
184. GOZAR, M.M., ET AL., *PLASMODIUM FALCIPARUM: IMMUNOGENICITY OF ALUM-ADSORBED CLINICAL-GRADE TBV25-28, A YEAST-SECRETED MALARIA TRANSMISSION-BLOCKING VACCINE CANDIDATE.* EXP PARASITOL, 2001. **97**(2): P. 61-9.
185. KASLOW, D.C. AND J. SHILOACH, *PRODUCTION, PURIFICATION AND IMMUNOGENICITY OF A MALARIA TRANSMISSION-BLOCKING VACCINE CANDIDATE: TBV25H EXPRESSED IN YEAST AND PURIFIED USING NICKEL-NTA AGAROSE.* BIOTECHNOLOGY (N Y), 1994. **12**(5): P. 494-9.
186. ZOU, L., ET AL., *EXPRESSION OF MALARIA TRANSMISSION-BLOCKING VACCINE ANTIGEN PFS25 IN PICHIA PASTORIS FOR USE IN HUMAN CLINICAL TRIALS.* VACCINE, 2003. **21**(15): P. 1650-7.
187. GREGORY, J.A., ET AL., *ALGAE-PRODUCED PFS25 ELICITS ANTIBODIES THAT INHIBIT MALARIA TRANSMISSION.* PLOS ONE, 2012. **7**(5): P. E37179.
188. JONES, C.S., ET AL., *HETEROLOGOUS EXPRESSION OF THE C-TERMINAL ANTIGENIC DOMAIN OF THE MALARIA VACCINE CANDIDATE PFS48/45 IN THE GREEN ALGAE CHLAMYDOMONAS REINHARDTII.* APPL MICROBIOL BIOTECHNOL, 2013. **97**(5): P. 1987-95.

189. GREGORY, J.A., ET AL., *ALGA-PRODUCED CHOLERA TOXIN-PFS25 FUSION PROTEINS AS ORAL VACCINES.* APPL ENVIRON MICROBIOL, 2013. **79**(13): P. 3917-25.
190. JONES, R.M., ET AL., *A PLANT-PRODUCED PFS25 VLP MALARIA VACCINE CANDIDATE INDUCES PERSISTENT TRANSMISSION BLOCKING ANTIBODIES AGAINST PLASMODIUM FALCIPARUM IN IMMUNIZED MICE.* PLOS ONE, 2013. **8**(11): P. E79538.
191. FARRANCE, C.E., ET AL., *ANTIBODIES TO PLANT-PRODUCED PLASMODIUM FALCIPARUM SEXUAL STAGE PROTEIN PFS25 EXHIBIT TRANSMISSION BLOCKING ACTIVITY.* HUM VACCIN, 2011. **7 SUPPL**: P. 191-8.
192. KUMAR, R., ET AL., *FUNCTIONAL EVALUATION OF MALARIA PFS25 DNA VACCINE BY IN VIVO ELECTROPORATION IN OLIVE BABOONS.* VACCINE, 2013. **31**(31): P. 3140-7.
193. FANNING, S.L., ET AL., *A GLYCOSYLPHOSPHATIDYLINOSITOL ANCHOR SIGNAL SEQUENCE ENHANCES THE IMMUNOGENICITY OF A DNA VACCINE ENCODING PLASMODIUM FALCIPARUM SEXUAL-STAGE ANTIGEN, PFS230.* VACCINE, 2003. **21**(23): P. 3228-35.
194. KONGKASURIYACHAI, D., ET AL., *POTENT IMMUNOGENICITY OF DNA VACCINES ENCODING PLASMODIUM VIVAX TRANSMISSION-BLOCKING VACCINE CANDIDATES PVS25 AND PVS28-EVALUATION OF HOMOLOGOUS AND HETEROLOGOUS ANTIGEN-DELIVERY PRIME-BOOST STRATEGY.* VACCINE, 2004. **22**(23-24): P. 3205-13.
195. LEBLANC, R., ET AL., *MARKEDLY ENHANCED IMMUNOGENICITY OF A PFS25 DNA-BASED MALARIA TRANSMISSION-BLOCKING VACCINE BY IN VIVO ELECTROPORATION.* VACCINE, 2008. **26**(2): P. 185-92.
196. ARAKAWA, T., ET AL., *NASAL IMMUNIZATION WITH A MALARIA TRANSMISSION-BLOCKING VACCINE CANDIDATE, PFS25, INDUCES COMPLETE PROTECTIVE IMMUNITY IN MICE AGAINST FIELD ISOLATES OF PLASMODIUM FALCIPARUM.* INFECT IMMUN, 2005. **73**(11): P. 7375-80.
197. ARAKAWA, T., ET AL., *SERUM ANTIBODIES INDUCED BY INTRANASAL IMMUNIZATION OF MICE WITH PLASMODIUM VIVAX PVS25 CO-ADMINISTERED WITH CHOLERA TOXIN COMPLETELY BLOCK PARASITE TRANSMISSION TO MOSQUITOES.* VACCINE, 2003. **21**(23): P. 3143-8.
198. MIYATA, T., ET AL., *PLASMODIUM VIVAX OOKINETE SURFACE PROTEIN PVS25 LINKED TO CHOLERA TOXIN B SUBUNIT INDUCES POTENT TRANSMISSION-BLOCKING IMMUNITY BY INTRANASAL AS WELL AS SUBCUTANEOUS IMMUNIZATION.* INFECT IMMUN, 2010. **78**(9): P. 3773-82.
199. COLLINS, W.E., ET AL., *ASSESSMENT OF TRANSMISSION-BLOCKING ACTIVITY OF CANDIDATE PVS25 VACCINE USING GAMETOCYTES FROM CHIMPANZEES.* AM J TROP MED HYG, 2006. **74**(2): P. 215-21.
200. WU, Y., ET AL., *SUSTAINED HIGH-TITER ANTIBODY RESPONSES INDUCED BY CONJUGATING A MALARIAL VACCINE CANDIDATE TO OUTER-MEMBRANE PROTEIN COMPLEX.* PROC NATL ACAD SCI U S A, 2006. **103**(48): P. 18243-8.
201. QIAN, F., ET AL., *CONJUGATING RECOMBINANT PROTEINS TO PSEUDOMONAS AERUGINOSA EXOPROTEIN A: A STRATEGY FOR ENHANCING IMMUNOGENICITY OF MALARIA VACCINE CANDIDATES.* VACCINE, 2007. **25**(20): P. 3923-33.
202. QIAN, F., ET AL., *ENHANCED ANTIBODY RESPONSES TO PLASMODIUM FALCIPARUM PFS28 INDUCED IN MICE BY CONJUGATION TO EXOPROTEIN A OF PSEUDOMONAS AERUGINOSA WITH AN IMPROVED PROCEDURE.* MICROBES INFECT, 2009. **11**(3): P. 408-12.
203. KUBLER-KIELB, J., ET AL., *LONG-LASTING AND TRANSMISSION-BLOCKING ACTIVITY OF ANTIBODIES TO PLASMODIUM FALCIPARUM ELICITED IN MICE BY PROTEIN CONJUGATES OF PFS25.* PROC NATL ACAD SCI U S A, 2007. **104**(1): P. 293-8.
204. BAUM, J., ET AL., *HOST-CELL INVASION BY MALARIA PARASITES: INSIGHTS FROM PLASMODIUM AND TOXOPLASMA.* TRENDS PARASITOL, 2008. **24**(12): P. 557-63.
205. YUDA, M., ET AL., *VON WILLEBRAND FACTOR A DOMAIN-RELATED PROTEIN, A NOVEL MICRONEME PROTEIN OF THE MALARIA OOKINETE HIGHLY CONSERVED THROUGHOUT PLASMODIUM PARASITES.* MOL BIOCHEM PARASITOL, 2001. **116**(1): P. 65-72.
206. TRUEMAN, H.E., ET AL., *FUNCTIONAL CHARACTERIZATION OF AN LCCL-LECTIN DOMAIN CONTAINING PROTEIN FAMILY IN PLASMODIUM BERGHEI.* J PARASITOL, 2004. **90**(5): P. 1062-71.
207. PRADEL, G., ET AL., *A MULTIDOMAIN ADHESION PROTEIN FAMILY EXPRESSED IN PLASMODIUM FALCIPARUM IS ESSENTIAL FOR TRANSMISSION TO THE MOSQUITO.* J EXP MED, 2004. **199**(11): P. 1533-44.
208. SAEED, S., ET AL., *TRANSLATIONAL REPRESSION CONTROLS TEMPORAL EXPRESSION OF THE PLASMODIUM BERGHEI LCCL PROTEIN COMPLEX.* MOL BIOCHEM PARASITOL, 2013. **189**(1-2): P. 38-42.

209. DESSENS, J.T., R.E. SINDEN, AND C. CLAUDIANOS, *LCCL PROTEINS OF APICOMPLEXAN PARASITES.* TRENDS PARASITOL, 2004. **20**(3): P. 102-8.
210. DESSENS, J.T., ET AL., *MALARIA CRYSTALLOIDS: SPECIALIZED STRUCTURES FOR PARASITE TRANSMISSION?* TRENDS PARASITOL, 2011. **27**(3): P. 106-10.
211. CARTER, V., ET AL., *PBSR IS SYNTHESIZED IN MACROGAMETOCYTES AND INVOLVED IN FORMATION OF THE MALARIA CRYSTALLOIDS.* MOL MICROBIOL, 2008. **68**(6): P. 1560-9.
212. SAEED, S., ET AL., *PLASMODIUM BERGHEI CRYSTALLOIDS CONTAIN MULTIPLE LCCL PROTEINS.* MOL BIOCHEM PARASITOL, 2010. **170**(1): P. 49-53.
213. LEMGRUBER, L. AND P. LUPETTI, *CRYSTALLOID BODY, REFRACTILE BODY AND VIRUS-LIKE PARTICLES IN APICOMPLEXA: WHAT IS IN THERE?* PARASITOLOGY, 2012. **139**(3): P. 285-93.
214. GARNHAM, P.C.C., *MALARIA PARASITES AND OTHER HAEMOSPORIDIA*. 1966, OXFORD: BLACKWELL SCIENTIFIC PUBLICATIONS. 1132.
215. GARNHAM, P.C., ET AL., *ELECTRON MICROSCOPE STUDIES ON MOTILE STAGES OF MALARIA PARASITES. VI. THE OOKINETE OF PLASMODIUM BERGHEI YOELII AND ITS TRANSFORMATION INTO THE EARLY OOCYST.* TRANS R SOC TROP MED HYG, 1969. **63**(2): P. 187-94.
216. SINDEN, R.E., R.H. HARTLEY, AND L. WINGER, *THE DEVELOPMENT OF PLASMODIUM OOKINETES IN VITRO: AN ULTRASTRUCTURAL STUDY INCLUDING A DESCRIPTION OF MEIOTIC DIVISION.* PARASITOLOGY, 1985. **91 (PT 2)**: P. 227-44.
217. DAVIES, E.E., *ULTRASTRUCTURAL STUDIES ON THE EARLY OOKINETE STAGE OF PLASMODIUM BERGHEI NIGERIENSIS AND ITS TRANSFORMATION INTO AN OOCYST.* ANN TROP MED PARASITOL, 1974. **68**(3): P. 283-90.
218. MEHLHORN, H., *THE FORMATION OF KINETES AND OOCYSTS IN PLASMODIUM GALLINACEUM (HAEMOSPORIDIA) AND CONSIDERATIONS ON PHYLOGENETIC RELATIONSHIPS BETWEEN HAEMOSPORIDIA, PIROPLASMA AND OTHER COCCIDIA.* PROTISTOLOGICA, 1980. **16**: P. 135–54.
219. TERZAKIS, J.A., J.P. VANDERBERG, AND M.M. WEISS, *VIRUSLIKE PARTICLES IN MALARIA PARASITES.* J PARASITOL, 1976. **62**(3): P. 366-71.
220. MEIS, J.F. AND T. PONNUDURAI, *ULTRASTRUCTURAL STUDIES ON THE INTERACTION OF PLASMODIUM FALCIPARUM OOKINETES WITH THE MIDGUT EPITHELIUM OF ANOPHELES STEPHENSI MOSQUITOES.* PARASITOL RES, 1987. **73**(6): P. 500-6.
221. DASGUPTA, B., *A POSSIBLE VIRUS DISEASE OF THE MALARIAL PARASITE.* TRANS ROY SOC TROP MED HYG, 1968. **62**: P. 730.
222. TERZAKIS, J.A., *A PROTOZOAN VIRUS.* MIL MED, 1969. **134**(10): P. 916-21.
223. TREFIAK, W.D. AND S.S. DESSER, *CRYSTALLOID INCLUSIONS IN SPECIES OF LEUCOCYTOZOON, PARAHAEMOPROTEUS, AND PLASMODIUM.* J PROTOZOOL, 1973. **20**(1): P. 73-80.
224. CLAUDIANOS, C., ET AL., *A MALARIA SCAVENGER RECEPTOR-LIKE PROTEIN ESSENTIAL FOR PARASITE DEVELOPMENT.* MOL MICROBIOL, 2002. **45**(6): P. 1473-84.
225. RAINE, J.D., ET AL., *FEMALE INHERITANCE OF MALARIAL LAP GENES IS ESSENTIAL FOR MOSQUITO TRANSMISSION.* PLOS PATHOG, 2007. **3**(3): P. E30.
226. LAVAZEC, C., ET AL., *ANALYSIS OF MUTANT PLASMODIUM BERGHEI PARASITES LACKING EXPRESSION OF MULTIPLE PBCCP GENES.* MOL BIOCHEM PARASITOL, 2009. **163**(1): P. 1-7.
227. JONES, M.L., ET AL., *ANALYSIS OF PROTEIN PALMITOYLATION REVEALS A PERVASIVE ROLE IN PLASMODIUM DEVELOPMENT AND PATHOGENESIS.* CELL HOST MICROBE, 2012. **12**(2): P. 246-58.
228. NADOLSKI, M.J. AND M.E. LINDER, *PROTEIN LIPIDATION.* FEBS J, 2007. **274**(20): P. 5202-10.
229. CORVI, M.M., A.M. ALONSO, AND M.C. CABALLERO, *PROTEIN PALMITOYLATION AND PATHOGENESIS IN APICOMPLEXAN PARASITES.* J BIOMED BIOTECHNOL, 2012: P. 483969.
230. JONES, M.L., C.L. TAY, AND J.C. RAYNER, *GETTING STUCK IN: PROTEIN PALMITOYLATION IN PLASMODIUM.* TRENDS PARASITOL, 2012. **28**(11): P. 496-503.
231. FAIRBANK, M., ET AL., *RING FINGER PALMITOYLATION OF THE ENDOPLASMIC RETICULUM GP78 E3 UBIQUITIN LIGASE.* FEBS LETT, 2012. **586**(16): P. 2488-93.
232. LAKKARAJU, A.K., ET AL., *PALMITOYLATED CALNEXIN IS A KEY COMPONENT OF THE RIBOSOME-TRANSLOCON COMPLEX.* EMBO J, 2012. **31**(7): P. 1823-35.
233. FRENAL, K., ET AL., *GLOBAL ANALYSIS OF APICOMPLEXAN PROTEIN S-ACYL TRANSFERASES REVEALS AN ENZYME ESSENTIAL FOR INVASION.* TRAFFIC, 2013. **14**(8): P. 895-911.
234. CHILD, M.A., ET AL., *SMALL-MOLECULE INHIBITION OF A DEPALMITOYLASE ENHANCES TOXOPLASMA HOST-CELL INVASION.* NAT CHEM BIOL, 2013. **9**(10): P. 651-6.

235. WANG, Y.X., ET AL., *FUSION OF DOCKED MEMBRANES REQUIRES THE ARMADILLO REPEAT PROTEIN VAC8P.* J BIOL CHEM, 2001. **276**(37): P. 35133-40.
236. SMOTRYS, J.E., ET AL., *THE VACUOLAR DHHC-CRD PROTEIN PFA3P IS A PROTEIN ACYLTRANSFERASE FOR VAC8P.* J CELL BIOL, 2005. **170**(7): P. 1091-9.
237. BECK, J.R., ET AL., *A TOXOPLASMA PALMITOYL ACYL TRANSFERASE AND THE PALMITOYLATED ARMADILLO REPEAT PROTEIN TGARO GOVERN APICAL ROPTRY TETHERING AND REVEAL A CRITICAL ROLE FOR THE RHOPTRIES IN HOST CELL INVASION BUT NOT EGRESS.* PLOS PATHOG, 2013. **9**(2): P. E1003162.
238. JENNINGS, B.C., ET AL., *2-BROMOPALMITATE AND 2-(2-HYDROXY-5-NITRO-BENZYLIDENE)-BENZO[B]THIOPHEN-3-ONE INHIBIT DHHC-MEDIATED PALMITOYLATION IN VITRO.* J LIPID RES, 2009. **50**(2): P. 233-42.
239. RESH, M.D., *USE OF ANALOGS AND INHIBITORS TO STUDY THE FUNCTIONAL SIGNIFICANCE OF PROTEIN PALMITOYLATION.* METHODS, 2006. **40**(2): P. 191-7.
240. ALONSO, A.M., ET AL., *PROTEIN PALMITOYLATION INHIBITION BY 2-BROMOPALMITATE ALTERS GLIDING, HOST CELL INVASION AND PARASITE MORPHOLOGY IN TOXOPLASMA GONDII.* MOL BIOCHEM PARASITOL, 2012. **184**(1): P. 39-43.
241. SHEN, B. AND L.D. SIBLEY, *TOXOPLASMA ALDOLASE IS REQUIRED FOR METABOLISM BUT DISPENSABLE FOR HOST-CELL INVASION.* PROC NATL ACAD SCI U S A, 2014. **111**(9): P. 3567-72.
242. RAIBAUD, A., ET AL., *CRYOFRACTURE ELECTRON MICROSCOPY OF THE OOKINETE PELLICLE OF PLASMODIUM GALLINACEUM REVEALS THE EXISTENCE OF NOVEL PORES IN THE ALVEOLAR MEMBRANES.* J STRUCT BIOL, 2001. **135**(1): P. 47-57.
243. DUBREMETZ, J.F., ET AL., *STRUCTURE DE LA PELLICULE DU SPOROZOITE DE PLASMODIUM YOELII: ÉTUDE PAR CRYOFRACTURE.* C R ACAD SCI PARIS SER D, 1979. **288**: P. 623-6.
244. FRENAL, K. AND D. SOLDATI-FAVRE, *[THE GLIDEOSOME, A UNIQUE MACHINERY THAT ASSISTS THE APICOMPLEXA IN GLIDING INTO HOST CELLS].* MED SCI (PARIS), 2013. **29**(5): P. 515-22.
245. HEINTZELMAN, M.B., *CELLULAR AND MOLECULAR MECHANICS OF GLIDING LOCOMOTION IN EUKARYOTES.* INT REV CYTOL, 2006. **251**: P. 79-129.
246. MENARD, R., *GLIDING MOTILITY AND CELL INVASION BY APICOMPLEXA: INSIGHTS FROM THE PLASMODIUM SPOROZOITE.* CELL MICROBIOL, 2001. **3**(2): P. 63-73.
247. SIBLEY, L.D., *INTRACELLULAR PARASITE INVASION STRATEGIES.* SCIENCE, 2004. **304**(5668): P. 248-53.
248. SIBLEY, L.D., *INVASION AND INTRACELLULAR SURVIVAL BY PROTOZOAN PARASITES.* IMMUNOL REV, 2011. **240**(1): P. 72-91.
249. MEISSNER, M., D.J. FERGUSON, AND F. FRISCHKNECHT, *INVASION FACTORS OF APICOMPLEXAN PARASITES: ESSENTIAL OR REDUNDANT?* CURR OPIN MICROBIOL, 2013. **16**(4): P. 438-44.
250. VLACHOU, D., ET AL., *THE DEVELOPMENTAL MIGRATION OF PLASMODIUM IN MOSQUITOES.* CURR OPIN GENET DEV, 2006. **16**(4): P. 384-91.
251. PIMENTA, P.F., M. TOURAY, AND L. MILLER, *THE JOURNEY OF MALARIA SPOROZOITES IN THE MOSQUITO SALIVARY GLAND.* J EUKARYOT MICROBIOL, 1994. **41**(6): P. 608-24.
252. MUELLER, A.K., ET AL., *INVASION OF MOSQUITO SALIVARY GLANDS BY MALARIA PARASITES: PREREQUISITES AND DEFENSE STRATEGIES.* INT J PARASITOL, 2010. **40**(11): P. 1229-35.
253. RODRIGUEZ, M.H. AND L. HERNANDEZ-HERNANDEZ FDE, *INSECT-MALARIA PARASITES INTERACTIONS: THE SALIVARY GLAND.* INSECT BIOCHEM MOL BIOL, 2004. **34**(7): P. 615-24.
254. CARRUTHERS, V.B. AND L.D. SIBLEY, *SEQUENTIAL PROTEIN SECRETION FROM THREE DISTINCT ORGANELLES OF TOXOPLASMA GONDII ACCOMPANIES INVASION OF HUMAN FIBROBLASTS.* EUR J CELL BIOL, 1997. **73**(2): P. 114-23.
255. DESSENS, J.T., ET AL., *SOAP, A NOVEL MALARIA OOKINETE PROTEIN INVOLVED IN MOSQUITO MIDGUT INVASION AND OOCYST DEVELOPMENT.* MOL MICROBIOL, 2003. **49**(2): P. 319-29.
256. CARRUTHERS, V.B. AND F.M. TOMLEY, *MICRONEME PROTEINS IN APICOMPLEXANS.* SUBCELL BIOCHEM, 2008. **47**: P. 33-45.
257. BROSSIER, F., ET AL., *A SPATIALLY LOCALIZED RHOMBOID PROTEASE CLEAVES CELL SURFACE ADHESINS ESSENTIAL FOR INVASION BY TOXOPLASMA.* PROC NATL ACAD SCI U S A, 2005. **102**(11): P. 4146-51.
258. BAKER, R.P., R. WIJETILAKA, AND S. URBAN, *TWO PLASMODIUM RHOMBOID PROTEASES PREFERENTIALLY CLEAVE DIFFERENT ADHESINS IMPLICATED IN ALL INVASIVE STAGES OF MALARIA.* PLOS PATHOG, 2006. **2**(10): P. E113.

259. KAPPE, S., ET AL., *CONSERVATION OF A GLIDING MOTILITY AND CELL INVASION MACHINERY IN APICOMPLEXAN PARASITES.* J CELL BIOL, 1999. **147**(5): P. 937-44.
260. EJIGIRI, I., ET AL., *SHEDDING OF TRAP BY A RHOMBOID PROTEASE FROM THE MALARIA SPOROZOITE SURFACE IS ESSENTIAL FOR GLIDING MOTILITY AND SPOROZOITE INFECTIVITY.* PLOS PATHOG, 2012. **8**(7): P. E1002725.
261. RUSSEL, D.G., *HOST CELL INVASION BY APICOMPLEXA: AN EXPRESSION OF THE PARASITE'S CONTRACTILE SYSTEM?* PARASITOLOGY, 1983. **87**(2): P. 199-209.
262. KING, C.A., *CELL MOTILITY OF SPOROZOAN PROTOZOA.* PARASITOL TODAY, 1988. **4**(11): P. 315-9.
263. STEWART, M.J. AND J.P. VANDERBERG, *MALARIA SPOROZOITES RELEASE CIRCUMSPOROZOITE PROTEIN FROM THEIR APICAL END AND TRANSLOCATE IT ALONG THEIR SURFACE.* J PROTOZOOL, 1991. **38**(4): P. 411-21.
264. STEWART, M.J. AND J.P. VANDERBERG, *MALARIA SPOROZOITES LEAVE BEHIND TRAILS OF CIRCUMSPOROZOITE PROTEIN DURING GLIDING MOTILITY.* J PROTOZOOL, 1988. **35**(3): P. 389-93.
265. ISHINO, T., Y. CHINZEI, AND M. YUDA, *TWO PROTEINS WITH 6-CYS MOTIFS ARE REQUIRED FOR MALARIAL PARASITES TO COMMIT TO INFECTION OF THE HEPATOCYTE.* MOL MICROBIOL, 2005. **58**(5): P. 1264-75.
266. DESSENS, J.T., ET AL., *KNOCKOUT OF THE RODENT MALARIA PARASITE CHITINASE PBCHT1 REDUCES INFECTIVITY TO MOSQUITOES.* INFECT IMMUN, 2001. **69**(6): P. 4041-7.
267. TSAI, Y.L., ET AL., *DISRUPTION OF PLASMODIUM FALCIPARUM CHITINASE MARKEDLY IMPAIRS PARASITE INVASION OF MOSQUITO MIDGUT.* INFECT IMMUN, 2001. **69**(6): P. 4048-54.
268. SILVIE, O., ET AL., *A ROLE FOR APICAL MEMBRANE ANTIGEN 1 DURING INVASION OF HEPATOCYTES BY PLASMODIUM FALCIPARUM SPOROZOITES.* J BIOL CHEM, 2004. **279**(10): P. 9490-6.
269. GIOVANNINI, D., ET AL., *INDEPENDENT ROLES OF APICAL MEMBRANE ANTIGEN 1 AND RHOPTRY NECK PROTEINS DURING HOST CELL INVASION BY APICOMPLEXA.* CELL HOST MICROBE, 2011. **10**(6): P. 591-602.
270. BARGIERI, D.Y., ET AL., *APICAL MEMBRANE ANTIGEN 1 MEDIATES APICOMPLEXAN PARASITE ATTACHMENT BUT IS DISPENSABLE FOR HOST CELL INVASION.* NAT COMMUN, 2013. **4**: P. 2552.
271. YAP, A., ET AL., *CONDITIONAL EXPRESSION OF APICAL MEMBRANE ANTIGEN 1 IN PLASMODIUM FALCIPARUM SHOWS IT IS REQUIRED FOR ERYTHROCYTE INVASION BY MEROZOITES.* CELL MICROBIOL, 2014. **16**(5): P. 642-56.
272. DESSENS, J.T., ET AL., *CTRP IS ESSENTIAL FOR MOSQUITO INFECTION BY MALARIA OOKINETES.* EMBO J, 1999. **18**(22): P. 6221-7.
273. YUDA, M., H. SAKAIDA, AND Y. CHINZEI, *TARGETED DISRUPTION OF THE PLASMODIUM BERGHEI CTRP GENE REVEALS ITS ESSENTIAL ROLE IN MALARIA INFECTION OF THE VECTOR MOSQUITO.* J EXP MED, 1999. **190**(11): P. 1711-6.
274. TEMPLETON, T.J., D.C. KASLOW, AND D.A. FIDOCK, *DEVELOPMENTAL ARREST OF THE HUMAN MALARIA PARASITE PLASMODIUM FALCIPARUM WITHIN THE MOSQUITO MIDGUT VIA CTRP GENE DISRUPTION.* MOL MICROBIOL, 2000. **36**(1): P. 1-9.
275. KADOTA, K., ET AL., *ESSENTIAL ROLE OF MEMBRANE-ATTACK PROTEIN IN MALARIAL TRANSMISSION TO MOSQUITO HOST.* PROC NATL ACAD SCI U S A, 2004. **101**(46): P. 16310-5.
276. KARIU, T., ET AL., *MAEBL IS ESSENTIAL FOR MALARIAL SPOROZOITE INFECTION OF THE MOSQUITO SALIVARY GLAND.* J EXP MED, 2002. **195**(10): P. 1317-23.
277. SAENZ, F.E., ET AL., *THE TRANSMEMBRANE ISOFORM OF PLASMODIUM FALCIPARUM MAEBL IS ESSENTIAL FOR THE INVASION OF ANOPHELES SALIVARY GLANDS.* PLOS ONE, 2008. **3**(5): P. E2287.
278. ISHINO, T., ET AL., *CELL-PASSAGE ACTIVITY IS REQUIRED FOR THE MALARIAL PARASITE TO CROSS THE LIVER SINUSOIDAL CELL LAYER.* PLOS BIOL, 2004. **2**(1): P. E4.
279. ISHINO, T., Y. CHINZEI, AND M. YUDA, *A PLASMODIUM SPOROZOITE PROTEIN WITH A MEMBRANE ATTACK COMPLEX DOMAIN IS REQUIRED FOR BREACHING THE LIVER SINUSOIDAL CELL LAYER PRIOR TO HEPATOCYTE INFECTION.* CELL MICROBIOL, 2005. **7**(2): P. 199-208.
280. ARREDONDO, S.A., ET AL., *STRUCTURE OF THE PLASMODIUM 6-CYSTEINE S48/45 DOMAIN.* PROC NATL ACAD SCI U S A, 2012. **109**(17): P. 6692-7.
281. VAN DIJK, M.R., ET AL., *GENETICALLY ATTENUATED, P36P-DEFICIENT MALARIAL SPOROZOITES INDUCE PROTECTIVE IMMUNITY AND APOPTOSIS OF INFECTED LIVER CELLS.* PROC NATL ACAD SCI U S A, 2005. **102**(34): P. 12194-9.

282. VAN DIJK, M.R., ET AL., *THREE MEMBERS OF THE 6-CYS PROTEIN FAMILY OF PLASMODIUM PLAY A ROLE IN GAMETE FERTILITY.* PLOS PATHOG, 2010. **6**(4): P. E1000853.
283. ANNOURA, T., ET AL., *ASSESSING THE ADEQUACY OF ATTENUATION OF GENETICALLY MODIFIED MALARIA PARASITE VACCINE CANDIDATES.* VACCINE, 2012. **30**(16): P. 2662-70.
284. LABAIED, M., ET AL., *PLASMODIUM YOELII SPOROZOITES WITH SIMULTANEOUS DELETION OF P52 AND P36 ARE COMPLETELY ATTENUATED AND CONFER STERILE IMMUNITY AGAINST INFECTION.* INFECT IMMUN, 2007. **75**(8): P. 3758-68.
285. SULTAN, A.A., ET AL., *TRAP IS NECESSARY FOR GLIDING MOTILITY AND INFECTIVITY OF PLASMODIUM SPOROZOITES.* CELL, 1997. **90**(3): P. 511-22.
286. MOTA, M.M., ET AL., *GENE TARGETING IN THE RODENT MALARIA PARASITE PLASMODIUM YOELII.* MOL BIOCHEM PARASITOL, 2001. **113**(2): P. 271-8.
287. MATUSCHEWSKI, K., ET AL., *PLASMODIUM SPOROZOITE INVASION INTO INSECT AND MAMMALIAN CELLS IS DIRECTED BY THE SAME DUAL BINDING SYSTEM.* EMBO J, 2002. **21**(7): P. 1597-606.
288. STEINBUECHEL, M. AND K. MATUSCHEWSKI, *ROLE FOR THE PLASMODIUM SPOROZOITE-SPECIFIC TRANSMEMBRANE PROTEIN S6 IN PARASITE MOTILITY AND EFFICIENT MALARIA TRANSMISSION.* CELL MICROBIOL, 2009. **11**(2): P. 279-88.
289. COMBE, A., ET AL., *TREP, A NOVEL PROTEIN NECESSARY FOR GLIDING MOTILITY OF THE MALARIA SPOROZOITE.* INT J PARASITOL, 2009. **39**(4): P. 489-96.
290. MOREIRA, C.K., ET AL., *THE PLASMODIUM TRAP/MIC2 FAMILY MEMBER, TRAP-LIKE PROTEIN (TLP), IS INVOLVED IN TISSUE TRAVERSAL BY SPOROZOITES.* CELL MICROBIOL, 2008. **10**(7): P. 1505-16.
291. HEISS, K., ET AL., *FUNCTIONAL CHARACTERIZATION OF A REDUNDANT PLASMODIUM TRAP FAMILY INVASIN, TRAP-LIKE PROTEIN, BY ALDOLASE BINDING AND A GENETIC COMPLEMENTATION TEST.* EUKARYOT CELL, 2008. **7**(6): P. 1062-70.
292. LACROIX, C. AND R. MENARD, *TRAP-LIKE PROTEIN OF PLASMODIUM SPOROZOITES: LINKING GLIDING MOTILITY TO HOST-CELL TRAVERSAL.* TRENDS PARASITOL, 2008. **24**(10): P. 431-4.
293. KAISER, K., ET AL., *DIFFERENTIAL TRANSCRIPTOME PROFILING IDENTIFIES PLASMODIUM GENES ENCODING PRE-ERYTHROCYTIC STAGE-SPECIFIC PROTEINS.* MOL MICROBIOL, 2004. **51**(5): P. 1221-32.
294. LABAIED, M., N. CAMARGO, AND S.H. KAPPE, *DEPLETION OF THE PLASMODIUM BERGHEI THROMBOSPONDIN-RELATED SPOROZOITE PROTEIN REVEALS A ROLE IN HOST CELL ENTRY BY SPOROZOITES.* MOL BIOCHEM PARASITOL, 2007. **153**(2): P. 158-66.
295. THOMPSON, J., ET AL., *PLASMODIUM CYSTEINE REPEAT MODULAR PROTEINS 1-4: COMPLEX PROTEINS WITH ROLES THROUGHOUT THE MALARIA PARASITE LIFE CYCLE.* CELL MICROBIOL, 2007. **9**(6): P. 1466-80.
296. ALEXANDER, D.L., ET AL., *IDENTIFICATION OF THE MOVING JUNCTION COMPLEX OF TOXOPLASMA GONDII: A COLLABORATION BETWEEN DISTINCT SECRETORY ORGANELLES.* PLOS PATHOG, 2005. **1**(2): P. E17.
297. LEBRUN, M., ET AL., *THE RHOPTRY NECK PROTEIN RON4 RE-LOCALIZES AT THE MOVING JUNCTION DURING TOXOPLASMA GONDII INVASION.* CELL MICROBIOL, 2005. **7**(12): P. 1823-33.
298. ALEXANDER, D.L., ET AL., *PLASMODIUM FALCIPARUM AMA1 BINDS A RHOPTRY NECK PROTEIN HOMOLOGOUS TO TGRON4, A COMPONENT OF THE MOVING JUNCTION IN TOXOPLASMA GONDII.* EUKARYOT CELL, 2006. **5**(7): P. 1169-73.
299. GONZALEZ, V., ET AL., *HOST CELL ENTRY BY APICOMPLEXA PARASITES REQUIRES ACTIN POLYMERIZATION IN THE HOST CELL.* CELL HOST MICROBE, 2009. **5**(3): P. 259-72.
300. PEI, Y., ET AL., *PLASMODIUM YOELII INHIBITOR OF CYSTEINE PROTEASES IS EXPORTED TO EXOMEMBRANE STRUCTURES AND INTERACTS WITH YOELIPAIN-2 DURING ASEXUAL BLOOD-STAGE DEVELOPMENT.* CELL MICROBIOL, 2013. **15**(9): P. 1508-26.
301. BOYSEN, K.E. AND K. MATUSCHEWSKI, *INHIBITOR OF CYSTEINE PROTEASES IS CRITICAL FOR MOTILITY AND INFECTIVITY OF PLASMODIUM SPOROZOITES.* MBIO, 2013. **4**(6).
302. MENARD, R., *THE JOURNEY OF THE MALARIA SPOROZOITE THROUGH ITS HOSTS: TWO PARASITE PROTEINS LEAD THE WAY.* MICROBES INFECT, 2000. **2**(6): P. 633-42.
303. SIDJANSKI, S.P., J.P. VANDERBERG, AND P. SINNIS, *ANOPHELES STEPHENSI SALIVARY GLANDS BEAR RECEPTORS FOR REGION I OF THE CIRCUMSPOROZOITE PROTEIN OF PLASMODIUM FALCIPARUM.* MOL BIOCHEM PARASITOL, 1997. **90**(1): P. 33-41.

304. MYUNG, J.M., P. MARSHALL, AND P. SINNIS, *THE PLASMODIUM CIRCUMSPOROZOITE PROTEIN IS INVOLVED IN MOSQUITO SALIVARY GLAND INVASION BY SPOROZOITES.* MOL BIOCHEM PARASITOL, 2004. **133**(1): P. 53-9.
305. SINNIS, P., ET AL., *MOSQUITO HEPARAN SULFATE AND ITS POTENTIAL ROLE IN MALARIA INFECTION AND TRANSMISSION.* J BIOL CHEM, 2007. **282**(35): P. 25376-84.
306. GHOSH, A.K., ET AL., *MALARIA PARASITE INVASION OF THE MOSQUITO SALIVARY GLAND REQUIRES INTERACTION BETWEEN THE PLASMODIUM TRAP AND THE ANOPHELES SAGLIN PROTEINS.* PLOS PATHOG, 2009. **5**(1): P. E1000265.
307. MORAHAN, B.J., L. WANG, AND R.L. COPPEL, *NO TRAP, NO INVASION.* TRENDS PARASITOL, 2009. **25**(2): P. 77-84.
308. JETHWANEY, D., ET AL., *FETUIN-A, A HEPATOCYTE-SPECIFIC PROTEIN THAT BINDS PLASMODIUM BERGHEI THROMBOSPONDIN-RELATED ADHESIVE PROTEIN: A POTENTIAL ROLE IN INFECTIVITY.* INFECT IMMUN, 2005. **73**(9): P. 5883-91.
309. MULLER, H.M., ET AL., *THROMBOSPONDIN RELATED ANONYMOUS PROTEIN (TRAP) OF PLASMODIUM FALCIPARUM BINDS SPECIFICALLY TO SULFATED GLYCOCONJUGATES AND TO HEPG2 HEPATOMA CELLS SUGGESTING A ROLE FOR THIS MOLECULE IN SPOROZOITE INVASION OF HEPATOCYTES.* EMBO J, 1993. **12**(7): P. 2881-9.
310. ROBSON, K.J., ET AL., *THROMBOSPONDIN-RELATED ADHESIVE PROTEIN (TRAP) OF PLASMODIUM FALCIPARUM: EXPRESSION DURING SPOROZOITE ONTOGENY AND BINDING TO HUMAN HEPATOCYTES.* EMBO J, 1995. **14**(16): P. 3883-94.
311. LOPEZ, R., ET AL., *PLASMODIUM FALCIPARUM: BINDING STUDIES OF PEPTIDE DERIVED FROM THE SPOROZOITE SURFACE PROTEIN 2 TO HEP G2 CELLS.* J PEPT RES, 2001. **58**(4): P. 285-92.
312. KANG, J.M., ET AL., *LIMITED SEQUENCE POLYMORPHISMS OF FOUR TRANSMISSION-BLOCKING VACCINE CANDIDATE ANTIGENS IN PLASMODIUM VIVAX KOREAN ISOLATES.* MALAR J, 2013. **12**: P. 144.
313. ZAKERI, S., S. RAZAVI, AND N.D. DJADID, *GENETIC DIVERSITY OF TRANSMISSION BLOCKING VACCINE CANDIDATE (PVS25 AND PVS28) ANTIGEN IN PLASMODIUM VIVAX CLINICAL ISOLATES FROM IRAN.* ACTA TROP, 2009. **109**(3): P. 176-80.
314. RICHARDS, J.S., N.J. MACDONALD, AND D.P. EISEN, *LIMITED POLYMORPHISM IN PLASMODIUM FALCIPARUM OOKINETE SURFACE ANTIGEN, VON WILLEBRAND FACTOR A DOMAIN-RELATED PROTEIN FROM CLINICAL ISOLATES.* MALAR J, 2006. **5**: P. 55.
315. HAFALLA, J.C., ET AL., *MINIMAL VARIATION IN THE PFS28 OOKINETE ANTIGEN FROM PHILIPPINE FIELD ISOLATES OF PLASMODIUM FALCIPARUM.* MOL BIOCHEM PARASITOL, 1997. **87**(1): P. 97-9.
316. JANSE, C.J., ET AL., *PLASMODIUM BERGHEI: GAMETOCYTE PRODUCTION, DNA CONTENT, AND CHROMOSOME-SIZE POLYMORPHISMS DURING ASEXUAL MULTIPLICATION IN VIVO.* EXP PARASITOL, 1989. **68**(3): P. 274-82.
317. JANSE, C.J., ET AL., *HIGH EFFICIENCY TRANSFECTION OF PLASMODIUM BERGHEI FACILITATES NOVEL SELECTION PROCEDURES.* MOL BIOCHEM PARASITOL, 2006. **145**(1): P. 60-70.
318. JANSE, C.J., J. RAMESAR, AND A.P. WATERS, *HIGH-EFFICIENCY TRANSFECTION AND DRUG SELECTION OF GENETICALLY TRANSFORMED BLOOD STAGES OF THE RODENT MALARIA PARASITE PLASMODIUM BERGHEI.* NAT PROTOC, 2006. **1**(1): P. 346-56.
319. SPACCAPELO, R., ET AL., *PLASMEPSIN 4-DEFICIENT PLASMODIUM BERGHEI ARE VIRULENCE ATTENUATED AND INDUCE PROTECTIVE IMMUNITY AGAINST EXPERIMENTAL MALARIA.* AM J PATHOL, 2010. **176**(1): P. 205-17.
320. JANSE, C.J., ET AL., *MALARIA PARASITES LACKING EEF1A HAVE A NORMAL S/M PHASE YET GROW MORE SLOWLY DUE TO A LONGER G1 PHASE.* MOL MICROBIOL, 2003. **50**(5): P. 1539-51.
321. YOSHIDA, N., ET AL., *HYBRIDOMA PRODUCES PROTECTIVE ANTIBODIES DIRECTED AGAINST THE SPOROZOITE STAGE OF MALARIA PARASITE.* SCIENCE, 1980. **207**(4426): P. 71-3.
322. TSUJI, M., ET AL., *DEMONSTRATION OF HEAT-SHOCK PROTEIN 70 IN THE SPOROZOITE STAGE OF MALARIA PARASITES.* PARASITOL RES, 1994. **80**(1): P. 16-21.
323. SANDERS, P.R., ET AL., *DISTINCT PROTEIN CLASSES INCLUDING NOVEL MEROZOITE SURFACE ANTIGENS IN RAFT-LIKE MEMBRANES OF PLASMODIUM FALCIPARUM.* J BIOL CHEM, 2005. **280**(48): P. 40169-76.
324. DI GIROLAMO, F., ET AL., *PLASMODIUM LIPID RAFTS CONTAIN PROTEINS IMPLICATED IN VESICULAR TRAFFICKING AND SIGNALLING AS WELL AS MEMBERS OF THE PIR SUPERFAMILY,*

POTENTIALLY IMPLICATED IN HOST IMMUNE SYSTEM INTERACTIONS. PROTEOMICS, 2008. **8**(12): P. 2500-13.
325. PATRA, K.P., ET AL., *PROTEOMIC ANALYSIS OF ZYGOTE AND OOKINETE STAGES OF THE AVIAN MALARIA PARASITE PLASMODIUM GALLINACEUM DELINEATES THE HOMOLOGOUS PROTEOMES OF THE LETHAL HUMAN MALARIA PARASITE PLASMODIUM FALCIPARUM.* PROTEOMICS, 2008. **8**(12): P. 2492-9.
326. LAL, K., ET AL., *CHARACTERISATION OF PLASMODIUM INVASIVE ORGANELLES; AN OOKINETE MICRONEME PROTEOME.* PROTEOMICS, 2009. **9**(5): P. 1142-51.
327. THATHY, V., ET AL., *LEVELS OF CIRCUMSPOROZOITE PROTEIN IN THE PLASMODIUM OOCYST DETERMINE SPOROZOITE MORPHOLOGY.* EMBO J, 2002. **21**(7): P. 1586-96.
328. SIRPIO, S., ET AL., *TLP18.3, A NOVEL THYLAKOID LUMEN PROTEIN REGULATING PHOTOSYSTEM II REPAIR CYCLE.* BIOCHEM J, 2007. **406**(3): P. 415-25.
329. BOULIN, T., ET AL., *POSITIVE MODULATION OF A CYS-LOOP ACETYLCHOLINE RECEPTOR BY AN AUXILIARY TRANSMEMBRANE SUBUNIT.* NAT NEUROSCI, 2012. **15**(10): P. 1374-81.
330. LIN, J.W., ET AL., *LOSS-OF-FUNCTION ANALYSES DEFINES VITAL AND REDUNDANT FUNCTIONS OF THE PLASMODIUM RHOMBOID PROTEASE FAMILY.* MOL MICROBIOL, 2013. **88**(2): P. 318-38.
331. MENARD, R., ET AL., *CIRCUMSPOROZOITE PROTEIN IS REQUIRED FOR DEVELOPMENT OF MALARIA SPOROZOITES IN MOSQUITOES.* NATURE, 1997. **385**(6614): P. 336-40.
332. JANSE, C.J. AND A.P. WATERS, *PLASMODIUM BERGHEI: THE APPLICATION OF CULTIVATION AND PURIFICATION TECHNIQUES TO MOLECULAR STUDIES OF MALARIA PARASITES.* PARASITOL TODAY, 1995. **11**(4): P. 138-43.
333. JANSE, C.J., ET AL., *IN VITRO FORMATION OF OOKINETES AND FUNCTIONAL MATURITY OF PLASMODIUM BERGHEI GAMETOCYTES.* PARASITOLOGY, 1985. **91 (PT 1)**: P. 19-29.
334. HOEIJMAKERS, W.A., ET AL., *LINEAR AMPLIFICATION FOR DEEP SEQUENCING.* NAT PROTOC, 2011. **6**(7): P. 1026-36.
335. TRAPNELL, C., ET AL., *DIFFERENTIAL ANALYSIS OF GENE REGULATION AT TRANSCRIPT RESOLUTION WITH RNA-SEQ.* NAT BIOTECHNOL, 2013. **31**(1): P. 46-53.
336. DE KONING-WARD, T.F., ET AL., *THE SELECTABLE MARKER HUMAN DIHYDROFOLATE REDUCTASE ENABLES SEQUENTIAL GENETIC MANIPULATION OF THE PLASMODIUM BERGHEI GENOME.* MOL BIOCHEM PARASITOL, 2000. **106**(2): P. 199-212.
337. BEETSMA, A.L., ET AL., *PLASMODIUM BERGHEI ANKA: PURIFICATION OF LARGE NUMBERS OF INFECTIOUS GAMETOCYTES.* EXP PARASITOL, 1998. **88**(1): P. 69-72.
338. REYNOLDS, E.S., *THE USE OF LEAD CITRATE AT HIGH PH AS AN ELECTRON-OPAQUE STAIN IN ELECTRON MICROSCOPY.* J CELL BIOL, 1963. **17**: P. 208-12.
339. LINDNER, S.E., ET AL., *TOTAL AND PUTATIVE SURFACE PROTEOMICS OF MALARIA PARASITE SALIVARY GLAND SPOROZOITES.* MOL CELL PROTEOMICS, 2013. **12**(5): P. 1127-43.
340. TREECK, M., ET AL., *THE PHOSPHOPROTEOMES OF PLASMODIUM FALCIPARUM AND TOXOPLASMA GONDII REVEAL UNUSUAL ADAPTATIONS WITHIN AND BEYOND THE PARASITES' BOUNDARIES.* CELL HOST MICROBE, 2011. **10**(4): P. 410-9.
341. SOLYAKOV, L., ET AL., *GLOBAL KINOMIC AND PHOSPHO-PROTEOMIC ANALYSES OF THE HUMAN MALARIA PARASITE PLASMODIUM FALCIPARUM.* NAT COMMUN, 2011. **2**: P. 565.
342. FRENAL, K., L.E. KEMP, AND D. SOLDATI-FAVRE, *EMERGING ROLES FOR PROTEIN S-PALMITOYLATION IN TOXOPLASMA BIOLOGY.* INT J PARASITOL, 2014. **44**: P. 121-31.
343. WEBB, Y., L. HERMIDA-MATSUMOTO, AND M.D. RESH, *INHIBITION OF PROTEIN PALMITOYLATION, RAFT LOCALIZATION, AND T CELL SIGNALING BY 2-BROMOPALMITATE AND POLYUNSATURATED FATTY ACIDS.* J BIOL CHEM, 2000. **275**(1): P. 261-70.
344. POULIN, B., ET AL., *UNIQUE APICOMPLEXAN IMC SUB-COMPARTMENT PROTEINS ARE EARLY MARKERS FOR APICAL POLARITY IN THE MALARIA PARASITE.* BIOL OPEN, 2013. **2**(11): P. 1160-70.
345. OEHRING, S.C., ET AL., *ORGANELLAR PROTEOMICS REVEALS HUNDREDS OF NOVEL NUCLEAR PROTEINS IN THE MALARIA PARASITE PLASMODIUM FALCIPARUM.* GENOME BIOL, 2012. **13**(11): P. R108.
346. PFANDER, C., ET AL., *A SCALABLE PIPELINE FOR HIGHLY EFFECTIVE GENETIC MODIFICATION OF A MALARIA PARASITE.* NAT METHODS, 2011. **8**(12): P. 1078-82.
347. LAURENTINO, E.C., ET AL., *EXPERIMENTALLY CONTROLLED DOWNREGULATION OF THE HISTONE CHAPERONE FACT IN PLASMODIUM BERGHEI REVEALS THAT IT IS CRITICAL TO MALE GAMETE FERTILITY.* CELL MICROBIOL, 2011. **13**(12): P. 1956-74.

348. SEYDEL, K.B., ET AL., *PLASMODIUM FALCIPARUM: CHARACTERIZATION OF A LATE ASEXUAL STAGE GOLGI PROTEIN CONTAINING BOTH ANKYRIN AND DHHC DOMAINS.* EXP PARASITOL, 2005. **110**(4): P. 389-93.
349. REN, J., ET AL., *CSS-PALM 2.0: AN UPDATED SOFTWARE FOR PALMITOYLATION SITES PREDICTION.* PROTEIN ENG DES SEL, 2008. **21**(11): P. 639-44.
350. WAN, J., ET AL., *PALMITOYLATED PROTEINS: PURIFICATION AND IDENTIFICATION.* NAT PROTOC, 2007. **2**(7): P. 1573-84.
351. LIEHL, P., ET AL., *PHOSPHOTHIOATE OLIGODEOXYNUCLEOTIDES INHIBIT PLASMODIUM SPOROZOITE GLIDING MOTILITY.* CELL MICROBIOL, 2010. **12**(4): P. 506-15.
352. FRISCHKNECHT, F., ET AL., *IMAGING MOVEMENT OF MALARIA PARASITES DURING TRANSMISSION BY ANOPHELES MOSQUITOES.* CELL MICROBIOL, 2004. **6**(7): P. 687-94.
353. HEGGE, S., ET AL., *AUTOMATED CLASSIFICATION OF PLASMODIUM SPOROZOITE MOVEMENT PATTERNS REVEALS A SHIFT TOWARDS PRODUCTIVE MOTILITY DURING SALIVARY GLAND INFECTION.* BIOTECHNOL J, 2009. **4**(6): P. 903-13.
354. RENIA, L., ET AL., *MALARIA SPOROZOITE PENETRATION. A NEW APPROACH BY DOUBLE STAINING.* J IMMUNOL METHODS, 1988. **112**(2): P. 201-5.
355. COMBET, C., ET AL., *NPS@: NETWORK PROTEIN SEQUENCE ANALYSIS.* TRENDS BIOCHEM SCI, 2000. **25**(3): P. 147-50.
356. SOLDATI, D. AND M. MEISSNER, *TOXOPLASMA AS A NOVEL SYSTEM FOR MOTILITY.* CURR OPIN CELL BIOL, 2004. **16**(1): P. 32-40.
357. RAIBAUD, A., ET AL., *DIFFERENTIAL GENE EXPRESSION IN THE OOKINETE STAGE OF THE MALARIA PARASITE PLASMODIUM BERGHEI.* MOL BIOCHEM PARASITOL, 2006. **150**(1): P. 107-13.
358. SCHREVEL, J., ET AL., *VESICLE TRAFFICKING DURING SPOROZOITE DEVELOPMENT IN PLASMODIUM BERGHEI: ULTRASTRUCTURAL EVIDENCE FOR A NOVEL TRAFFICKING MECHANISM.* PARASITOLOGY, 2008. **135**(PT 1): P. 1-12.
359. PATRA, K.P. AND J.M. VINETZ, *NEW ULTRASTRUCTURAL ANALYSIS OF THE INVASIVE APPARATUS OF THE PLASMODIUM OOKINETE.* AM J TROP MED HYG, 2012. **87**(3): P. 412-7.
360. HEGGE, S., ET AL., *DIRECT MANIPULATION OF MALARIA PARASITES WITH OPTICAL TWEEZERS REVEALS DISTINCT FUNCTIONS OF PLASMODIUM SURFACE PROTEINS.* ACS NANO, 2012. **6**(6): P. 4648-62.
361. BOETTIGER, D., *QUANTITATIVE MEASUREMENTS OF INTEGRIN-MEDIATED ADHESION TO EXTRACELLULAR MATRIX.* METHODS ENZYMOL, 2007. **426**: P. 1-25.
362. MEDALIA, O. AND B. GEIGER, *FRONTIERS OF MICROSCOPY-BASED RESEARCH INTO CELL-MATRIX ADHESIONS.* CURR OPIN CELL BIOL, 2010. **22**(5): P. 659-68.
363. MUNEVAR, S., Y.L. WANG, AND M. DEMBO, *DISTINCT ROLES OF FRONTAL AND REAR CELL-SUBSTRATE ADHESIONS IN FIBROBLAST MIGRATION.* MOL BIOL CELL, 2001. **12**(12): P. 3947-54.
364. WEHRLE-HALLER, B. AND B.A. IMHOF, *ACTIN, MICROTUBULES AND FOCAL ADHESION DYNAMICS DURING CELL MIGRATION.* INT J BIOCHEM CELL BIOL, 2003. **35**(1): P. 39-50.
365. HEGGE, S., ET AL., *MULTISTEP ADHESION OF PLASMODIUM SPOROZOITES.* FASEB J, 2010. **24**(7): P. 2222-34.
366. MUNTER, S., ET AL., *PLASMODIUM SPOROZOITE MOTILITY IS MODULATED BY THE TURNOVER OF DISCRETE ADHESION SITES.* CELL HOST MICROBE, 2009. **6**(6): P. 551-62.
367. MONTAGNA, G.N., ET AL., *CRITICAL ROLE FOR HEAT SHOCK PROTEIN 20 (HSP20) IN MIGRATION OF MALARIAL SPOROZOITES.* J BIOL CHEM, 2012. **287**(4): P. 2410-22.
368. SHIN, S.C., J.P. VANDERBERG, AND J.A. TERZAKIS, *DIRECT INFECTION OF HEPATOCYTES BY SPOROZOITES OF PLASMODIUM BERGHEI.* J PROTOZOOL, 1982. **29**(3): P. 448-54.
369. CARVALHO, T.G., ET AL., *CONDITIONAL MUTAGENESIS USING SITE-SPECIFIC RECOMBINATION IN PLASMODIUM BERGHEI.* PROC NATL ACAD SCI U S A, 2004. **101**(41): P. 14931-6.
370. COMBE, A., ET AL., *CLONAL CONDITIONAL MUTAGENESIS IN MALARIA PARASITES.* CELL HOST MICROBE, 2009. **5**(4): P. 386-96.
371. LACROIX, C., ET AL., *FLP/FRT-MEDIATED CONDITIONAL MUTAGENESIS IN PRE-ERYTHROCYTIC STAGES OF PLASMODIUM BERGHEI.* NAT PROTOC, 2011. **6**(9): P. 1412-28.
372. PINO, P., ET AL., *A TETRACYCLINE-REPRESSIBLE TRANSACTIVATOR SYSTEM TO STUDY ESSENTIAL GENES IN MALARIA PARASITES.* CELL HOST MICROBE, 2012. **12**(6): P. 824-34.
373. ADAM, R.D., *BIOLOGY OF GIARDIA LAMBLIA.* CLIN MICROBIOL REV, 2001. **14**(3): P. 447-75.

374. TOUZ, M.C., J.T. CONRAD, AND T.E. NASH, *A NOVEL PALMITOYL ACYL TRANSFERASE CONTROLS SURFACE PROTEIN PALMITOYLATION AND CYTOTOXICITY IN GIARDIA LAMBLIA.* MOL MICROBIOL, 2005. **58**(4): P. 999-1011.
375. MERINO, M.C., ET AL., *IDENTIFICATION OF GIARDIA LAMBLIA DHHC PROTEINS AND THE ROLE OF PROTEIN S-PALMITOYLATION IN THE ENCYSTATION PROCESS.* PLOS NEGL TROP DIS, 2014. **8**(7): P. E2997.
376. TEWARI, R., ET AL., *THE SYSTEMATIC FUNCTIONAL ANALYSIS OF PLASMODIUM PROTEIN KINASES IDENTIFIES ESSENTIAL REGULATORS OF MOSQUITO TRANSMISSION.* CELL HOST MICROBE, 2010. **8**(4): P. 377-87.
377. MCROBERT, L., ET AL., *GAMETOGENESIS IN MALARIA PARASITES IS MEDIATED BY THE CGMP-DEPENDENT PROTEIN KINASE.* PLOS BIOL, 2008. **6**(6): P. E139.
378. BILLKER, O., ET AL., *CALCIUM AND A CALCIUM-DEPENDENT PROTEIN KINASE REGULATE GAMETE FORMATION AND MOSQUITO TRANSMISSION IN A MALARIA PARASITE.* CELL, 2004. **117**(4): P. 503-14.
379. TEWARI, R., ET AL., *AN ATYPICAL MITOGEN-ACTIVATED PROTEIN KINASE CONTROLS CYTOKINESIS AND FLAGELLAR MOTILITY DURING MALE GAMETE FORMATION IN A MALARIA PARASITE.* MOL MICROBIOL, 2005. **58**(5): P. 1253-63.
380. REININGER, L., ET AL., *AN ESSENTIAL ROLE FOR THE PLASMODIUM NEK-2 NIMA-RELATED PROTEIN KINASE IN THE SEXUAL DEVELOPMENT OF MALARIA PARASITES.* J BIOL CHEM, 2009. **284**(31): P. 20858-68.
381. BILLKER, O., S. LOURIDO, AND L.D. SIBLEY, *CALCIUM-DEPENDENT SIGNALING AND KINASES IN APICOMPLEXAN PARASITES.* CELL HOST MICROBE, 2009. **5**(6): P. 612-22.
382. MOON, R.W., ET AL., *A CYCLIC GMP SIGNALLING MODULE THAT REGULATES GLIDING MOTILITY IN A MALARIA PARASITE.* PLOS PATHOG, 2009. **5**(9): P. E1000599.
383. SMYTHE, E. AND K.R. AYSCOUGH, *THE ARK1/PRK1 FAMILY OF PROTEIN KINASES. REGULATORS OF ENDOCYTOSIS AND THE ACTIN SKELETON.* EMBO REP, 2003. **4**(3): P. 246-51.
384. GUTTERY, D.S., ET AL., *GENOME-WIDE FUNCTIONAL ANALYSIS OF PLASMODIUM PROTEIN PHOSPHATASES REVEALS KEY REGULATORS OF PARASITE DEVELOPMENT AND DIFFERENTIATION.* CELL HOST MICROBE, 2014. **16**(1): P. 128-40.
385. TALMAN, A.M., ET AL., *PBGEST MEDIATES MALARIA TRANSMISSION TO BOTH MOSQUITO AND VERTEBRATE HOST.* MOL MICROBIOL, 2011. **82**(2): P. 462-74.
386. NUNES, J.K., ET AL., *DEVELOPMENT OF A TRANSMISSION-BLOCKING MALARIA VACCINE: PROGRESS, CHALLENGES, AND THE PATH FORWARD.* VACCINE, 2014.
387. LEROY, D., ET AL., *DEFINING THE BIOLOGY COMPONENT OF THE DRUG DISCOVERY STRATEGY FOR MALARIA ERADICATION.* TRENDS PARASITOL, 2014.